

Treatment-resistant ophthalmoplegia in myasthenia gravis:  
Clinical, molecular and functional studies of patient-derived  
orbital tissues

A thesis presented to the Division of Neurology,  
Department of Medicine, Faculty of Health Sciences,  
University of Cape Town

By Dr Tarin Europa, MBChB

For the degree of PhD (Medicine)

Supervisor: Prof Jeannine Heckmann, PhD

Co-supervisor: Dr Melissa Nel, PhD

The copyright of this thesis vests in the author. No quotation from it or information derived from it is to be published without full acknowledgement of the source. The thesis is to be used for private study or non-commercial research purposes only.

Published by the University of Cape Town (UCT) in terms of the non-exclusive license granted to UCT by the author.

**Table of Contents**

Abstract.....	2
Plagiarism declaration.....	4
Acknowledgments.....	5
Foreword.....	6
Introduction.....	7
Chapter 1: Myasthenic ophthalmoparesis: time to resolution after initiating immune therapies .....	19
Chapter 2: A review of the histopathological findings in myasthenia gravis: clues to the pathogenesis of treatment-resistance in extraocular muscles .....	40
Chapter 3: Gene expression profiling of patient-derived peri-orbital and extraocular muscle in treatment-resistant ophthalmoplegic myasthenia gravis .....	67
Chapter 4: Gene expression in human extraocular and orbicularis oculi muscles .....	114
Chapter 5: Mitochondrial genetic and dynamic studies in ocular fibroblasts of myasthenia gravis patients with ophthalmoplegia: a pilot study.....	138
Chapter 6: Concluding remarks.....	166
References .....	171
List of abbreviations .....	173

## Abstract

**Introduction:** Myasthenia gravis (MG) is an immune-mediated disorder affecting the neuromuscular junction. Weakness of the extraocular muscles (EOMs) occurs frequently in MG and typically responds to immune therapies similarly to the non-ocular muscles. Susceptible individuals with the ophthalmoplegic subphenotype of MG (OP-MG), which occurs almost exclusively in acetylcholine receptor positive MG (AChR-MG), may manifest treatment-resistant extraocular muscle weakness despite the use of standard immune therapies. The pathogenetic mechanisms involved in the development of treatment-resistant ophthalmoplegia in MG are still unknown and no effective treatment currently exists. **Aim:** To investigate the molecular-genetic pathogenesis of the OP-MG subphenotype. **Methods:** Triangulation of data from clinical observations, review of MG muscle biopsy histopathology, gene expression studies in OP-MG patient-derived orbital muscles (AChR-MG) and bioenergetic studies in highly specialised perimysial ocular fibroblasts of these OP-MG cases was used to identify the underlying pathogenetic mechanisms of OP-MG and to verify previous hypotheses generated by next generation sequencing studies. **Results:** Myasthenic ophthalmoparesis may persist despite immune therapies in 40% of cases in the first year of immune treatment. Delay to diagnosis of MG and therefore initiation of treatment (>1 year) was an unfavourable prognostic factor for resolution of ophthalmoparesis and suggested that with prolonged weakness, pathological changes may occur at the level of the muscle. Review of the literature documenting histopathology in MG muscle biopsies showed that neurogenic atrophy and features of mitochondrial stress, which may be secondary consequences of functional denervation and reduced contractility, are frequently observed in MG muscle biopsies and the EOMs may be particularly susceptible, demonstrating features of fatty and fibrocellular replacement of myofibres. Gene expression studies performed in the orbital muscles of OP-MG and non-MG control cases supported the hypotheses of previous unbiased genomic studies showing that genes harbouring OP-MG associated gene variants may be involved in a dysregulated network of genes including genes in pathways involved in atrophy signalling, muscle contractility and mitochondrial homeostasis. Several genes were significantly downregulated in the OP-MG orbital muscles compared with controls. MicroRNAs which are biological regulators of gene expression, were hypothesized to be a potential pathogenetic mechanism causing downregulation of these genes in OP-MG orbital muscles and several microRNAs highly expressed in EOMs were associated with the significantly repressed genes in OP-MG orbital muscle using available data in public microRNA databases. Preliminary dynamic bioenergetic assays in perimysial ocular fibroblasts derived from the EOM myotendons of OP-MG and non-MG control cases suggested that regulation of

mitochondrial homeostasis may be altered in the context of MG. **Conclusion:** Gene expression analyses in patient-derived orbital muscles support the hypotheses of previous genomic studies suggesting that pathogenetic mechanisms involving pathways relating to muscle atrophy, contractility and mitochondrial homeostasis may be triggered in the EOMs in the context of MG. Dysregulation of these pathways is likely to impact EOM regeneration in the context of MG-induced complement-mediated attack as well as contractility in this specialized muscle allotype with a high firing rate. These complex aberrant molecular-genetic interactions may contribute to persistent ophthalmoplegia despite adequate immune therapies in OP-MG cases.

**Plagiarism declaration**

“This thesis/dissertation has been submitted to the Turnitin module (or equivalent similarity and originality checking software) and I confirm that my supervisor has seen my report and any concerns revealed by such have been resolved with my supervisor.”

Name: Tarin Europa

Student number: ERPTAR001

Date: 14/12/2022

## **Acknowledgments**

I would like to thank the following people for their contributions to this project:

Professor JM Heckmann for her consistent support, encouragement, and inspiration throughout the duration of this project and for her invaluable expertise and insight as a specialist in neuromuscular diseases.

Dr M Nel for her support as my co-supervisor and excellent teaching in laboratory techniques and statistical analysis, whose genomic research in OP-MG provided the basis for this project.

Professor S Prince for providing access to her laboratory and technical support during my experimental work.

Professor A Murray and Dr M Lenake for performing the surgeries which provided access to the orbital tissues necessary for this project.

Dr M Lebeko for his teaching and assistance in techniques of bioenergetic assays and flow cytometry and Prof N Khumalo for providing access to her laboratory for these experiments.

Dr D Bouwers for her teaching in methods of cell culture.

Dr A Shoko for performing the custom qPCR arrays on the orbital muscles.

**Foreword**

Ophthalmoplegic myasthenia gravis (OP-MG) refers to a rare subphenotype of a neuromuscular disorder called myasthenia gravis (MG). Individuals with the ophthalmoplegic complication of MG develop severe, treatment-resistant weakness of the orbital muscles causing impaired vision. At present, there is no effective treatment for OP-MG.

The OP-MG subphenotype was recognized and characterized in South African MG cases by the principle investigator of the Neurology Research Group (NRG), Professor JM Heckmann, who observed the manifestation of treatment-resistant ophthalmoplegia in patients attending the MG clinic at Groote Schuur Hospital (GSH) in Cape Town, South Africa, over the past two decades. Although this is a rare condition, the previous research conducted by Prof Heckmann and the NRG over the past two decades has established a database of OP-MG cases who have attended the MG clinic at Groote Schuur Hospital. Previous genetic research in OP-MG, including whole genome sequencing (WGS) of extreme phenotype cases, has provided the background for the research described in this thesis, which forms part of the larger body of work investigating the molecular genetic pathogenesis of OP-MG. The main objectives of this project are to verify the hypotheses generated by comprehensive next generation sequencing techniques and further interrogate the molecular genetic pathogenesis of OP-MG to inform potential future development of novel, targeted therapies.

## Introduction

In autoimmune myasthenia gravis (MG), antibodies target the neuromuscular junction causing a neurotransmission defect that manifests clinically as varying degrees of muscle weakness ranging from fatigability to paralysis (Gilhus 2016). The extraocular muscles (EOMs), which enable eye movements, are frequently and severely weakened in MG, but similarly to non-ocular muscles, typically improve with immune therapies (Benatar, McDermott et al. 2016). However, a subphenotype of myasthenia gravis cases has been described in which susceptible individuals develop treatment-resistant paralysis of the EOMs although the non-ocular muscles respond to treatment (Heckmann and Nel 2017). This is referred to as the ophthalmoplegic myasthenia gravis subphenotype (OP-MG). Myasthenia gravis is a rare disease, and OP-MG occurs in less than twenty per cent of MG cases attending the MG clinic at Groote Schuur Hospital (GSH) (Heckmann and Nel 2017). Although OP-MG only affects a small proportion of our population, those affected experience severe visual impairment that impacts schooling, employment and quality of life. At present, there are no effective therapies for OP-MG.

### 1. Clinical manifestations of MG

The South African annual incidence rate of MG is 8.5 cases per million persons, which is similar to international rates (Bateman, Schinkel et al. 2007, Mombaur, Lesosky et al. 2015, Gilhus 2016). Extraocular muscle (EOM) weakness presenting as drooping of the eyelids (ptosis) and/or double vision (diplopia) occurs in 85% of cases and is the first clinical manifestation of myasthenia gravis in two-thirds of cases (Kupersmith, Latkany et al. 2003). Of those with EOM weakness as the initial presentation of MG, 50 - 60% develop generalized weakness within two years affecting the limb, respiratory or bulbar muscles (Benatar and Kaminski 2006, Kupersmith 2009). Ocular myasthenia, in which the weakness remains confined to the ocular muscles, is defined after an arbitrary period of 2 years, based on the rarity of generalization occurring after the first 2 years of symptoms (Kupersmith and Ying 2005, Wong, Huda et al. 2014).

MG is diagnosed based on a history and physical examination consistent with fatigable weakness as well as one or more of the following;

- a positive response to acetylcholinesterase inhibitors
- positive assays for pathogenic antibodies (acetylcholine receptor or muscle-specific kinase antibodies)
- and/or a decremental response on single-fibre electromyography (SFEMG) or repetitive nerve stimulation (RNS) (Gilhus 2016).

Diagnosis may also be retrospectively affirmed by a response to immune therapies. In cases with proven acetylcholine receptor antibodies, computed tomography (CT) imaging of the mediastinum may be indicated to investigate for a thymoma (Gilhus 2016).

## 2. The antibody-mediated effects on the neuromuscular junction in myasthenia gravis

In most cases of MG, antibodies target the acetylcholine receptors (AChR) of the neuromuscular junction (Gilhus 2016). Antibodies may block or destroy AChRs; as complement initiation by IgG-1 antibodies may cause injury to the muscle endplate or antibody cross-linkage of AChRs (Drachman, Angus et al. 1978). In 85% of MG cases, circulating AChR antibodies are detectable by radioimmunoassay while approximately 10% have detectable antibodies targeting the muscle-specific kinase (MuSK) which is involved in clustering of AChRs on the muscle endplate (Skeie, Apostolski et al. 2010). Cases without detectable antibodies to AChR or MuSK may either have antibodies against other muscle endplate proteins including lipoprotein receptor-related protein 4 (LRP4) and agrin, or low-level titres of anti-AChR or MuSK antibodies below the detectable limit of current radioimmunoassays (Skeie, Apostolski et al. 2010, Gilhus 2016).

## 3. Ocular manifestations of myasthenia gravis

Weakness of the extraocular muscles (EOMs), levator palpebrae superiors and/or orbicularis oculi results in ptosis and diplopia in patients with ocular manifestations of MG. Dysfunction of even one EOM can result in significant functional difficulties due to visual impairment. Ocular symptoms may manifest as fatigable or persistent weakness. As with generalized MG, the diagnosis is based on suggestive history and examination findings with support from serology, electrophysiology (repetitive nerve stimulation and/or single fiber electromyography) and response to acetylcholinesterase inhibitors and/or immune therapies however, only 50% of ocular MG cases have detectable antibodies in the serum (vs 85% in generalized MG) (Wong, Huda et al. 2014).

The extraocular muscles are thought to be more susceptible to the effects of MG than non-ocular muscles, as they have lower expression of complement regulators, a lower safety factor and simpler synaptic folds (Wong, Huda et al. 2014).

## 4. Treatment of myasthenia gravis

Acetylcholinesterase inhibitors (AChEIs) may provide transient symptomatic relief by inhibiting the breakdown of acetylcholine in the synaptic cleft (Gilhus 2016). In cases where there is partial or no response to AChEIs, or cases with severe disease, immunosuppression is indicated (Skeie, Apostolski et al. 2010). Most frequently an oral corticosteroid (prednisone) is initiated at low doses and titrated upwards until symptoms have improved or resolved

(Heckmann, Owen et al. 2007, Heckmann, Rawoot et al. 2011, Benatar, McDermott et al. 2016). If longer term corticosteroid use is required, a steroid-sparing agent such as methotrexate (Heckmann, Rawoot et al. 2011) or azathioprine (Palace, Newsom-Davis et al. 1998) may be added to the treatment regimen. MG is graded according to the Myasthenia Gravis Foundation of America (MGFA) scale, which ranges from Grade 1 (ocular symptoms only) to grade 5 (severe respiratory muscle involvement requiring intubation and ventilation) (Jaretzki, Barohn et al. 2000). In severe cases (Grade 4 – 5), “rescue therapies” such as intravenous immunoglobulin (IVIG) or plasma exchange (PLEX) may be required. In cases where thymomas are visualised on computed tomography (CT), thymectomy may be indicated (Marx, Pfister et al. 2012). The standard treatment protocol at our clinic is comparable to others internationally (Heckmann, Rawoot et al. 2011, Benatar, McDermott et al. 2016). Immune therapies are generally effective in improving myasthenic weakness, and the EOMs typically respond to treatment similarly to non-ocular muscles (Benatar, McDermott et al. 2016). However, in this project I will be focusing on the treatment-resistant ophthalmoplegic subphenotype of myasthenia gravis which is characterised by myasthenic EOM weakness that does not respond to immune therapies (Heckmann and Nel 2017).

#### 5. Treatment-resistant ophthalmoplegia in MG

It has previously been described internationally that a proportion of patients with ocular manifestations of myasthenia gravis do not respond to immune therapies (Kupersmith and Ying 2005, Wong, Huda et al. 2014). In patients attending the Myasthenia gravis clinic at Groote Schuur Hospital, those with treatment-resistant ophthalmoplegia have been described as having the ophthalmoplegic myasthenia gravis (OP-MG) subphenotype (Heckmann and Nel 2017). Most frequently, these are individuals with generalized MG but with persistent and often severe extraocular muscle weakness (ophthalmoplegia) (Heckmann and Nel 2017). The onset of symptoms in most OP-MG cases is most frequently before the age of 18 years (juvenile MG), however several cases with late-onset MG (older than 50 years) have been reported (Heckmann and Nel 2017). The OP-MG subphenotype is most frequently observed in patients with African-genetic ancestry and with detectable circulating acetylcholine receptor antibodies (AChR positive MG) although a few cases have been reported having MuSK-MG or triple seronegative MG (Heckmann and Nel 2017).

The inclusion criteria for OP-MG used in the MG clinic at our institution (Groote Schuur Hospital/ University of Cape Town) is moderate to severe weakness of more than half of the EOMs ( $\geq 6$  of 12) and/or levator palpebrae superioris for a minimum duration of two years despite immune therapies (Heckmann and Nel 2017). Although some cases demonstrate treatment-resistant ocular manifestations from the time of initiation of immune therapies,

others may initially respond well to treatment and later develop treatment-resistance after a critical event such as an MG crisis, relapse or cessation of immune therapies (Heckmann and Nel 2017). As the clinical course varies, it is unclear at initial consultations with newly diagnosed MG cases which individuals with MG will develop the ophthalmoplegic complication. Therefore, one of the aims of this project was to analyse clinical observations of MG cases with weak EOMs from the first consultation and through the first year of immune therapies, to determine whether there are common clinical features or patterns that might aid in prognostication early in the course of the disease (see Chapter 1).

## 6. Management of visual impairment in OP-MG

As current medical treatments for MG are ineffective in resolving ophthalmoplegia in OP-MG cases, alternative strategies to assist patients with visual impairment were developed (Findlay 2017). As a non-surgical option for improvement of ptosis, “ptosis crutches” were developed. These are 3D printed devices designed to lift the eyelid by attachment to spectacles. This option was beneficial for OP-MG cases where all 12 EOMs are paralysed (complete ophthalmoplegia) and the eyes are correctly aligned but ptosis of the eyelids impaired vision. As the ptosis crutch does not allow for blinking it can only be worn intermittently but helps to achieve temporary vision.

In highly selected cases, where there has been no improvement of ophthalmoplegia despite years of immune therapies, surgical correction of ptosis or strabismus might be considered. Patients considered for surgery should be in MG remission without diurnal fluctuation of their ocular symptoms. For ptosis surgeries, a prerequisite is that the patient has good eye closure to prevent lagophthalmos and exposure keratitis as a post-surgical complication. Ocular re-alignment and ptosis surgeries have been successful in improving vision in MG patients with chronic ptosis and ophthalmoplegia in our setting. During these procedures, it has been possible for us to opportunistically sample orbital tissues of OP-MG cases with informed consent.

## 7. Histopathology of EOMs and non-ocular muscles in MG

Light and electron microscopy were previously performed on an EOM sampled during the ocular re-alignment surgery of a patient with OP-MG after 3.5 years of ocular symptoms (Rautenbach, Pillay et al. 2017). This sample showed atrophic fibres, mitochondrial abnormalities and fibrocellular infiltrates similarly to one other case report although the symptoms were of shorter duration (<6 months) (Gratton, Herro et al. 2014, Rautenbach, Pillay et al. 2017). As these findings were from 2 cases, and due to the sparseness of histopathological data in EOMs of MG cases, a systematic review of histopathology of MG muscle biopsies was conducted to ascertain whether the changes seen in the paralysed EOMs

of MG cases have been previously reported in the muscles of MG cases (EOMs or non-ocular) and to identify the changes that occur at the level of the muscle that may contribute to the manifestation of treatment-resistance of the EOMs in MG (see Chapter 2).

#### 8. Mitochondrial function in MG

In addition to the hints of ultrastructural features of mitochondrial stress in the OP-MG EOM biopsy, evidence of increased mitochondrial metabolism and/or stress in actively and passively induced experimental autoimmune myasthenia gravis (EAMG) and the serum proteins of humans with MG has been reported (Zhou, Kaminski et al. 2014, Kaminski, Himuro et al. 2016, Adamczyk-Sowa, Bieszczad-Bedrejczuk et al. 2017). As the EOMs are dependent on mitochondrial metabolism to sustain their high firing rates and may be particularly susceptible to changes in mitochondrial function, dynamic mitochondrial functional tests were performed on the ocular fibroblasts that support EOMs to determine whether mitochondrial function is altered in MG and whether it may contribute to the pathogenesis of OP-MG (Chapter 3).

The EOMs require energy to perform both rapid, precision ocular movements as well as sustained non-fatiguing tonus (Martinez, Hay et al. 1976). They therefore have an abundance of mitochondria as well as several metabolic adaptations that optimise energy production (Porter and Baker 1996, Patel, Gamboa et al. 2009).

These adaptations are summarized in the schematic Figure 1. A detailed comparison between EOM and non-ocular muscle metabolism is shown in Appendix table 1.

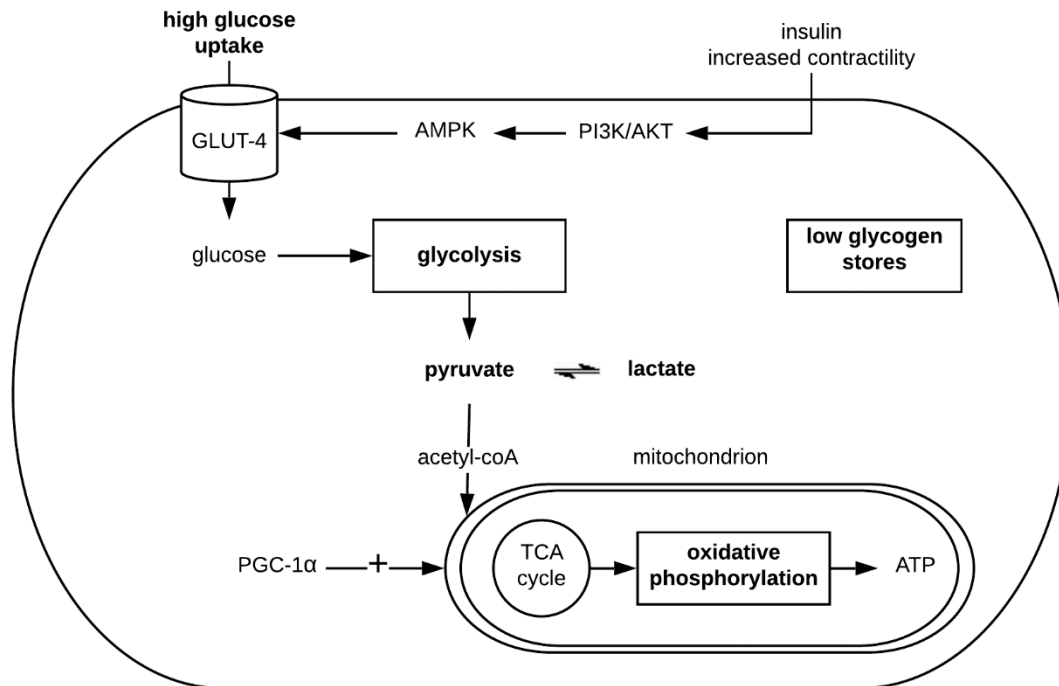


Figure 1. Extraocular muscle (EOM) metabolism. Processes that are optimised in EOMs compared with non-ocular muscles are shown in bold text. “GLUT-4” refers to a glucose receptor which translocates to the cell surface via mediation of the phosphoinositide-3 kinase (PI3K/AKT) and AMP-activated protein kinase pathways on stimulation by insulin or contractile activity. Mitochondrial biogenesis and oxidative metabolism are regulated by the peroxisome proliferator-activated receptor- $\gamma$  coactivator (PGC-1 $\alpha$ ) pathway. Tricarboxylic acid (TCA) cycle. Adenosine triphosphate (ATP).

As the EOMs require a continuous supply of energy, efficient glucose uptake is essential. The increased vascularity of the EOMs aids delivery of circulating glucose and similarly to non-ocular muscles, glucose uptake is regulated to meet demand by insulin and contractility via PI3K/AKT and AMPK translocation of the GLUT-4 receptors to the cell membrane (Garcia-Cazarin, Fisher et al. 2010). Several lines of evidence from studies of both rat and human EOMs have shown that EOMs synthesize less glycogen than non-ocular muscles, are less dependent on glycogen to drive glycolysis during periods of intense activity and preferentially use circulating glucose (Fischer, Gorospe et al. 2002, Fischer, Budak et al. 2005, Garcia-Cazarin, Fisher et al. 2010). Differential isoform expression of several regulatory enzymes in glycolysis (Fischer, Gorospe et al. 2002), as well as expression of the lactate dehydrogenase isoform that preferentially converts lactate to pyruvate, suggests efficient and economical use of glycolysis (Andrade and McMullen 2006). Although lactate has traditionally been considered

a waste product of glycolysis and associated with fatigue, the EOMs can utilize lactate for oxidative metabolism.

Although the EOMs have high energy demands, they exhibit slower respiration than limb muscles (Patel, Gamboa et al. 2009). It is thought that the EOMs have greater oxidative efficiency than non-ocular muscles due to their abundance of mitochondria, together with differential expression, content and activity of mitochondrial proteins and respiratory complexes (Patel, 2006). For example, lower expression of the uncoupling protein *UCP3* may increase coupling efficiency in the EOMs (Fischer, Budak et al. 2005).

In summary, in order to meet great energy demands, EOM metabolism differs from non-ocular muscles in glycogen and lactate utilization, subunit expression of glycolytic enzymes and mitochondrial respiratory complexes and coupling efficiency.

## 9. Genetic research in OP-MG

Previous research suggested that the pathogenesis of OP-MG is complex. Previously, two single nucleotide polymorphisms (SNPs) in the promoter regions of *DAF/CD55* (Heckmann, Uwimpuhwe et al. 2010) and *TGFB1* (Nel, Buys et al. 2016) associated with juvenile myasthenia gravis and were shown to reduce the expression of these genes. Reduced expression of the complement regulatory protein encoded by *DAF/CD55* and the myokine encoded by *TGFB1*, may increase EOM susceptibility to complement attack and impair important muscle regeneration pathways (Nel, Buys et al. 2016). Recently, unbiased next generation sequencing (NGS) studies using extreme-phenotype sampling, comparing genomic data of OP-MG cases to control-MG cases i.e. MG cases with EOM weakness that responded well to immune therapies, identified several potentially functional gene variants that were more frequent in OP-MG cases vs control-MG (Nel, Jalali Sefid Dashti et al. 2017, Nel, Mulder et al. 2019). Functional gene variants identified in this study were overrepresented in pathways of muscle regeneration and atrophy signalling.

As the gene variants identified by next generation sequencing techniques required functional validation, the expression of genes harbouring OP-MG susceptibility variants discovered by whole exome sequencing (WES) was investigated in patient-derived myocytes derived from transdifferentiated dermal fibroblasts (Nel, Jalali Sefid Dashti et al. 2017, Nel, Prince et al. 2019). Comparing OP-MG transdifferentiated myocytes to control-MG myocytes, i.e., myocytes derived from cases whose EOMs responded to immune therapies, differential gene expression of four genes suspected to be harbouring OP-MG associated variants was identified including *PPP1R2*, *CANX*, *FAM69A* and *FAM136A* (Nel, Prince et al. 2019). Strong

cross correlations between OP-MG genes and genes previously shown to be differentially expressed in models of experimental myasthenia gravis were demonstrated in the OP-MG myocytes but not in control-MG myocytes (Nel, Prince et al. 2019). However, as EOMs represent a unique muscle allotype and splice variants may produce different effects in different tissues, gene expression in the model myocytes, although informative as a surrogate for gene expression in muscle tissue, were not representative of unique EOM gene expression signatures. Therefore, one of the aims of this project was to investigate the expression of genes harbouring OP-MG susceptibility gene variants identified by WES and WGS in patient-derived EOMs (see Chapter 3).

It is suspected that the pathogenetic mechanisms underlying the OP-MG subphenotype may be complex and may vary between OP-MG cases i.e. not all OP-MG cases may have the same genetic variants; although similar muscle pathways may be impacted. Epigenetic mechanisms may contribute to the development of treatment-resistant EOMs in OP-MG e.g. DNA methylation and/or histone modification may inhibit the binding of transcriptional regulators thereby affecting transcription of genes differentially expressed in the EOMs and non-ocular muscles. Circulating microRNAs may impact transcription of genes in pathways important for EOM function. In this project, investigation of the gene expression in OP-MG orbital muscles (Chapter 3) was performed to provide clues to the pathogenetic mechanisms underlying the development of the OP-MG subphenotype.

#### 10. Knowledge gap

At present, there are no clinical or laboratory predictive markers for the early identification of susceptible individuals with MG who may develop treatment-resistant ophthalmoplegia. Although there is consensus amongst experts regarding the standard therapeutic regimens for the treatment of MG, currently there is no effective treatment for OP-MG. To inform the potential future development of novel, targeted therapeutic strategies, the molecular genetic pathogenesis of OP-MG must be investigated. In summary, the overall aim of this project was to investigate the molecular genetic pathogenesis of OP-MG by addressing the following specific objectives:

1. To determine by analysis of clinical observations in newly diagnosed MG cases, how quickly MG-associated EOM weakness should be expected to resolve in the first year of immune therapies with the purpose of identifying predictors for persistent EOM weakness.
2. To identify clues to the pathogenesis of OP-MG by review of histopathology in the EOMs and non-ocular muscles of MG cases compared to EOMs with reduced contractility in other conditions.

3. To investigate the expression of genes harbouring OP-MG susceptibility variants (identified by unbiased next generation sequencing studies) and their downstream pathways by comparing the gene expression of patient-derived OP-MG and control orbital tissues.
4. To determine by gene expression and live-cell metabolic assays in ocular fibroblasts derived from EOM myotendons, whether mitochondrial function differs between OP-MG and control ocular fibroblasts.

The following chapters describe the clinical and laboratory-based studies performed to achieve these objectives.

## References

- Adamczyk-Sowa, M., E. Bieszczad-Bedrejcuk, S. Galiniak, I. Rozmiłowska, D. Czyżewski, G. Bartosz and I. Sadowska-Bartosz (2017). "Oxidative modifications of blood serum proteins in myasthenia gravis." J. Neuroimmunol. **305**: 145-153.
- Andrade, F. H. and C. A. McMullen (2006). "Lactate is a metabolic substrate that sustains extraocular muscle function." Pflugers Arch. **452**(1): 102-108.
- Bateman, K. J., M. Schinkel, F. Little, L. Liebenberg, A. Vincent and J. M. Heckmann (2007). "Incidence of seropositive myasthenia gravis in Cape Town and South Africa." South African Medical Journal **97**: 959+.
- Benatar, M. and H. Kaminski (2006). "Medical and surgical treatment for ocular myasthenia." Cochrane Database Syst Rev(2): CD005081.
- Benatar, M., M. P. McDermott, D. B. Sanders, G. I. Wolfe, R. J. Barohn, R. J. Nowak, M. Hehir, V. Juel, H. Katzberg, R. Tawil and G. Muscle Study (2016). "Efficacy of prednisone for the treatment of ocular myasthenia (EPITOME): A randomized, controlled trial." Muscle Nerve **53**(3): 363-369.
- Drachman, D. B., C. W. Angus, R. N. Adams, J. D. Michelson and G. J. Hoffman (1978). "Myasthenic antibodies cross-link acetylcholine receptors to accelerate degradation." New England Journal of Medicine **298**(20): 1116-1122.
- Findlay, M. (2017). A modular and adjustable ptosis crutch as a non-surgical solution to elevating the upper eyelid of myasthenia gravis patients, University of Cape Town.
- Fischer, M. D., M. T. Budak, M. Bakay, J. R. Gorospe, D. Kjellgren, F. Pedrosa-Domellof, E. P. Hoffman and T. S. Khurana (2005). "Definition of the unique human extraocular muscle allotype by expression profiling." Physiol Genomics **22**(3): 283-291.
- Fischer, M. D., J. R. Gorospe, E. Felder, S. Bogdanovich, F. Pedrosa-Domellof, R. S. Ahima, N. A. Rubinstein, E. P. Hoffman and T. S. J. P. g. Khurana (2002). "Expression profiling reveals metabolic and structural components of extraocular muscles." Physiol. Genomics **9**(2): 71-84.
- Garcia-Cazarin, M. L., T. M. Fisher and F. H. Andrade (2010). "Glucose Uptake in Rat Extraocular Muscles: Effect of Insulin and Contractile Activity." Invest. Ophthalmol. Vis. Sci. **51**(12): 6364-6368.
- Gilhus, N. E. (2016). "Myasthenia Gravis." N Engl J Med **375**(26): 2570-2581.
- Gratton, S. M., A. Herro, J. A. Bermudez-Magner and J. Guy (2014). "Atrophy and Fibrosis of Extra-Ocular Muscles in Anti-Acetylcholine Receptor Antibody Myasthenia Gravis." Open Journal of Ophthalmology **4**(04): 117.
- Heckmann, J. M. and M. Nel (2017). "A unique subphenotype of myasthenia gravis." Ann. N. Y. Acad. Sci.

- Heckmann, J. M., E. P. Owen and F. Little (2007). "Myasthenia gravis in South Africans: racial differences in clinical manifestations." Neuromuscul. Disord. **17**(11-12): 929-934.
- Heckmann, J. M., A. Rawoot, K. Bateman, R. Renison and M. Badri (2011). "A single-blinded trial of methotrexate versus azathioprine as steroid-sparing agents in generalized myasthenia gravis." BMC Neurol **11**: 97.
- Heckmann, J. M., H. Uwimpuhwe, R. Ballo, M. Kaur, V. B. Bajic and S. Prince (2010). "A functional SNP in the regulatory region of the decay-accelerating factor gene associates with extraocular muscle pareses in myasthenia gravis." Genes Immun **11**(1): 1-10.
- Jaretzki, A., 3rd, R. J. Barohn, R. M. Ernstoff, H. J. Kaminski, J. C. Keeseey, A. S. Penn and D. B. Sanders (2000). "Myasthenia gravis: recommendations for clinical research standards. Task Force of the Medical Scientific Advisory Board of the Myasthenia Gravis Foundation of America." Neurology **55**(1): 16-23.
- Kaminski, H. J., K. Himuro, J. Alshaikh, B. Gong, G. Cheng and L. L. Kusner (2016). "Differential RNA Expression Profile of Skeletal Muscle Induced by Experimental Autoimmune Myasthenia Gravis in Rats." Front Physiol **7**: 524.
- Kupersmith, M. and G. Ying (2005). "Ocular motor dysfunction and ptosis in ocular myasthenia gravis: effects of treatment." British journal of ophthalmology **89**(10): 1330-1334.
- Kupersmith, M. J. (2009). "Ocular myasthenia gravis: treatment successes and failures in patients with long-term follow-up." J Neurol **256**(8): 1314-1320.
- Kupersmith, M. J., R. Latkany and P. Homel (2003). "Development of generalized disease at 2 years in patients with ocular myasthenia gravis." Archives of neurology **60**(2): 243-248.
- Kupersmith, M. J. and G. Ying (2005). "Ocular motor dysfunction and ptosis in ocular myasthenia gravis: effects of treatment." Br J Ophthalmol **89**(10): 1330-1334.
- Martinez, A. J., S. Hay and K. W. McNeer (1976). "Extraocular muscles light microscopy and ultrastructural features." Acta Neuropathologica **34**(3): 237-253.
- Marx, A., F. Pfister, B. Schalke, W. Nix and P. Strobel (2012). "Thymus pathology observed in the MGTX trial." Ann N Y Acad Sci **1275**: 92-100.
- Mombaur, B., M. R. Lesosky, L. Liebenberg, H. Vreede and J. M. Heckmann (2015). "Incidence of acetylcholine receptor-antibody-positive myasthenia gravis in South Africa." Muscle & Nerve **51**(4): 533-537.
- Nel, M., J. M. Buys, R. Rautenbach, S. Mowla, S. Prince and J. M. Heckmann (2016). "The African-387 C>T TGFB1 variant is functional and associates with the ophthalmoplegic complication in juvenile myasthenia gravis." J Hum Genet **61**(4): 307-316.
- Nel, M., M. Jalali Sefid Dashti, J. Gamielidien and J. M. Heckmann (2017). "Exome sequencing identifies targets in the treatment-resistant ophthalmoplegic subphenotype of myasthenia gravis." Neuromuscul Disord.

- Nel, M., N. Mulder, T. A. Europa and J. M. Heckmann (2019). "Using Whole Genome Sequencing in an African Subphenotype of Myasthenia Gravis to Generate a Pathogenetic Hypothesis." Front Genet **10**(136).
- Nel, M., S. Prince and J. M. Heckmann (2019). "Profiling of patient-specific myocytes identifies altered gene expression in the ophthalmoplegic subphenotype of myasthenia gravis." Orphanet J Rare Dis **14**(1): 24.
- Palace, J., J. Newsom-Davis, B. Lecky and M. G. S. Group (1998). "A randomized double-blind trial of prednisolone alone or with azathioprine in myasthenia gravis." Neurology **50**(6): 1778-1783.
- Patel, S. P., J. L. Gamboa, C. A. McMullen, A. Rabchevsky and F. H. Andrade (2009). "Lower Respiratory Capacity in Extraocular Muscle Mitochondria: Evidence for Intrinsic Differences in Mitochondrial Composition and Function." Investigative Ophthalmology & Visual Science **50**(1): 180-186.
- Porter, J. D. and R. S. Baker (1996). "Muscles of a different 'color': The unusual properties of the extraocular muscles may predispose or protect them in neurogenic and myogenic disease." Neurology **46**(1): 30-37.
- Rautenbach, R. M., K. Pillay, A. D. N. Murray and J. M. Heckmann (2017). "Extraocular Muscle Findings in Myasthenia Gravis Associated Treatment-Resistant Ophthalmoplegia: A Case Report." J Neuroophthalmol.
- Skeie, G., S. Apostolski, A. Evoli, N. Gilhus, I. Illa, L. Harms, D. Hilton-Jones, A. Melms, J. Verschuuren and H. J. E. J. o. N. Horge (2010). "Guidelines for treatment of autoimmune neuromuscular transmission disorders." **17**(7): 893-902.
- Wong, S. H., S. Huda, A. Vincent and G. T. Plant (2014). "Ocular myasthenia gravis: controversies and updates." Curr Neurol Neurosci Rep **14**(1): 421.
- Zhou, Y., H. J. Kaminski, B. Gong, G. Cheng, J. M. Feuerman and L. Kusner (2014). "RNA expression analysis of passive transfer myasthenia supports extraocular muscle as a unique immunological environment." Invest. Ophthalmol. Vis. Sci. **55**(7): 4348-4359.

## Chapter 1: Myasthenic ophthalmoparesis: time to resolution after initiating immune therapies

### Abstract

**Introduction:** Although immune therapies such as prednisone are effective in treating weakness in myasthenia gravis (MG), their effect on the resolution of myasthenic-induced persistent ophthalmoparesis is unknown. **Methods:** MG patients were observed during their first year of immune therapies and ophthalmoplegia scores and drug doses were documented. **Results:** Of seventy-six cases with persistent ophthalmoparesis on immune therapies, the median time to resolution of ophthalmoparesis was 7 months and 37% resolved within 3 months. Those starting therapy within 12 months of symptom onset were twice as likely to have resolution in the first year ( $p=0.028$ ). Resolution of ophthalmoparesis within 3 months, compared to later, was associated with higher initial prednisone doses (mean 0.5 vs. 0.3 mg/kg/day;  $p = 0.014$ ). Although 25% of the higher-dose group also received intravenous immunoglobulin or plasma exchange, the trend remained after their exclusion. **Conclusion:** While a third of cases with myasthenic-ophthalmoparesis resolved within 3 months of immunotherapy, more aggressive immunotherapy in this period correlated with improved responses.

Reference: Europa, T. A., et al. (2018). "Myasthenic ophthalmoparesis: Time to resolution after initiating immune therapies." Muscle Nerve 58(4): 542-549.

## 1. Introduction

Ocular manifestations in myasthenia gravis (MG) occur frequently and early in the course of disease. The extraocular muscles (EOMs) may manifest fatigable or persistent weakness, resulting in symptoms of diplopia and/or ptosis. Approximately half of MG cases who develop EOM weakness (ophthalmoparesis), develop generalized MG within two years of onset of symptoms (Grob, Brunner et al. 1981).

Previous clinical observational data in MG cases reporting EOM responses to immune therapies are sparse. The available evidence from a few reports suggests that ocular manifestations of MG frequently improve in response to immune therapies (Kupersmith and Ying 2005, Benatar, McDermott et al. 2016). In a cohort of myasthenic patients treated with low doses of prednisone (mean dose = 20 mg daily) and using the visual subscores of the quantified MG (QMG) score, (Jaretzki, Barohn et al. 2000) reflecting outcomes related to fatigable diplopia and ptosis, 3 of 27 cases (11%) with ocular manifestations of MG resolved in 2 months (Bhanushali, Wu et al. 2008). A small, but blinded randomized trial using prednisone, found 5 of 6 (83%) of cases with ocular manifestations of MG achieved resolution of their symptoms at a median of 14 weeks with a prednisone dose of 15 mg/day, although only half of the cases had severe visual QMG subscores which would be comparable to the cases of interest in this study with persistent ophthalmoparesis rather than fatigable weakness (Benatar, McDermott et al. 2016).

However, in South Africa (Heckmann and Nel 2017) and internationally (Oosterhuis and Bethlem 1973, Wong, Huda et al. 2014), it has been recognised that some individuals with MG may have ocular symptoms that do not respond to immune therapies. For research purposes, the ophthalmoplegic subphenotype of myasthenia gravis was previously defined by the recognition of severe cases with persistent and significant weakness of  $\geq 6$  (of 12) EOMs and/or levator palpebrae superioris despite at least two years of standard immune therapies (Heckmann and Nel 2017). The development of treatment-resistance however, may occur earlier in the course of the disease. We were therefore interested in the early identification of susceptible individuals with MG who may develop the ophthalmoplegic subphenotype. Ocular manifestations of MG were documented in a cohort of myasthenia gravis cases, mostly with persistent ophthalmoparesis rather than fatigable weakness, in their first year of treatment to evaluate responses to standard immune therapies.

## Aims:

1. To determine by analysis of clinical observational data, how quickly patients with MG-associated ophthalmoparesis responded to immunotherapy in the first year of treatment using our standard clinic protocol.
2. To identify clinical predictors for persistent ophthalmoparesis.

## 2. Methods

### 2.1. Patient selection

Clinical observations were recorded on consecutive patients diagnosed with MG at the Myasthenia Clinic at Groote Schuur Hospital in Cape Town, South Africa between 2007 and 2017. Patients were excluded if they had previously been treated with prednisone or another immunosuppressive agent prior to their first study examination or had laboratory-based evidence of uncontrolled concomitant disease such as thyroid disease, diabetes, or HIV-infection. In addition, only those patients who could attend at least one follow-up consultation at our clinic, were included in the study.

### 2.2. Diagnostic criteria for MG

MG was diagnosed by a suggestive history, demonstration of fatigable weakness on clinical examination and at least one of the following: response to acetylcholinesterase inhibitors (intramuscular or oral), the presence of circulating acetylcholine receptor (AChR) or muscle kinase (MuSK) antibodies, a decremental response (>10%) to 3Hz repetitive nerve stimulation, and/or a positive response to immune therapies. Participants were examined by the same experienced neurologist (JMH) using a standardized template.

### 2.3. Ophthalmoplegia score

Clinical data was recorded using a standardized template and examinations were performed by the same neurologist at each visit (JMH). MG scores such as the QMG score, grade fatigable diplopia but in this study, we were interested in patients with immediate and persistent weakness of one or more EOMs, which would get the maximum penalty. Patients with a suggestive history and examination were therefore scored using the ophthalmoplegia score (Vivian and Morris 1993, Heckmann, Owen et al. 2007, Cleary, Williams et al. 2008) at their first visit, although the other criteria for MG diagnostic confirmation were only fulfilled at a later date when the test results and/or treatment responses were available. The ophthalmoplegia score allowed for systematic recording of weakness of each EOM at each

clinic visit. Briefly, ophthalmoparesis was assessed for each EOM and scored between mild weakness (25% limitation) and severe weakness (100% limitation) (see Fig. 1).

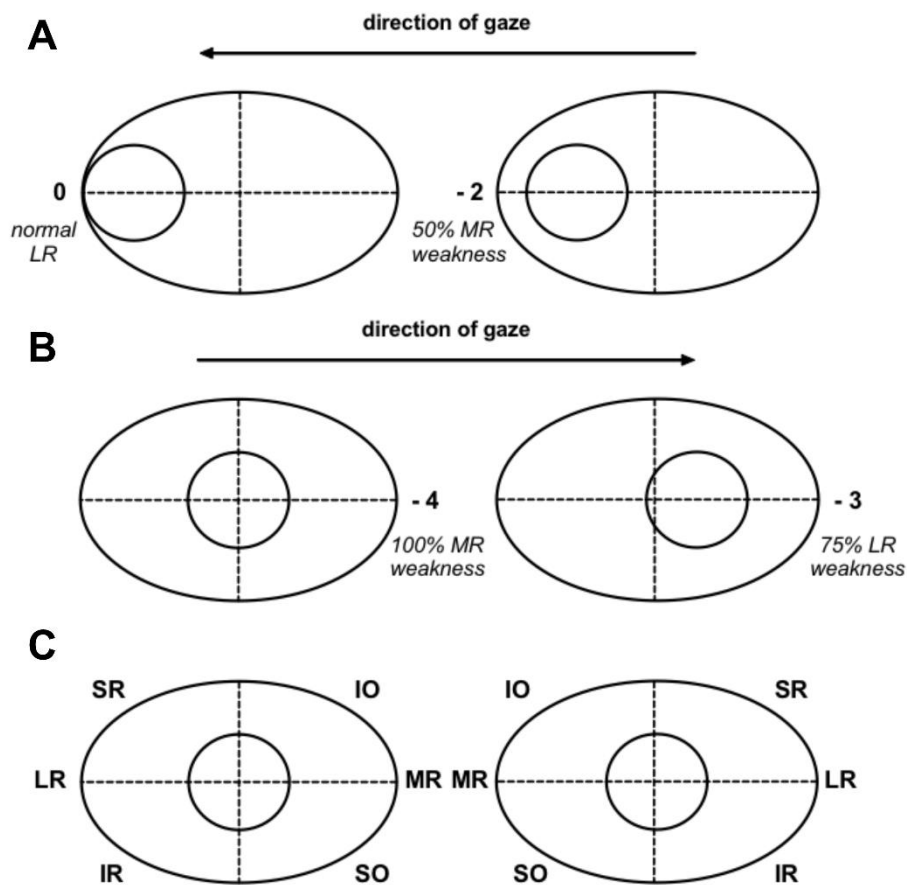


Figure 1: A schematic to illustrate the ophthalmoplegia score (Vivian and Morris 1993). A. Weakness of the left medial rectus (MR) on right gaze. B. Weakness of the right medial rectus and left lateral rectus (LR) on left gaze. C. All twelve extraocular muscles are assessed individually. Superior rectus (SR); inferior oblique (IO); inferior rectus (IR); superior oblique (SO).

#### 2.4. MG treatment protocol

Patients were treated according to the standard clinic protocol, which is comparable to international treatment protocols for MG (Heckmann, Owen et al. 2007, Benatar, McDermott et al. 2016, Huda, Woodhall et al. 2016, Wolfe, Kaminski et al. 2016). After the initial diagnosis of MG, based on history and examination findings and positive response to anticholinesterase therapy, immune therapies were initiated within a few days if the patient remained symptomatic on anticholinesterase therapy alone. Prednisone was started at doses of 15-20 mg daily and titrated upwards as needed over several weeks to a maximum of 1 mg/kg for cases with generalized myasthenia gravis and lower for those with ocular manifestations only, until the patients' symptoms resolved, or steroid-related side effects limited the dose. Non-

steroid immunosuppressive therapies were started soon after prednisone in generalized myasthenia gravis cases, and in those with ocular manifestations when prednisone therapy was required for more than a few weeks. Non-steroid immunosuppressive therapies were started earlier if prednisone was contraindicated. Azathioprine and methotrexate were most frequently used (Heckmann, Lambson et al. 2005, Heckmann, Rawoot et al. 2011). Four patients were enrolled into the MG thymectomy trial (not randomized to surgery), and did not receive steroid-sparing agents as per protocol (Wolfe, Kaminski et al. 2016). Exact doses of prednisone (mg/kg/day) and steroid-sparing agents were recorded at each visit. Rescue therapies including intravenous immunoglobulin (IVIg) or plasma exchange for severe generalized symptoms (MGFA grade IVB or V) were also recorded.

### 2.5. Ethics approval

Ethics approval for this study analysis was obtained from the University of Cape Town's Health Sciences Faculty research ethics committee (HREC 257/2012).

### 2.6. Data collection

The overall severity of symptoms was graded using the MG Foundation of America (MGFA) classification (Jaretzki, Barohn et al. 2000) and ophthalmoparesis was graded using the ophthalmoplegia score. Patients who demonstrated symptoms of extraocular muscle weakness only with sustained gaze (i.e., fatigability), scored 0. Ptosis was graded independently for each eye with the patient in a seated position and with the head maintained in a neutral position (Benatar, McDermott et al. 2016). A 4-point grading system was used and maximum degree of ptosis was recorded, seen either spontaneously or soon after upgaze (<10 seconds) (Benatar, McDermott et al. 2016).

### 2.7. Statistical analysis

Raw data were entered into Microsoft Excel. Statistical analysis was completed using Prism Graphpad 7 (GraphPad Software, La Jolla, CA), IBM SPSS 24 (IBM, Armonk, NY) and EZR (Kanda 2013). Normally distributed continuous variables were presented as the mean with standard deviation (SD) and comparisons between continuous variables were performed using student's t-tests (2 groups, 2-tailed) or one-way ANOVA ( $\geq 3$  groups). Non-parametric data were presented as the median with interquartile ranges and compared using Mann-Whitney U or Kruskal-Wallis tests. Categorical data was analysed using Fisher's exact test (2 groups) or the  $\chi^2$  test ( $\geq 3$  groups). Statistical significance was set at  $p < 0.05$ .

### 2.8. Kaplan Meier analysis

Kaplan Meier analyses were used to determine the influence of single dependent variables on the clinical outcome of resolution of ophthalmoparesis. Cases with complete resolution of persistent ophthalmoparesis (although they may have had residual fatigable weakness), were considered as having a successful outcome, while those not achieving this outcome in the treatment period of 12 (+2) months were censored in the survival analyses. Kaplan Meier graphs were generated in Prism Graphpad. and compared using the Log rank and Gehan-Breslow-Wilcoxon tests. We evaluated the following patient characteristics as predictors for resolution of ophthalmoparesis: age ( $\leq 45$  years), sex (men), race (African-genetic ancestry), delay to diagnosis/ treatment initiation ( $< 12$  months), positive AChR-ab assay and generalized MG. Patients self-identified their race as per South African racial census categories (Black-, mixed-African-, (Heckmann and Nel 2017) White/European- and Indian-genetic ancestry). For the analysis, we grouped race into two groups, viz. African-genetic ancestry (Black and mixed-African-genetic ancestry) and non-African-genetic ancestry (European- and Indian-genetic ancestry). This binary classification was necessary for two reasons; a) we previously identified African-genetic ancestry to be associated with the treatment-resistant ophthalmoplegic subphenotype and b) small sub-sample sizes. The effect of variables on the resolution of ophthalmoparesis was reported as the 'resolution ratio' (RsR) instead of the 'hazard ratio' with 95% confidence interval (CI).

### 2.9. Multivariate analysis

Cox regression analyses were performed using SPSS to evaluate the influence of multiple variables on the clinical outcome (resolution of ophthalmoparesis). Multiple models were tested, and the "best fit" model was presented. The proportional 'hazards' assumption was tested by analysis of the Schoenfeld residuals.

## 3. Results

### 3.1. Cohort characteristics

After 176 patients were excluded, the cohort comprised 87 MG patients, who had either persistent ophthalmoplegia and/or ptosis (see Fig. 1). Thirteen patients presented with ocular manifestations only (OM) and 74 with additional evidence of generalized MG (GMG) (Table 1). MG was diagnosed by a positive response to anticholinesterase therapy, albeit incomplete for the ocular manifestations. The diagnosis was supported by detecting either AChR-abs (n=58) or MuSK-abs (n=8) in the sera, or abnormal electrophysiology (decremental response n=5 or increased jitter n=4) in those without detectable circulating antibodies.

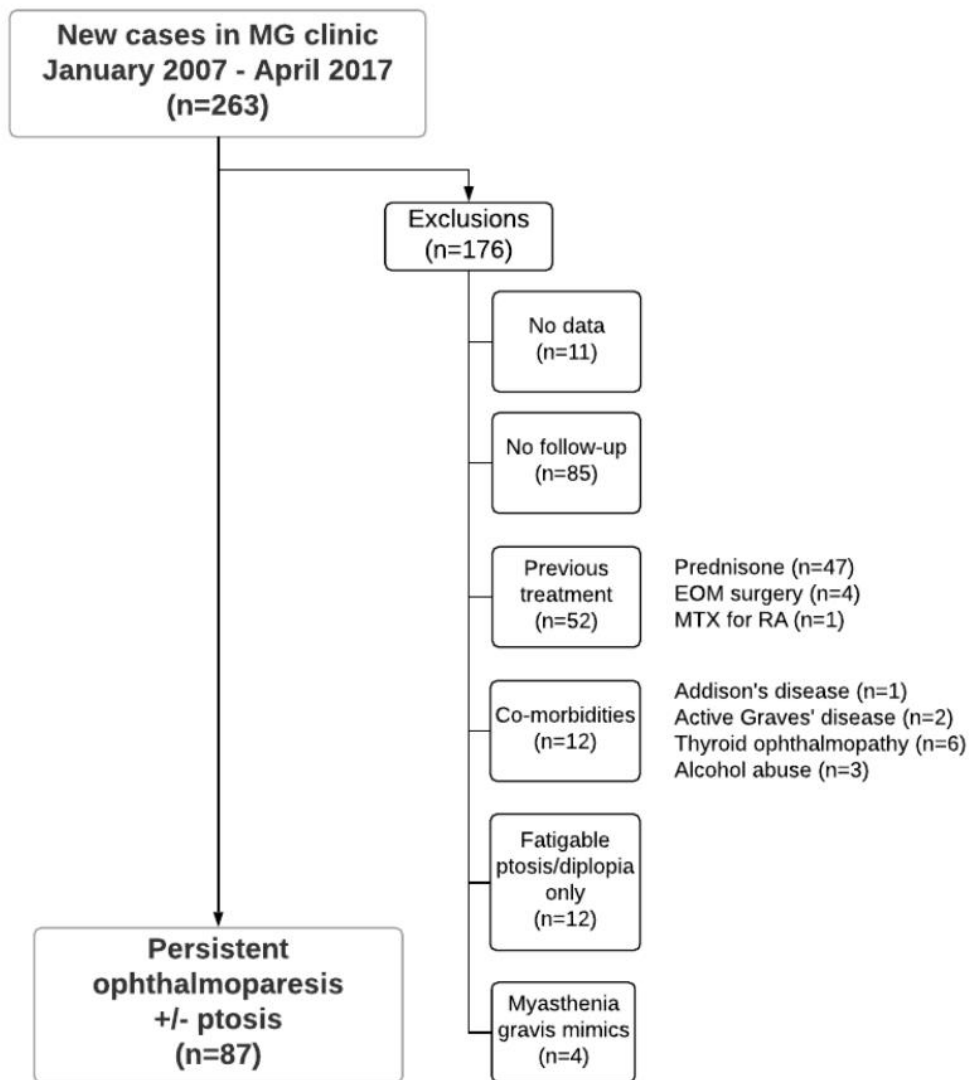


Figure 2. Flow diagram of patients included in the study observations and the reasons for exclusion from further analysis. Extraocular muscle (EOM); myasthenia gravis (MG); methotrexate (MTX); rheumatoid arthritis (RA).

**Table 1: Demographic and clinical characteristics of the cohort at baseline**

	Ocular manifestations n = 13	Generalized MG n = 74	p value
Median age (IQR)	56 (42; 63)	34 (24; 52)	<b>0.006*</b>
Men (%)	8 (61.5%)	21 (28.4)	<b>0.002†</b>
Genetic ancestry: African	5 (38.5)	60 (81.1)	<b>0.003†</b>
Time to therapy, months median (IQR)	3.6 (1.8; 24)	10.8 (4.0; 24)	0.41*
AChR-ab positive, n (%)	8 (61.5)‡	52 (70.3)	>0.53†
<u>Stable comorbid disease</u>			
HIV-positive, n (%)	0	4 (5.4)	>0.99†
Thyroid disease, n (%)	3 (23.1)	12 (16.2)	>0.70†
Diabetes mellitus, n (%)	1 (7.1%)	5 (5.4%)	>0.58†
<u>Ptosis severity, n (%)</u>			
Mild persistent ptosis (≥ 25%)	6 (46.2)	25 (33.8)	0.65†
Severe persistent ptosis (≥ 50%)	7 (53.8)	49 (66.2)	
<u>Ophthalmoparesis severity</u>			
No. EOM ≥25% weakness, median (IQR)	5 (5: 10)	7 (3:11)	0.39*
No. EOM ≥50% weakness, median (IQR)	4 (2:10)	6 (4:10)	0.06*

Table 1. \*Mann-Whitney U test, †Fisher's exact test, ‡4/8 OM with AChR-abs transformed into generalized MG during the observation period. Ocular manifestations of myasthenia refers to persistent signs confined to the extraocular muscles; Time to therapy refers to the delay between onset of MG symptoms and the initiation of immunotherapies; No. refers to number of extraocular muscles (EOMs); AChR-ab: Acetylcholine receptor antibody; IQR: Interquartile range; HIV: Human immunodeficiency virus. Those with a history of thyroid disease were euthyroid on treatment, those with pre-existing diabetes mellitus were well-controlled on treatment and those known with HIV-infection were on effective antiretroviral therapy (viral loads <20 RNA copies/ml). Bold text indicates statistically significant results.

Patients presenting with OM were older and more frequently men with European-genetic ancestry. The median delay from MG symptoms onset to initiation of immune therapies was 10.8 months (IQR 3.6; 24), and similar in OM and GMG. However, men were 3.5 times more likely to have an early diagnosis (<12 months) ( $p = 0.013$ ) and this was independent of age, race or whether they have OM only or GMG ( $p = 0.002$ ).

Prior to initiation of immune therapies, 94% of the cohort had persistent ptosis of which the ptosis was bilateral in 63% of cases. At least one EOM showed persistent weakness in 87%

of the cohort. The median number of EOMs affected in the OM (n=5 EOMs) and GMG (n=7 EOMs) groups were similar, although there was a trend towards more EOMs having moderate to severe weakness among those with GMG ( $p=0.06$ ; Table 1). Seventeen patients had persistent weakness of all 12 EOMs, of whom 82% had GMG ( $p = 0.53$ ).

### 3.2. Immunosuppressive treatment

Although all patients had a minimum of two visits within 3 months, 94% had  $\geq 6$  months of follow-up and 84% having 12-14 months of follow-up data. Eleven patients had their last visit at 13-14 months and the follow-up period was therefore extended to include this information. All patients with persistent ophthalmoparesis or ptosis, except five, were started on prednisone within days of diagnosis. The reasons for not using prednisone, but instead starting non-steroid immunotherapies (indicated in brackets), included two patients with MGFA grade I or II and diabetes mellitus (methotrexate), one patient (MGFA grade IIB) elected not to use prednisone (azathioprine), and two patients with MGFA grade IVB disease developed neuropsychiatric symptoms within days of starting prednisone which was then stopped (azathioprine + IVIg and mycophenolate mofetil + plasma exchange, respectively). A non-steroid immunosuppressive therapy was introduced in 59 of the 76 cases of ophthalmoparesis usually shortly after the prednisone initiation and 11 required either IVIg or plasma exchange for MGFA grade IVB or V in the first 3 months (Table 2). The doses of immunotherapies, calculated per patient according to their weight and per day (for prednisone and azathioprine), are summarized as the mean dose for the treatment period specified (Table 2).

Table 2. Immunosuppressive doses used in the treatment intervals

Time periods	Pred only	Pred+AZA	Pred+MTX	Other
0–3 months, n	24	33	24	2*
Pred, mg/kg	0.34 (0.15) <sup>†</sup>	0.38 (0.26;0.46) <sup>‡</sup>	0.37 (0.24;0.47) <sup>‡</sup>	
NSIT, mg/kg <sup>§</sup>	ND	1.83 (0.56) <sup>†</sup>	15 (12.5;15) <sup>‡</sup>	
Rescue therapies: 1–3 months, n <sup>#</sup>	ND	6	3	2
Pred adverse effects, n (%)	1 (9)	5 (15)	4 (17)	1
3-6 months, n	15	33	32	2
Pred, mg/kg	0.34 (0.19) <sup>†</sup>	0.35 (0.17) <sup>†</sup>	0.35 (0.18) <sup>†</sup>	0.13
NSIT <sup>§</sup>	ND	2.05 (0.56) <sup>†</sup> (mg/kg)	15 (12.5;17.5) <sup>‡</sup> (mg weekly)	
6-12 months, n	6	32	36	2
Pred, mg/kg	0.43 (0.26)	0.22 (0.13) <sup>†</sup>	0.24 (0.16) <sup>†</sup>	ND
NSIT <sup>§</sup>	ND	2.00 (0.53) <sup>†</sup> (mg/kg)	15 (15;17.5) <sup>‡</sup> (mg weekly)	ND

No data (ND); azathioprine (AZA), dose reflected as mg/kg daily; interquartile range (IQR); intravenous immunoglobulin (IVIg); Myasthenia Gravis Foundation of America (MGF); methotrexate (MTX, dose reflected as mg weekly); nonsteroid immunosuppressive therapy (NSIT); plasma exchange (PLEX); prednisone (Pred). \*These 2 patients received cyclosporine (100mg twice daily) and mycophenolate mofetil (1,000mg twice daily) and IVIg or PLEX at each time interval. The patients in the other groups did not receive rescue therapy after the 3-month interval. Few patients who received AZA (n=4)/MTX (n=2) in the 3–6-mo period did not receive prednisone. <sup>†</sup>Mean ( $\pm$ SD). <sup>‡</sup>Median (IQR). <sup>§</sup>Patients who started NSITs after 2 months are not reflected in the 0–3 month interval. <sup>#</sup>Rescue therapy refers to IVIg or PLEX for MGFA grade 4 or 5.

### 3.3. Resolution of ophthalmoparesis

Of the 76 patients with persistent ophthalmoparesis, 59% had complete resolution of ophthalmoparesis within 12 (+2) months of immunosuppressive treatment (Fig. 3). Patients with fewer EOMs affected (1 – 5 EOMs), were more likely to have resolution of symptoms in the first year of treatment as opposed to those with 6 or more EOMs affected (odds ratio 3.6, CI: 1.3 – 9.1; p = 0.017). Of the 17 with complete ophthalmoparesis at baseline (12 EOMs  $\geq$

25% weakness), 47% had complete resolution of symptoms within the study period, 29% showed a reduction in the number of EOMs with persistent weakness albeit not complete resolution, and 24% had persistent, complete ophthalmoparesis for 12-14 months, although one was lost to follow up at 4 months.

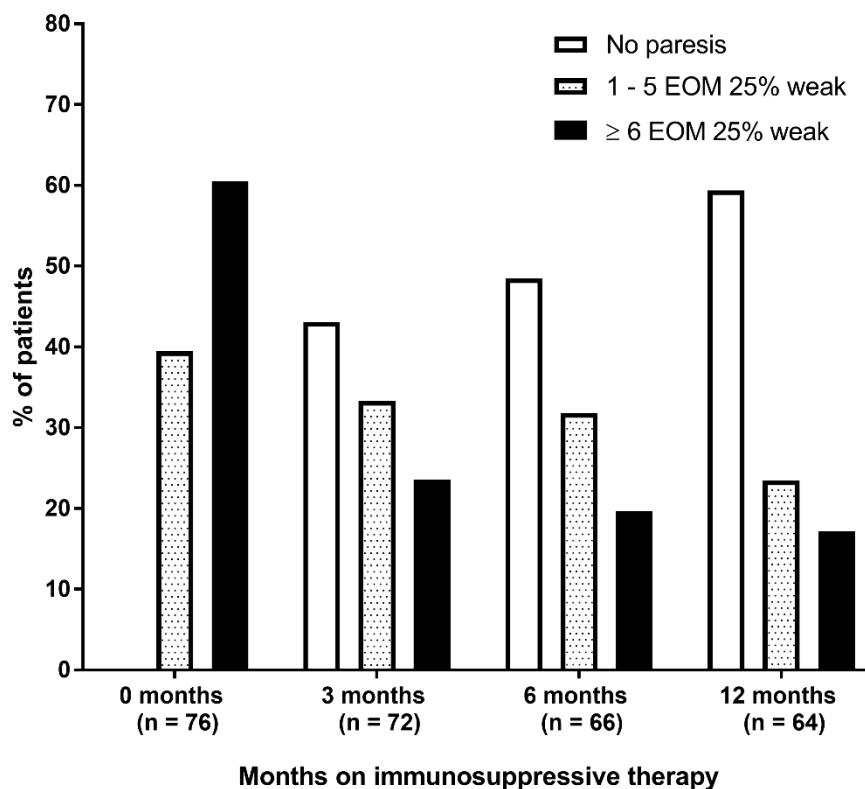


Figure 3. Histogram of the proportions of patients with ophthalmoparesis, and the number of weak extraocular muscles, over the treatment period. “No paresis” refers to patients with either normal extraocular muscle function or those that show fatigable weakness or diplopia only. “1-5 EOMs 25% weak” refers to at least mild weakness of one to five EOMs and “≥ 6 EOMs 25% weak” refers to at least mild weakness of six to twelve EOMs. Four patients had their second clinic visit after 3 months, therefore, the bar at 3 months represents a percentage of the 72 patients who had 2 clinic visits in this period.

The median time to resolution in the overall study cohort, as determined by Kaplan Meier analysis, was 7 months after initiation of immune therapies. At 3 months, 37% showed complete resolution of their ophthalmoparesis. There was no clear discrepancy between responsiveness of treatment of the extraocular muscles vs the non-ocular muscles although this was not the primary focus of this study. Figure 4A shows that patients with ophthalmoparesis who were started on treatment within 12 months of symptom onset (early treatment group), had twice the chance of complete resolution of ophthalmoparesis when compared to those in whom the diagnosis/ initiation of immune therapies was delayed for >

12 (delayed treatment group) ( $p = 0.028$ ). The median time to resolution for the early-treatment group was 4 months compared to 14 months for the group with delayed treatment. Patients with ophthalmoparesis who were AChR-ab positive improved more quickly than the AChR-ab negative group (median resolution time 5 vs 13 months, respectively (Fig. 4B;  $p = 0.020$ ). Ophthalmoparesis in patients  $\leq 45$  years tended to respond more quickly than older patients (median time 4 months vs 12 months, respectively,  $p = 0.095$ ) (Fig. 4C), but there was no significant difference between those with generalized MG and those with ocular manifestations only (Fig. 4D,  $p = 0.31$ ). The Kaplan Meier curves for men and women were similar (not shown,  $p = 0.43$ ).

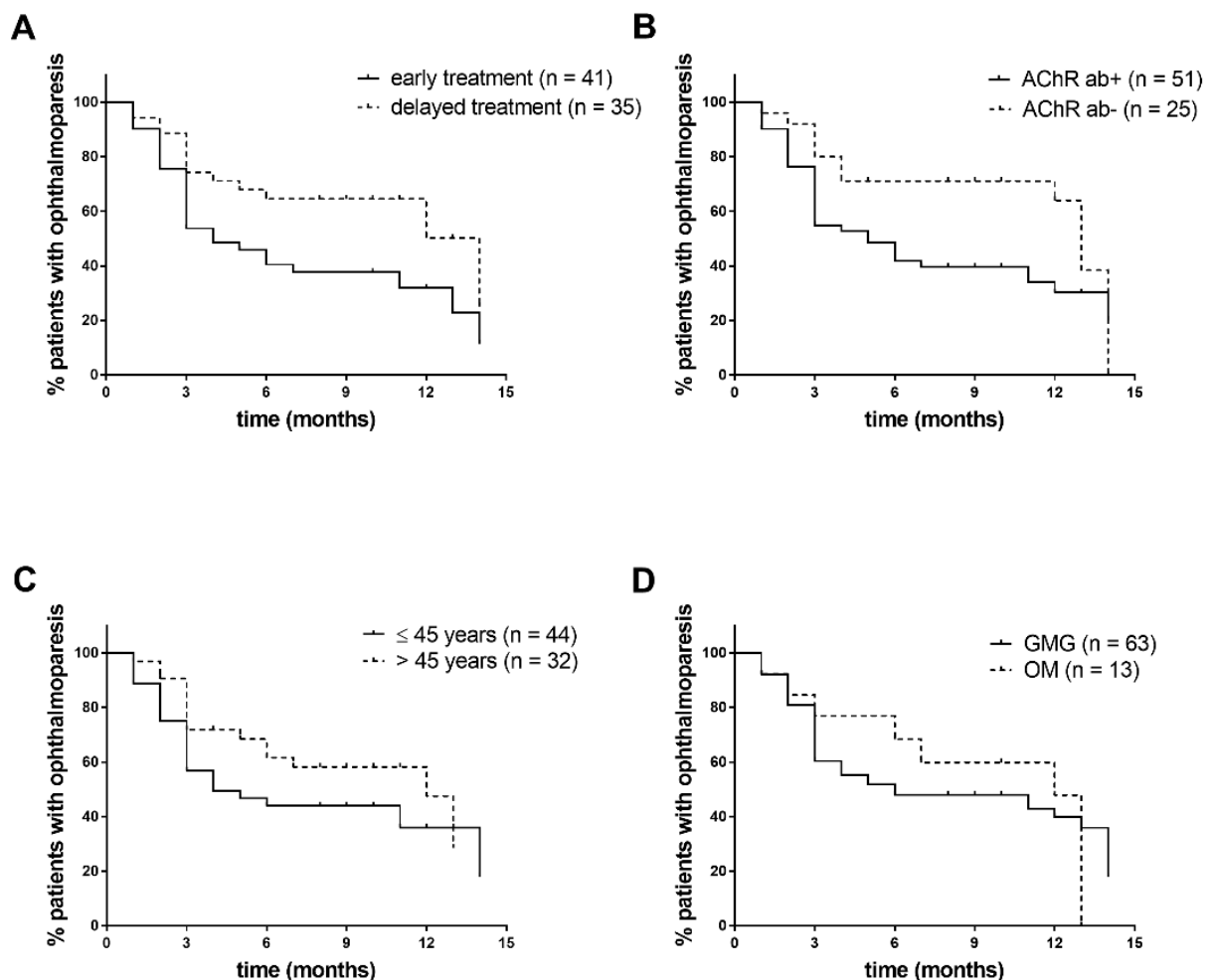


Figure 4. Kaplan Meier curves illustrating the resolution of ophthalmoparesis in the cohort with strata for the variables of interest. Resolution ratio (RsR); 95% confidence interval is shown in brackets. A. RsR 2.0 (1.1; 3.8),  $p = 0.028$ . B. RsR 1.9 (1.0; 3.4),  $p = 0.020$ . C. RsR 1.4 (0.8; 2.7),  $p = 0.095$ . D. RsR 1.2, (0.5; 2.7),  $p = 0.37$ .

Because the previously described treatment-resistant ophthalmoplegic MG subphenotype showed racial bias, and more frequently occurred among those developing MG before the age of 20 (Heckmann, Owen et al. 2007, Heckmann, Hansen et al. 2012, Heckmann 2017, Heckmann and Nel 2017), we were interested in whether race and age would predict treatment responses of ophthalmoparesis in this cohort of newly-diagnosed MG patients. There were only 10 cases with symptom onset before age 20 (median age 17; IQR 16:18), all of whom had African-genetic ancestry and generalized MG. In this group, the severity of persistent ophthalmoparesis prior to immunosuppressive therapy was similar to the rest of the cohort (median number of EOMs 25% weak = 9; median EOMs 50% weak = 6). Nine of the patients with juvenile-onset MG completed 12 months follow-up. Five showed complete resolution of ophthalmoparesis in a similar time to the other age groups, whereas four remained with persistent ophthalmoparesis at 12 months. This juvenile sub-sample was too small to draw meaningful conclusions.

A Cox regression was performed to assess the collective influence of the respective variables on the RsR (Table 3). A multivariate analysis (model 1) including all the variables of interest showed interaction between the variables that nullified the influence of sex and race (73% of those with African-genetic ancestry were <45 years old at symptom onset). A second multivariate model is also presented, including only factors that contributed to the model as based on their Wald coefficients and RsR values, i.e. early immunotherapy, positive AChR antibody assay and age  $\leq$  45 years. Initiation of immunotherapy <12 months from symptom onset shows the strongest association with resolution of ophthalmoparesis and is relatively independent from the other variables in both multivariate models.

**Table 3: Multivariate analysis to identify collective influences on the resolution of ophthalmoparesis**

	Univariate analysis		Multivariate analysis			
			Model 1		Model 2	
	RsR (95% CI)	P value	RsR (95% CI)	P value	RsR (95% CI)	P value
Immunotherapy <12 months of symptom onset	1.92 (1.03; 3.58)	<b>0.039</b>	1.86 (0.95; 3.66)	0.07	1.80 (0.95; 3.39)	<b>0.07</b>
AChR-ab positive	1.87 (0.94; 3.69)	0.07	1.60 (0.78; 3.27)	0.20	1.56 (0.77; 3.15)	0.21
Age ≤ 45 years	1.39 (0.75; 2.56)	0.29	1.43 (0.65; 3.14)	0.37	1.36 (0.73; 2.53)	0.33
Generalized MG	1.18 (0.52; 2.66)	0.69	1.02 (0.38; 2.78)	0.97	-	-
Male sex	1.21 (0.66; 2.21)	0.54	0.92 (0.47; 1.79)	0.80	-	-
African-genetic ancestry	1.34 (0.68; 2.65)	0.40	0.89 (0.34; 2.35)	0.81	-	-

Table 3. Resolution ratio (RsR). 95% confidence interval is shown in brackets. Acetylcholine receptor antibody (AChR-ab). Statistically significant results are shown in bold.

*Prednisone dosing and resolution of ophthalmoparesis:* Resolution of ophthalmoparesis within the first 3 months of starting immunosuppressive therapies (n=28), compared to resolution between 4 to 14 months (n=17), was associated with higher mean prednisone dose in the first 3 months (mean 0.45 mg/kg/day, SD ± 0.22 vs. 0.29, SD ± 0.18; p = 0.014). However, 25% of the higher dose group also received rescue therapies (IVIg/plasma exchange)(Fig. 5). Nevertheless, if patients who received rescue therapies in the first 3 months (n=8) were excluded, there remained a trend towards higher prednisone dosing in the early ophthalmoparesis resolution group compared to the later resolution group (mean =0.38 mg/kg/day vs 0.29 respectively; p=0.116).

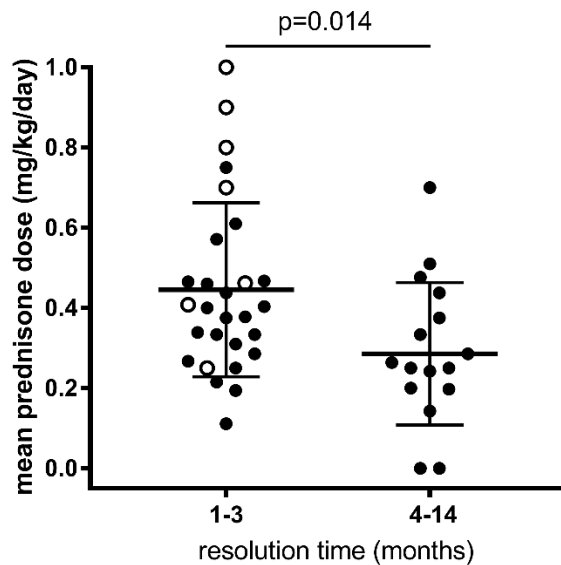


Figure 5: Grouped comparisons of the mean prednisone doses in the first 3 months in those who showed resolution of ophthalmoparesis (n=28) within 3 months compared to those showing resolution within 4-14 months (n=17). The open circles represent those who also received either IVIg or plasma exchange as rescue therapies in the first 3 months; after excluding these individuals a trend remained towards higher doses of prednisone in the early resolution group compared to the later group (mean =0.38 mg/kg/day, SD  $\pm$  0.15 vs 0.29, SD  $\pm$ 0.18 respectively; p=0.116).

*Resolution of ophthalmoparesis in patients with comorbidities.* Of the five diabetic patients (all >60 years), only one showed resolution of ophthalmoparesis in the study period. However, other factors may have played a role as not all were treated with prednisone. Eleven patients with ophthalmoparesis and stable thyroid disease on therapy showed a similar rate of resolution of ophthalmoparesis compared to those without thyroid disease. Three HIV-positive patients had ophthalmoparesis at baseline. They all required immunotherapy for generalized MG within the first year of symptoms but only one had resolution of ophthalmoparesis in the study period.

*Ptosis and responses to prednisone:* Of the 82 patients with ptosis at baseline, 58 had resolution of ptosis, of whom 43 (74%) had resolution within the first 3 months of immunosuppressive therapy while 15 (26%) had resolution between 4-14 months. Ptosis completely resolved in 85% of patients with mild/grade 1 ptosis, while the percentage of patients with resolution of grades 2, 3 and 4 were 72%, 63% and 38% respectively, which

suggests that more severe ptosis takes longer to improve. The mean prednisone dose of the group with earlier resolution of ptosis was significantly higher than those who had later resolution of ptosis (0.40 vs. 0.30 mg/kg/day respectively,  $p = 0.030$ ), but some of these patients overlap with the cases who also received IVIg/plasma exchange).

*Conversion of ocular manifestations to generalized MG.* Over the follow-up period, four (31%) OM cases developed generalized MG; three developed generalized disease in the first month of starting prednisone treatment and one relapsed with generalized and bulbar symptoms after cessation of treatment subsequent to remission at 3 months. Of the remaining nine OM cases with a mean follow-up of 9 months, four remained on low doses of prednisone and four were in clinical remission without therapy.

#### 4. Discussion

Ocular manifestations of MG frequently cause substantial functional disability and requires immune therapies (Benatar, McDermott et al. 2016). At the initial presentation, patients and clinicians question how quickly improvement in ocular symptoms is to be expected after starting prednisone, and which factors may impact on the resolution of extraocular muscle weakness. In this observational study, documenting myasthenic ophthalmoparesis in a group of newly diagnosed and mostly generalized MG patients for at least 3 months after starting immunosuppressive therapy, we found that the most important predictor of early resolution of persistent ophthalmoparesis was the initiation of steroid therapy within 12 months of symptom onset. A third of the cohort showed resolution of ophthalmoparesis within 3 months and 50% at 7 months. Those exposed to more aggressive immunotherapy, such as higher prednisone doses ( $\pm$  IVIg or plasma exchange as rescue therapy) showed quicker resolution of persistent ophthalmoparesis and ptosis.

Steroid doses in patients with ocular manifestations of MG are still debated amongst experts internationally (Wong, Huda et al. 2014, Narayanaswami, Sanders et al. 2021). The only double-blind randomized trial in OM showed that half the patients treated with  $\approx 0.2$  mg/kg/day had resolution of ocular symptoms by 14 weeks, but the study sample comprised few cases and most had fatigable diplopia as opposed to persistent ophthalmoparesis (Benatar, McDermott et al. 2016). Steroid doses have been considered with some caution by neurologists due to the risk of clinical deterioration following steroid initiation at high doses (Drachman 1994, Wolfe, Kaminski et al. 2016). However, ophthalmologists have used a different strategy with rapid escalation of prednisone doses over a week, approaching 0.9 mg/kg/day (Wong, Huda et al. 2014). Extrapolating dosing over the first 4 weeks as reported by Kupersmith *et al.* (Kupersmith and Ying 2005) and others (Wong, Huda et al. 2014), the average 70 kg patient with OM is exposed to a mean of 0.66 mg/kg/day prednisone over the first 4 weeks. In a retrospective study, two-thirds of cases showed resolution of 'ocular muscle dysfunction' after 4 weeks using high doses (Kupersmith and Ying 2005). In this study, we used a dosing regimen similar to other multi-centered randomized MG studies (Benatar, McDermott et al. 2016, Wolfe, Kaminski et al. 2016). Those with more severe generalized disease received more rapid escalation of prednisone with/without other rapidly acting rescue therapies such as IVIg and plasma exchange (Gajdos, Chevret et al. 2012) and appeared to have quicker resolution of ophthalmoparesis. Doses of non-steroid immunosuppressive therapies were similar and these agents would not be expected to have induced immunosuppression within the first 3 months (Palace, Newsom-Davis et al. 1998, Heckmann, Rawoot et al. 2011).

Based on the 'complement hypothesis' (Soltys, Gong et al. 2008) which suggests that EOMs are particularly vulnerable to the complement-mediated attack triggered by MG, and previous in-vitro work in which we showed that prednisone, in the presence of MG sera, repressed the expression of a critical complement regulating protein, muscle decay accelerating factor (DAF) (Auret, Abrahams et al. 2014), prednisone dosing was practiced with caution in the clinical MG setting where the emphasis was on treating EOMs dysfunction. However, the results of this observational study suggest that we need to re-consider this assumption. Although  $\approx 20\%$  of our cohort, remained with persistent treatment-resistant ophthalmoparesis after 1 year of immunosuppressive therapies, and without a specific biomarker to determine who is at risk and whether prednisone influences this risk, using higher prednisone dosing in the first 3 months appeared to have improved the chances of early resolution of severe myasthenic ophthalmoparesis for the remainder of the group. Half of the patients with juvenile-onset MG had resolution of ophthalmoparesis, but this sample was too small to assess whether they should be treated differently. The effects of prednisone at the EOM endplate in myasthenia is still unknown however, a study in 15 MG cases assessing the metabolomic response in sera to treatment with low doses of prednisone ( $\approx 0.29$  mg/kg/day) in the first 12 weeks, showed upregulation of membrane associated glycerophospholipids and downregulation of pro-inflammatory pathways (Sengupta, Cheema et al. 2014). Previous work has shown that the pathogenetic mechanisms underlying the ophthalmoplegic treatment-resistant MG subphenotype, may in part be due to aberrant muscle endplate membrane repair and stability, and specifically implicated gangliosphingolipid metabolism (Heckmann and Nel 2017, Nel, Jalali Sefid Dashti et al. 2017). By the end of the treatment period, a NSIT had been initiated in most cases. However, this did not appear to impact EOM weakness and the effects of these medications would not be expected to be seen in the first 3-6 months.

That we did not assess the effects of treatment on the patients' quality of life was a limitation, although we were particularly interested in responses of the EOMs to immune therapies. The association of higher prednisone doses with earlier resolution of ophthalmoparesis in this study will require further study in a randomized controlled trial to establish recommendations for treatment.

In conclusion, early initiation of immunotherapies, that is, within 12 months from onset of symptoms, is a favourable prognostic factor for resolution of myasthenic-related persistent ophthalmoparesis. Our results suggest that more aggressive immunotherapy such as higher doses of prednisone ( $\approx 0.45$  mg/kg/day) in the first 3 months (this study), which is in keeping with the doses used by neuro-ophthalmologists for ocular manifestations ( $\approx 0.66$  mg/kg/day in the first 4 weeks), (Kupersmith and Ying 2005, Wong, Huda et al. 2014) may impact positively on the resolution of persistent and severe extraocular muscle weakness in myasthenia gravis.

## References

- Auret, J., A. Abrahams, S. Prince and J. M. Heckmann (2014). "The effects of prednisone and steroid-sparing agents on decay accelerating factor (CD55) expression: implications in myasthenia gravis." Neuromuscul Disord **24**(6): 499-508.
- Benatar, M., M. P. McDermott, D. B. Sanders, G. I. Wolfe, R. J. Barohn, R. J. Nowak, M. Hehir, V. Juel, H. Katzberg, R. Tawil and G. Muscle Study (2016). "Efficacy of prednisone for the treatment of ocular myasthenia (EPITOME): A randomized, controlled trial." Muscle Nerve **53**(3): 363-369.
- Bhanushali, M. J., J. Wu and M. Benatar (2008). "Treatment of ocular symptoms in myasthenia gravis." Neurology **71**(17): 1335-1341.
- Cleary, M., G. J. Williams and R. A. Metcalfe (2008). "The pattern of extra-ocular muscle involvement in ocular myasthenia." Strabismus **16**(1): 11-18.
- Drachman, D. B. (1994). "Myasthenia gravis." N Engl J Med **330**(25): 1797-1810.
- Gajdos, P., S. Chevret and K. V. Toyka (2012). "Intravenous immunoglobulin for myasthenia gravis." Cochrane Database Syst Rev **12**: CD002277.
- Grob, D., N. G. Brunner and T. Namba (1981). "THE NATURAL COURSE OF MYASTHENIA GRAVIS AND EFFECT OF THERAPEUTIC MEASURES." Annals of the New York Academy of Sciences **377**(1): 652-669.
- Heckmann, J. M. (2017). "Juvenile myasthenia gravis." Eur J Paediatr Neurol **21**(5): 696.
- Heckmann, J. M., P. Hansen, R. Van Toorn, E. Lubbe, E. Janse van Rensburg and J. M. Wilmshurst (2012). "The characteristics of juvenile myasthenia gravis among South Africans." S. Afr. Med. J. **102**(6): 532-536.
- Heckmann, J. M., E. M. Lambson, F. Little and E. P. Owen (2005). "Thiopurine methyltransferase (TPMT) heterozygosity and enzyme activity as predictive tests for the development of azathioprine-related adverse events." J Neurol Sci **231**(1-2): 71-80.
- Heckmann, J. M. and M. Nel (2017). "A unique subphenotype of myasthenia gravis." Ann. N. Y. Acad. Sci.
- Heckmann, J. M., E. P. Owen and F. Little (2007). "Myasthenia gravis in South Africans: racial differences in clinical manifestations." Neuromuscul. Disord. **17**(11-12): 929-934.
- Heckmann, J. M., A. Rawoot, K. Bateman, R. Renison and M. Badri (2011). "A single-blinded trial of methotrexate versus azathioprine as steroid-sparing agents in generalized myasthenia gravis." BMC Neurol **11**: 97.
- Huda, S., M. R. Woodhall, A. Vincent and J. M. Heckmann (2016). "Characteristics Of acetylcholine-receptor-antibody-negative myasthenia gravis in a South African cohort." Muscle Nerve **54**(6): 1023-1029.

- Jaretzki, A., 3rd, R. J. Barohn, R. M. Ernstoff, H. J. Kaminski, J. C. Keeseey, A. S. Penn and D. B. Sanders (2000). "Myasthenia gravis: recommendations for clinical research standards. Task Force of the Medical Scientific Advisory Board of the Myasthenia Gravis Foundation of America." Neurology **55**(1): 16-23.
- Kanda, Y. (2013). "Investigation of the freely available easy-to-use software 'EZR' for medical statistics." Bone marrow transplantation **48**(3): 452-458.
- Kupersmith, M. and G. Ying (2005). "Ocular motor dysfunction and ptosis in ocular myasthenia gravis: effects of treatment." British journal of ophthalmology **89**(10): 1330-1334.
- Kupersmith, M. J. and G. Ying (2005). "Ocular motor dysfunction and ptosis in ocular myasthenia gravis: effects of treatment." Br J Ophthalmol **89**(10): 1330-1334.
- Narayanaswami, P., D. B. Sanders, G. Wolfe, M. Benatar, G. Cea, A. Evoli, N. E. Gilhus, I. Illa, N. L. Kuntz, J. Massey, A. Melms, H. Murai, M. Nicolle, J. Palace, D. Richman and J. Verschuuren (2021). "International Consensus Guidance for Management of Myasthenia Gravis." 2020 Update **96**(3): 114-122.
- Nel, M., M. Jalali Sefid Dashti, J. Gamielidien and J. M. Heckmann (2017). "Exome sequencing identifies targets in the treatment-resistant ophthalmoplegic subphenotype of myasthenia gravis." Neuromuscul Disord **27**(9): 816-825.
- Oosterhuis, H. and J. Bethlem (1973). "Neurogenic muscle involvement in myasthenia gravis. A clinical and histopathological study." J Neurol Neurosurg Psychiatry **36**(2): 244-254.
- Palace, J., J. Newsom-Davis and B. Lecky (1998). "A randomized double-blind trial of prednisolone alone or with azathioprine in myasthenia gravis. Myasthenia Gravis Study Group." Neurology **50**(6): 1778-1783.
- Sengupta, M., A. Cheema, H. J. Kaminski, L. L. Kusner and G. Muscle Study (2014). "Serum metabolomic response of myasthenia gravis patients to chronic prednisone treatment." PLoS One **9**(7): e102635.
- Soltys, J., B. Gong, H. J. Kaminski, Y. Zhou and L. L. Kusner (2008). "Extraocular muscle susceptibility to myasthenia gravis: unique immunological environment?" Ann N Y Acad Sci **1132**: 220-224.
- Vivian, A. J. and R. J. Morris (1993). "Diagrammatic representation of strabismus." Eye (Lond) **7 ( Pt 4)**: 565-571.
- Wolfe, G. I., H. J. Kaminski, I. B. Aban, G. Minisman, H. C. Kuo, A. Marx, P. Strobel, C. Mazia, J. Oger, J. G. Cea, J. M. Heckmann, A. Evoli, W. Nix, E. Cifaloni, G. Antonini, R. Witoonpanich, J. O. King, S. R. Beydoun, C. H. Chalk, A. C. Barboi, A. A. Amato, A. I. Shaibani, B. Katirji, B. R. Lecky, C. Buckley, A. Vincent, E. Dias-Tosta, H. Yoshikawa, M. Waddington-Cruz, M. T. Pulley, M. H. Rivner, A. Kostera-Pruszczyk, R. M. Pascuzzi, C. E. Jackson, G. S. Garcia Ramos, J. J. Verschuuren, J. M. Massey, J. T. Kissel, L. C. Werneck, M. Benatar, R. J. Barohn, R. Tandan, T. Mozaffar, R. Conwit, J. Odenkirchen, J. R. Sonett, A.

Jaretzki, 3rd, J. Newsom-Davis, G. R. Cutter and M. S. Group (2016). "Randomized Trial of Thymectomy in Myasthenia Gravis." N Engl J Med **375**(6): 511-522.

Wong, S. H., S. Huda, A. Vincent and G. T. Plant (2014). "Ocular myasthenia gravis: controversies and updates." Curr Neurol Neurosci Rep **14**(1): 421.

## Chapter 2: A review of the histopathological findings in myasthenia gravis: clues to the pathogenesis of treatment-resistance in extraocular muscles

### Abstract

**Introduction:** In most cases of myasthenia gravis (MG), autoantibodies initiate a complement-mediated attack on the muscle endplate. Previous research has shown that the extraocular muscles express lower levels of complement regulators such as *DAF/CD55* which may make them more susceptible to complement-mediated immune attack compared with non-ocular muscles. **Methods:** A systematic review of the peer-reviewed publications reporting histopathology in muscle biopsies of MG cases over the past 65 years was performed to determine whether histopathological changes in extraocular (EOMs) differ from non-ocular muscles. As it is known that muscles with impaired contractility undergo structural changes, and the EOMs comprise a unique muscle allotype which may manifest different structural changes to non-ocular muscles, histopathology observed in the EOMs of MG cases were compared with EOMs in strabismus. **Results:** Neurogenic changes were frequently reported in the non-ocular muscles of MG cases. Ultrastructural features of mitochondrial stress/damage were also frequent and may be more prominent in muscle-specific kinase antibody positive MG. Although paralysed EOMs in MG demonstrated prominent fibrocellular and fatty replacement and mitochondrial alterations, these features appeared commonly in paralysed EOMs of any cause. **Conclusions:** In addition to the potential increased susceptibility to complement attack, the secondary effects of poor contractility in MG may be more pronounced in EOMs. Atrophy signalling and altered mitochondrial homeostasis may be triggered, contributing to the development of treatment-resistant myasthenic ophthalmoplegia. Therefore, we propose that early strategies to improve force generation in EOMs are critical.

Reference: Europa, T. A., et al. (2019). "A review of the histopathological findings in myasthenia gravis: clues to the pathogenesis of treatment-resistance in extraocular muscles." Neuromuscul. Disord.

## 1. Introduction

In cases with the treatment-resistant ophthalmoplegic subphenotype of MG (OP-MG), the non-ocular muscles improve in response to immune therapies, while the EOMs manifest treatment-resistance (Heckmann and Nel 2017). Extraocular muscles (EOMs) are a unique muscle allotype and may be differentially susceptible to the complement-mediated attack at the muscle endplate that occurs in acetylcholine receptor positive MG (AChR-ab positive MG) due to lower expression of complement regulators such as *DAF/CD55* (Soltys, Gong et al. 2008, Heckmann, Uwimpuhwe et al. 2010). Clinical observations in myasthenia gravis (MG) cases in the first year of immune therapies showed that delayed diagnosis and initiation of treatment in MG is an unfavorable prognostic factor for MG-associated ophthalmoparesis (Chapter 1). The poorer response to therapies in the EOMs of these cases may be a consequence of disuse or ongoing complement-mediated damage at the muscle endplate in untreated MG. Rautenbach et al. observed histopathological changes in the medial rectus muscle of a case of OP-MG which showed atrophy, fibrocellular and fatty infiltrates and evidence of mitochondrial stress (Rautenbach, Pillay et al. 2017). Here, a review of histopathology reports in MG was performed, to provide clues to the molecular underpinnings of OP-MG pathogenesis and compare the effects of MG on the histopathology of EOMs and non-ocular muscles.

In brief, a systematic search of histopathology reports in MG spanning 65 years was conducted. Observations from light and electron microscopy were summarized and compared between EOMs and non-ocular muscles in MG cases. Comparisons were drawn between the different MG serotypes i.e. acetylcholine receptor (AChR) positive MG and muscle-specific kinase (MuSK) MG from reports after the discovery of radioimmunoassays. As the EOMs are a unique muscle allotype and may manifest different changes in response to prolonged inactivity compared with non-ocular muscles, several reports of histopathology in cases of strabismus were included for comparison. Although it may be expected that the pathological changes in humans with MG may be the consequence of more chronic disease than in experimental autoimmune MG (EAMG) models where the animals are sacrificed soon after the development of weakness, we have also included histopathological reports in EAMG as it may provide clues to the early muscle changes in antibody-mediated MG.

Aims:

1. To summarize the histopathology in non-ocular muscles of MG cases.
2. To compare the histopathology between AChR-MG and MuSK-MG.
3. To summarize the histopathology of EOMs in MG cases.

4. To summarize the histopathological findings in experimental autoimmune myasthenia gravis (EAMG).
5. To summarize the histopathological findings in non-MG strabismus cases to assess which pathological changes are unique to ophthalmoplegia in MG.

## 2. Methods

The NCBI Pubmed database was searched for all articles on structural changes in the muscles of patients with myasthenia gravis. Studies on myasthenia gravis (MG) as well as experimental autoimmune MG (EAMG) models in rodents were included. Search terms included “extraocular”, “ophthalmoplegia”, “muscle” and “myasthenia” in addition to “microscopy”, “histology”, “ultrastructure” “mitochondria”, “mitochondrial respiration”, “oxidative phosphorylation”, “mitochondrial dysfunction”, “COX negative fibres”, “ragged red fibres”, “citrate synthase”, “swollen mitochondria” and “oxidative stress”. Secondary manual searches were conducted on citations of articles in our primary search results.

For each report, where the information was available, we documented the age of the subjects, the muscle biopsied, severity of MG, MG serotype and the light microscopy and/or electron microscopy findings. We focused specifically on the pathological features of the muscle and not of the neuromuscular junction.

The reports were grouped according to those described prior to radio-immunoassays and those after radio-immunoassays by pathogenic serotype. One report (Nakano and Engel 1993) included a subset of patients in whom AChR antibody testing had been performed, but we have grouped these with the pre-availability of radio-immunoassays as most of the cohort were not serologically tested for AChR antibodies and their treatment program resembled the pre-assay era.

## 3. Results

In this review, we have included 25 histopathological reports on MG-associated changes in human muscles, of which 15 preceded serotyping of MG by pathogenic antibodies. Four reports were excluded as there was no accompanying English text.

- 3.1. Histopathological features of non-ocular muscles in MG prior to the era of antibody assays

These reports were published between 1953 and 1993. The muscle biopsies were mostly taken from patients aged 25 - 50 years, with variable duration of MG symptoms (3 months – 34 years) (Supplementary table 1).

Where the severity of muscle weakness at the time of biopsy was not reported, an approximation of the Osserman severity grade (in (Oosterhuis and Bethlem 1973)) was applied. As MG-associated antibodies were not assayed in this period, the cases from this period may have included patients with congenital myasthenic syndromes who had shown acetylcholinesterase inhibitor (AChEI) responsiveness. However, a substantial proportion of the cases had thymic abnormalities (thymic hyperplasia and thymoma), which is expected in 75% of MG cases (Russell 1953, Stortebecker 1955, Rowland, Hofer et al. 1956, Castleman 1966, Brownell, Oppenheimer et al. 1972, Oosterhuis and Bethlem 1973). The most recent series in this group (1993) performed AChR-antibody assays on 12 (of 30) cases, and 10/12 were positive of AChR antibodies (Nakano and Engel 1993). Three series (Russell 1953, Rowland, Hofer et al. 1956, Oosterhuis and Bethlem 1973) included post-mortem biopsies although not all cases died of MG-related complications.

#### 3.1.1. Atrophic changes in non-ocular MG muscle biopsies

Non-specific atrophic changes were consistently reported in the limb muscle biopsies of MG cases. Neurogenic atrophic changes, including grouped fibre atrophy and small angulated fibres were suspected to be a consequence of functional denervation at the motor endplate (Russell 1953, Rowland, Hofer et al. 1956, Fenichel and Shy 1963, Engel and McFarlin 1966, Bergman, Johns et al. 1971, Oosterhuis and Bethlem 1973). Fenichel (Fenichel 1966) suggested that atrophic changes with fatty replacement of muscle fibres were more frequently associated with prolonged disease duration. Muscle fibre atrophy was reported in almost half of the cases (Engel and McFarlin 1966) and mostly involved type II fibres (Russell 1953, Fenichel and Shy 1963, Engel and McFarlin 1966). Brownell *et al.* reported severe neurogenic atrophy of the tongue with fatty replacement of atrophic fibres in 2 cases after >5 years of MG symptoms (Brownell, Oppenheimer et al. 1972). It is possible that these may have been cases of MuSK-MG, as they had severe bulbar weakness with triple furrowing of the tongue and neostigmine-resistant weakness (Brownell, Oppenheimer et al. 1972); features now recognized as strongly suggestive of MuSK-MG (Farrugia, Robson et al. 2006). Architectural alterations such as myofibrillary disruption and Z-line streaming, centralization of nuclei and occasionally increased connective tissue deposition were reported (Russell 1953, Fenichel 1966).

### 3.1.2. Inflammatory infiltrates

Lymphocyte-predominant, isolated inflammatory infiltrates were described surrounding small blood vessels or rarely, degenerating muscle fibres (termed 'necrosis') (Russell 1953, Fenichel and Shy 1963, Engel and McFarlin 1966, Bergman, Johns et al. 1971, Nakano and Engel 1993). These infiltrates, termed "lymphorrhages", reported in between 23% (Engel and McFarlin 1966) and 32% (Fenichel and Shy 1963) of biopsies, were suggested to be more likely in muscle biopsies taken early in the disease process and/or prior to steroid therapy (Fenichel 1966, Nakano and Engel 1993). Beekman *et al.* associated lymphorrhages with the presence of thymomas as observed in 9/13 patients with thymoma-MG (Beekman, Kuks et al. 1997), although this finding was not replicated by others (Nakano and Engel 1993). The presence of inflammatory cells did not appear to correlate with disease severity grade (Nakano and Engel 1993).

### 3.1.3. Mitochondrial and other ultrastructural changes

The few ultrastructural studies reported disintegration of the myofibrillar structures with regions devoid of myofibrils, increased intramyocellular lipid, thickening of the basement membrane and abnormal mitochondria that appeared enlarged/swollen and collecting as subsarcolemmal aggregates (Bergman, Johns et al. 1971, Marchiori, Levy et al. 1989). One case was reported with increased numbers of mitochondria (Marchiori, Levy et al. 1989).

From these early reports on muscle biopsies from individuals with MG who were infrequently treated with adrenocorticotrophic hormone (ACTH) or prednisone, we can conclude that limb (and/or diaphragm) muscle showed more neurogenic compared to myopathic features in addition to inflammatory mononuclear cells, either single or few cells (common) or small focal collections (less common) in the endomysium or perivascular regions of the myasthenic endplate (Nakano and Engel, Hong, Khang et al. 2000).

## 3.2. Comparison of histopathology of non-ocular muscles in AChR- and MuSK-MG

Since the identification of pathogenic antibodies by radio-immunoassays, a few case series and case reports (Selcen, Fukuda et al. 2004, Samuraki, Furui et al. 2007) compared or described the histopathological features in limb muscles of AChR-MG and MuSK-MG (Supplementary table 2).

Rostedt-Punga et al. compared limb muscle biopsies of AChR-MG and MuSK-MG cases taken between 17 and 43 years after symptom onset. Most cases had either recovered or only had moderately affected myasthenic weakness at the time of muscle biopsy (Rostedt Punga, Ahlqvist et al.). Although most of the patients were older than 50 years, and the MuSK-MG cases were on average 10 years older than the AChR-MG cases, they reported atrophic fibres,

cytochrome C oxidase (COX) negative fibres and ragged red fibres with similar frequency in both the MuSK- and AChR-MG groups (Rostedt Punga, Ahlqvist et al.).

In a smaller cohort, atrophic fibres were reported more frequently in AChR-MG than MuSK-MG cases (6/7 vs 2/6 respectively) despite the biopsied muscles having normal strength, however the AChR-MG cases were notably older than the MuSK-MG cases (Martignago, Fanin et al. 2009). Minicores (areas devoid of mitochondria) found in most specimens suggested mitochondrial stress and electron microscopic features of myofibrillary disarray and subsarcolemmal mitochondrial aggregates were seen with similar frequency in AChR- and MuSK-MG. Only two patients were younger than 40, and therefore not expected to have COX negative fibres although the MuSK-MG case (and not the AChR-MG case) had scattered COX-negative fibres (<0.5% of fibres) (Martignago, Fanin et al. 2009).

In another small series, in which almost all cases were on immune therapies, mild neurogenic changes (including atrophic fibres, myofibrillary disarray, Z-line streaming) were more prominent in AChR-MG, whereas the MuSK-MG group overall showed more severe mitochondrial damage with degenerated mitochondria (with fragmented cristae) and subsarcolemmal aggregates (AChR-MG 1/7 vs MuSK-MG 7/7), although the MuSK-MG cases were younger than the AChR-MG cases (Cenacchi, Papa et al. 2011). However, quantified scores of the mitochondrial enzyme immunohistochemistry were more frequently abnormal in the AChR-MG group compared to MuSK-MG muscles (Cenacchi, Papa et al. 2011). Moreover, ragged red fibres (or the appearance of rims with subsarcolemmal mitochondrial accumulations) were as frequent in AChR-MG as MuSK-MG (Martignago, Fanin et al. 2009, Cenacchi, Papa et al. 2011).

Therefore, although there is overlap in the pathological findings in limb muscles, the AChR-MG may have predominant neurogenic features with less frequent mitochondrial changes whereas MuSK-MG muscle showed more evidence of mitochondrial damage (Rostedt Punga, Ahlqvist et al. , Martignago, Fanin et al. 2009, Cenacchi, Papa et al. 2011). With the exception of lymphocytic infiltrates reported in earlier literature, the light microscopy findings were similar to those reported prior to 1994.

### 3.3. Histopathological findings in myasthenic extraocular muscles

Extraocular muscle (EOM) biopsies of MG cases were described in six case reports and series from 1953 – 2017, of which two reports described histopathological findings of postmortem EOM biopsies (Supplementary table 3).

#### 3.3.1. Lymphocytic infiltrates and fibrofatty change

Oosterhuis and Bethlem (1973) (Oosterhuis and Bethlem 1973) reported EOM histopathology in postmortem biopsies of seven cases, mostly with generalized MG symptoms for less than two years (5 of 7 cases). Lymphocytic infiltrates were reported in the EOMs and non-ocular muscles in three cases. Total external ophthalmoplegia (duration unknown) was reported in two cases and the EOMs were noted to be “almost completely replaced with fat”. Russell (1953) also described lymphorrhages in the EOMs and eyelids of MG cases at post mortem on average 3 years after symptom onset, but does not mention the antemortem clinical status of the EOMs (Russell 1953). While Sakimoto et al. (Sakimoto and Cheng-Minoda 1970) focused on the endplate junctions of the EOMs of myasthenic patients who underwent biopsies within months of showing non-responsiveness to cholinesterase inhibitors, and reported increased post-junctional folds in 4/10 biopsies, they reported normal myofibre and mitochondrial ultrastructure. The increase in post-junctional folds for EOMs was interpreted as compensatory response to denervation.

### 3.3.2. Ultrastructural mitochondrial changes

More recent case reports describe similar fibrofatty changes in EOMs which showed treatment-resistant ophthalmoplegia in AChR-MG (after 1.2 years), and triple seronegative MG (after 3.5 years), but without lymphorrhages (Gratton, Herro et al. 2014, Rautenbach, Pillay et al. 2017) similarly to Hoogenraad et al (Deutman and Cruysberg 1978). The ultrastructural evidence of mitochondrial stress was similar to the reports in non-ocular muscles in MG (Table 3) (Rautenbach, Pillay et al. 2017). Although based on only a few reports, the histopathology of EOMs, which were also very weak, was reported to show more fibrocellular and fatty replacement of the extraocular muscle fibres compared to the descriptions in limb muscles.

### 3.4. Comparisons with muscle pathology in experimental MG models

Evidence of mitochondrial stress was observed in both MuSK- and AChR-MG induced experimental autoimmune MG (EAMG) models, although the rodents were sacrificed soon after EAMG induction (Supplementary table 4). Enlarged mitochondria with abnormal cristae were noted within 24 hours of passive transfer of AChR-antibodies in rodents (Kusner, Halperin et al. 2013) and one week after active AChR-EAMG induction (Wu, She et al. 2013) (supplementary Table 1). However, after 8 weeks from the active induction of AChR-EAMG and MuSK-EAMG the latter showed 2-fold more frequent ragged red fibres (Ozkok, Durmus et al. 2015). Of interest, Zhou et al. (2014) compared EOMs with non-ocular muscle histology at 48 hours after passive AChR-EAMG and noted more lymphocytic infiltrates in the EOMs compared to the limb and diaphragm muscles (Zhou, Kaminski et al. 2014).

### 3.5. Comparing the EOMs histopathological findings in strabismus with those in MG

Histopathological features of paresed or paralysed EOMs without the influence of MG conditions were compared to the findings in EOMs of MG cases. Surprisingly, the histopathological reports in EOMs of patients with strabismus were similar to the descriptions in MG (Supplementary Table 5). The most severe cases with EOM and levator muscle paralysis showed excessive extracellular deposition of connective tissue and fibrofatty replacement of atrophic fibres, in addition to myofibrillar disarray and ragged red fibres (Martinez, Hay et al. 1976, Berard-Badier, Pellissier et al. 1978, Martínez, Biglan et al. 1980, Domenici-Lombardo, Corsi et al. 1992, Clark, Kemp et al. 1995, Baldwin and Manners 2002, Wabbels, Schroeder et al. 2007, Surve, Sharma et al. 2018). The ultrastructure of these EOMs, irrespective of whether the muscles were weak or completely paralysed, showed mitochondrial abnormalities ranging from pyknotic appearance in those with milder misalignment (Yao, Wang et al. 2016) to enlarged abnormal aggregations and degenerate mitochondria with abnormal cristae (Berard-Badier, Pellissier et al. 1978, Martínez, Biglan et al. 1980, Hamdi, El-Hawary et al. 2013). The severity of the pathological changes appears to correlate somewhat with the degree of paralysis; those cases who could still generate force despite ocular misalignment (e.g. sensory esotropia in the blind eye or pendular nystagmus), showed normal histology including ultrastructure (Wabbels, Schroeder et al. 2007, Rautenbach, Pillay et al. 2017). Taken together we conclude that the structural mitochondrial changes noted in the EOMs may in part be a secondary consequence of severe muscle weakness (Spencer and McNeer 1980).

The main findings of this review are summarized in Table 1.

Table 1. Summarizing the histopathological changes in the non-ocular and extraocular muscles in myasthenia gravis and comparisons with strabismus from other (non-myasthenic) causes

Muscle type	Light microscopy (n)	Electron microscopy (EM)	
		EM general (n)	EM mitochondria (n)
MG limb before serotyping (n=13)*	AF type II >> type I (6), N-atrophy (6), MFD (4), LI (4), FCMR (2), lymphorrhages (2), minicores/targets (1), necrosis (2)	ZBS (2), IMCL (2)	Enlarged (2), SSA (2), abn. cristae (2)
MG limb (AChR+) (n=5)	N-atrophy (3), AF type II >> type I (5), MFD (1), rims (2), minicores (2)	ZBS (1), IMCL (1)	Enlarged (1), SSA (2), abn. cristae (2)

MG limb (MuSK+) (n=5)**	N-atrophy (2), AF (4), MFD (4), rims (2), minicores (1)	ZBS (2), IMCL (2)	Enlarged (1), SSA (1), abn. cristae (1)
MG EOM (n=6)#	N-atrophy (2), AF (3), MFD (1), FCMR (3), lymphorrhages (1), LI (1), degenerative fibres (1)	ZBS (1), IMCL (1)	Enlarged (1), SSA (1)
Strabismus EOM (n=9)	AF (3), MFD (5), FCMR (3), rims (2), degenerative fibres (1), LI (1)	ZBS (5), IMCL (4)	Enlarged (3), SSA (3), abn. cristae (6), degenerated (1)

Table 1. number of reports (n); myasthenia gravis (MG); “N-atrophy” refers to neurogenic atrophy; atrophic fibers (AF); myofibrillary disarray (MFD); fibrocellular ± fatty muscle replacement (FCMR); lymphocytic infiltrates (LI); Z-band streaming (ZBS); intramyocellular lipid (IMCL); subsarcolemmal infiltrates (SSA); abnormal (abn.) cristae refers to fragmented, disrupted or abnormally arranged cristae; AChR+ refers to acetylcholine receptor antibody positive MG; “rims” refer to peripherally located mitochondrial aggregates on Gömori Trichrome stain; minicores (or target fibres) refers to central areas devoid of mitochondria; MuSK+ refers to muscle specific kinase antibody positive MG; extraocular muscle (EOM); \*only 2 reports on ultrastructure before serotyping; \*\*only 1 report on ultrastructure in MuSK+ MG; #1 report on ultrastructure in EOMs in MG.

#### 4. Discussion

In summarizing the histopathology in muscle biopsies of myasthenic individuals, albeit based on relatively few reports, two predominant themes emerged. Firstly, in non-ocular muscles, irrespective of the MG serotype, there were substantial structural changes, mainly type II fibre atrophy, suspected to be consequent to functional denervation. Secondly, varying degrees of mitochondrial stress and damage are described, possibly more consistently in MuSK-MG. Interestingly type II fibres have been noted to contain fewer mitochondria than type I fibres (McKelvie, Satchi et al. 2012), which may explain their increased susceptibility to mitochondrial stress. An important aim of the review was to focus on the extraocular muscle changes in MG. Compared to limb muscles, EOMs showed similar, albeit more severe, pathological features, but the few reports which exist are based on EOMs with severe weakness in contrast to the limb muscle biopsies which were mostly reported to have mild weakness or normal strength. The pathology in the EOMs was not specific to MG, but also found in paralysed EOMs due to other causes.

In AChR-MG, a complement mediated attack, triggered by pathogenic immunoglobulin (Ig)G1 and IgG3 antibodies, results in AChR blockade and destruction thereby functionally denervating the muscle endplate (Nakano and Engel, Soltys, Gong et al. 2008, Grativol, Silva et al. 2017). Although the IgG4 antibodies in MuSK-MG are not complement activating, a reduction in the density of AChRs at the muscle endplate (Niks, Kuks et al. 2010, Verschuuren, Huijbers et al. 2013) and evidence of neurogenic atrophy were observed (Cenacchi, Papa et al. 2011). It is therefore not surprising that features of functional denervation are described in both AChR-MG and MuSK-MG. The mitochondrial changes observed in MG muscle biopsies may be more frequent or more pronounced in MuSK-MG, even in cases without substantial weakness (Cenacchi, Papa et al. 2011). In AChR-EAMG models, gene expression changes in both EOM and limb muscles were most prominent in pathways related to metabolism, and suggested that increased oxidative metabolism may occur in response to induced MG (Kaminski, Himuro et al. 2016). As the EOMs possess unique metabolic characteristics such as high firing rates and energy requirements, they may be particularly susceptible to this metabolic shift which may impact generation of muscle force (Kaminski, Himuro et al. 2016). Indeed, in EAMG rodent models and *in vitro* muscle treated with MG sera, a prominent effect was noted on muscle contractility which was over and above the neuromuscular junction transmission defect (Pagala, Nandakumar et al. 1990, Van Lunteren, Moyer et al. 2004). Poor muscle force generation would further impact mitochondrial biogenesis (Andrade, McMullen et al. 2005) and trigger atrophy signaling (Yu Wai Man, Chinnery et al. 2005, Patel, Gamboa et al. 2009). Several lines of evidence from animal models and *in vitro* C2C12 myotube cycle stretch experiments (Soltow, Zeanah et al. 2013) have shown that preventing muscle/myotubes from generating a force for  $\geq 48$  hours (vs continued stretching), resulted in downstream transcriptional signaling changes and myofiber atrophy. EOMs may be more susceptible to these effects.

The EOMs also differ from limb skeletal muscle in their response to botulinum toxin (Botox) and certain growth factors (Ugalde, Christiansen et al. 2005). Pre-synaptic 'denervation' with Botox in chick embryos showed severe limb muscle atrophy with almost complete fatty replacement within 7 days (Drachman and Sokoloff 1966) whereas EOMs injected with Botox did not develop muscle atrophy despite transient paralysis, a phenomena which is thought to be explained by continued EOM satellite cell activation and the potential for remodeling (Ugalde, Christiansen et al. 2005, Verma, Fitzpatrick et al. 2017). However, a single injection of certain muscle growth factors (BMP4, TGFB1, Wnt3A) into mouse EOMs had a profound reduction of force generation and muscle fibre diameter when examined after 7 days (Anderson, Christiansen et al. 2008).

Substantial muscle force reduction activates atrophy signaling pathways via downregulation of the anabolic IGF1/Akt pathway, which inhibits protein degradation and promotes muscle protein synthesis (Soltow, Zeanah et al. 2013). Knock-down of critical genes in the IGF1/Akt/mTOR signaling pathway also had a negative effect on muscle contractility and mitochondrial biogenesis (Schiaffino and Mammucari 2011). Dysfunctional mitochondria further trigger atrophy signaling pathways by excessive production of reactive oxygen species. Recently, Graham et al. (2018) reported substantial transcriptomic changes in denervated muscle after 7 days, and a shift from mitochondrial fusion to fission and fragmentation (Iqbal, Ostojic et al. 2013, Graham, Harlow et al. 2018).

In conclusion, neurogenic muscle changes are frequent in MG. Mitochondrial homeostasis is impacted even in mildly affected muscles in the setting of MG. We hypothesized that the extraocular muscles may be more susceptible to mitochondrial damage secondary to reduced contractility, resulting in a cascade of atrophy signaling pathways which may contribute to the development of treatment-resistant and persistent ophthalmoplegia in MG (Figure 1). Therefore, strategies to improve contractility in weak EOMs early in MG, are critical.

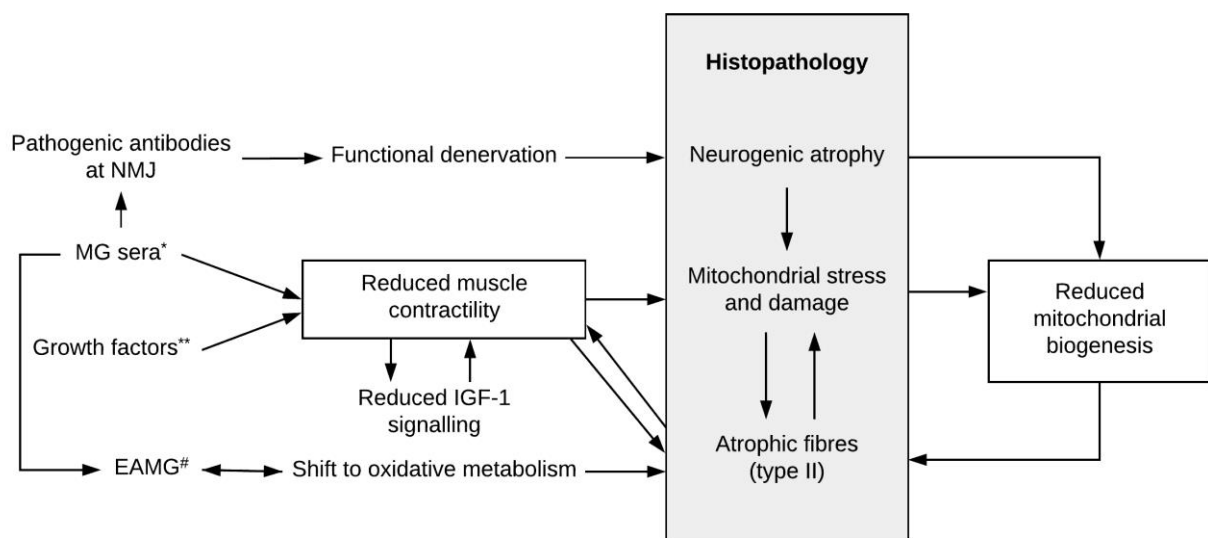


Figure 1. Histopathological changes in muscle inform hypothesis of pathogenetic mechanisms resulting in treatment-resistant ophthalmoplegia. Pathogenic antibodies in myasthenia gravis (MG) result in functional denervation at the neuromuscular junction (NMJ) and reduced muscle contractility resulting in neurogenic atrophy and altered mitochondrial metabolism. On a molecular level, transcriptional changes induced in MG inhibit insulin-like growth factor 1 (IGF-1) signaling which lifts inhibition of muscle proteolytic and apoptotic pathways. Dysfunctional mitochondria cause oxidative stress which potentiates atrophy signaling. #EAMG: experimental autoimmune myasthenia gravis.

## References

- Anderson, B. C., S. P. Christiansen and L. K. McLoon (2008). "Myogenic growth factors can decrease extraocular muscle force generation: a potential biological approach to the treatment of strabismus." Investigative ophthalmology & visual science **49**(1): 221-229.
- Andrade, F. H., C. A. McMullen and R. E. Rumbaut (2005). "Mitochondria are fast Ca<sup>2+</sup> sinks in rat extraocular muscles: a novel regulatory influence on contractile function and metabolism." Investigative ophthalmology & visual science **46**(12): 4541-4547.
- Baldwin, H. C. and R. M. Manners (2002). "Congenital blepharoptosis: a literature review of the histology of levator palpebrae superioris muscle." Ophthalmic Plast Reconstr Surg **18**(4): 301-307.
- Beekman, R., J. B. Kuks and H. J. Oosterhuis (1997). "Myasthenia gravis: diagnosis and follow-up of 100 consecutive patients." J Neurol **244**(2): 112-118.
- Berard-Badier, M., J. Pellissier, M. Toga, N. Mouillac and P. Berard (1978). "Ultrastructural studies of extraocular muscles in ocular motility disorders." Albrecht von Graefes Archiv für klinische und experimentelle Ophthalmologie **208**(1-3): 193-205.
- Bergman, R. A., R. J. Johns and A. K. J. A. o. t. N. Y. A. o. S. Afifi (1971). "Ultrastructural alterations in muscle from patients with myasthenia gravis and Eaton-Lambert syndrome." **183**(1): 88-122.
- Brownell, B., D. R. Oppenheimer and J. M. Spalding (1972). "Neurogenic muscle atrophy in myasthenia gravis." J Neurol Neurosurg Psychiatry **35**(3): 311-322.
- Castleman, B. (1966). "The pathology of the thymus gland in myasthenia gravis." Ann N Y Acad Sci **135**(1): 496-505.
- Cenacchi, G., V. Papa, M. Fanin, E. Pegoraro and C. Angelini (2011). "Comparison of muscle ultrastructure in myasthenia gravis with anti-MuSK and anti-AChR antibodies." J Neurol **258**(5): 746-752.
- Clark, B. J., E. G. Kemp, W. M. Behan and W. R. Lee (1995). "Abnormal extracellular material in the levator palpebrae superioris complex in congenital ptosis." Arch Ophthalmol **113**(11): 1414-1419.
- Deutman, A. F. and J. R. M. Cruysberg (1978). "Ophthalmoplegia due to myasthenia gravis histological and histochemical observations in the inferior oblique muscle." Deutman, August F, And J R M Cruysberg (Ed ) Documenta Ophthalmologica Proceedings Series, Vol 17 Neurogenetics And Neuro-Ophthalmology 5th International Congress, Nijmegen, The Netherlands(Ed): The Hague, The Netherlands: Boston, Mass , Usa Isbn 90-6193-6159-6192 6127-6134.

- Domenici-Lombardo, L., M. Corsi, R. Mencucci, M. Scrivanti, M. Faussonne-Pellegrini and G. Salvi (1992). "Extraocular muscles in congenital strabismus: muscle fiber and nerve ending ultrastructure according to different regions." Ophthalmologica **205**(1): 29-39.
- Drachman, D. B. and L. Sokoloff (1966). "The role of movement in embryonic joint development." Developmental Biology **14**(3): 401-420.
- Engel, W. K. and D. E. J. A. o. t. N. Y. A. o. S. McFarlin (1966). "Discussion." **135**(1): 68-78.
- Farrugia, M. E., M. D. Robson, L. Clover, P. Anslow, J. Newsom-Davis, R. Kennett, D. Hilton-Jones, P. M. Matthews and A. Vincent (2006). "MRI and clinical studies of facial and bulbar muscle involvement in MuSK antibody-associated myasthenia gravis." Brain **129**(Pt 6): 1481-1492.
- Fenichel, G. M. (1966). "Muscle lesions in myasthenia gravis." Ann N Y Acad Sci **135**(1): 60-67.
- Fenichel, G. M. and G. M. Shy (1963). "Muscle Biopsy Experience in Myasthenia Gravis." Arch Neurol **9**: 237-243.
- Graham, Z. A., L. Harlow, W. A. Bauman and C. P. Cardozo (2018). "Alterations in mitochondrial fission, fusion, and mitophagic protein expression in the gastrocnemius of mice after a sciatic nerve transection." Muscle & nerve **58**(4): 592-599.
- Grativvol, R. S., A. M. S. d. Silva, B. F. Guedes, E. d. P. Estephan, R. d. H. Mendonça, A. A. Zambon, C. O. Heise and E. Zanoteli (2017). "Facial and bulbar muscle atrophy in acetylcholine receptor antibody-positive myasthenia gravis." Arquivos de neuro-psiquiatria **75**(3): 197-198.
- Gratton, S. M., A. Herro, J. A. Bermudez-Magner and J. Guy (2014). "Atrophy and Fibrosis of Extra-Ocular Muscles in Anti-Acetylcholine Receptor Antibody Myasthenia Gravis." Open Journal of Ophthalmology **4**(04): 117.
- Hamdi, M. M., G. R. El-Hawary, N. G. El-Hefnawy and M. I. Salman (2013). "Histopathological and electron microscopic study for different grades of inferior oblique muscle overaction." Clinical Ophthalmology (Auckland, NZ) **7**: 917.
- Heckmann, J. M. and M. Nel (2017). "A unique subphenotype of myasthenia gravis." Ann. N. Y. Acad. Sci.
- Heckmann, J. M., H. Uwimpuhwe, R. Ballo, M. Kaur, V. B. Bajic and S. Prince (2010). "A functional SNP in the regulatory region of the decay-accelerating factor gene associates with extraocular muscle pareses in myasthenia gravis." Genes Immun **11**(1): 1-10.
- Hong, S. M., S. K. Khang, K. K. Kim, Y. Bae and S. H. Park (2000). "A case of myasthenia gravis proven by ultrastructural study." J Korean Med Sci **15**(2): 251-254.
- Iqbal, S., O. Ostojic, K. Singh, A. M. Joseph and D. A. Hood (2013). "Expression of mitochondrial fission and fusion regulatory proteins in skeletal muscle during chronic use and disuse." Muscle & nerve **48**(6): 963-970.

- Kaminski, H. J., K. Himuro, J. Alshaikh, B. Gong, G. Cheng and L. L. Kusner (2016). "Differential RNA Expression Profile of Skeletal Muscle Induced by Experimental Autoimmune Myasthenia Gravis in Rats." Front Physiol **7**: 524.
- Kusner, L. L., J. A. Halperin and H. J. Kaminski (2013). "Cell surface complement regulators moderate experimental myasthenia gravis pathology." Muscle & nerve **47**(1): 33-40.
- Marchiori, P. E., J. Levy, M. S. Lusvardi, A. M. Tsanaclis, J. Assis and M. Scaff (1989). "Mitochondrial dysfunction in myasthenia gravis: report of a case." Arquivos de neuro-psiquiatria **47**(3): 355-358.
- Martignago, S., M. Fanin, E. Albertini, E. Pegoraro and C. Angelini (2009). "Muscle histopathology in myasthenia gravis with antibodies against MuSK and AChR." Neuropathol Appl Neurobiol **35**(1): 103-110.
- Martínez, A. J., A. W. Biglan and D. A. Hiles (1980). "Structural features of extraocular muscles of children with strabismus." Archives of ophthalmology **98**(3): 533-539.
- Martinez, A. J., S. Hay and K. W. McNeer (1976). "Extraocular muscles light microscopy and ultrastructural features." Acta Neuropathologica **34**(3): 237-253.
- McKelvie, P., K. Satchi, A. A. McNab and P. Kennedy (2012). "Orbicularis oculi: morphological changes mimicking mitochondrial cytopathy in a series of control normal muscles." Clin Exp Ophthalmol **40**(5): 497-502.
- Nakano, S. and A. G. Engel (1993). "Myasthenia gravis: quantitative immunocytochemical analysis of inflammatory cells and detection of complement membrane attack complex at the end-plate in 30 patients." (0028-3878 (Print)).
- Niks, E. H., J. B. Kuks, J. H. Wokke, H. Veldman, E. Bakker, J. J. Verschuuren and J. J. Plomp (2010). "Pre- and postsynaptic neuromuscular junction abnormalities in musk myasthenia." Muscle Nerve **42**(2): 283-288.
- Oosterhuis, H. and J. Bethlem (1973). "Neurogenic muscle involvement in myasthenia gravis. A clinical and histopathological study." J Neurol Neurosurg Psychiatry **36**(2): 244-254.
- Ozkok, E., H. Durmus, B. Yetimler, H. Tasli, N. Trakas, C. Ulusoy, G. Lagoumintzis, S. Tzartos and E. Tuzun (2015). "Reduced muscle mitochondrial enzyme activity in MuSK-immunized mice." Clin Neuropathol **34**(6): 359-363.
- Pagala, M. K. D., N. V. Nandakumar, S. A. T. Venkatachari, K. Ravindran, T. Namba and D. Grob (1990). "Responses of intercostal muscle biopsies from normal subjects and patients with myasthenia gravis." Muscle Nerve **13**(11): 1012-1022.
- Patel, S. P., J. L. Gamboa, C. A. McMullen, A. Rabchevsky and F. H. Andrade (2009). "Lower Respiratory Capacity in Extraocular Muscle Mitochondria: Evidence for Intrinsic Differences in

- Mitochondrial Composition and Function." Investigative Ophthalmology & Visual Science **50**(1): 180-186.
- Rautenbach, R. M., K. Pillay, A. D. N. Murray and J. M. Heckmann (2017). "Extraocular Muscle Findings in Myasthenia Gravis Associated Treatment-Resistant Ophthalmoplegia: A Case Report." J Neuroophthalmol.
- Rostedt Punga, A., K. Ahlqvist, E. Bartoccioni, F. Scuderi, M. Marino, A. Suomalainen, H. Kalimo and E. V. Stålberg "Neurophysiological and mitochondrial abnormalities in MuSK antibody seropositive myasthenia gravis compared to other immunological subtypes." Clinical Neurophysiology **117**(7): 1434-1443.
- Rowland, L. P., P. F. Hoefler, H. Aranow, Jr. and H. H. Merritt (1956). "Fatalities in myasthenia gravis; a review of 39 cases with 26 autopsies." Neurology **6**(5): 307-326.
- Russell, D. S. (1953). "Histological changes in the striped muscles in myasthenia gravis." The Journal of Pathology and Bacteriology **65**(2): 279-289.
- Sakimoto, T. and K. Cheng-Minoda (1970). "Fine structure of neuromuscular junctions in myasthenic extraocular muscles." Investigative Ophthalmology & Visual Science **9**(4): 316-324.
- Samuraki, M., E. Furui, K. Komai, M. Takamori and M. Yamada (2007). "Myasthenia gravis presenting with unusual neurogenic muscle atrophy." Muscle Nerve **36**(3): 394-399.
- Schiaffino, S. and C. Mammucari (2011). "Regulation of skeletal muscle growth by the IGF1-Akt/PKB pathway: insights from genetic models." Skelet Muscle **1**(1): 4.
- Selcen, D., T. Fukuda, X. M. Shen and A. G. Engel (2004). "Are MuSK antibodies the primary cause of myasthenic symptoms?" Neurology **62**(11): 1945-1950.
- Soltow, Q. A., E. H. Zeanah, V. A. Lira and D. S. Criswell (2013). "Cessation of cyclic stretch induces atrophy of C2C12 myotubes." Biochemical and biophysical research communications **434**(2): 316-321.
- Soltys, J., B. Gong, H. J. Kaminski, Y. Zhou and L. L. Kusner (2008). "Extraocular muscle susceptibility to myasthenia gravis: unique immunological environment?" Ann N Y Acad Sci **1132**: 220-224.
- Spencer, R. F. and K. W. McNeer (1980). "Structural alterations in overacting inferior oblique muscles." Arch Ophthalmol **98**(1): 128-133.
- Stortebecker, T. P. (1955). "Signs of myositis in myasthenia gravis and in myopathy clinically resembling progressive muscular dystrophy." Acta Med Scand **151**(6): 452-464.
- Surve, A., M. C. Sharma, N. Pushker, M. S. Bajaj, R. Meel and S. Kashyap (2018). "A study of changes in levator muscle in congenital ptosis." Int Ophthalmol.

- Ugalde, I., S. P. Christiansen and L. K. McLoon (2005). "Botulinum toxin treatment of extraocular muscles in rabbits results in increased myofiber remodeling." Investigative ophthalmology & visual science **46**(11): 4114-4120.
- Van Lunteren, E., M. Moyer and H. J. J. J. o. A. P. Kaminski (2004). "Adverse effects of myasthenia gravis on rat phrenic diaphragm contractile performance." **97**(3): 895-901.
- Verma, M., K. R. Fitzpatrick and L. K. McLoon (2017). "Extraocular muscle repair and regeneration." Current ophthalmology reports **5**(3): 207-215.
- Verschuuren, J. J., M. G. Huijbers, J. J. Plomp, E. H. Niks, P. C. Molenaar, P. Martinez-Martinez, A. M. Gomez, M. H. De Baets and M. Losen (2013). "Pathophysiology of myasthenia gravis with antibodies to the acetylcholine receptor, muscle-specific kinase and low-density lipoprotein receptor-related protein 4." Autoimmunity reviews **12**(9): 918-923.
- Wabbels, B., J. A. Schroeder, B. Voll, H. Siegmund and B. Lorenz (2007). "Electron microscopic findings in levator muscle biopsies of patients with isolated congenital or acquired ptosis." Graefes Archive for Clinical and Experimental Ophthalmology **245**(10): 1533-1541.
- Wu, H., S. She, Y. Liu, W. Xiong, Y. Guo, H. Fang, H. Chen and J. Li (2013). "Protective effect of Sijunzi decoction on neuromuscular junction ultrastructure in autoimmune myasthenia gravis rats." J Tradit Chin Med **33**(5): 669-673.
- Yao, J., X. Wang, H. Ren, G. Liu and P. Lu (2016). "Ultrastructure of medial rectus muscles in patients with intermittent exotropia." Eye (Lond) **30**(1): 146-151.
- Yu Wai Man, C. Y., P. F. Chinnery and P. G. Griffiths (2005). "Extraocular muscles have fundamentally distinct properties that make them selectively vulnerable to certain disorders." Neuromuscular Disorders **15**(1): 17-23.
- Zhou, Y., H. J. Kaminski, B. Gong, G. Cheng, J. M. Feuerman and L. Kusner (2014). "RNA expression analysis of passive transfer myasthenia supports extraocular muscle as a unique immunological environment." Invest. Ophthalmol. Vis. Sci. **55**(7): 4348-4359.

## Appendices

Supplementary table 1. Histopathology of skeletal muscle biopsies (non-ocular) before antibody assays

Ref.	Age* (n), MG grade	MG diagnosis (n)	Muscle biopsied	MG duration, years, (range)	Light microscopy	Electron microscopy	
						general	mitochondria
Russel, 1953	43 (8), ≥ II	AChEI+, TH, Thym.	**UL; LL; DIA; IC	3.2 (0.7 – 13)	N-atrophy, 'Necrosis', lymphorrhages,	ND	ND
Stortebecker, 1955	41 (13), NS	AChEI+, Thym.	Trap; DIA; temporalis	NS (3 – 30)	AF, lymphorrhages	ND	ND
Rowland, 1956	41 (39), NS	AChEI+, Thym., TH	**NS	2.8 (0.2 – 12)	LI, AF, MFD	ND	ND
Fenichel, 1963	NS (37), NS	AChEI+, RNS	UL; LL	7 (1 – 34)	AF, FCMR, MFD, LI (12), N-atrophy (11)	ND	ND
Engel, 1966	NS (30), II	NS	NS	NS	N-atrophy (19), 'Necrosis' (9), AF (15), LI (7)	ND	ND
Brody, 1964	3 (1), ≥ IIIb	AChEI+, RNS	UL, LL	32	N-atrophy, AF, "targets"	ND	ND
Bergman, 1971	29 (3), ≥ IIb	AChEI+, RNS, SF	LL	2.5 (0.2 – 7)	MFD	ZBS, IMCL	enlarged, SSA, abn. cristae

Brownell, 1972	46 (2), ≥ IVb	AChEI+, RNS, Thym.	Tongue	7.5 (10 – 15)	AF, MFD	ND	ND
Oosterhuis, 1973	46: 54 <sup>#</sup> (46), NS	AChEI+, SF, Thym.	UL, LL, IC	≥ 6	AF, FCMR, N-atrophy, LI	ND	ND
Korényi-Both, 1973	12-73 (23), <sup>†</sup> V	NS, Thym. (n=1)	UL, LL	NS	AF, N-atrophy (3), MFD	ZBS, ZLM, DSR	enlarged, SSA, abn. cristae
Isaacs, 1974	11-55 (12), NS	AChEI+, RNS, TH (1)	UL	2-28	AF (3), N-atrophy (6), LI (2), MFD (7)	ZBS (5), ZLM (1), DSR (3)	NS
Marchiori, 1989	11 (1), NS	AChEI+, RNS	UL	1	'Necrosis'	IMCL	Increased
Nakano, 1993	<sup>‡</sup> 36 (30), I- IIb	RNS, Thym, TH	UL, IC	3 (0.3 – 14)	LI	ND	ND

Legend: Supplementary table 1. Reference (ref) listed chronologically according to year of publication; \* mean age of individuals at the time of biopsy and n refers to the number of cases; Myasthenia gravis (MG); MG grade refers to the Osserman grade of MG severity (or approximation) e.g. near normal strength interpreted as grade II [5]; MG diagnosis refers to support for the diagnosis of MG; MG duration refers to the mean years of MG symptoms before biopsy; Acetylcholinesterase inhibitor responsive (AChEI+); thymic hyperplasia (TH); thymoma (Thym.); \*\* muscle biopsied post mortem; upper limb (UL); lower limb (LL); diaphragm (DIA); intercostal (IC); N-atrophy refers to neurogenic atrophy with myofibre grouping and angulated fibres; 'necrosis' refers to degenerating fibres surrounded by inflammatory cells; not done (ND); NS refers to "not specified"; Trapezius (Trap.); atrophic fibres (AF); lymphocytic infiltrates (LI);

myofibrillary disarray (MFD); repetitive nerve stimulation (RNS); fibrocellular  $\pm$  fatty muscle replacement (FCMR); cores or “targets” which refer to areas devoid of staining; single fibre electromyography (SF); Z-band streaming (ZBS); intramyocellular lipid (IMCL); subsarcolemmal aggregates of mitochondria (SSA); abnormal (abn) cristae refers to fragmented, disrupted or abnormally arranged cristae; #mean ages were noted for groups with/without clinical atrophy;  $\dagger$  severity grades not stated although 8/17 were MGFA V; ZLM refers to Z-line material or rod-shaped Z-line structures; DSR refers to dilated sarcoplasmic reticulum;  $\ddagger$ 12/36 had acetylcholine receptor (AChR) antibody assays.

Supplementary table 2. Histopathology of limb skeletal muscle biopsies from MG cases by MG serotype

Ref.	MG serotype	Age* (n), MGFA grade	MG Diagnosis	Muscle biopsied	MG duration, years, (range)	Light microscopy (n)	Electron microscopy (n)	
							general	mitochondria
Hong, 2000	AChR+	18 (1), ≥IIIb	AChEI+, RNS, TH	LL	3	AF-type II, MFD	NS	Enlarged, SSA abn. cristae
Selcen, 2004	MuSK+	34 (1), IIIb	RNS	IC	13	AF-type II, MFD	ZBS	NS
Rostedt Punga, 2006	MuSK+	64 (10), I-IVb	AChEI+, RNS+	UL, LL	17 (0.5-55)	AF-type II>I (3), Rims (2)	ND	ND
	AChR-; MuSK-	58 (9), IIa-IVb	AChEI+, RNS+	UL ±N	17 (2-33)	AF-type II=I (2), Rims (3); CNF 0.07% (1)	ND	ND
	AChR+	54 (31), I-V	AChEI+, RNS+	UL ±N	25 (1-57)	AF-type II>I (7), Rims (3); CNF 0.02% (1)	ND	ND
Samuraki, 2007	AChR+	28 (1), ≥IIa	AChEI+, RNS	UL	0.5	AF-type I/II, N-atrophy	ND	ND

Martignago, 2009	AChR+	71 (7), IIa - IVa	RNS	UL, LL	NS	AF (5), N-atrophy (6), MFD, cores/Rims (5), CNF<2% (6)	NS	NS
	MuSK+	39 (6), IIa - IIb	RNS	UL, LL	NS	AF (3); N-atrophy (2), MFD, cores/rims (5), CNF 0.5% (1)	NS	NS
Niks, 2010	MuSK+	29 (1), IVb	AChEI+, RNS+	IC	<1	NS, MFD	NS	NS
Cenacchi, 2011	AChR+	67 (7), IIa, b	RNS	UL, LL ±N	6 (1 – 32)	AF, N-Atrophy, MFD, cores	ZBS; IMCL	SSA, Abn. cristae**(1)
	MuSK+	45 (7), mms-IIIb	RNS	UL, LL ±N	9 (1 – 31)	AF, N-atrophy, MFD	ZBS; IMCL	Enlarged, SSA Abn. cristae**(3)

Legend. Supplementary table 2. Reference (ref) listed chronologically according to year of publication; Myasthenia gravis (MG); \*mean age (years) at the time of biopsy and n refers to the number of cases; MGFA grade refers to either the specified MG Foundation of America grade of severity or an approximation; MG diagnosis refers to support for the diagnosis of MG; MG duration refers to the mean years of MG symptoms before biopsy; AChR+/- refers to whether acetylcholine receptor antibodies were detected; Acetylcholinesterase inhibitor responsive (AChEI+); repetitive nerve stimulation (RNS) and RNS+ refers to single fibre electromyography; thymic hyperplasia (TH); lower limb (LL); atrophy/ atrophic fibres (AF); type I/ II refers to type I/ II fibre atrophy; myofibrillary disarray (MFD); not specified (NS); subsarcolemmal aggregates of mitochondria (SSA); abnormal (abn) cristae refers to fragmented, disrupted or abnormally

arranged cristae; MuSK+/- refers to whether muscle specific kinase antibodies were detected; intercostal muscle (IC); upper limb (UL); Rims refer to peripherally located mitochondrial aggregates on Gömori Trichrome stain; not done (ND); "± N" includes muscles that were normal and not clinically weak; cytochrome oxidase negative fibres (CNF), % CNF only depicted for patients <40 years of age when it is considered abnormal (Punga); N-atrophy refers to neurogenic atrophy; Z-band streaming (ZBS); cores refer to areas devoid of mitochondria; intramyocellular lipid (IMCL); minimal manifestations of MG (mms). \*\*refers to pronounced mitochondrial alterations.

Supplementary table 3: Histopathology of extraocular muscles in myasthenia gravis

Ref.	MG serotype	Age <sup>*</sup> (n), MGFA grade	MG diagnosis	EOM biopsied	MG duration, years (range)	Light microscopy	Electron microscopy	
							General	Mitochondria
Russel, 1953	NS	43 (8), ≥ II	AChEI+, TH; thymoma	**EOMs/LPS	3.2 (0.7 – 13)	Lymphorrhages, N-atrophy	ND	ND
Sakimoto, 1970	NS	15 (10), I, II	AChEI+, RNS	EOMs/LPS	1.7 (0.2 – 7)	NS	N	N
Oosterhuis, 1973	NS	52 (12), ≥ IIb	AChEI+, ± thymoma, RNS	**EOMs	5 (1.5-11)	FCMR, N-atrophy, LI	ND	ND
Hoogenraad, 1979	NS	53 (3), I	AChEI+, SF	IO	0.3, 14, NS	AF, degenerating fibres	ND	ND
Gratton, 2014	AChR+	66 (1), I	AChEI+	MR	1.2	AF, FCMR	ND	ND
Rautenbach, 2017	AChR-, MuSK-, LRP4-	45 (1), IIIb	AChEI+, RNS, immune therapy	MR	3.5	AF, FCMR, MFD	ZBS, IMCL	SSA, enlarged

Legend. Supplementary table 3. Reference (ref) listed chronologically according to year of publication; Myasthenia gravis (MG); \*mean age of individuals at the time of biopsy and n refers to the number of cases. Severity grade refers to the Osserman or MG Foundation of America (MGFA) grade of severity (or approximation) [5]. MG diagnosis refers to support the diagnosis of MG; Extraocular muscle (EOM); MG duration (mean in years) refers to the duration of symptoms before the biopsy; not specified (NS); Acetylcholinesterase inhibitor responsive (AChEI+); thymic hyperplasia (TH); \*\*post mortem (PM) biopsy; levator palpebrae superioris (LPS); N-atrophy refers to neurogenic atrophy; not done (ND); repetitive nerve stimulation (RNS); "N" refers to normal findings; fibrocellular ± fatty muscle replacement (FCMR); single fibre electromyography (SFEMG); lymphocytic infiltrates (LI); single fibre electromyography (SF); inferior oblique (IO); atrophic fibres (AF); acetylcholine receptor positive (AChR+); medial rectus (MR); AChR-, MuSK-, LRP4- refers to no detectable antibodies to AChR-, muscle specific kinase (MuSK-) or low density lipoprotein receptor 4 (LRP4); myofibrillary disarray (MFD); Z-band streaming (ZBS); intramyocellular lipid (IMCL); subsarcolemmal aggregates of mitochondria (SSA).

Supplementary table 4: Histopathological findings in the muscle in Experimental Autoimmune Myasthenia Gravis (EAMG) rodent models

Ref.	EAMG type	Muscle	Time of sacrifice	Light microscopy	Electron microscopy	
					General	Mitochondria
Kusner, 2013	AChR (passive)	DIA, LL	24 hours	“Moth-eaten” fibres	NS	Enlarged, abnormal cristae
Wu, 2013	AChR (active)	LL	1 week	MFD	NS	Fewer, vacuolated
Zhou, 2014	AChR (passive)	EOM, DIA, LL	48 hours	Lymphocytic infiltrates EOM >LL/DIA	ND	ND
Ozkok, 2015	AChR (active)	UL	8 weeks	AF (3%); RRF (2%)	ND	ND
	MuSK (active)	UL	8 weeks	AF (19%); Rims (7%)	ND	ND

Legend. Supplementary table 4. Reference (ref); Experimental autoimmune myasthenia gravis (EAMG); Acetylcholine receptor (AChR); Passive or active refers to the type of EAMG model. diaphragm (DIA); lower limb (LL); not specified (NS); “abnormal cristae” refers to fragmented, disrupted or abnormally arranged cristae; myofibrillary disarray (MFD); extraocular muscle (EOM); not done (ND); upper limb (UL); atrophic fibres (AF); ragged red fibres (RRF); Muscle specific kinase (MuSK).

Supplementary Table 5: Histopathological findings in extraocular muscle biopsies of patients with strabismus

Ref.	Cases	Diagnosis	Age, range, years	Muscle biopsied	Years of symptoms*	Light microscopy (n)	Electron microscopy	
							General	Mitochondria (n)
Martinez, 1976	n=13	Strabismus, various**	2 – 80	MR, IO	NS	MFD, FCMR, rims	IMCL, ZBS	Enlarged, abn. cristae
Berard-Badier, 1978	n=24	Strabismus	2 – 30	EOM	NS	MFD, AF	IMCL	abn. cristae
Martínez, 1980	n=62	Cong. strabismus	0.5- 18	EOM	NS	MFD, FCMR, rims	IMCL, ZBS	Enlarged, SSA, abn. cristae
Spencer, 1980	n=18	Overacting IO <sup>#</sup>	2 – 29	IO	4.3	AF, MFD, degenerate fibres	DSR	Enlarged, abn. cristae
Domenici-Lombardo, 1992	n=15	Cong. strabismus <sup>†</sup>	8 (3 – 35)	MR, LR	8.4	MFD	ZBS	Enlarged, SSA, abn. cristae
Wabbels, 2007	n=11	Cong. Ptosis	4 – 29	LPS	4 – 29	NS	NS	Enlarged, abn. cristae
	n=2	Pendular nystagmus <sup>‡</sup>	13; 32	LPS	13; 4	NS	N	N

Hamdi, 2013	n=7	Overacting IO <sup>#</sup>	3 – 35	IO	≥3	FCMR, Inflamm. infiltrates (3)	IMCL, ZBS	SSA, degenerate
Yao, 2016	n=20	Intermittent exotropia	3 – 38	MR	≥3.7	AF, MFD, FCMR	ZBS	Pyknotic
Rautenbach, 2017	n=1	Sensory esotropia <sup>‡</sup>	32	MR	3.5	N	N	N

Legend. Supplementary table 5. Reference (ref); Age refers to age at biopsy; \* mean years of ocular symptoms before biopsy; “n” refers to the number of cases; \*\*Biopsies of various pathologies were included such as palsies of cranial nerves III or VI; Brown syndrome and double elevator palsy; Null-point nystagmus; medial rectus (MR); inferior oblique (IO), not specified (NS), myofibrillary disarray (MFD), fibrocellular ± fatty muscle replacement (FCMR); “rims” refers to peripherally located mitochondrial aggregates on Gömori Trichrome stain; intramyocellular lipid (IMCL); Z-band streaming (ZBS); abnormal (abn) cristae refers to fragmented, disrupted or abnormally arranged cristae; extraocular muscle (EOM) - presumed MR and LR but not specified; atrophic fibres (AF); Congenital (Cong.); subsarcolemmal aggregates of mitochondria (SSA); <sup>#</sup>“Overaction of inferior oblique” defined as either primary congenital overaction of IO or secondary to weakness of antagonists; DSR refers to dilated sarcoplasmic reticulum; <sup>†</sup>deviation +29°; lateral rectus (LR); levator palpebrae superioris (LPS); “N” refers to normal findings; Inflammatory (inflamm.). <sup>‡</sup>non-paralytic strabismus due to blindness, either RP [46] or traumatic blindness [36].

### Chapter 3: Gene expression profiling of patient-derived peri-orbital and extraocular muscle in treatment-resistant ophthalmoplegic myasthenia gravis

#### Abstract

**Introduction:** Genomic studies were previously used to identify potentially functional gene variants associated with the ophthalmoplegic myasthenia gravis (OP-MG) subphenotype by comparing the extreme phenotypes of OP-MG and control-MG subjects, and to generate hypotheses regarding pathogenetic mechanisms. To validate the findings of the unbiased NGS studies, we investigated the expression of the OP-MG genes and pathways identified by NGS single variant and gene-based analyses in patient-derived orbital muscles. **Methods:** Orbicularis oculi muscles (OOM) and one paralysed extraocular muscle (EOM) were sampled from six individuals with OP-MG during blepharoptosis and re-alignment surgeries, respectively. For controls, OOMs were sampled from four individuals without myasthenia undergoing surgery for non-muscle causes of ptosis, and one non-paralysed EOM was sampled during strabismus surgery. Using a custom qPCR array, the expression of 120 genes was compared in OP-MG and control orbital muscles including the putative “OP-MG” genes, genes in related biological pathways and genes previously reported to be dysregulated in MG cases or experimental MG models and in the EOMs of cases with strabismus. Normalization was performed with two stable reference genes for the OOMs and one for the EOMs. Differential gene expression was compared between OP-MG and control samples using the  $\Delta\Delta Cq$  method. Gene co-expression was analysed in OP-MG and control OOMs by pairwise correlation of gene transcripts to infer expression networks. Differential gene co-expression analysis was performed using the DiffCorr algorithm in OP-MG and control OOMs. **Results:** In the OP-MG OOMs, eight genes were significantly downregulated compared with controls ( $>2$ -fold;  $p \leq 0.016$ ), including *TFAM*, a mitochondrial transcription factor, and genes related to the following pathways: atrophy signalling; muscle regeneration and contraction; glycogen synthesis; and extracellular matrix remodelling. Several microRNAs, known to be highly expressed in EOMs, are predicted to regulate some of these genes. Co-expression analyses of gene pairs suggested high interconnectedness of gene expression networks in OP-MG muscle, but not controls ( $r > 0.96$ ,  $p < 0.01$ ). Functional modules included OP-MG genes with as yet poorly characterized biological function (*FAM92A1* and *PEF1*). Significant inverse directions of gene-pair correlations were noted in OP-MG versus controls OOM networks ( $r \geq 0.92$ ,  $p < 0.001$ ) involving most OP-MG genes overlapping prominently with muscle atrophy/contractility and oxidative metabolism genes. **Conclusion:** The gene expression in orbital muscles derived from OP-MG individuals compared with normal controls, support the pathogenic hypotheses previously generated from whole genome sequence analyses.

Repression of gene transcripts in OP-MG orbital muscle implicate tissue-specific regulatory mechanisms, which may inform future biomarker discovery approaches.

Reference: Europa, T. A., et al. (2020). "Gene expression profiling of orbital muscles in treatment-resistant ophthalmoplegic myasthenia gravis." Orphanet J Rare Dis **15**(1): 1-12.

## 1. Introduction

Previously, next generation sequencing (NGS) was used to dissect the molecular pathogenesis underlying the development of treatment-resistant ophthalmoplegic myasthenia gravis (OP-MG) (Nel, Jalali Sefid Dashti et al. 2017, Nel, Mulder et al. 2019). Several OP-MG susceptibility gene variants were identified (Nel, Jalali Sefid Dashti et al. 2017, Nel, Mulder et al. 2019). Genes identified as either harbouring OP-MG susceptibility variants or having a higher cumulative variant burden suggested potential pathogenetic pathways that were postulated to be altered in OP-MG (Nel, Mulder et al. 2019). The overall aim of the experiments discussed in this chapter, which describes the first investigations of OP-MG gene/pathway expression in patient-derived orbital muscles, is to verify the hypotheses generated by unbiased NGS studies in tissues relevant to the subphenotype.

Aims:

1. To compare gene expression in OP-MG and control extraocular muscles.
2. To compare gene expression in OP-MG and control orbicularis oculi muscles as surrogate orbital muscles due to limited availability of EOMs from live donors with the rare subphenotype of OP-MG.

### 1.1. Previous identification of putative OP-MG genes

In brief, Nel et al. first performed whole exome sequencing (WES), comparing well-characterized OP-MG cases with "control-MG" cases whose EOMs had responded well to immune therapies (Nel, Jalali Sefid Dashti et al. 2017). Next, whole genome sequencing (WGS) was performed using the same 'extreme-phenotype' sampling strategy (Nel, Mulder et al. 2019) to more comprehensively identify variants, including those in the non-coding genome. Subjects were matched for age, genetic ancestry and seropositivity (acetylcholine receptor positive MG). Single variant association analysis identified gene variants that were more frequent in OP-MG cases than control-MG cases and a tissue-based prioritization strategy was used to identify variants that had biological relevance in important muscle pathways. Some of these variants overlapped regulatory features active in muscle. Of these, variants in genes *FAM92A1* and *PEF1* were validated in a larger sample (Nel, Mulder et al.

2019). Although *FAM92A1* and *PEF1* have been shown to be expressed in skeletal muscle by RNA sequencing (Lonsdale, Thomas et al. 2013), their biological function is poorly characterized (Nel, Mulder et al. 2019).

In addition to the single variant analysis, Nel et al. performed a gene-based analysis in which variants identified as more frequent in OP-MG cases than control-MG cases were mapped to genes and those with a higher cumulative variant burden were prioritized based on their expression in skeletal muscle rather than EOMs for which availability of gene expression data is limited (see Chapter 5) (Lonsdale, Thomas et al. 2013, Nel, Mulder et al. 2019). The top genes identified by this strategy converged on common biological processes including muscle regeneration and atrophy signalling. Although the aim of this tissue-based prioritization approach was to select genes with biological relevance, a limitation of this approach was that the selection of genes was based on their expression and biological roles in skeletal muscle, rather EOMs for which there was lack of gene expression data. For simplicity, genes from both single-variant and gene-based analyses will be referred to in this study as putative “OP-MG genes”.

## 1.2. Rationale for investigating expression of OP-MG genes/ pathways in patient-derived orbital muscles

The comprehensive discovery of OP-MG associated gene variants posed the challenge of distinguishing disease-causing gene variants from benign individual variation (MacArthur, Manolio et al. 2014). This is particularly important in studies involving subjects with African genetic ancestry, as African genomes demonstrate a high degree of genetic diversity and are currently underrepresented in public databases (Nel, Mulder et al. 2019). This means that the burden of benign African-specific variants identified by association studies can be a significant limitation even with appropriate ancestry matching of case and control samples (Fan, Kelly et al. 2019).

It is also possible that the variant associations may be spurious (detected due to chance) (MacArthur, Manolio et al. 2014). The variant association signals in the WGS study did not reach genome-wide significance (Nel, Mulder et al. 2019), however this may be expected given the small sample size.

Although the OP-MG associated gene variants were predicted to be deleterious by *in silico* prediction algorithms (Nel, Mulder et al. 2019), it was important to verify these functional consequences *in vivo*. Even validated loss-of-function variants, once considered highly pathogenic since they completely disrupt the function of protein-coding genes, are found in healthy human genomes and may not necessarily contribute to the mechanisms underlying a specific phenotype (MacArthur, Balasubramanian et al. 2012, MacArthur, Manolio et al. 2014).

Therefore, to support the gene variant prioritization analyses and bioinformatics predictions which led to the identification of putative OP-MG susceptibility genes, we aimed to investigate the functionality of these candidates at the RNA level by investigating gene expression in patient-derived orbital muscles.

### 1.3. Rationale for tissue selection

The EOMs constitute a unique muscle allotype, having structural and functional characteristics that differ from other skeletal muscles (see Chapter 4) (Fischer, Budak et al. 2005, Porter, Israel et al. 2006). As we were investigating a subphenotype of MG characterized by treatment-resistant ophthalmoplegia, and differences in gene expression between OP-MG cases and controls were hypothesized to impact tissue-specific regulatory mechanisms, it was considered ideal to investigate the expression of putative OP-MG genes in EOMs.

Sampling of EOMs was opportunistic and limited to ocular re-alignment surgeries of OP-MG cases which is only considered in exceptional cases. Ocular re-alignment surgeries are considered in cases where the EOM weakness has not responded to years of immune therapies and without fluctuation in ocular symptoms despite the non-ocular symptoms being in remission (Heckmann and Nel 2017). As MG is a rare disease and the OP-MG subphenotype occurs in <20% of MG cases in our clinic (Heckmann and Nel 2017), few EOM samples could be obtained. We therefore widened our sampling strategy to include orbicularis oculi muscle (OOM), obtained during oculoplastic procedures for correction of ptosis in OP-MG cases and which are performed more frequently than ocular re-alignment surgeries in our setting (Heckmann and Nel 2017). Although the EOMs constitute a unique muscle allotype, it was considered that orbicularis oculi, a facial muscle that surrounds the orbit and is responsible for eye closure, may also be informative as it is comparable to the EOM allotype in structure and function in contrast with non-orbital muscles (Nelson and Blaivas 1991). In order to maintain ocular alignment and perform reflex and voluntary eye movements, the EOMs have fast firing rates, demonstrate fatigue resistance and high oxidative capacities and are capable of constant regeneration (Fischer, Budak et al. 2005, Verma, Fitzpatrick et al. 2017). As OOMs are responsible for eye closure, they demonstrate similar characteristics with faster firing rates and a greater capacity for oxidative metabolism than non-orbital muscles, although not to the same extent as the EOMs (Goodmurphy and Ovalle 1999, Sekulic-Jablanovic, Palmowski-Wolfe et al. 2015). Table 1 shows the similarities and differences between extraocular muscles, orbicularis oculi muscles and limb skeletal muscle.

Table 1. Comparison of extraocular muscles, orbicularis oculi and limb muscles

	Extraocular muscles	Orbicularis oculi	Limb skeletal muscle
Embryogenesis <sup>1,2</sup>	Pre-otic somitomeres	Second pharyngeal arch	Paraxial somites
Fibre composition <sup>3-5</sup>	Type II predominance	Type II predominance	Type I and II
Firing rate <sup>6</sup>	Fast, fatigue-resistant	Fast	Slower
Innervation <sup>5,7</sup>	MIF	SIF	SIF
Regeneration <sup>8,9</sup>	Constant	Intermittent	Intermittent
Mitochondrial content <sup>5,10</sup>	High	High	Variable

Table 1. Multiply-innervated fibres (MIF); singly-innervated fibres (SIF). References: 1. (Sevel 1986); 2. (Sevel 1988) 3. (Spencer and Porter 2006); 4. (McLoon and Wirtschafter 1991); 5. (Porter and Baker 1996); 6. (Cheng, Liao et al. 2007), 7. (Lander, Wirtschafter et al. 1996); 8. (Zhou, Cheng et al. 2009); 9. (Shih, Gross et al. 2007); 10. (Goodmurphy and Ovalle 1999).

The diagnosis of ocular myasthenia, the manifestation of MG that is persistently limited to ocular symptoms (see Chapter 1), excludes the involvement of all non-ocular muscles besides OOMs, and may be diagnosed on demonstration of “jitter” in OOMs on single fibre electromyography (SFEMG) (Milone, Monaco et al. 1993, Jaretzki, Barohn et al. 2000, Kupersmith and Ying 2005). That OOMs frequently manifest concurrent weakness with the EOMs in ocular myasthenia while non-orbital muscles remain unaffected, suggests a similar susceptibility to myasthenic molecular-genetic triggers.

For comparison with the OP-MG samples, we sampled EOMs and OOMs from control cases, i.e. individuals who do not have MG, during strabismus surgeries and oculoplastic procedures for conditions unrelated to muscle disorders (see Methods, section 2.1).

#### 1.4. Selection of genes for profiling in orbital tissues

It was hypothesized that the putative “OP-MG genes” function in a dysregulated gene network, triggered by MG molecular events, in which the EOMs are rendered more susceptible compared to limb muscles (Nel, Jalali Sefid Dashti et al. 2017, Nel, Mulder et al. 2019). Therefore, in addition to the putative OP-MG genes, genes in biological pathways related to

the functions of these genes were also profiled. To investigate the transcriptional effects of MG, genes previously shown to be up- or downregulated by MG in human limb muscles or *in vitro* models of experimental autoimmune myasthenia gravis (EAMG) were also included (Zhou, Kaminski et al. 2014, Kaminski, Himuro et al. 2016). In order to investigate the effects of reduced contractility on the regulation of biological pathways in EOMs, to which we previously postulated that the EOMs are particularly susceptible (see Chapter 2), we also profiled genes previously reported to have altered regulation in the EOMs of strabismus cases with ocular misalignment from causes other than MG (Altick, Feng et al. 2012, Agarwal, Feng et al. 2016). The rationale for populating each category of the array of genes was as follows:

a) Putative OP-MG genes and OP-MG pathways

The primary objective was to investigate the expression of putative “OP-MG genes” identified by unbiased NGS analyses (Nel, Mulder et al. 2019). Known biological functions of the OP-MG genes were informative in generating hypotheses regarding possible pathogenic pathways underlying OP-MG susceptibility. OP-MG genes therefore served as “seed queries” which informed the broader enquiry of additional gene candidates in related pathways. Pathogenetic themes generated by the OP-MG genes included muscle regeneration, atrophy signalling and mitochondrial function, pathways that were also implicated by histopathological evidence of atrophy and mitochondrial stress in MG muscle biopsies (Chapter 2) (Europa, Nel et al. 2019).

b) MG pathways

As the OP-MG muscle samples were compared to muscle from non-MG cases, the expression of genes associated with MG (“MG pathways”) were investigated; including a) genes encoding the antigenic targets in MG (nicotinic acetylcholine receptor and muscle-specific kinase) and b) genes shown to have altered expression in EOMs and other muscles of rodents with experimental autoimmune myasthenia gravis (EAMG) (Zhou, Kaminski et al. 2014, Kaminski, Himuro et al. 2016).

c) Strabismus pathways

Strabismus refers to ocular misalignment, which may be due to EOM paralysis or causes without intrinsic EOM weakness. In these cases, there may be abnormal EOM motility resulting from congenital or acquired abnormalities including altered innervation of the EOMs (other than denervation) or misalignment due to reduced sensory input caused by blindness (Altick, Feng et al. 2012, Agarwal, Feng et al. 2016). We therefore profiled the genes reported to show altered expression levels in the EOMs of cases with strabismus which may be

expected to be altered in the EOMs of OP-MG cases but not the OOMs which demonstrated good contractility clinically (Altick, Feng et al. 2012, Agarwal, Feng et al. 2016).

### 1.5. Strategies for analysing gene expression data

In conditions with complex molecular-genetic aetiology, the expression of multiple genes, often comprising a biological pathway, may be up- or downregulated as a result of abnormal co-regulation by common transactivators or repressors (Kostka and Spang 2004, van Dam, Vösa et al. 2017). It has been postulated that traditional methods of analysing gene expression in which the absolute levels of gene expression are compared between healthy and disease states, may be insufficient to detect patterns of abnormal gene co-regulation, which can manifest in small differences in gene expression unlikely to be identified with statistical significance by first order statistical methods of comparison such as student's t tests or analysis of variance (ANOVA) (Kostka and Spang 2004). We therefore reasoned that in analysing the gene expression data in this investigation of a subphenotype of myasthenia gravis suspected to have complex molecular-genetic aetiology, with limited sample size, and where the cumulative effect of multiple gene variants may alter the co-regulation of a network of genes in the EOMs (Nel, Jalali Sefid Dashti et al. 2017, Nel, Mulder et al. 2019), that in addition to identifying differentially expressed genes by first order statistics, second order statistical methods analysing co-variance should be used to investigate gene co-expression.

In a co-expression analysis, pairwise correlation of gene expression levels identifies genes with similar patterns of expression across a group of samples. These co-expressed genes frequently indicate important biological pathways (Chowdhury, Bhattacharyya et al. 2019). Potentially disease-causing genes and pathways are then identified by comparing gene co-expression between case and control phenotypes.

Genes may be co-expressed (strong positive correlation) in one phenotype but not the other (weak correlation) (figure 1A). Alternatively, genes may be co-expressed in one phenotype (strong positive correlation) but inversely co-expressed in the other (strong negative correlation), i.e. the directionality of correlation differs between the two phenotypes (figure 1B). The pathogenetic relevance of this type of differential co-expression (as illustrated in Figure 1B), referred to as a "switching mechanism", is that it identifies situations where a transcription factor acts as a transactivator in one phenotype but as a repressor in another (Kayano, Takigawa et al. 2011).

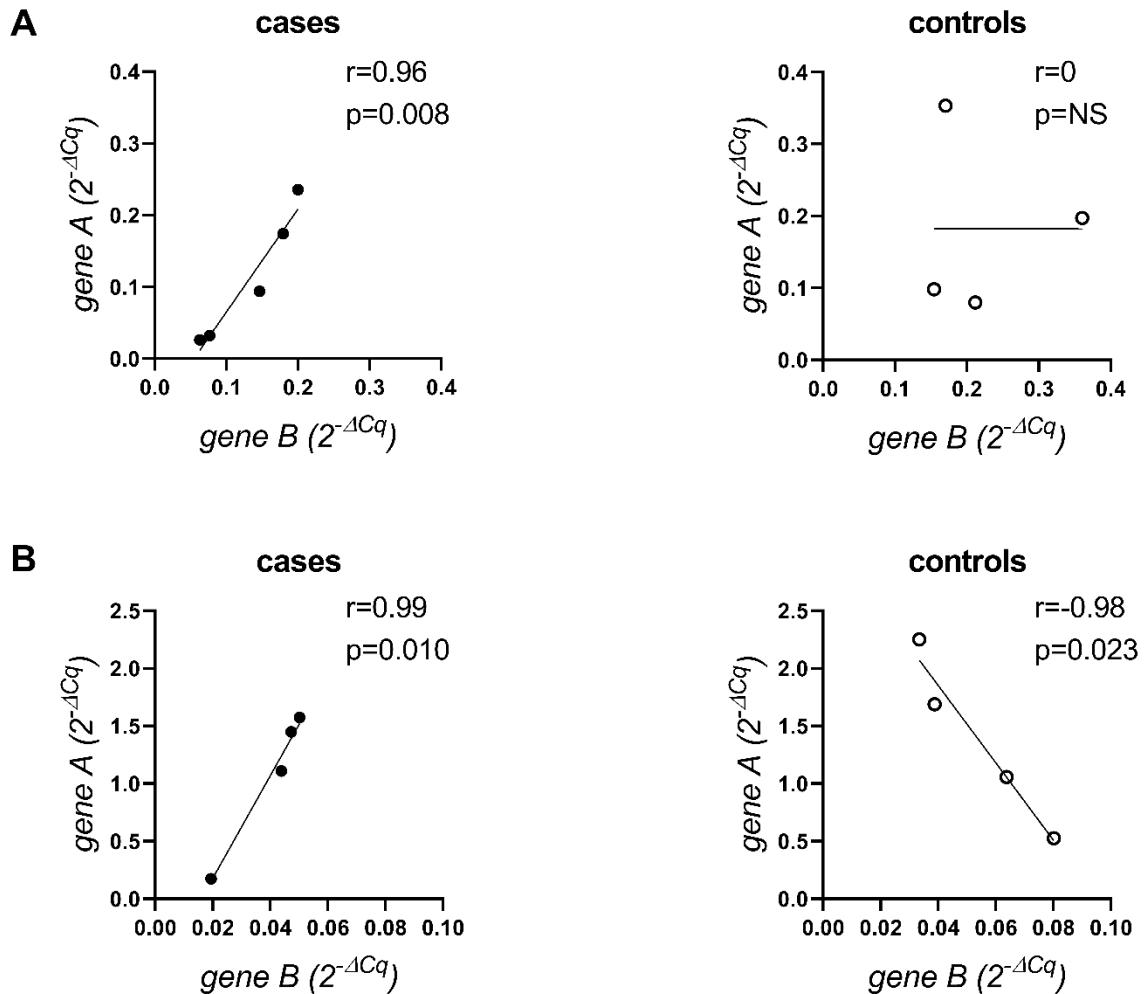


Figure 1. Graphs illustrating examples of differential co-expression between two phenotypes. A. Strong positive correlation between expression of gene A and gene B in case samples (co-expressed) but not in controls. B. Strong positive correlation between expression of gene A and gene B in cases (co-expressed) but strong negative correlation between expression of gene A and gene B in control samples (inversely co-expressed). Quantitation cycle value (Cq). The “r” value indicates the strength of correlation. P values  $>0.05$  are considered non-significant (NS). Data used to generate graphs were from the results of this study (see later) but produced here as examples.

In comparing gene co-expression between phenotypes, correlation plots may be informative in identifying differing patterns of co-expression. Co-expression network analysis has the additional advantage of providing insight into the functional relationships between genes, by analysis of their position and interconnections in the network. Genes of interest may be identified including a) co-expressed genes clustered in modules that frequently indicate biological pathways (Chowdhury, Bhattacharyya et al. 2019), b) highly interconnected genes that are key indicators of the main biological function of a module of co-expressed genes or

the entire network (van Dam, Vösa et al. 2017) and c) genes connecting modules which may serve regulatory functions (van Dam, Vösa et al. 2017). Using similar strategies, co-expression network analysis has recently been informative in identifying diagnostic biomarkers and novel therapeutic targets in Parkinson's disease and Alzheimer's disease (George, Singh et al. 2019, Wu, Chen et al. 2019). Another advantage of gene co-expression network analysis is that it may be useful in associating genes with unknown biological function with biological processes using the "guilt-by-association" approach (Chowdhury, Bhattacharyya et al. 2019).

Differential co-expression analysis refers to the statistical comparison of the correlations between gene pairs in each phenotype and identifies gene pairs that differ between phenotypes with statistical significance (Fukushima 2013, Chowdhury, Bhattacharyya et al. 2019). This type of analysis identifies genes that are co-expressed in one phenotype but inversely co-expressed in the other (as seen in Figure 1B).

In this study, the aforementioned strategies were used together to more comprehensively identify differentially expressed and co-expressed genes underlying the pathogenesis of OP-MG.

## 2. Methods

### 2.1. Patients and tissue collection

In selected treatment-resistant cases with ophthalmoplegic MG, surgery may be required to improve ptosis or ocular alignment (Heckmann and Nel 2017). These are exceptional cases in which the EOM weakness has been unresponsive to treatment despite years of immune therapies and where there is no diurnal fluctuation in ocular symptoms despite the non-ocular symptoms being in remission (Heckmann and Nel 2017). With written informed consent, we opportunistically sampled orbital muscles from OP-MG cases during oculoplastic procedures for ocular re-alignment (EOMs) and ptosis (OOMs). For controls, EOM samples were obtained from patients with strabismus and OOM samples were obtained from patients with ptosis due to causes other than MG. We obtained six OP-MG orbital muscle samples (1 EOM; 5 OOMs) and eight control orbital muscle samples (4 EOMs; 4 OOMs) (Table 2). The EOM samples consisted of either medial or lateral rectus muscle samples. In cases who underwent ptosis correction surgeries, where resection of orbital muscle was not required for the surgical procedure, patients consented to biopsy of the OOM. Samples were obtained with approval from the institutional Human Research Ethics Committee (HREC 257/2012 and 602/2020).

All patients from whom samples were obtained, self-identified according to South African racial census categories as having African genetic ancestry, comprising those who identified as

Black Africans or having mixed-African genetic ancestry, i.e. South African Cape “coloureds” who may mostly have Khoi San genetics as well as contributions from black Africans, Europeans and Asians, as previously determined by genome-wide studies by de Wit *et al.* (De Wit, Delpont *et al.* 2010, Heckmann and Nel 2017, Nel, Mulder *et al.* 2019). The OP-MG cases all had acetylcholine receptor positive MG (AChR-MG). Of the patients who were included in this study, only one was previously included in the WGS study. The aim here was to look for genetic signatures common to the OP-MG subphenotype rather than the profiling of each individual.

Importantly, OP-MG patients were only eligible for ptosis surgery if they had good OOM contractility as a precautionary measure to avoid post-operative exposure keratitis (Lenake and McNab 2017). Therefore, the OOMs of the OP-MG cases had reasonably good contractility. The EOMs of OP-MG cases however, had been paralysed for several years (Table 2). The EOM and OOM samples were dissected without cautery or clamping, immediately placed in RNAlater stabilization solution (Ambion, Texas, USA) and stored at -80°C according to the manufacturer’s protocol to preserve RNA integrity.

Table 2. Patient-derived extraocular muscle and orbicularis oculi muscle samples

Age at surgery (y)	Muscle samples	Diagnosis	MG duration (y)
27	EOM	OP-MG	15
52	EOM	Secondary esotropia*	NA
14	EOM	Congenital strabismus	NA
31	EOM	Secondary esotropia*	NA
77	EOM	Secondary esotropia*	NA
42	OOM	OP-MG	18
15	OOM**	OP-MG	7
27	OOM	OP-MG	10
34	OOM	OP-MG	14
55	OOM**	Levator dehiscence <sup>#</sup>	NA
51	OOM	Levator trauma <sup>#</sup>	NA
56	OOM	Canalicular obstruction <sup>#</sup>	NA

Table 1. Years (y); myasthenia gravis (MG) duration was taken from onset of symptoms. Extraocular muscle (EOM); ophthalmoplegic myasthenia gravis (OP-MG); \*esotropia secondary to blindness resulting from trauma, glaucoma or congenital blindness; orbicularis oculi (OOM). \*\*samples obtained from both eyes; <sup>#</sup> normal control OOM biopsied. Cases and controls were matched for genetic ancestry (African-genetic ancestry).

## 2.2. RNA isolation

### 2.2.1. Optimization of RNA isolation protocol using mouse skeletal muscle

Due to the fibrous nature of muscle tissue, RNA isolation from muscles requires thorough tissue disruption. The RNA isolation protocol was therefore optimized using mouse muscle samples before proceeding with the patient-derived orbital muscle samples. With consent from the institutional Animal Ethics Committee (AEC) (FHS AEC 018/001/JH), postmortem limb muscle samples (1-2mm) were dissected from mice who had already been euthanized under anaesthesia for the purpose of lab population control. A total of fifteen mouse skeletal muscle

samples (mostly tibialis anterior or gastrocnemius) were collected from three different mice and frozen in RNAlater stabilization solution at  $-80^{\circ}\text{C}$ .

Disruption of the mouse muscle in liquid nitrogen by mortar and pestle resulted in low RNA yields and RNA degradation. In the process of disruption, some of the sample was lost as it could not be completely retrieved from the mortar. Thawing of the sample during manual disruption likely contributed to RNA degradation. In comparison with manual disruption, homogenization of the muscle samples in TRI Reagent (Sigma-Aldrich, Missouri, USA) using a handheld homogenizer and sterile pellet tips (Pellet Pestle, Fisherbrand, Pittsburgh, USA) optimised RNA yield, preserved RNA integrity and helped to avoid contamination.

Phenol/chloroform precipitation has been reported to produce the greatest RNA yields from fibrous tissues (Nolan, Hands et al. 2006). However, it is possible for phenol, guanidine or ethanol contaminants to be co-eluted with the RNA and cause inhibition in downstream applications like qPCR. Alternatively, column-based methods with in-column DNase digestion produce purer RNA but often with lower yield (Nolan, Hands et al. 2006). Therefore, both methods of RNA isolation were tested on the mouse muscles samples. A combination of these methods, i.e., phenol/chloroform precipitation (TRI Reagent, Thermofisher, Massachusetts, USA) followed by spin-column purification with DNase digestion (Direct-zol Miniprep kit, Zymo Research, California, USA) produced the highest RNA yield ( $\approx 750\text{ng}$  total RNA) with acceptable spectrophotometric ratios ( $A_{260}/_{280} > 1.8$ ;  $A_{260}/_{230} > 1.2$ ) in the mouse muscle samples.

#### 2.2.2. RNA isolation, quantification and quality assessment in patient-derived orbital muscles

The optimized RNA isolation protocol as described in section 2.2.1 was used for the patient-derived orbital muscles. RNA was quantified using Nanodrop 1000 software (v3.5.2, Inqaba Biotechnical industries, Pretoria, RSA) and RNA integrity (RIN) was evaluated using the PicoChip Bioanalyzer (Agilent, California, USA). The muscle sample weights were 3 – 26mg yielding RNA concentrations of 5 – 49ng/ $\mu\text{L}$ . The  $A_{260}/_{280}$  (1.3 – 1.9) and  $A_{260}/_{230}$  (0.3 – 1.6) suggested some contamination by co-eluted reagents. RNA integrity (RIN) ranged between 5.2 and 7.6. The remaining protein was not kept for subsequent protein work. All patient-derived samples were reverse transcribed and used in the qPCR array. Table 3 shows the details of quality assessment for all patient-derived orbital muscle samples.

Table 3. Quality assessment of RNA extracted from the EOMs and OOMs

Tissue characteristics							Expression of reference genes		Expression of target genes	
Phenotype	Muscle	Weight (mg)	RIN	Conc.	A260/280	A260/230	(#expressed*/ #profiled)	Mean/median Cq (SD/IQR)	(#expressed*/ #profiled)	Mean/median Cq (SD/IQR)
OP-MG	EOM	21	5.2	49.0	1.9	1.6	5/5	20.1 (±3.63)	120/120	24.8 (±2.68)
<b>C</b>	<b>EOM</b>	<b>5</b>	<b>7.2</b>	<b>4.9</b>	<b>1.3</b>	<b>0.4</b>	<b>2/5</b>	<b>34.6 (34.4: 34.8)</b>	<b>14/120</b>	<b>33.8 (±0.67)</b>
<b>C</b>	<b>EOM</b>	<b>6</b>	<b>6.7</b>	<b>9.9</b>	<b>1.5</b>	<b>0.3</b>	<b>3/5</b>	<b>30.7 (±2.81)</b>	<b>45/120</b>	<b>32.9 (±1.29)</b>
<b>C</b>	<b>EOM</b>	<b>23</b>	<b>7.3</b>	<b>25.9</b>	<b>1.5</b>	<b>0.4</b>	<b>3/5</b>	<b>29.4 (±2.52)</b>	<b>76/120</b>	<b>31.8 (30.6: 33.1)</b>
C	EOM	8	7.5	40.1	1.9	0.8	5/5	20.8 (±3.45)	120/120	25.7 (±2.68)
OP-MG	OOM	7	7.6	11.3	1.7	0.9	5/5	22.4 (±3.58)	119/120	27.7 (±2.63)
OP-MG	OOM	3	7.3	15.6	1.6	0.4	5/5	26.8 (±2.82)	100/120	31.4 (29.4: 32.6)
OP-MG	OOM	8	6.1	9.3	1.8	0.8	5/5	24.0 (±3.25)	117/120	28.4 (±2.54)
OP-MG	OOM	6	6.9	18.6	1.6	0.5	5/5	25.5 (±3.60)	113/120	29.1 (±2.35)
OP-MG	OOM	6	6.6	35.3	1.6	0.4	5/5	25.3 (±3.23)	104/120	30.3 (28.9: 31.8)
C	OOM	11	7.4	11.8	1.8	1.0	5/5	22.1 (±3.37)	118/120	27.7 (26.2: 29.4)
C	OOM	9	7.0	18.3	1.7	0.5	5/5	23.4 (±3.73)	119/120	28.5 (±2.91)
C	OOM	12	6.7	4.9	1.6	0.3	5/5	26.5 (±3.91)	105/120	31.3 (29.5: 32.8)
C	OOM	26	5.5	39.7	1.9	0.7	5/5	27.4 (±3.15)	101/120	29.9 (28.1: 31.1)

Table 3. Measures determining sample quality and performance in qPCR array. Samples indicated in bold were excluded from data analyses based on the number of reference genes expressed by that sample and/or high average Cq values in comparison with other samples of that tissue type. RNA integrity number (RIN); concentration (conc.) measured in ng/μL; quantitation cycle (Cq). The Cq values indicated are the mean or median with the standard deviation (SD) or interquartile range (IQR) depending on data distribution (Shapiro-Wilk test of normality). \*Cq values<35. Ophthalmoplegic myasthenia gravis (OP-MG); control (C); extraocular muscle (EOM); orbicularis oculi (OOM).

### 2.3. Custom array plate

A total of 120 target genes and 5 reference genes were included in custom qPCR array plates (Qiagen, Hilden, Germany). The primer assay sequences are proprietary and therefore not included. The target genes were categorized into OP-MG genes, OP-MG pathways, MG pathways and strabismus pathways (Figure 2A). The reference genes were selected from genes that have previously been validated in human (Fischer, Budak et al. 2005, Andrade and McMullen 2006, Altick, Feng et al. 2012, Agarwal, Feng et al. 2016) and rodent EOMs (Fischer, Gorospe et al. 2002, Zhou, Kaminski et al. 2014, Kaminski, Himuro et al. 2016) (Figure 2A). We included those that showed stability across OP-MG and control-MG phenotypes in transdifferentiated myocytes (OP-MG vs control-MG) (Nel, Prince et al. 2019) and ocular fibroblasts (OP-MG and non-MG strabismus controls) (see Chapter 5). Gene categorization as shown in Figure 2 was based on the source of evidence for their relationship to OP-MG, MG or strabismus, however there is overlap between the different categories.



(ECM). “Strabismus pathways” refers to genes with altered expression in human strabismic extraocular muscles. References: 1. (Nel, Mulder et al. 2019); 2. (Nel, Jalali Sefid Dashti et al. 2017); 3. (McLoon and Wirtschafter 2003) 4. (Anderson, Christiansen et al. 2008) 5. (Verma, Fitzpatrick et al. 2017) 6. (McLoon, Harandi et al. 2014) 7. (Tryon, Vainshtein et al. 2014); 8. (Zhou, Kaminski et al. 2014); 9. (Kaminski, Himuro et al. 2016); 10. (Altick, Feng et al. 2012); 11. (Agarwal, Feng et al. 2016); 12. (Nel, Prince et al. 2019); 13. (Sekulic-Jablanovic, Ullrich et al. 2016).

#### 2.4. Reverse transcription and qPCR

For each orbital muscle RNA sample (OP-MG and controls), 40ng of RNA was reverse transcribed using the RT<sup>2</sup> First Strand Kit (Qiagen) according to the standard protocol of the manufacturer and qPCR was performed using the RT<sup>2</sup> SYBR Green Mastermix (Qiagen) on the QuantStudio 12K Flex thermocycler following standard cycling conditions as per the manufacturer’s instructions.

#### 2.5. Quality control

No genomic DNA contamination was detected in the samples (genomic DNA control Cq >35). The positive plate controls (PPC) showed no evidence of PCR inhibition (Cq<22). No inhibition of reverse transcription (RT) was evident (Cq<sub>RT</sub>-Cq<sub>PPC</sub> <5) despite some impurities in the RNA samples. However, three control EOM samples with the lowest RNA concentrations and RIN values were excluded from data analysis for quantitation cycle (Cq) values >35 for at least 15% of genes in the array (see Table 3).

#### 2.6. Reference gene selection

Reference genes for data normalization were selected separately for the EOMs and OOMs. For each muscle type, reference gene stability was assessed across all samples and between phenotypes (OP-MG and controls) to prevent bias in comparison of gene expression between phenotypes.

For the EOM samples, the exclusion of three control samples (Section 2.3.2, Table 2) necessitated the use of the variation in reference gene expression between only two EOM samples (OP-MG and control) for selection of the reference gene for normalization (Figure 3). As more OOM samples were available, suitable reference genes for normalization of this data

were selected using geNorm (Vandesompele, De Preter et al. 2002) and Bestkeeper methods (Pfaffl, Tichopad et al. 2004) (Figure 3). Appendix table 1 shows the details of this analysis.

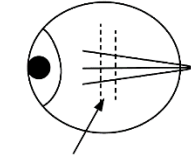
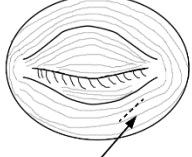
	ocular re-alignment surgeries	ptosis surgeries
<b>Sample source</b>	 extraocular muscle (EOM)	 orbicularis oculi (OOM)
<b>Samples that passed QC for data analysis (n)</b>	OP-MG (1) controls (1)	OP-MG (5) controls (4)
<b>Reference gene selection:</b>		
<b>Fold change (OP-MG/controls), t test</b>	Yes, ND	Yes, p=NS
<b>Bestkeeper</b>	ND	lowest SD and CV
<b>geNorm</b>	ND	lowest m value
<b>Differential gene expression analysis:</b>		
<b>Fold change (OP-MG/controls)</b>	Yes	Yes
<b>t tests</b>	ND	unpaired t tests/Mann-Whitney U
<b>correction for multiple testing</b>	ND	Benjamini-Hochberg correction
<b>Gene co-expression analyses:</b>		
<b>Correlation plots</b>	ND	OP-MG and control correlation matrices Hierarchical clustering (median)
<b>Gene co-expression networks (Cytoscape)</b>	ND	OP-MG and control co-expression networks Topological clustering
<b>Differential gene co-expression analysis (DiffCorr)</b>	ND	OP-MG vs controls

Figure 3. Workflow of experiments and data analysis. Patient-derived orbital muscle samples were acquired during ocular re-alignment or ptosis surgeries. RNA isolated from ophthalmoplegic myasthenia gravis (OP-MG) and control orbital muscles was used in a custom quantitative polymerase chain reaction (qPCR) array. “n” refers to the number of samples. “Not done” (ND) refers to statistical tests that could not be performed due to the small sample size. Non-significant p values (NS). Standard deviation (SD); coefficient of variance (CV). The geNorm m value is calculated by the geometric mean.

## 2.7. Differential gene expression

Raw quantitation cycle (Cq) values were captured and analysed in Microsoft Excel using the  $\Delta\Delta C_t$  method (Schmittgen and Livak 2008). Differences between OP-MG and controls were expressed as fold change (OP-MG/controls) or  $\log_2$  fold change for the purposes of graphical presentation by heatmap (Prism Graphpad v.8).

Comparison of only two EOM samples (1 OP-MG EOM vs 1 control EOM), precluded rigorous assessment of reference gene stability and tests of statistical significance. Therefore, the distribution of the  $\log_2$  fold change values (OP-MG/ control) was analysed and only outlying values with the greatest magnitude of fold change were considered as differentially expressed.

For the OOMs (OP-MG=5; controls=4), more robust statistical analyses were possible. In comparing OOMs of OP-MG and control cases, unpaired student's t tests were performed for normally distributed  $2^{-\Delta C_q}$  values and Mann-Whitney U tests for non-parametric data. Shapiro Wilk tests were performed to assess normality. As we performed multiple tests of statistical significance, the Benjamini Hochberg correction was performed on the results of the t tests and Mann-Whitney U tests (Benjamini and Hochberg 1995) (Figure 3). For one OP-MG case and one control, OOMs were obtained from both eyes. Although these samples came from the same individuals, the procedures for each eye were performed months apart these samples were therefore not treated as replicates in the data analyses.

## 2.8. Gene co-expression analyses

### 2.8.1. Identification of co-expressed genes by pairwise correlation of gene expression levels

Pairwise Pearson's correlations were performed on the normalised gene expression values ( $2^{-\Delta C_q}$ ) for all possible gene-pair permutations. Five genes that were not expressed in >1 sample were excluded from this analysis.

In Rstudio v.3.5.3, the "rcorr" function of the Harrel Miscellaneous ("Hmisc") R package (Harrell Jr 2019) was used to perform the pairwise correlation analysis for the five OP-MG OOMs. The "hclust" function was used to hierarchically cluster the resulting correlation matrix into modules of strongly correlated genes. As Hmisc requires a minimum of five samples, pairwise correlation of  $2^{-\Delta C_q}$  values for the 4 control samples was performed using Prism Graphpad v.8. The resulting correlation matrix was then manually re-ordered to the same gene-gene configuration as the clustered OP-MG correlation matrix for comparison.

### 2.8.2. Correlation plots

The aforementioned OP-MG and control correlation matrices were visualised as separate correlation plots using the "corrplot" function of the Corrplot R package in Rstudio v. 3.5.3. For

the correlation plots, an arbitrary correlation p value cut-off of 0.01 was decided a priori in order to show only the most significant gene-pair correlations. To compare patterns of co-expression, the hierarchically clustered OP-MG correlation plot was compared with the control correlation plot (section 2.8.1).

### 2.8.3. Co-expression network analysis

OP-MG and control co-expression networks were generated using Cytoscape (v.3.71), open source software used to generate network graphs in which genes, visualised as nodes, are connected by lines (edges) representing the correlation of expression levels between genes (Shannon, Markiel et al. 2003).

#### *Processing and import of data into Cytoscape*

In Rstudio, the “tidyr” package was used to organise the pairwise correlation data into tables which were written to Microsoft Excel files using the “xlsx” package. The data were filtered in Excel, identifying the same highly correlated gene pairs visualised in the correlation plots ( $p < 0.01$ ) (section 2.8.3). This data, consisting of the gene pairs, r values and p values, were imported into Cytoscape to generate the co-expression networks. Network “nodes” representing different genes were colour-coded for easier identification of the putative OP-MG genes within the network.

#### *Network layout*

For clear visual presentation, the prefuse force-directed layout, which prevents overlapping of nodes and edges, was applied to both OP-MG and control networks. Force-directed graphs are a well-established method of displaying data based on a mathematical algorithm in which repulsive forces between nodes and attractive forces between edge points are balanced for clear visualization of each gene-gene interaction. No additional attributes, for example r value, were used to influence the layout. Instead, r values and p values were shown in the networks by edge width or type. Edge width was used to show the strength of correlation between genes, with the most strongly correlated gene pairs having thicker edges (lowest p values, higher r values). Positively correlated genes pairs were shown with solid lines and negatively correlated pairs were shown with dotted lines.

#### *Network analysis*

The “network analysis” function in Cytoscape was used to calculate the node “degree”, an indicator of the interconnectedness of nodes. This enabled identification of the most highly interconnected nodes, or “hubs”, which are central to the function of the network. Clusters/modules of genes were identified visually and by the MCODE Cytoscape plug-in which makes

use of a topological clustering algorithm. Genes connecting modules (intermodular genes) which may have regulatory function were also identified.

#### 2.8.4. Statistical comparison of gene co-expression

The DiffCorr R package (Fukushima 2013) was used to perform a differential correlation analysis (Figure 3). In this analysis, correlation Z scores were used to calculate differences between OP-MG and control correlation matrices by means of Fisher's Z tests. Gene expression data ( $2^{-\Delta Cq}$  values) were imported into Rstudio to compute the differential correlation analysis using the "comp.2.cc.fdr" function. Gene pairs with a local false discovery rate  $>0.6$  (Efron 2007) were excluded.

#### 2.9. Identification of microRNAs that may alter gene expression in OP-MG orbital muscles

Here, the aim was to identify miRNAs potentially responsible for altered gene expression in the OP-MG OOMs. First, as the consequence of miRNA action is downregulation of mRNA, all genes downregulated  $\geq 1.5$ -fold in the OP-MG orbital muscles were identified. Next, a systematic search was performed in miRTarBase to identify miRNAs previously associated with the downregulated genes (Chou, Shrestha et al. 2018). Those previously reported to have  $\geq 2$ -fold higher expression in EOMs than limb muscle (Zeiger and Khurana 2010) were selected.

### 3. Results

#### 3.1. Differential gene expression analysis comparing OP-MG and control orbital muscles

##### 3.1.1. Extraocular muscle

The gene expression data from only two EOM samples (OP-MG 1; control 1) passed data quality analysis (Section 2.3.2, Table 2). Although the comparison of only two samples is a substantial limitation, this was the first opportunity to investigate the expression of OP-MG genes/pathways in the EOM of an OP-MG case. The paralysed medial rectus muscle of an OP-MG case was compared with the non-paralytic medial rectus muscle of a patient with ocular misalignment secondary to severe glaucoma. The reference gene *ACTB* was used for normalization as it showed similar expression levels across the two samples ( $SD=0.06$ ) (see Appendix table 1). The comparison of gene expression between only two samples necessitated stringent criteria for identifying differentially expressed genes.

The distribution of  $\log_2$  fold change values as illustrated in the quantile-quantile plot in Figure 4A, demonstrates that 50% of the genes showed 2-fold upregulation which may represent individual or chance variation rather than differences in gene expression due to pathology. However, five genes at the extremes of the dataset demonstrated an unexpected degree of difference in gene expression and are more likely to indicate pathological differences in gene expression. These five genes are presented in Figure 4B ( $\geq 10$ -fold).

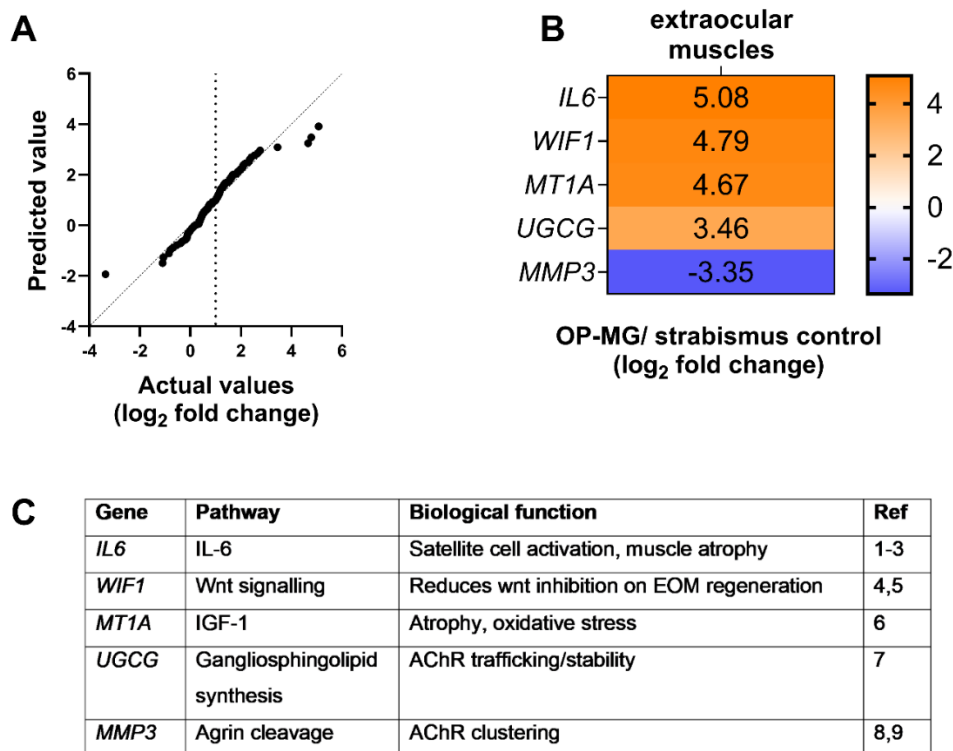


Figure 4. Genes differentially expressed between ophthalmoplegic myasthenia gravis (OP-MG) and controls. A. Quantile-quantile plot showing the distribution of  $\log_2$  fold change values between the OP-MG EOM and control EOM. The diagonal line of identity shows normally distributed values. The vertical dotted line represents the median  $\log_2$  fold change value. Outlying data points representing the genes with the greatest fold change in gene expression (OP-MG EOM/control EOM, fold change  $\geq 10$ ) are listed in the heatmap in Figure 4B. C. Functions of the genes in important muscle pathways. 1. (Maurer, Bougoïn et al. 2015). 2. (Haddad, Zaldivar et al. 2005). 3. (Munoz-Canoves, Scheele et al. 2013). 4. (McLoon, Harandi et al. 2014). 5. (Cisternas, Henriquez et al. 2014). 6. (Summermatter, Bouzan et al. 2017). 7. (Baier and Barrantes 2007). 8. (VanSaun and Werle 2000). 9. (Werle and VanSaun 2003).

The genes shown to be differentially expressed between OP-MG and control EOM samples (*IL6*, *WIF1*, *MT1A*, *UGCG* and *MMP3*), are found in muscle pathways relating to regeneration,

atrophy signalling and AChR stability/clustering on the muscle endplate (Figure 4C). Although this comparison is between two EOM samples, the results suggest that these muscle pathways may be dysregulated in OP-MG EOMs. Importantly, 2 of the 5 genes implicated are involved in AChR stability/clustering on the muscle endplate which may be expected to be altered in MG.

### 3.1.2. Orbicularis oculi muscle

Although the OP-MG cases had active MG, the orbicularis oculi muscles (OOMs) were not clinically weak unlike the OP-MG EOM. All OOMs (OP-MG 5; control 4) passed data quality analysis. Data normalization was performed using the average values for reference genes *RPLP0* and *ACTN2*. Genes that showed >2-fold change in expression (OP-MG/controls) with statistical significance after Benjamini Hochberg correction (false discovery rate (FDR) = 15%;  $p < 0.01$ ) were considered differentially expressed by phenotype, i.e. OP-MG vs control, and are presented in Figure 5A. Here, all the significantly differentially expressed genes were downregulated in the OP-MG muscles compared to the normal controls.

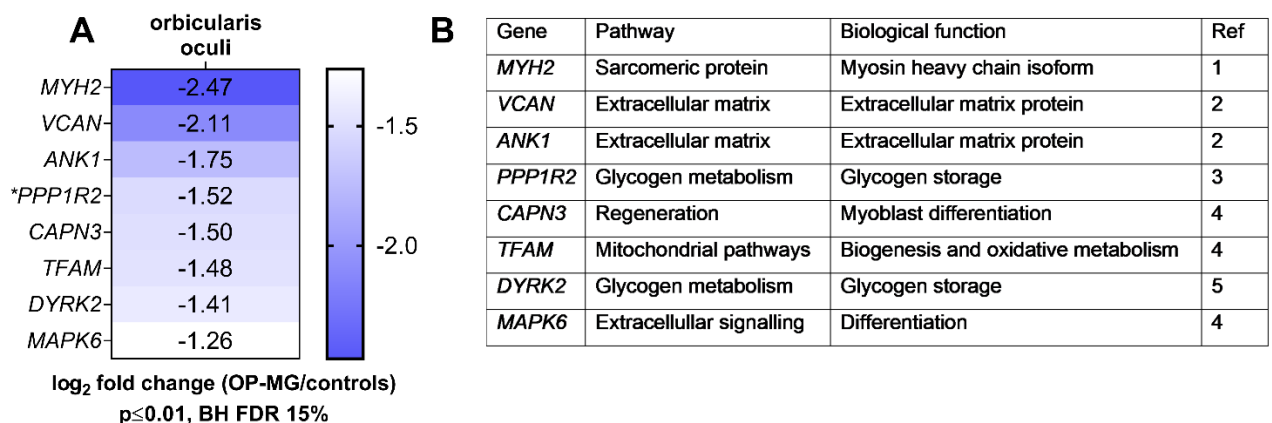


Figure 5. A. Significantly differentially expressed genes between the OP-MG and control orbicularis oculi muscles (fold change  $\geq 2$ ). P values were determined by unpaired t tests except for \**PPP1R2* ( $p = 0.016$ ) (Mann-Whitney U test). Benjamini Hochberg false discovery rate (BH FDR). B. Functions of the genes in important muscle pathways. 1. (Zhou, Liu et al. 2010). 2. (Altick, Feng et al. 2012). 3. (Nel, Mulder et al. 2019). 4. (Tryon, Vainshtein et al. 2014). 5. (Skurat and Dietrich 2004).

The known functions of the downregulated genes are summarized in Figure 5B. Genes related to muscle regeneration pathways, encoding structural proteins like *MYH2* which encodes the myosin heavy chain 2a isoform abundant in OOMs and EOMs (Cheng, Liao et al. 2007) (Park, Lim et al. 2012) and genes encoding extracellular matrix proteins versican (*VCAN*) and

ankyrin-1 (*ANK1*) (Altick, Feng et al. 2012) were downregulated in the OP-MG OOMs  $\geq 3$ -fold ( $p \leq 0.008$ ) (Altick, Feng et al. 2012). *CAPN3* encoding the protease calpain-3 and *MAPK6* encoding an extracellular signalling kinase (OP-MG pathways), are involved in sarcomeric remodelling and myoblast differentiation in regenerating muscle and were downregulated  $\geq 2$ -fold together with *TFAM* (OP-MG pathways), a major mitochondrial transcription factor which regulates mitochondrial biogenesis (Taveau, Bourg et al. 2003, Coulombe and Meloche 2007, Tryon, Vainshtein et al. 2014) ( $p < 0.009$ ). *DYRK2* (MG pathways) encoding dual specificity tyrosine phosphorylation regulated kinase-2, involved in glycogen storage was downregulated ( $p = 0.003$ ) (Skurat and Dietrich 2004). Of the eighteen putative OP-MG genes, *PPP1R2*, a gene identified by an unbiased whole genome sequencing analysis (as described by Nel, 2019) and encoding an inhibitory subunit of protein phosphatase-1, involved in myosin II phosphorylation and glycogen metabolism, was downregulated 2.9-fold ( $p = 0.016$ ), although this was not significant after correction for multiple testing (Figure 5A).

These results show statistically significant differences in gene expression between OP-MG and control OOM myotranscripts. Downregulation of genes in pathways relating to muscle regeneration and mitochondrial biogenesis, together with genes encoding structural muscle proteins suggested that although these muscles were not clinically weak, there was differential gene expression between OP-MG and controls in pathways important for muscle function.

### 3.2. Differential co-expression

#### 3.2.1. Visual comparison of gene-co-expression in orbicularis oculi muscle by phenotype

Using strongly correlated gene pairs ( $r > 0.96$ ,  $p < 0.01$ ) from pairwise correlation analysis of 115 genes in OP-MG OOMs (232 gene pairs) and control OOMs (92 gene pairs), correlation plots were generated. Hierarchical clustering of gene pairs (k-median) in the OP-MG correlation plot showed modules of co-expressed genes that may be functionally related (Figure 6A). For the same configuration of gene pairs, these modules were not observed in the controls suggesting that these genes are differentially regulated in OP-MG (Figure 6B).

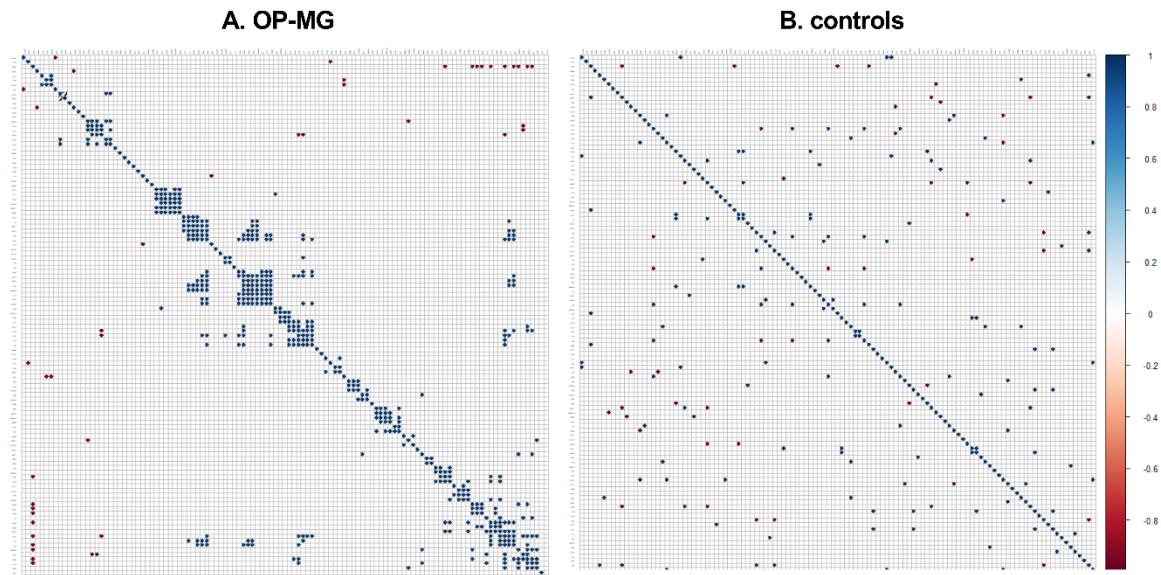


Figure 6. Visual comparison of gene co-expression between OP-MG and control orbicularis oculi muscle samples. Correlation plots A (OP-MG) and B (controls) show differing patterns of gene co-expression between OP-MG and control phenotypes. A. OP-MG correlation plot ordered by median hierarchical clustering ( $r > 0.96$ ;  $p < 0.01$ ). B. Controls correlation plot with gene pairs ordered to match configuration of OP-MG correlation matrix for comparison ( $r > 0.98$ ;  $p < 0.01$ ). Blue indicates positive correlations and red negative correlations.

### 3.2.2. Comparison of OP-MG and control OOM gene co-expression networks

Here, co-expression networks inferred from pairwise correlation of gene expression levels were analysed. Genes shown in each network, demonstrating strong correlations with others ( $p < 0.01$ ), are suggestive of having important functional roles in the orbital muscle and may even be disease-causing (van Dam, Vösa et al. 2017). The position and interconnectivity of genes in each network was used to infer potentially functional relationships and to draw comparisons between the OP-MG and control networks. As expected, based on the correlation plots, the OP-MG co-expression network (Figure 6) was densely clustered while that in controls (not shown) showed little interconnectivity consisting of small, discrete clusters.

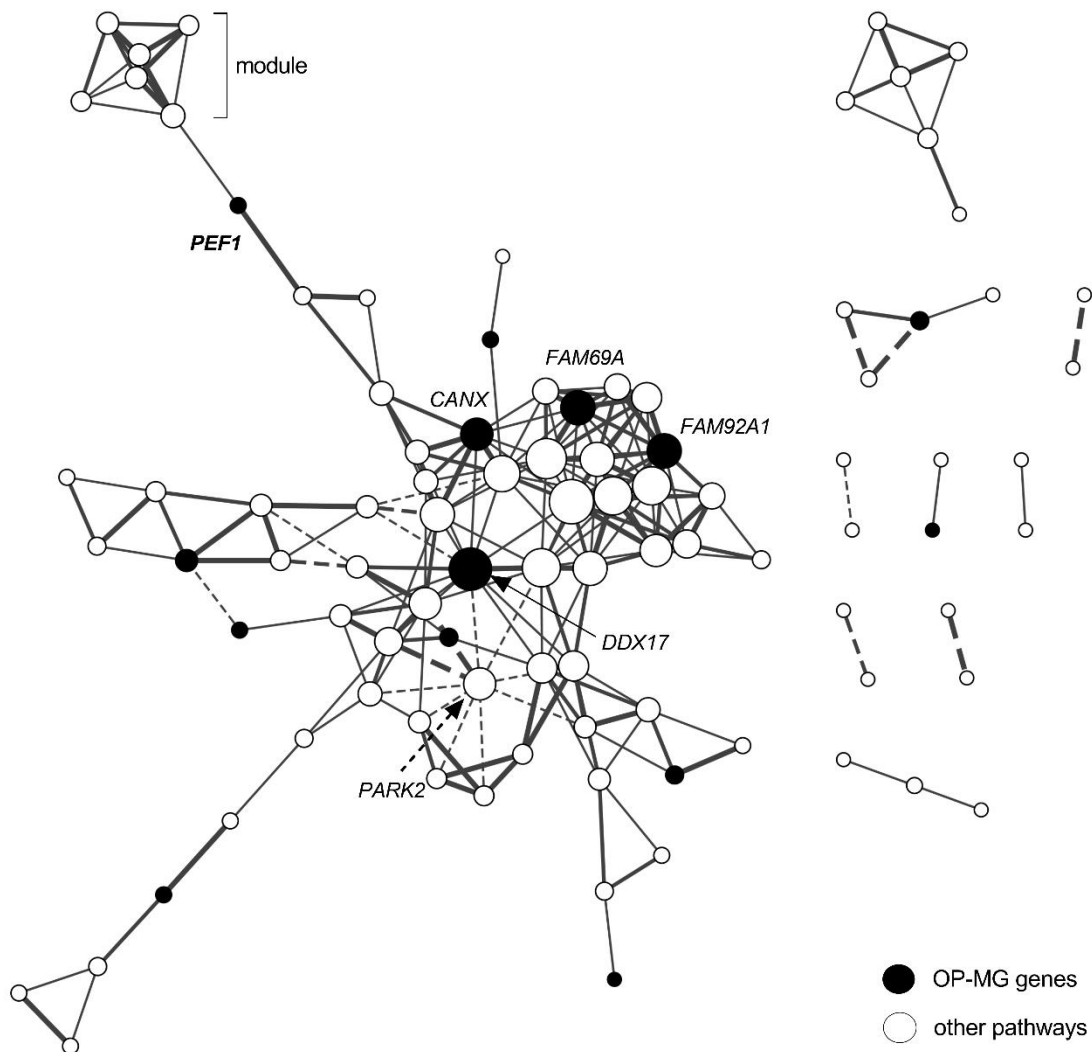


Figure 6. Gene co-expression network of ophthalmoplegic myasthenia gravis (OP-MG) orbicularis oculi muscles. A highly interconnected central module of genes connects to a smaller module by an intermodular, potentially regulatory gene *PEF1* (bold text). Degree of interconnectivity is shown by greater node size. Highly interconnected OP-MG genes, important to the function of the network, are labelled in plain text. Edges (interconnecting lines) are weighted by strength of correlation. Dotted lines indicate negative correlations vs solid lines indicating significantly positive correlations ( $r > 0.96$ ;  $p < 0.01$ ) (from Europa *et al*, 2020).

Putative OP-MG genes formed strong correlations in both OP-MG and control networks, suggesting that these genes have important functional roles in orbital muscles however, these gene interactions differed by phenotype, frequently being positively correlated in OP-MG and negatively correlated in controls, which suggests differential co-regulation between

phenotypes. The degree of interconnectivity of the OP-MG genes, which is suggestive of functional relevance, also differed between the two networks as seen in Table 4.

Table 4. Degree of interconnectedness of putative OP-MG genes compared by phenotype

Gene origin		Genes	Degree of interconnectivity	
			Controls network	OP-MG network
WGS gene-based analysis (Nel et al., 2019)		<i>AKT1S1</i>	2	-
		<i>MKNK2</i>	3	-
		<i>PPP1R2</i>	4	-
		<i>ZFP36L2</i>	-	2
		<i>MYL12B</i>	1	3
		<i>PPP1R12C</i>	1	3
		<i>SH3BGR</i>	1	5
		<i>FAM92A1</i>	3	11
WGS single-variant analysis (Nel et al., 2019)		<i>PEF1</i>	5	2
		<i>CANX</i>	4	10
WES single-variant analysis (Nel et al., 2017)		<i>DDX17</i>	3	15
		<i>FAM136A</i>	1	2
		<i>FAM69A</i>	2	11
		<i>IL6R</i>	4	3
		<i>PPP6R2</i>	2	1
		<i>SPTLC3</i>	4	1
		<i>ST8SIA1</i>	-	2

Table 4. The number of gene-gene interactions involving each of the putative ophthalmoplegic myasthenia gravis (OP-MG) genes (degree of interconnectivity) was compared in OP-MG and control co-expression networks. Genes are categorized by the next generation sequencing

analysis in which they were identified (Nel, Jalali Sefid Dashti et al. 2017, Nel, Mulder et al. 2019). Whole genome sequencing (WGS); whole exome sequencing (WES).

In the OP-MG network, *FAM92A1* and *PEF1*, identified by a genome-wide unbiased, single variant association with OP-MG (Table 1), and with poorly characterized biological function, showed multiple connections to other OP-MG genes/ pathways which were not observed in controls.

*FAM92A1* formed part of a large, central module including other highly interconnected OP-MG genes (*FAM69A*, *DDX17* and *CANX*) each interacting with  $\geq 10$  other genes involved in the regulation of muscle regeneration and atrophy signalling pathways. *FAM92A1* has recently been shown to have an important role in the maintenance of the mitochondrial inner membrane (Wang, Yan et al. 2019). Previously, using bioinformatics tools, *FAM69A* was predicted to form part of a novel family of kinases with EF-hand  $\text{Ca}^{2+}$  binding domains (Dudkiewicz, Lenart et al. 2012). *DDX17* is a master transcriptional regulator, coordinating different levels of gene expression in the process of myoblast differentiation (Dardenne, Espinoza et al. 2014). *CANX* encodes calnexin which is involved in the assembly of AChR subunits (Chang, Gelman et al. 1997). *PARK2* encoding parkin, a regulator of mitochondrial biogenesis/degradation and mitochondrial protein import (Jacoupy, Hamon-Keromen et al. 2019), negatively correlated with *DDX17* as well as with 10 other genes involved in mitochondrial biogenesis and muscle regeneration in the main network module (Figure 6).

*PEF1* was seen connecting this large module to a smaller module of co-expressed genes involved in mitochondrial biogenesis and oxidative metabolism, and its intermodular position in the network suggests regulatory function (Tryon, Vainshtein et al. 2014, Ketsawatsomkron, Keen et al. 2016). *PEF1* encodes an EF-hand protein involved in endoplasmic reticulum to golgi transport and may be involved in the regulation of apoptosis (Sargeant, Costain et al. 2020). The genes which were co-expressed with *PEF1* are listed in Table 5. Most of these genes previously showed altered expression in EAMG (Kaminski, Himuro et al. 2016). Although the exact functions of *PEF1* in muscle are still unclear, guilt-by-association in the OP-MG network suggests that *PEF1* may have a regulatory role, influencing the expression of genes relating to mitochondrial function and extracellular matrix remodelling.

Table 5. Genes co-expressed with *PEF1*

Gene	Function (biological pathway)
<i>ANGPTL4</i>	Mitochondrial metabolism (PGC-1 $\alpha$ )
<i>PPARG</i>	Mitochondrial biogenesis (PGC-1 $\alpha$ )
<i>FMO2</i>	Oxidation of foreign substances
<i>BCL2</i>	Activation of mitochondrial apoptosis (PGC-1 $\alpha$ )
<i>TIMP4</i>	Inhibitor of metalloproteinases (ECM remodelling)
<i>MMP16</i>	Metalloproteinase; attenuation of oxidative stress (ECM remodelling)

Table 5. Peroxisome proliferator-activated receptor gamma coactivator 1 $\alpha$  (PGC-1 $\alpha$ ), extracellular matrix (ECM), interleukin-6 (IL-6), “p53” refers to the biological pathway involving the tumour suppressor protein p53.

To summarise, gene co-expression network analysis demonstrated that a) putative OP-MG genes, identified from previous unbiased genomic data association analyses comparing extreme phenotypes of OP-MG and control-MG cases, were predicted to be involved in complex network interactions in OP-MG orbital muscle but not independent controls b) genes in pathways predicted to be involved in OP-MG and relating to muscle regeneration, atrophy signalling and mitochondrial metabolism were differentially co-expressed between OP-MG and control orbital muscles and c) an OP-MG gene with poorly characterized biological function (*PEF1*) showed potentially regulatory function in the co-expression network, connecting with genes relating to mitochondrial function and regulation of extracellular matrix composition. Although co-expression network analysis was useful in qualitatively identifying differences in gene co-expression between phenotypes, differential co-expression analysis was next used to quantitatively identify significant differences in gene co-expression.

### 3.2.3. Differentially co-expressed gene pairs between OP-MG and control OOMs

Statistical comparison of gene co-expression between OP-MG and control OOMs identified 110 strongly correlated gene pairs that showed positive correlations in one phenotype but

negative correlations in the other (Fisher's Z tests,  $p < 0.01$ ). As expected, based on the topology of the co-expression networks (section 3.2.2), most gene pairs were positively correlated in OP-MG ( $n=80$ ) suggesting co-activation of genes in pathways predicted to be involved in the pathogenesis of OP-MG, while these were negatively correlated in controls (see section 1.5). The remaining 30 gene pairs were negatively correlated in OP-MG but positively correlated in controls. Positively correlated (co-expressed) genes in OP-MG OOMs mostly involved muscle atrophy (44%) and mitochondrial pathways (24%) (Tryon, Vainshtein et al. 2014), while negatively correlated genes pairs (inversely co-expressed) mostly involved stress-signal pathways (43%) (Kaminski, Himuro et al. 2016) and genes encoding myosin heavy chain isoforms highly expressed in EOMs (*MYH1*, *MYH3* and *MYH13*) (40%) (Fischer, Budak et al. 2005).

One third of the differentially co-expressed gene pairs (37/110) involved the putative OP-MG genes, although OP-MG genes only constituted 15% of all genes profiled in the array. These gene pairs, involving the OP-MG genes and showing significant inverse correlations, were visualized in a co-expression network shown in Figure 7.

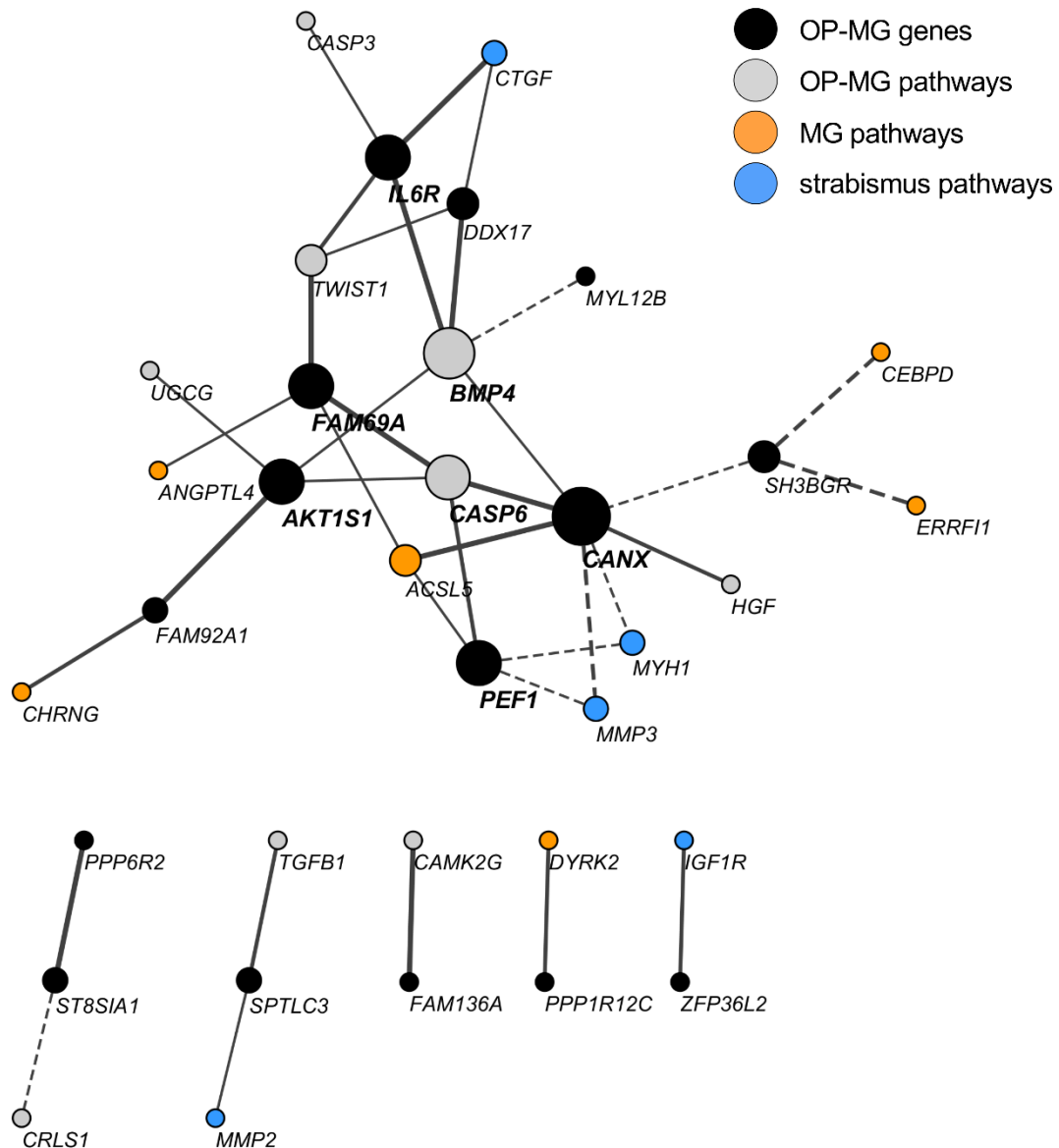


Figure 7. Differential co-expression between ophthalmoplegic myasthenia gravis (OP-MG) and control OOMs ( $p < 0.01$ ). Gene pairs involving the putative OP-MG genes ( $n = 37$ ) were visualised as a co-expression network. Solid lines indicate positively correlated gene pairs while dotted lines indicate negatively correlated gene pairs. All positively correlated genes in this network (OP-MG orbicularis oculi muscle) showed significant negative correlations in the control orbicularis oculi muscles as depicted in Figure 1.

Importantly, three genes identified in the genome-wide association study (Nel, Mulder et al. 2019) as having a significantly higher cumulative variant burden in OP-MG cases compared to control-MG cases, (*AKT1S1*, *MYL12B* and *SH3BGR*), were involved in a module of interconnected differentially co-expressed genes, including the genes identified by single variant analysis (*FAM92A1* and *PEF1*) as well as several genes previously identified by WES

association study (*CANX*, *FAM69A*, *DDX17* and *IL6R*). Although it was expected that the OP-MG genes would be shown to interact with genes in similar biological pathways (OP-MG pathways), they were also seen to interact with genes previously shown to have altered expression in EAMG (MG pathways), suggesting that aberrant regulation of this network of genes may be triggered by MG stimuli.

The most significant gene pairs identified in the differential co-expression analysis ( $n=13$ ,  $p\leq 0.001$ ) are shown in Figure 8A. More than half (8/13) of these gene-pairs include genes previously shown to be dysregulated in EAMG (Zhou, Kaminski et al. 2014, Kaminski, Himuro et al. 2016). Categorization of these gene pairs by the known functions of these genes in muscle (Figure 8B) suggested that muscle atrophy pathways are substantially altered in OP-MG OOMs compared with controls, viz. ubiquitin protease system (*CASP6*, *TMBIM6*), TGF $\beta$ /BMP4 superfamily (*BMP4*, *GADD45A*), IL6-pathway (*IL6R*) and IGF1-signalling pathway (*IGF1R*, *PIK3R1* and *MTOR*). The dysregulation of these muscle atrophy pathways may impact several other important processes in muscle including muscle regeneration and oxidative metabolism (Figure 8B).



### 3.3. Downregulated genes in OP-MG orbital muscle vs control muscle may be regulated by microRNAs

Differential gene expression analysis comparing OP-MG and control OOMs (Figure 4C), showed significant downregulation of several genes in OP-MG OOMs compared with control muscles. Post-transcriptional repression by microRNAs (miRNAs) is a potential mechanism by which these genes may have been downregulated (Zou, Kang et al. 2018). Gene variants in miRNA binding sites in the 3'UTR regions may result in altered miRNA binding and cause differential expression of a gene transcript.

MicroRNAs (miRNA) are small non-coding RNAs that regulate gene expression at a post-transcriptional level by binding to and degrading messenger RNA (mRNA) (Wang and Zhang 2020). It is estimated that one third of the human genome is regulated by miRNAs and deficiency (or excess) of miRNAs has been linked to many human diseases. MiRNAs are being increasingly studied in various autoimmune conditions including MG as potential diagnostic and prognostic biomarkers (Wang and Zhang 2020). They may also serve as potential novel therapeutic targets with the advancement of RNA molecular delivery technology (Wang and Zhang 2020). We therefore aimed to identify the miRNAs associated with genes that are shown to be downregulated in OP-MG orbital muscles compared with control muscles, to identify miRNAs that may be contributing to dysregulated pathways in OP-MG.

To determine which miRNAs may be involved in the potential miR-mediated mechanism of gene downregulation in OP-MG orbicularis oculi muscles, genes that were downregulated  $\geq 1.5$ -fold in OP-MG OOMs compared with controls were identified and miRNAs previously shown to be highly expressed in EOMs by Zeiger et al. were associated with these genes by experimentally validated data in the miRTarBase database (Zeiger and Khurana 2010, Chou, Shrestha et al. 2018). These predicted interactions are shown in Figure 9.

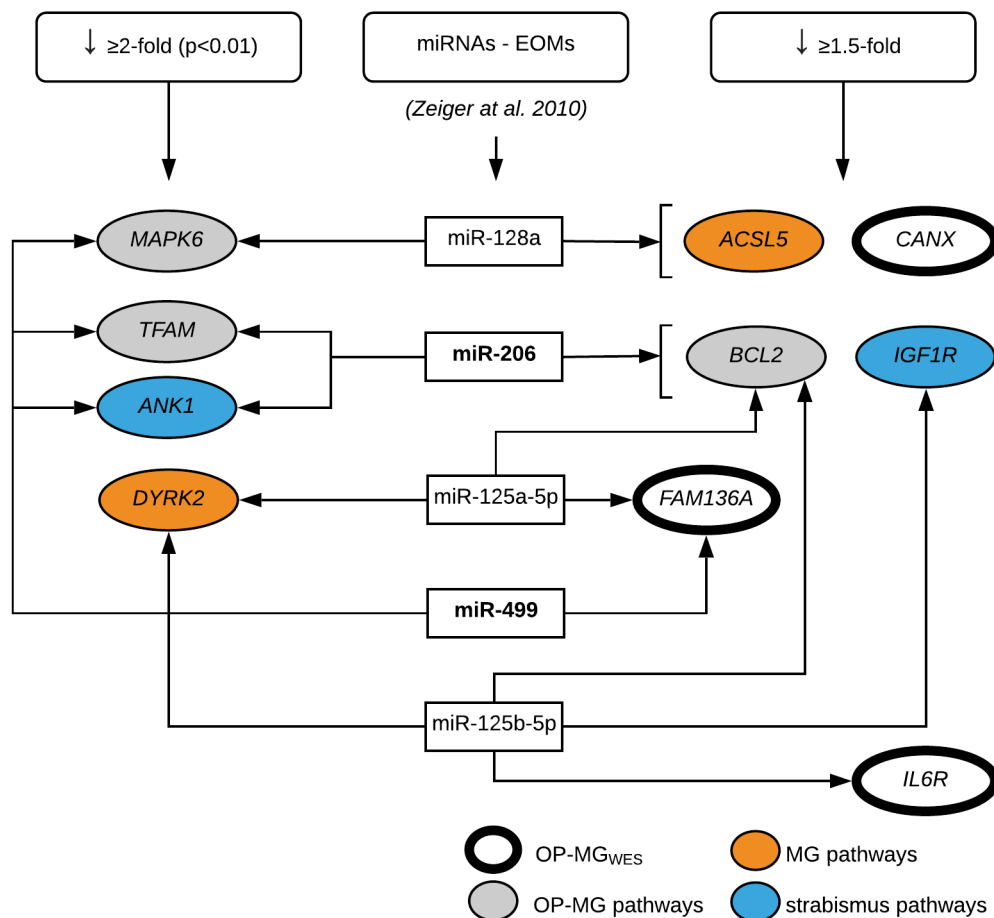


Figure 9. Potential messenger RNA (mRNA) and microRNAs (miRNAs) regulatory networks in extraocular muscle. Differentially downregulated genes in OP-MG orbicularis oculi muscle (Fig. 4) and differentially co-expressed genes (Figs. 6, 7) are listed in the columns to show potential mRNA-miRNA interaction with miRs known to be highly expressed in extraocular muscles (EOMs). Downward-facing arrows ( $\downarrow$ ) indicate downregulation. OP-MG<sub>WES</sub> refers to genes identified by whole exome sequencing analysis (Nel, Jalali Sefid Dashti et al. 2017). Downregulation of genes in ophthalmoplegic myasthenia gravis (OP-MG) orbital muscle may be mediated by microRNAs (miRNAs) that are highly expressed in extraocular muscles (EOMs).

MicroRNAs miR-206 and miR-499 were the most highly expressed in mouse EOMs (Zeiger and Khurana 2010) and in Figure 9 are shown to potentially interact with at least 3 downregulated genes in OP-MG OOMs. *CANX*, *FAM136A* and *IL6R*, OP-MG genes identified by whole exome sequencing by Nel et al., harbour 3'UTR OP-MG associated variants, which may alter microRNA binding in OP-MG muscles thereby decreasing mRNA expression (Nel, Prince et al. 2019). Therefore, the miRNAs depicted here may be causing downregulation of

the aforementioned transcripts in OP-MG orbital muscles and contributing to the pathogenesis of OP-MG.

#### 4. Discussion

Expression profiling was performed in patient-derived orbital muscles, investigating putative genes and pathways previously postulated to contribute to the pathogenesis of ophthalmoplegic myasthenia gravis (OP-MG) by unbiased, genome-wide studies (Nel, Jalali Sefid Dashti et al. 2017, Nel, Mulder et al. 2019). Genes and pathways previously prioritized as harbouring OP-MG associated variants were shown to be differentially regulated in OP-MG orbital muscles compared to independent controls and these findings therefore support their involvement in the pathogenesis of OP-MG.

Although previous gene association studies used an extreme-phenotype approach comparing OP-MG cases with MG cases whose EOMs responded well to immune therapies (control-MG) (Nel, Mulder et al. 2019), here we attempted to validate these associations by comparing the gene expression in the orbital muscles of OP-MG and non-MG control cases. Although gene expression was only investigated in two EOMs in this study, similar pathway dysregulation was observed in the EOMs as the orbicularis oculi muscles for which more robust data analysis was possible.

Genes related to the actin/myosin cytoskeleton and extracellular matrix proteins were significantly repressed in OP-MG orbicularis oculi muscles compared to controls. Although the orbicularis oculi muscles taken from MG cases were not paralysed i.e. demonstrated only mild to no spontaneous weakness although there have been fatigable weakness, muscle atrophy pathways appeared to be activated in these muscles compared to the non-MG controls. We previously postulated that reduced contractility in MG may drive OP-MG pathogenesis and that the EOMs may be most susceptible (Chapters 1 and 2)(Europa, Nel et al. 2019). However, activation of atrophy signalling in the non-paralytic OP-MG orbicularis oculi muscles suggests that stimuli other than reduced contractility may be activating atrophy signalling in the context of MG. Activation of pro-atrophy pathways may impact the regulation of mitochondrial function (Sandri 2008). Indeed, *TFAM* encoding a major mitochondrial transcription factor and genes involved in glycogen storage (*DYRK2* and *PPP1R2*) were also repressed in the OP-MG OOMs. Individuals with gene variants in these important muscle pathways relating to regeneration/atrophy and contractility, may be particularly susceptible to the molecular triggers in active MG and resultant loss of contractility. Although clinical observations of cases with myasthenic ophthalmoparesis in the first year of immune therapies (Chapter 1) suggested improved outcomes with higher doses of oral steroids, previous work has shown that dexamethasone can induce muscle atrophy by activation of E3-ubiquitin ligases resulting in downregulation of myosin heavy chain transcripts (Clarke, Drujan et al. 2007). In the clinical

context, as it is not known which individuals carry gene variants in these pathways, this may be an important consideration in decisions relating to immune therapies.

OP-MG genes identified by previous unbiased genomic association studies, including *FAM92A1* and *PEF1* (Nel, Mulder et al. 2019), featured prominently in the dysregulated gene networks suggesting that these genes may contribute to the aberrant gene regulation underlying the pathogenesis of OP-MG. Guilt-by association in the OP-MG network implicated *PEF1*, an EF-hand protein with potential kinase activity (Sargeant, Costain et al. 2020) as having a regulatory role involving genes related to mitochondrial function and extracellular matrix remodelling. Interestingly, since the prioritization of these genes, it was shown that *FAM92A1* is important for maintenance of the mitochondrial inner membrane (Wang, Yan et al. 2019). It has previously been suggested that mitochondrial metabolism, which is essential for EOM function, may be altered in the context of MG, as genes involved in the regulation of oxidative metabolism were shown to be upregulated in rodent EOMs in an experimental model of autoimmune myasthenia gravis (Kaminski, Himuro et al. 2016). Based on ultrastructural evidence of mitochondrial stress in the EOMs (and other muscles) of MG cases, thought to be secondary to reduced contractility, and the fact that the EOMs have unique metabolic requirements to support their constant firing rates, we hypothesized that the extraocular muscles may be more susceptible than other muscles to the effects of mitochondrial dysfunction in the context of MG (see Chapter 5).

As differential expression analysis mostly showed significantly downregulated transcripts, and it was posited that this may be a consequence of miRNA binding, five miRNAs highly expressed in EOMs (Zeiger and Khurana 2010) and previously shown experimentally to interact with the downregulated genes in OP-MG muscles, were identified by literature searches and use of an miRNA database (Chou, Shrestha et al. 2018). The downregulation of these transcripts may be the result of variants in 3'UTR regions. Identification of the miRNAs potentially involved in the altered regulation of these genes may be informative in subsequent research as diagnostic/ prognostic biomarkers or novel therapeutic targets.

The limited number of samples was a substantial limitation in this study however, because the opportunity to evaluate the expression of putative OP-MG genes in orbital tissue of a well-characterized OP-MG case is a rarity, even the comparison of a single OP-MG EOM to a control case was considered a valuable investigation. Stringent criteria were therefore used in the identification of differentially expressed genes between the single OP-MG and control EOM samples, although this may have contributed to type II error as only a few genes with the highest fold change were reported as differentially expressed. Although the orbicularis

oculi muscles share some characteristics with EOMs, they may not be fully representative of processes in EOMs.

In conclusion, the profiling of patient-derived orbital muscles supports the previous hypotheses regarding the pathogenesis of OP-MG generated using an extreme phenotype gene association approach. The findings suggest altered co-regulation of a network of genes in which putative OP-MG genes may have key functional roles and including pathways involved in muscle atrophy, muscle contractility and mitochondrial homeostasis. Co-expression analyses showed crosstalk between the OP-MG genes and those previously shown to be up- or downregulated in MG, suggesting that dysregulation of OP-MG pathways may be triggered in the context of MG. In the EOMs of susceptible individuals with MG, dysregulation of these pathways may contribute to the development of treatment resistant ophthalmoplegia.

## References

- Agarwal, A. B., C. Y. Feng, A. L. Altick, D. R. Quilici, D. Wen, L. A. Johnson and C. S. von Bartheld (2016). "Altered Protein Composition and Gene Expression in Strabismic Human Extraocular Muscles and Tendons." *Invest Ophthalmol Vis Sci* **57**(13): 5576-5585.
- Altick, A. L., C.-Y. Feng, K. Schlauch, L. A. Johnson and C. S. Von Bartheld (2012). "Differences in gene expression between strabismic and normal human extraocular muscles." *Investigative ophthalmology & visual science* **53**(9): 5168-5177.
- Anderson, B. C., S. P. Christiansen and L. K. McLoon (2008). "Myogenic growth factors can decrease extraocular muscle force generation: a potential biological approach to the treatment of strabismus." *Investigative ophthalmology & visual science* **49**(1): 221-229.
- Andrade, F. H. and C. A. McMullen (2006). "Lactate is a metabolic substrate that sustains extraocular muscle function." *Pflugers Arch.* **452**(1): 102-108.
- Baier, C. and F. Barrantes (2007). "Sphingolipids are necessary for nicotinic acetylcholine receptor export in the early secretory pathway." *Journal of neurochemistry* **101**(4): 1072-1084.
- Benjamini, Y. and Y. Hochberg (1995). "Controlling the False Discovery Rate: A Practical and Powerful Approach to Multiple Testing." *Journal of the Royal Statistical Society: Series B (Methodological)* **57**(1): 289-300.
- Chang, W., M. S. Gelman and J. M. Prives (1997). "Calnexin-dependent enhancement of nicotinic acetylcholine receptor assembly and surface expression." *Journal of Biological Chemistry* **272**(46): 28925-28932.
- Cheng, N.-C., S.-L. Liao, I.-J. Wang, I.-C. Lin and Y.-B. Tang (2007). "Fiber type and myosin heavy chain compositions of adult pretarsal orbicularis oculi muscle." *Journal of Molecular Histology* **38**(3): 177-182.
- Chou, C.-H., S. Shrestha, C.-D. Yang, N.-W. Chang, Y.-L. Lin, K.-W. Liao, W.-C. Huang, T.-H. Sun, S.-J. Tu, W.-H. Lee, M.-Y. Chiew, C.-S. Tai, T.-Y. Wei, T.-R. Tsai, H.-T. Huang, C.-Y. Wang, H.-Y. Wu, S.-Y. Ho, P.-R. Chen, C.-H. Chuang, P.-J. Hsieh, Y.-S. Wu, W.-L. Chen, M.-J. Li, Y.-C. Wu, X.-Y. Huang, F. L. Ng, W. Buddhakosai, P.-C. Huang, K.-C. Lan, C.-Y. Huang, S.-L. Weng, Y.-N. Cheng, C. Liang, W.-L. Hsu and H.-D. Huang (2018). "miRTarBase update 2018: a resource for experimentally validated microRNA-target interactions." *Nucleic acids research* **46**(D1): D296-D302.
- Chowdhury, H. A., D. K. Bhattacharyya and J. K. Kalita (2019). "(Differential) Co-Expression Analysis of Gene Expression: A Survey of Best Practices." *IEEE/ACM Trans Comput Biol Bioinform.*
- Cisternas, P., J. P. Henriquez, E. Brandan and N. C. Inestrosa (2014). "Wnt signaling in skeletal muscle dynamics: myogenesis, neuromuscular synapse and fibrosis." *Mol Neurobiol* **49**(1): 574-589.

- Clarke, B. A., D. Drujan, M. S. Willis, L. O. Murphy, R. A. Corpina, E. Burova, S. V. Rakhilin, T. N. Stitt, C. Patterson and E. Latres (2007). "The E3 Ligase MuRF1 degrades myosin heavy chain protein in dexamethasone-treated skeletal muscle." Cell metabolism **6**(5): 376-385.
- Coulombe, P. and S. Meloche (2007). "Atypical mitogen-activated protein kinases: Structure, regulation and functions." Biochimica et Biophysica Acta (BBA) - Molecular Cell Research **1773**(8): 1376-1387.
- Dardenne, E., M. P. Espinoza, L. Fattet, S. Germann, M.-P. Lambert, H. Neil, E. Zonta, H. Mortada, L. Gratadou and M. Deygas (2014). "RNA helicases DDX5 and DDX17 dynamically orchestrate transcription, miRNA, and splicing programs in cell differentiation." Cell reports **7**(6): 1900-1913.
- De Wit, E., W. Delpont, C. E. Rugamika, A. Meintjes, M. Möller, P. D. Van Helden, C. Seoighe and E. G. Hoal (2010). "Genome-wide analysis of the structure of the South African Coloured Population in the Western Cape." Human genetics **128**(2): 145-153.
- Dudkiewicz, M., A. Lenart and K. Pawłowski (2012). "A novel predicted calcium-regulated kinase family implicated in neurological disorders." Nature Precedings.
- Efron, B. (2007). "Size, power and false discovery rates." The Annals of Statistics **35**(4): 1351-1377.
- Europa, T. A., M. Nel and J. M. Heckmann (2019). "A review of the histopathological findings in myasthenia gravis: clues to the pathogenesis of treatment-resistance in extraocular muscles." Neuromuscul. Disord.
- Fan, S., D. E. Kelly, M. H. Beltrame, M. E. B. Hansen, S. Mallick, A. Ranciaro, J. Hirbo, S. Thompson, W. Beggs, T. Nyambo, S. A. Omar, D. W. Meskel, G. Belay, A. Froment, N. Patterson, D. Reich and S. A. Tishkoff (2019). "African evolutionary history inferred from whole genome sequence data of 44 indigenous African populations." Genome Biology **20**(1): 82.
- Fischer, M. D., M. T. Budak, M. Bakay, J. R. Gorospe, D. Kjellgren, F. Pedrosa-Domellof, E. P. Hoffman and T. S. Khurana (2005). "Definition of the unique human extraocular muscle allotype by expression profiling." Physiol Genomics **22**(3): 283-291.
- Fischer, M. D., J. R. Gorospe, E. Felder, S. Bogdanovich, F. Pedrosa-Domellof, R. S. Ahima, N. A. Rubinstein, E. P. Hoffman and T. S. J. P. g. Khurana (2002). "Expression profiling reveals metabolic and structural components of extraocular muscles." Physiol. Genomics **9**(2): 71-84.
- Fukushima, A. (2013). "DiffCorr: an R package to analyze and visualize differential correlations in biological networks." Gene **518**(1): 209-214.
- George, G., S. Singh, S. B. Lokappa and J. Varkey (2019). "Gene co-expression network analysis for identifying genetic markers in Parkinson's disease - a three-way comparative approach." Genomics **111**(4): 819-830.
- Goodmurphy, C. W. and W. K. Ovalle (1999). "Morphological study of two human facial muscles: Orbicularis oculi and corrugator supercilii." Clinical Anatomy **12**(1): 1-11.

- Haddad, F., F. Zaldivar, D. M. Cooper and G. R. Adams (2005). "IL-6-induced skeletal muscle atrophy." Journal of applied physiology **98**(3): 911-917.
- Harrell Jr, F. E. (2019). "Package 'Hmisc'." CRAN2018: 235-236.
- Heckmann, J. M. and M. Nel (2017). "A unique subphenotype of myasthenia gravis." Ann. N. Y. Acad. Sci.
- Jacoupy, M., E. Hamon-Keromen, A. Ordureau, Z. Erpapazoglou, F. Coge, J. C. Corvol, O. Nosjean, C. Mannoury la Cour, M. J. Millan, J. A. Boutin, J. W. Harper, A. Brice, D. Guedin, C. A. Gautier and O. Corti (2019). "The PINK1 kinase-driven ubiquitin ligase Parkin promotes mitochondrial protein import through the presequence pathway in living cells." Scientific Reports **9**(1): 11829.
- Jaretzki, A., 3rd, R. J. Barohn, R. M. Ernstoff, H. J. Kaminski, J. C. Keesey, A. S. Penn and D. B. Sanders (2000). "Myasthenia gravis: recommendations for clinical research standards. Task Force of the Medical Scientific Advisory Board of the Myasthenia Gravis Foundation of America." Neurology **55**(1): 16-23.
- Kaminski, H. J., K. Himuro, J. Alshaikh, B. Gong, G. Cheng and L. L. Kusner (2016). "Differential RNA Expression Profile of Skeletal Muscle Induced by Experimental Autoimmune Myasthenia Gravis in Rats." Front Physiol **7**: 524.
- Kayano, M., I. Takigawa, M. Shiga, K. Tsuda and H. Mamitsuka (2011). "ROS-DET: robust detector of switching mechanisms in gene expression." Nucleic Acids Research **39**(11): e74-e74.
- Ketsawatsomkron, P., H. L. Keen, D. R. Davis, K.-T. Lu, M. Stump, T. M. De Silva, A. M. Hilzendeger, J. L. Grobe, F. M. Faraci and C. D. Sigmund (2016). "Protective role for tissue inhibitor of metalloproteinase-4, a novel peroxisome proliferator-activated receptor- $\gamma$  target gene, in smooth muscle in deoxycorticosterone acetate-salt hypertension." Hypertension **67**(1): 214-222.
- Kostka, D. and R. Spang (2004). "Finding disease specific alterations in the co-expression of genes." Bioinformatics **20 Suppl 1**: i194-199.
- Kupersmith, M. and G. Ying (2005). "Ocular motor dysfunction and ptosis in ocular myasthenia gravis: effects of treatment." British journal of ophthalmology **89**(10): 1330-1334.
- Lander, T., J. D. Wirtschafter and L. K. McLoon (1996). "Orbicularis oculi muscle fibers are relatively short and heterogeneous in length." Invest Ophthalmol Vis Sci **37**(9): 1732-1739.
- Lenake, M. N. and A. A. McNab (2017). "The Posterior Approach Tarsal Switch Procedure for Myopathic Ptosis: A Modified Technique." Ophthalmic Plast Reconstr Surg **33**(2): 129-131.
- Lonsdale, J., J. Thomas, M. Salvatore, R. Phillips, E. Lo, S. Shad, R. Hasz, G. Walters, F. Garcia, N. Young, B. Foster, M. Moser, E. Karasik, B. Gillard, K. Ramsey, S. Sullivan, J. Bridge, H. Magazine, J. Syron, J. Fleming, L. Siminoff, H. Traino, M. Mosavel, L. Barker, S. Jewell, D. Rohrer, D. Maxim, D. Filkins, P. Harbach, E. Cortadillo, B. Berghuis, L. Turner, E.

Hudson, K. Feenstra, L. Sobin, J. Robb, P. Branton, G. Korzeniewski, C. Shive, D. Tabor, L. Qi, K. Groch, S. Nampally, S. Buia, A. Zimmerman, A. Smith, R. Burges, K. Robinson, K. Valentino, D. Bradbury, M. Cosentino, N. Diaz-Mayoral, M. Kennedy, T. Engel, P. Williams, K. Erickson, K. Ardlie, W. Winckler, G. Getz, D. DeLuca, D. MacArthur, M. Kellis, A. Thomson, T. Young, E. Gelfand, M. Donovan, Y. Meng, G. Grant, D. Mash, Y. Marcus, M. Basile, J. Liu, J. Zhu, Z. Tu, N. J. Cox, D. L. Nicolae, E. R. Gamazon, H. K. Im, A. Konkashbaev, J. Pritchard, M. Stevens, T. Flutre, X. Wen, E. T. Dermitzakis, T. Lappalainen, R. Guigo, J. Monlong, M. Sammeth, D. Koller, A. Battle, S. Mostafavi, M. McCarthy, M. Rivas, J. Maller, I. Rusyn, A. Nobel, F. Wright, A. Shabalina, M. Feolo, N. Sharopova, A. Sturcke, J. Paschal, J. M. Anderson, E. L. Wilder, L. K. Derr, E. D. Green, J. P. Struwing, G. Temple, S. Volpi, J. T. Boyer, E. J. Thomson, M. S. Guyer, C. Ng, A. Abdallah, D. Colantuoni, T. R. Insel, S. E. Koester, A. R. Little, P. K. Bender, T. Lehner, Y. Yao, C. C. Compton, J. B. Vaught, S. Sawyer, N. C. Lockhart, J. Demchok and H. F. Moore (2013). "The Genotype-Tissue Expression (GTEx) project." Nature Genetics **45**: 580.

MacArthur, D., T. Manolio, D. Dimmock, H. Rehm, J. Shendure, G. Abecasis, D. Adams, R. Altman, S. Antonarakis and E. Ashley (2014). "Guidelines for investigating causality of sequence variants in human disease." Nature **508**(7497): 469.

MacArthur, D. G., S. Balasubramanian, A. Frankish, N. Huang, J. Morris, K. Walter, L. Jostins, L. Habegger, J. K. Pickrell, S. B. Montgomery, C. A. Albers, Z. D. Zhang, D. F. Conrad, G. Lunter, H. Zheng, Q. Ayub, M. A. DePristo, E. Banks, M. Hu, R. E. Handsaker, J. A. Rosenfeld, M. Fromer, M. Jin, X. J. Mu, E. Khurana, K. Ye, M. Kay, G. I. Saunders, M.-M. Suner, T. Hunt, I. H. A. Barnes, C. Amid, D. R. Carvalho-Silva, A. H. Bignell, C. Snow, B. Yngvadottir, S. Bumpstead, D. N. Cooper, Y. Xue, I. G. Romero, J. Wang, Y. Li, R. A. Gibbs, S. A. McCarroll, E. T. Dermitzakis, J. K. Pritchard, J. C. Barrett, J. Harrow, M. E. Hurles, M. B. Gerstein and C. Tyler-Smith (2012). "A Systematic Survey of Loss-of-Function Variants in Human Protein-Coding Genes." Science **335**(6070): 823-828.

Maurer, M., S. Bougoin, T. Feferman, M. Frenkian, J. Bismuth, V. Mouly, G. Clairac, S. Tzartos, E. Fadel, B. Eymard, S. Fuchs, M. C. Souroujon and S. Berrih-Aknin (2015). "IL-6 and Akt are involved in muscular pathogenesis in myasthenia gravis." Acta Neuropathol Commun **3**(1): 1.

McLoon, L. K., V. M. Harandi, T. Brännström, P. M. Andersen, J.-X. J. I. o. Liu and v. science (2014). "Wnt and extraocular muscle sparing in amyotrophic lateral sclerosis." **55**(9): 5482-5496.

McLoon, L. K. and J. Wirtschafter (2003). "Activated satellite cells in extraocular muscles of normal adult monkeys and humans." Invest Ophthalmol Vis Sci **44**(5): 1927-1932.

McLoon, L. K. and J. D. Wirtschafter (1991). "Regional differences in the orbicularis oculi muscle: conservation between species." Journal of the neurological sciences **104**(2): 197-202.

- Milone, M., M. L. Monaco, A. Evoli, S. Servidei and P. Tonali (1993). "Ocular myasthenia: diagnostic value of single fibre EMG in the orbicularis oculi muscle." J Neurol Neurosurg Psychiatry **56**(6): 720-721.
- Munoz-Canoves, P., C. Scheele, B. K. Pedersen and A. L. Serrano (2013). "Interleukin-6 myokine signaling in skeletal muscle: a double-edged sword?" FEBS J **280**(17): 4131-4148.
- Nel, M., M. Jalali Sefid Dashti, J. Gamielidien and J. M. Heckmann (2017). "Exome sequencing identifies targets in the treatment-resistant ophthalmoplegic subphenotype of myasthenia gravis." Neuromuscul Disord.
- Nel, M., N. Mulder, T. A. Europa and J. M. Heckmann (2019). "Using Whole Genome Sequencing in an African Subphenotype of Myasthenia Gravis to Generate a Pathogenetic Hypothesis." Front Genet **10**(136).
- Nel, M., S. Prince and J. M. Heckmann (2019). "Profiling of patient-specific myocytes identifies altered gene expression in the ophthalmoplegic subphenotype of myasthenia gravis." Orphanet J Rare Dis **14**(1): 24.
- Nelson, C. C. and M. Blaivas (1991). "Orbicularis oculi muscle in children. Histologic and histochemical characteristics." Investigative Ophthalmology & Visual Science **32**(3): 646-654.
- Nolan, T., R. E. Hands and S. A. J. N. p. Bustin (2006). "Quantification of mRNA using real-time RT-PCR." **1**(3): 1559.
- Park, K.-A., J. Lim, S. Sohn and S. Y. Oh (2012). "Myosin heavy chain isoform expression in human extraocular muscles: Longitudinal variation and patterns of expression in global and orbital layers." Muscle & Nerve **45**(5): 713-720.
- Pfaffl, M. W., A. Tichopad, C. Prgomet and T. P. Neuvians (2004). "Determination of stable housekeeping genes, differentially regulated target genes and sample integrity: BestKeeper–Excel-based tool using pair-wise correlations." Biotechnol. Lett. **26**(6): 509-515.
- Porter, J. D. and R. S. Baker (1996). "Muscles of a different 'color': The unusual properties of the extraocular muscles may predispose or protect them in neurogenic and myogenic disease." Neurology **46**(1): 30-37.
- Porter, J. D., S. Israel, B. Gong, A. P. Merriam, J. Feuerman, S. Khanna and H. J. Kaminski (2006). "Distinctive morphological and gene/protein expression signatures during myogenesis in novel cell lines from extraocular and hindlimb muscle." Physiol Genomics **24**(3): 264-275.
- Sandri, M. (2008). "Signaling in muscle atrophy and hypertrophy." Physiology **23**(3): 160-170.
- Sargeant, J., T. Costain, C. Madreiter-Sokolowski, D. E. Gordon, A. A. Peden, R. Mali, W. F. Graier and J. C. Hay (2020). "Calcium Sensors ALG-2 and Peflin Bind ER Exit Sites in Alternate States to Modulate Secretion in Response to Calcium Signaling." bioRxiv: 2020.2002.2022.944264.
- Schmittgen, T. D. and K. J. Livak (2008). "Analyzing real-time PCR data by the comparative C(T) method." Nat Protoc **3**(6): 1101-1108.

- Sekulic-Jablanovic, M., A. Palmowski-Wolfe, F. Zorzato and S. J. B. J. Treves (2015). "Characterization of excitation–contraction coupling components in human extraocular muscles." **466**(1): 29-36.
- Sekulic-Jablanovic, M., N. D. Ullrich, D. Goldblum, A. Palmowski-Wolfe, F. Zorzato and S. J. T. J. o. g. p. Treves (2016). "Functional characterization of orbicularis oculi and extraocular muscles." jgp. 201511542.
- Sevel, D. (1986). "The origins and insertions of the extraocular muscles: development, histologic features, and clinical significance." Transactions of the American Ophthalmological Society **84**: 488-526.
- Sevel, D. (1988). "A reappraisal of the development of the eyelids." Eye **2**(2): 123-129.
- Shannon, P., A. Markiel, O. Ozier, N. S. Baliga, J. T. Wang, D. Ramage, N. Amin, B. Schwikowski and T. Ideker (2003). "Cytoscape: a software environment for integrated models of biomolecular interaction networks." Genome research **13**(11): 2498-2504.
- Shih, H. P., M. K. Gross and C. Kioussi (2007). "Expression pattern of the homeodomain transcription factor Pitx2 during muscle development." Gene Expression Patterns **7**(4): 441-451.
- Skurat, A. V. and A. D. Dietrich (2004). "Phosphorylation of Ser640 in muscle glycogen synthase by DYRK family protein kinases." The Journal of biological chemistry **279**(4): 2490-2498.
- Spencer, R. F. and J. D. J. P. i. b. r. Porter (2006). "Biological organization of the extraocular muscles." **151**: 43-80.
- Summermatter, S., A. Bouzan, E. Pierrel, S. Melly, D. Stauffer, S. Gutzwiller, E. Nolin, C. Dornelas, C. Fryer and J. Leighton-Davies (2017). "Blockade of metallothioneins 1 and 2 increases skeletal muscle mass and strength." Molecular and cellular biology **37**(5): e00305-00316.
- Taveau, M., N. Bourg, G. Sillon, C. Roudaut, M. Bartoli and I. Richard (2003). "Calpain 3 Is Activated through Autolysis within the Active Site and Lyses Sarcomeric and Sarcolemmal Components." Molecular and Cellular Biology **23**(24): 9127-9135.
- Tryon, L. D., A. Vainshtein, J. M. Memme, M. J. Crilly and D. A. Hood (2014). "Recent advances in mitochondrial turnover during chronic muscle disuse." Integr Med Res **3**(4): 161-171.
- van Dam, S., U. Vösa, A. van der Graaf, L. Franke and J. P. de Magalhães (2017). "Gene co-expression analysis for functional classification and gene–disease predictions." Briefings in Bioinformatics **19**(4): 575-592.
- Vandesompele, J., K. De Preter, F. Pattyn, B. Poppe, N. Van Roy, A. De Paepe and F. Speleman (2002). "Accurate normalization of real-time quantitative RT-PCR data by geometric averaging of multiple internal control genes." Genome Biol. **3**(7): research0034.0031.

- VanSaun, M. and M. J. Werle (2000). "Matrix metalloproteinase-3 removes agrin from synaptic basal lamina." Journal of Neurobiology **43**(2): 140-149.
- Verma, M., K. R. Fitzpatrick and L. K. McLoon (2017). "Extraocular muscle repair and regeneration." Current ophthalmology reports **5**(3): 207-215.
- Wang, L., Z. Yan, H. Vihinen, O. Eriksson, W. Wang, R. Soliymani, Y. Lu, Y. Xue, E. Jokitalo, J. Li and H. Zhao (2019). "FAM92A1 is a BAR domain protein required for mitochondrial ultrastructure and function." The Journal of Cell Biology **218**(1): 97-111.
- Wang, L. and L. Zhang (2020). "Emerging Roles of Dysregulated MicroRNAs in Myasthenia Gravis." Frontiers in Neuroscience **14**(507).
- Werle, M. J. and M. VanSaun (2003). "Activity dependent removal of agrin from synaptic basal lamina by matrix metalloproteinase 3." Journal of Neurocytology **32**(5): 905-913.
- Wu, J., L. Chen, C. Zheng, S. Xu, Y. Gao and J. Wang (2019). "Co-expression Network Analysis Revealing the Potential Regulatory Roles of lncRNAs in Alzheimer's Disease." Interdisciplinary Sciences: Computational Life Sciences.
- Zeiger, U. and T. S. Khurana (2010). "Distinctive patterns of microRNA expression in extraocular muscles." Physiological Genomics **41**(3): 289-296.
- Zhou, Y., G. Cheng, L. Dieter, T. A. Hjalt, F. H. Andrade, J. S. Stahl, H. J. J. I. o. Kaminski and v. science (2009). "An altered phenotype in a conditional knockout of Pitx2 in extraocular muscle." **50**(10): 4531-4541.
- Zhou, Y., H. J. Kaminski, B. Gong, G. Cheng, J. M. Feuerman and L. Kusner (2014). "RNA expression analysis of passive transfer myasthenia supports extraocular muscle as a unique immunological environment." Invest. Ophthalmol. Vis. Sci. **55**(7): 4348-4359.
- Zhou, Y., D. Liu and H. J. Kaminski (2010). "Myosin heavy chain expression in mouse extraocular muscle: more complex than expected." Investigative ophthalmology & visual science **51**(12): 6355-6363.
- Zou, X., L. Kang, M. Yang, J. Wu and H. Guan (2018). "MicroRNA binding mediated Functional sequence variant in 3'-UTR of DNA repair Gene XPC in Age-related Cataract." Scientific Reports **8**(1): 15198.

Appendix table 1. Reference gene selection

Tissue/cells ( <i>n</i> OP-MG; <i>n</i> controls)	Extraocular muscles (1; 1)			
	Average fold change (OP-MG/controls)	p value	geNorm (m value)	Bestkeeper (SD; CV)
<i>RPLP0</i>	1.68	-	0.35	0.37; 1.43
<b><i>ACTB</i></b>	<b>0.94</b>	-	<b>0.71</b>	<b>0.04; 0.21</b>
<i>GAPDH</i>	1.41	-	0.40	0.25; 1.31
<i>CSNK2A2</i>	1.92	-	0.39	0.47; 2.70
<i>ACTN2</i>	2.77	-	0.67	0.74; 4.04
Average <i>ACTB-GAPDH</i>	1,15	-	0.29	0.10; 0.51
Average <i>RPLP0-CSNK2A2</i>	1.79	-	0.13	0.42; 1.94
Tissue/cells ( <i>n</i> OP-MG; <i>n</i> controls)	Orbicularis oculi (4; 5)			
	Average fold change (OP-MG/controls)	p value	geNorm (m value)	Bestkeeper (SD; CV)
<i>RPLP0</i>	0,98	0.977	1.58	1.13; 3.78
<i>ACTB</i>	0.40	0.439	1.71	2.11; 8.17
<i>GAPDH</i>	0.55	0.565	2.08	2.41; 10.33
<i>CSNK2A2</i>	0.91	0.891	1.40	1.70; 7.44
<i>ACTN2</i>	1.39	0.559	1.50	1.05; 4.74

<b>Average</b>	<b><i>RPLP0-</i></b>	<b>1.19</b>	<b>0.769</b>	<b>0.44</b>	<b>1.09; 4.19</b>
<b><i>ACTN2</i></b>					

Appendix table 1. Table. “*n*” refers to the number of samples. Ophthalmoplegic myasthenia gravis (OP-MG); Fold change =  $2^{-\Delta Cq}$  ( $\Delta Cq = OP-MG Cq^{ref} - controls Cq^{ref}$ ). “Average fold change” refers to the arithmetic mean of OP-MG  $2^{-Cq}$  divided by the arithmetic mean of the controls. The p value of unpaired t tests comparing OP-MG and control  $2^{-Cq}$  values is presented for orbicularis oculi samples where the number of samples (OP-MG and controls) ( $n > 2$ ). For the EOMs, only the fold change is presented ( $n = 2$ ). The “geNorm m value” refers to the average expression stability value calculated using the geometric mean. SD is the standard deviation and CV is the coefficient of variance. Four RNA samples with low concentrations and spectrophometric evidence of impurity, were excluded from this analysis as their Cq values were significantly higher than others of the same tissue type although there was no evidence of reverse transcription of PCR inhibition based on the plate controls (RTC-PPC < 5, PPC < 22).

## Chapter 4: Gene expression in human extraocular and orbicularis oculi muscles

### Abstract

**Introduction:** The extraocular muscles (EOMs) constitute a unique muscle allotype and may be differentially susceptible in neuromuscular diseases. As human EOMs are rarely available for biopsy, gene expression data for human EOMs from live donors in public databases are sparse. The craniofacial orbicularis oculi muscles (OOMs) have similar embryological origin and share some functional characteristics with the EOMs but are more accessible for biopsy. Here, novel gene expression data in human EOMs and OOMs are reported, with a comparison of gene expression in the two muscle allotypes in a custom array. **Methods:** EOMs were sampled from two patients undergoing ocular re-alignment surgery and OOMs from seven patients undergoing oculoplastic procedures. A quantitative polymerase chain reaction (qPCR) array was used to quantify the expression of 120 genes in important muscle pathways including 70 genes not previously profiled in human EOMs/OOMs by qPCR (but expected to be expressed) and 5 reference genes. Gene expression was compared between EOM and orbicularis oculi muscle samples using the comparative CT ( $\Delta\Delta Cq$ ) method using *RPLP0* and *ACTN2* as reference genes. **Results:** All genes of interest (n=120) were expressed in the 2 EOMs, but 7 genes were not expressed in  $\geq 4/9$  OOM samples. Differential expression between EOM and OOM allotypes was shown for 10 genes ( $p < 0.029$ ) although only 2 genes showed statistically significant differences after Benjamini-Hochberg correction (FDR 5%,  $p < 0.0001$ ). *MYH3* encoding the embryonic myosin heavy chain isoform was upregulated 9-fold in the EOMs ( $p < 0.00001$ ) compared to OOM while the adult isoforms (*MYH1* and *MYH2*) and the EOM-specific isoform *MYH13* were similarly expressed in EOMs and OOMs ( $p > 0.44$ ). Acetylcholine receptor subunit expression differed significantly between EOMs and OOMs with expression of the  $\alpha$ -subunit (*CHRNA1*) being upregulated 10-fold in the EOMs ( $p = 0.0003$ ) and the  $\epsilon$ -subunit 3-fold ( $p = 0.021$ ). *MYOG*, *ANKRD1*, *CTGF* and *TNC* encoding genes relating to muscle regeneration and extracellular matrix regulation were upregulated  $>2$ -fold in the EOMs ( $p < 0.029$ ). The expression of 31 genes relating to muscle metabolism was similar in EOMs and OOMs ( $p > 0.15$ ). **Conclusion:** Orbicularis oculi muscles showed similar gene expression in 118 genes studied to EOMs and may serve as a reasonable surrogate tissue for EOMs in gene expression analyses.

## 1. Introduction

Although it was not the primary aim, gene expression profiling in patient-derived extraocular and orbicularis oculi muscles (Chapter 4), produced novel gene expression data of specialised skeletal muscles for which publicly available gene expression data is currently sparse. The extraocular muscles (EOMs) are considered a unique muscle allotype due to their unique fibre composition, firing rate, fatigue-resistance and metabolic characteristics (Fischer, Gorospe et al. 2002, Porter, Israel et al. 2006). Although published data exist of gene expression in EOMs, few are based on live human biopsy samples and are mostly limited to animal and post-mortem human samples and even less gene expression data is available for orbicularis oculi muscle. The gene expression of EOMs and orbicularis oculi muscles, opportunistically sampled from live patients and measured by a highly sensitive method of gene quantitation, viz. quantitative polymerase chain reaction (qPCR), is described in this chapter.

### 1.1. Previous work investigating gene expression in extraocular and orbicularis oculi muscles

#### 1.1.1. Extraocular muscle gene expression

A systematic search of the literature was conducted to establish prior knowledge of gene expression in EOMs and orbicularis oculi muscles in order to identify the novel contributions in our data. First, the Pubmed database was searched using the terms “gene expression”, “extraocular muscles”, “qPCR” and “microarray” which retrieved 161 English publications. Figure 1 shows the exclusion of articles that were not relevant to EOM gene expression or described semi-quantitative methods of analysing gene expression. Articles describing gene expression in levator palpebrae superioris, other cranial muscles and non-muscle orbital cells were excluded. Relevant reports were then categorized by method of investigation.

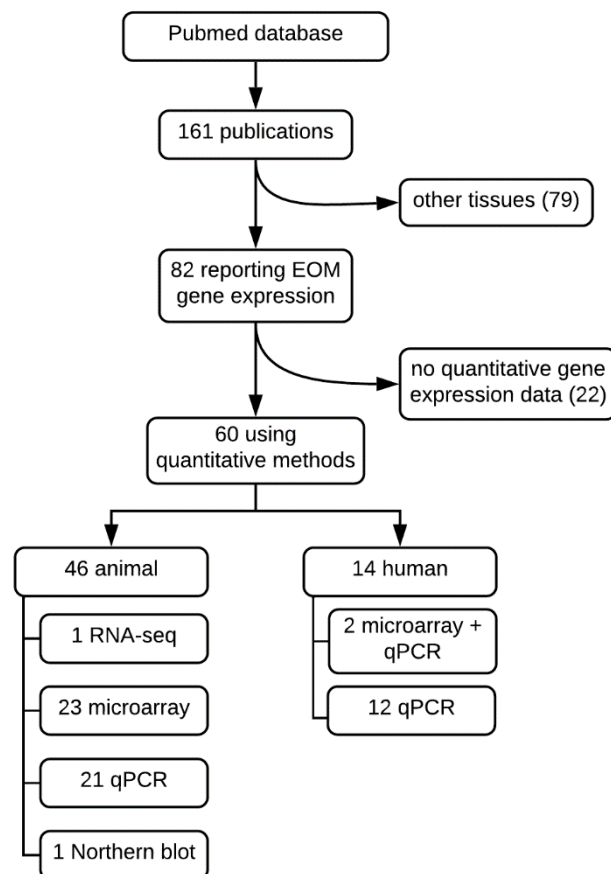


Figure 1. Flow diagram of literature search for publications reporting quantitative gene expression data for rectus or oblique extraocular muscles (EOMs). “Other tissues” includes levator palpebrae superioris or other cranial muscles, as well as EOM satellite cells and perimysial ocular fibroblasts. Quantitative polymerase chain reaction (qPCR); RNA sequencing (RNA-seq).

As sampling of EOMs requires surgery, study of gene expression in human EOMs has been limited to samples acquired opportunistically from patients undergoing surgery or from organ donors. Therefore, of the 60 articles using quantitative measures of gene expression, including qPCR, microarrays, RNA sequencing and northern blots, only one third were performed on human samples. However, due to differences in physiology and disease phenotype in animal models of human disease, it is difficult to infer transcriptional differences between animal EOMs and limb muscles on human EOMs (Fischer, Budak et al. 2005). Differences between animal and human EOMs have previously been shown in myosin heavy chain isoform expression and calcium homeostasis indicating that important differences exist between species at a transcriptional level (Fischer, Budak et al. 2005).

In the 14 studies profiling human EOMs, samples were mostly acquired post-mortem from organ donors or resected during surgeries for ocular misalignment due to strabismus or thyroid ophthalmopathy. However, the study of gene expression in post-mortem samples is not optimal as RNA integrity may be compromised after death affecting downstream applications such as qPCR (Koppelkamm, Vennemann et al. 2011). Investigation of gene expression in surgical specimens from live donors is therefore preferable however, it must be considered that gene expression in these samples may be altered by existing pathology or reduced contractility.

RNA-sequencing has recently been performed in rabbit EOMs which allowed a genome-wide survey of the EOM transcriptome however, this has not yet been replicated in human EOMs (Rodríguez, Sandgren Hochhard et al. 2019). At present, human EOM gene expression data is limited to few studies using microarrays and quantitative polymerase reaction (qPCR). Two studies have profiled hundreds of genes in human EOMs using microarrays (Fischer, Budak et al. 2005, Altick, Feng et al. 2012) however, both studies used post-mortem samples. Compared with qPCR, microarrays are less sensitive and genes with low expression levels may result in absent calls (Etienne, Meyer et al. 2004). Hybridization specificity is also a limitation in microarray studies (Koltai and Weingarten-Baror 2008). Therefore, qPCR, which has greater specificity and sensitivity, was used to validate a few of the top differentially expressed genes in both microarray studies. Although qPCR in human EOMs has also been performed in 12 additional studies, the number of genes that may be profiled with this method is much smaller than high-throughput methods such as RNA-sequencing and microarrays and therefore qPCR data in human EOMs is still very limited (see Table 1).

Table 1. Studies reporting gene expression data in human EOMs and orbicularis oculi muscle

Ref	Tissues and source of samples	Method	Genes (n)
1	EOMs, strabismus vs control (PM)	qPCR arrays	417
2	EOMs, TAO vs control (strabismus)	qPCR	7
3	EOMs, strabismus vs control (PM)	qPCR arrays	410
4	EOMs (strabismus) vs orbicularis oculi (surg.)* vs limb (surg.)	qPCR	11
5	EOMs (TAO) vs EOMs (strabismus)	qPCR	4
6	EOMs (strabismus), limb (surg.)	qPCR	16
7	EOMs, strabismus vs control (PM)	qPCR	9
8	EOMs, strabismus vs control (PM)	Microarray + qPCR array	89
9	EOMs (PM) vs limb** (biopsy)	Microarray + semi-quantitative qPCR	8
10	EOMs (strabismus)	Radiolabelled cDNA array	48
11	EOMs (TAO) vs non-ocular tissues (surg.)	qPCR	2
12	EOMs (TAO)	qPCR	10
13	EOMs (TAO)	qPCR	1
14	EOMs vs intercostal vs limb (all PM)	qPCR	2

Table 1. Ref (reference). “n” refers to the number of genes profiled by quantitative polymerase chain reaction (qPCR). Extraocular muscles (EOMs). “PM” refers to postmortem EOM specimens. “Surg.” refers to surgical specimens taken from live donors. \*only publication reporting gene expression data in orbicularis oculi muscle. \*\*EOMs compared with limb muscle from diagnostic biopsies for undiagnosed neuromuscular disorders and therefore potentially abnormal muscle. Thyroid-associated ophthalmopathy (TAO). References: 1. (Agarwal, Christensen et al. 2017); 2. (Romero-Kusabara, Filho et al. 2017); 3. (Agarwal, Feng et al. 2016); 4. (Sekulic-Jablanovic, Ullrich et al. 2016); 5. (Cheng, Yin et al. 2016); 6. (Sekulic-Jablanovic, Palmowski-Wolfe et al. 2015); 7. (Zhu, Deng et al. 2013); 8. (Altick, Feng et al. 2012); 9. (Fischer, Budak et al. 2005); 10. (Kitada, Matsuo et al. 2003); 11. (Agretti, Chiovato et al. 2002); 12. (Hiromatsu, Yang et al. 2000); 13. (Wu, Yang et al. 1999); 14. (MacLennan, Beeson et al. 1997).

#### 1.1.2. Reports on gene expression in orbicularis oculi muscles

The Pubmed database was searched using terms “orbicularis oculi”, “biopsies”, “gene expression”, “qPCR”, “microarrays” and “northern blots”. Much fewer reports on orbicularis oculi muscle exist. Most of the previous experimental work involving orbicularis oculi related

to oculoplastic procedures for ptosis or blepharospasm and the reports are mostly limited to histology and immunohistochemistry (Cheng, Liao et al. 2007, Choi, Charlton et al. 2012). Quantitative gene expression data in orbicularis oculi muscles is limited to one report (see Table 1) in which selected genes relating to contractile function were profiled and expression was compared between human EOMs, orbicularis oculi muscles and limb muscles (Sekulic-Jablanovic, Ullrich et al. 2016). Based on physiological characteristics, there is some evidence to suggest that orbicularis oculi gene expression may differ from limb and other cranial muscles and bare some similarities to EOM gene expression. However, due to the paucity of quantitative gene expression data in orbicularis oculi, this has not yet been proven.

As gene expression data was available from qPCR profiling of 125 genes in human EOMs and orbicularis oculi (see Chapter 4), here novel gene expression data in human EOMs and orbicularis oculi muscle is reported for a) genes not previously profiled in EOMs/ orbicularis oculi b) genes only previously shown to be expressed in EOMs in animal studies and c) genes only previously reported to be expressed in EOMs by microarray or RNA-sequencing and requiring validation by qPCR.

Aims:

1. Identify the genes that are most highly expressed in EOMs.
2. Determine whether the putative OP-MG genes (see Chapter 3), are expressed in EOMs and whether levels of gene expression are similar in EOMs and OOMs.
3. Describe novel gene expression data in human EOMs and OOMs and identify differences between the EOMs and OOMs.

## 2. Methods

### 2.1. Collection and processing of the orbital muscle samples

In brief, extraocular (n=2) and orbicularis oculi muscle samples (9) were obtained from live patients undergoing strabismus or ptosis surgeries and harvested without the use of clamps or cautery. Both EOM samples were taken from the belly of medial rectus muscles, including both orbital and global layers. The orbicularis oculi samples were collected as biopsies from the pre-septal portion and was therefore considered as orbital muscle rather than peri-orbital. The muscle samples were immediately preserved in RNAlater stabilization solution upon resection and stored at -80°C to protect RNA integrity. RNA was isolated using phenol/chloroform precipitation with subsequent spin-column purification and in-column DNase treatment to avoid genomic DNA contamination. The detailed methods of the orbital muscle processing are reported in Chapter 4. RNA was quantified using Nanodrop 1000

software (v3.5.2, Ingqaba Biotechnical industries) and showed A260/280 ratios of 1.3 – 1.9 and A260/230 ratios of 0.3 – 1.6. RNA integrity (RIN) values were measured using the Agilent 2100 Bioanalyzer and ranged between 5.2 and 7.6.

## 2.2. Selection of genes for profiling in human extraocular and orbicularis oculi muscles

Selected genes were profiled in EOMs and orbicularis oculi with the aim of investigating the molecular genetic pathogenesis of OP-MG (see Chapter 4). This array included putative “OP-MG genes”, identified by Nel et al. in previous unbiased analyses of next generation sequencing data (Nel, Jalali Sefid Dashti et al. 2017, Nel, Mulder et al. 2019) as either a) harbouring OP-MG susceptibility variants or b) having a higher cumulative variant burden in a gene-based analysis, in which case genes were prioritized based on their expression in limb skeletal muscle (Lonsdale, Thomas et al. 2013) as no previous expression data for these genes were available in EOMs. It was therefore important to establish whether these genes were expressed in EOMs, which suggests biological relevance of the putative genes identified by unbiased genome-wide analyses, and whether they were expressed in orbicularis oculi muscle, which was hypothesized to be informative as a surrogate orbital muscle for EOMs.

## 2.3. Reference gene selection

The average Cq values obtained from qPCR differed between the EOM (n=2) and OOM (n=9) sample groups. For example, average Cq values across the OOMs for 120 genes of interest and 5 reference genes, was substantially higher than the average Cq values for the EOMs (IQR<sub>orbicularis</sub> 28; 31 vs IQR<sub>EOMs</sub> 23; 27) ( $p < 0.0001$ , Mann-Whitney U test). This was uniformly observed across all genes profiled and likely relates to the RNA sample concentration (average concentration was 44.6 ng/ $\mu$ L in the EOMs vs 18.3 ng/ $\mu$ L in the OOMs). Although 40ng of RNA was reverse transcribed for each sample, pipetting error may have contributed to the difference in overall Cq values. The differences in the ranges of Cq values complicated the selection of stable reference genes. Reference genes were selected using Bestkeeper and geNorm methods (Rstudio v.3.5.3) as shown in Appendix table 1 and an average of *RPLP0* and *ACTN2*, the two most stable reference genes selected by these algorithms was used for normalization, although all reference genes profiled showed significant differences between EOMs and orbicularis oculi muscles ( $p < 0.004$ ).

## 2.4. Data analysis

Genes with Cq values  $< 35$  were considered as expressed. Differential gene expression analysis between EOMs and orbicularis oculi muscles was performed using the  $\Delta\Delta C_t$  method

(Schmittgen and Livak 2008). Unpaired student's t tests were performed for normally distributed  $2^{-\Delta Cq}$  values and Mann-Whitney U tests for non-parametric data. Benjamini Hochberg correction was performed for multiple tests of statistical significance (FDR 5%). Shapiro Wilk tests were performed to assess normality. Graphs were generated using Prism Graphpad V.8.

### 3. Results

Two high-quality EOM samples expressed all 125 genes profiled ( $Cq < 35$ ) including 120 genes of interest and 5 reference genes. As previously described in Chapter 4, three EOM samples with low spectrophotometric ratios and RIN values (see Chapter 4, table 3) were excluded based on data quality analysis. Seven genes were not expressed in  $\geq 4$  of the 9 OOM samples ( $Cq > 35$ ). These included 5 genes relating to muscle regeneration/atrophy (*WNT3*, *TWIST1*, *TNF*, *AKT1S1* and *PAX6*) and 2 genes relating to extracellular matrix function (*NRCAM* and *MMP3*).

The average Cq values for reference genes *RPLP0* and *ACTN2* were used for normalization. Despite large differences in raw Cq values between EOMs and orbicularis oculi muscles, after normalization these datasets were comparable as shown in Figure 2A ( $p=0.72$ ).

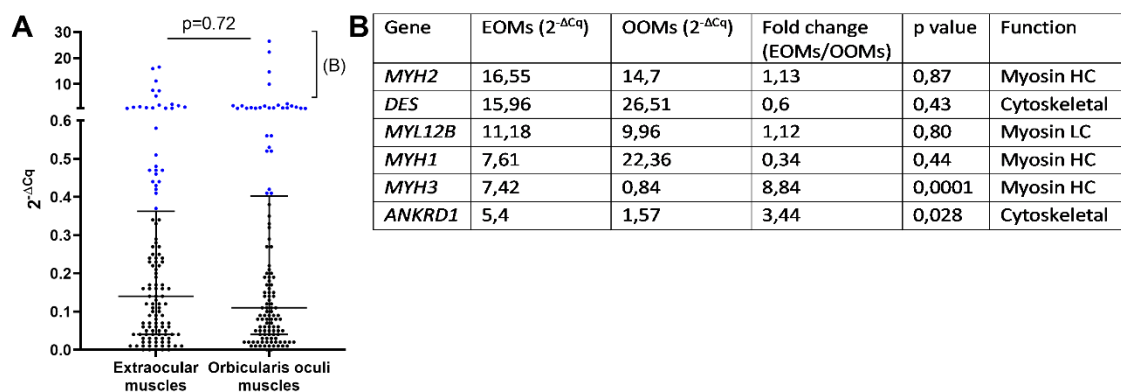


Figure 2. Gene expression in extraocular muscles (EOMs) and orbicularis oculi muscles (OOMs). A. Distribution of gene expression levels in EOMs and OOMs. Each data point represents the average  $2^{-\Delta Cq}$  value for a single gene ( $n=120$ ). Error bars indicate the median and interquartile range. The distribution and average of the  $2^{-\Delta Cq}$  values were similar for the EOMs and OOMs were similar ( $p=0.72$ ; Mann-Whitney U test) suggesting that data normalization was effective. Highly expressed genes in the 3<sup>rd</sup> quartile are shown in blue. B. The top expressed genes in EOMs and OOMs. Myosin heavy chain isoforms (Myosin HC). Myosin light chain isoforms (Myosin LC).

### 3.1. Highly expressed genes in the extraocular muscles

As expected in muscle tissue, the most highly expressed genes in the EOMs encoded structural muscle proteins and those relating to contractile function (Figure 2B). Importantly, gene expression was similar in the EOMs and OOMs for four of the 6 most highly expressed genes ( $p \geq 0.44$ ). For the purposes of stratifying the genes based on levels of expression in EOMs and OOMs, which suggests biological importance in these muscles, here genes in the 3<sup>rd</sup> quartile (see Figure 2A), with levels of expression higher than 75% of the genes in the EOM and OOM datasets will be referred to as the “highly expressed genes”. Based on this categorization, 30 genes in each dataset were considered highly expressed with overlap of 26 commonly highly expressed genes between EOM and OOM datasets. This is shown in Figure 3 where the highly expressed genes are categorized by biological pathway.

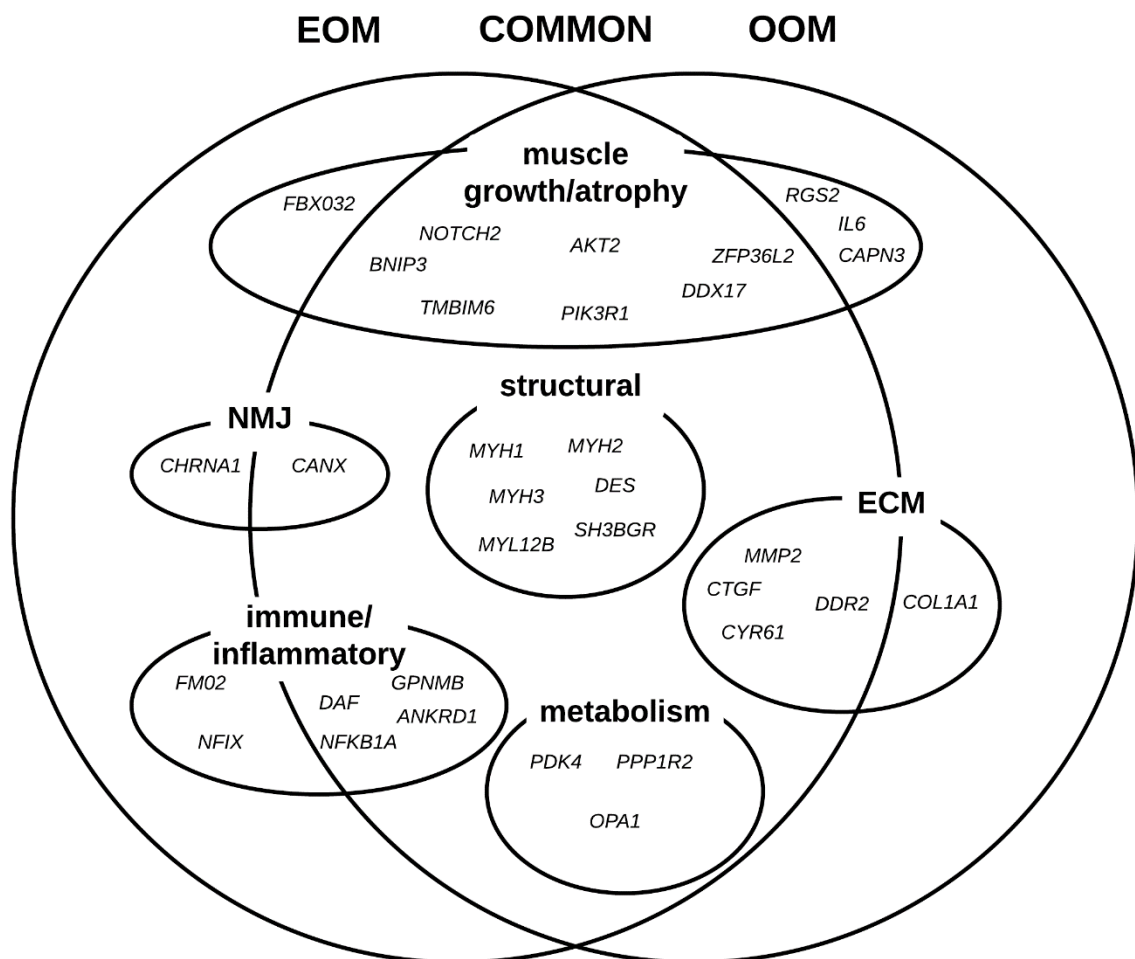


Figure 3. Highly expressed genes in EOMs and OOMs categorized by biological pathway. Neuromuscular junction (NMJ). Extracellular matrix (ECM).

The array of genes profiled here is not comprehensive and the highly expressed genes may not be indicative of the most highly expressed genes in EOMs and OOMs however, the genes included form part of major muscle pathways and may be representative of pathways that are most significant in the functioning of these muscles. Genes related to muscle regeneration and atrophy featured prominently in the highly expressed genes which is consistent with the high regenerative capacity of the EOMs (Fischer, Budak et al. 2005). Notably, these genes were also highly expressed in the OOMs. EOM metabolism differs from that of other muscles as they need a constant energy supply to fuel their fast contractility (Andrade, McMullen et al. 2005, Fischer, Budak et al. 2005). Three of the highly expressed genes relate to metabolism but were highly expressed in both EOMs and OOMs. It is hypothesized that the unique immune environment of the EOMs contributes to their differential susceptibility in autoimmune diseases (Porter, Khanna et al. 2001, Soltys, Gong et al. 2008). Here, several genes relating to immune function were highly expressed. It is known that EOM neuromuscular junction function and extracellular matrix distribution/composition have unique properties that contribute to their specialized contractility and genes in these functional pathways were therefore expected to be highly expressed (MacLennan, Beeson et al. 1997, Liu and Domellöf 2021).

Genes encoding the adult myosin heavy chain isoforms (MyHC) encoded by *MYH1*, *MYH2*, the embryonic MyHC isoform encoded by *MYH3* and a gene encoding myosin light chain 12B (*MYL12B*) comprised 4 of the 6 most highly expressed genes. It was previously reported that EOMs have unique MyHC expression, expressing both mature and developmental MyHC isoforms as well as an EOM-specific isoform encoded by *MYH13*, which together are suspected to provide the EOMs with their unique contractile properties (Briggs and Schachat 2002, Kjellgren, Thornell et al. 2003). Here, the adult MyHC isoforms *MYH1* and *MYH2* are similarly expressed in EOMs and orbicularis oculi muscles (Figure 2), while the developmental isoform encoded by *MYH3* is more highly expressed in EOMs (fold change=8.8,  $p=0.0001$ ). The EOM-specific isoform *MYH13* was expressed in the two EOMs and seven of 9 OOMs and did not show a statistically significant difference in gene expression between the two muscle allotypes ( $p=0.58$ ). This suggests that this MyHC isoform is also expressed in the OOMs which supports the findings of one previous report (Sekulic-Jablanovic, Ullrich et al. 2016).

Genes previously identified as putative OP-MG associated gene variants (Nel, Jalali Sefid Dashti et al. 2017, Nel, Mulder et al. 2019) (see Chapter 3), viz., *SH3BGR*, *ZFP36L2*, *PPP1R2* ( $p>0.46$ ) and *DDX17* ( $p=0.16$ ) showed similar levels of expression between EOMs and OOMs. *CANX* was more highly expressed in the EOMs than OOMs (fold change 2.16,  $p=0.033$ ) although this did not reach statistical significance after correction for multiple tests of

significance. The expression of the OP-MG genes in the EOMs is explored in greater depth in Section 3.2.

*ANKRD1*, *NFKBIA*, *GPNMB* and *PDK4* were previously profiled by microarray in the EOMs of rodents in an experimental model of autoimmune myasthenia gravis (EAMG) (Kaminski, Himuro et al. 2016) and show high levels of expression here in human EOMs. The transcription factor encoded by *ANKRD1* has been reported to provide feedback inhibition on NF-kB activity, modulating inflammatory responses and atrophy signalling induced by NF-kB (Liu, Bauman et al. 2015). *GPNMB* which encodes osteoactivin is a transmembrane protein thought to regulate immune responses in muscle (Kaminski, Himuro et al. 2016). *PDK4* is involved in glucose metabolism which is essential in EOMs (Andrade and McMullen 2006). *NFKBIA*, *PDK4* and *GPNMB* showed similar expression between EOMs and OOMs in this study ( $p>0.36$ ), but *ANKRD1* was more highly expressed in the EOMs ( $p=0.028$ ).

Genes *CTGF*, *DDR2*, *MMP3* and *CYR61*, which were previously profiled in the EOMs of cases with strabismus and are involved in ECM regulation were highly expressed in the EOMs. *CTGF* was more highly expressed in the EOMs than OOMs ( $p=0.007$ ). *MMP3* showed a trend towards higher expression levels in EOMs than OOMs ( $p=0.092$ ). *DDR2* and *CYR61* were similarly expressed in EOMs and OOMs ( $p>0.63$ ).

*DAF/CD55*, a regulator of complement, was previously reported to have lower expression in EOMs than limb skeletal muscles (Fischer, Gorospe et al. 2002, Kaminski, Li et al. 2004). Here, *DAF* featured in the upper quartile of genes expressed in EOMs but this was in comparison to a small selected panel of genes and is not necessarily representative of the relative expression of *DAF* in the entire EOM transcriptome. The *DAF* transcript levels in this study were similar in EOMs and OOMs (fold change=0.38,  $p=0.27$ ).

Overall, the highly expressed genes in EOMs mostly showed similar expression levels in OOMs. These genes are known to be involved in muscle pathways integral to the function of these highly active muscles.

### 3.2. Putative OP-MG genes

Seven genes were identified by gene-based analysis and prioritized based on their expression in limb skeletal muscle rather than EOMs due to the lack of EOM expression data for these genes (Nel, Mulder et al. 2019). It was therefore important to determine whether these genes are indeed expressed in the EOMs to establish whether they have biological relevance. As in Chapter 3 expression of these genes was also interrogated in OP-MG and control OOMs as a surrogate orbital muscle for EOMs, here the expression of the OP-MG genes is compared between the EOMs and OOMs.

All the OP-MG genes were expressed in the human EOMs in this study (Table 2) although *AKT1S1*, which has been reported as being highly expressed in limb skeletal muscle (GTex) (Lonsdale, Thomas et al. 2013), showed lower levels of expression compared to the other OP-MG genes. All OP-MG genes showed similar expression levels in EOMs and orbicularis oculi ( $p > 0.41$ ), except for gene *MKNK2* for which EOM gene expression was lower than orbicularis oculi muscles but this difference did not reach statistical significance (2-fold,  $p = 0.16$ ). Previous evidence comparing rodent EOMs with non-ocular muscles by microarray supports lower expression of *MKNK2* in EOM myoblasts compared with limb and masseter myoblasts (Porter, Israel et al. 2006). As levels of expression for the OP-MG genes were similar between EOMs and OOMs, these findings support the use of orbicularis oculi muscle as a surrogate tissue for EOMs in the investigation of putative OP-MG genes in Chapter 3).

Table 2. Comparing the gene expression of the OP-MG genes in EOMs and OOMs

Gene	Average $2^{-\Delta Cq}$ EOMs	Average $2^{-\Delta Cq}$ OOMs	Fold change (EOMs/OOMs)	P value
<i>MYL12B</i>	11,18	9,96	1,12	0,81
<i>SH3BGR</i>	1,32	2,41	0,55	0,54
<i>ZFP36L2</i>	0,75	0,71	1,05	0,88
<i>PPP1R2</i>	0,44	0,84	0,53	0,46
<i>PEF1</i>	0,16	0,12	1,37	0,43
<i>FAM92A1</i>	0,16	0,15	1,09	0,91
<i>PPP1R12C</i>	0,14	0,15	0,96	0,89
<i>MKNK2</i>	0,04	0,09	0,42	0,16
<i>AKT1S1</i>	0.002	0.003	0.80	0.42

Table 2. The OP-MG genes are listed in order of highest expression in extraocular muscles (EOMs). Expression levels for the orbicularis oculi muscles (OOMs) are listed for comparison together with the fold change values and p values calculated by Student's unpaired t tests.

### 3.3. Differentially expressed genes between extraocular muscles and orbicularis oculi

Of 120 genes of interest profiled, only 2 genes were differentially expressed after Benjamini-Hochberg correction for multiple testing. The most significantly upregulated gene was *MYH3* encoding the embryonic myosin heavy chain isoform (fold change 8.84,  $p < 0.0001$ ). The  $\alpha$ -

subunit of the acetylcholine receptor encoded by *CHRNA1* was upregulated 10-fold in the EOMs ( $p=0.0003$ ). Although the differences in gene expression was not a study aim, we nevertheless analysed the few EOM samples available and report the top differentially expressed genes with  $p<0.05$  and upregulated 2-fold in EOMs (Figure 4A). Except for *MYH3* and *CHRNA1*, the differences in gene expression did not reach statistical significance after correction for multiple testing.

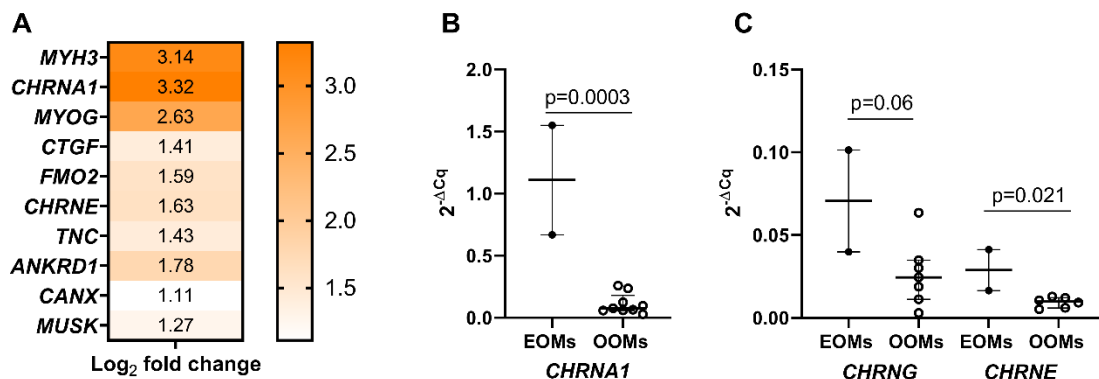


Figure 4. Differentially expressed genes between extraocular muscles (EOMs) and orbicularis oculi muscles (OOMs) ( $p<0.035$ ). A. Log<sub>2</sub> fold change values are shown by heatmap and listed according to p value. Acetylcholine receptor subunit expression compared between EOMs and OOMs is shown in figures 3B and 3C.

In addition to the  $\alpha$ -subunit of the acetylcholine receptor (*CHRNA1*) which was upregulated 10-fold in the EOMs compared to the OOMs (Figure 4B), the  $\epsilon$ -acetylcholine receptor subunit (*CHRNE*) was upregulated 3-fold (Figure 4C), similar to rodents (Porter, Israel et al. 2006). The fetal  $\gamma$ -subunit, which was previously reported to be differentially expressed in EOMs compared with non-ocular muscles, showed a trend towards upregulation in the EOMs ( $p=0.06$ ) (Figure 4C) (Kaminski, Kusner et al. 1995). The muscle-kinase specific receptor (*MUSK*) which is involved in the clustering of acetylcholine receptors on the muscle endplate, was upregulated 2-fold ( $p=0.034$ ). *CANX* encodes a chaperone protein involved in the assembly of AChR subunits (Chang, Gelman et al. 1997) and was upregulated 2-fold ( $p=0.033$ ).

The remaining genes with upregulated transcripts in EOMs compared to OOMs relate to muscle repair and extracellular matrix regulation. The EOMs are known for their capacity for constant regeneration. Here, the myogenesis transcription factor *MYOG* was upregulated in the EOMs (2.6-fold;  $p=0.002$ ). Genes previously shown to be dysregulated in the EOMs of cases with strabismus suggesting that these genes are significant in the function of EOMs, *CTGF*, *ANKRD1* and *TNC*, were upregulated 3-fold in the EOMs ( $p<0.029$ ) (Altick, Feng et al.

2012). *CTGF* encoding connective tissue growth factor was also previously shown to be upregulated in human EOMs vs limb muscles (Fischer, Budak et al. 2005) and EOM myoblasts vs masseter myoblasts (Porter, Israel et al. 2006). *FMO2* encoding flavin containing monooxygenase 2, was upregulated 3-fold ( $p=0.014$ ). The flavin containing monooxygenases are responsible for oxidation of foreign substances and are thought to have a role in energy homeostasis (Veeravalli, Omar et al. 2014).

As the EOM metabolism is highly specialised to support their fast contractility, differences between the EOMs and OOMs in the expression of genes relating to metabolic pathways were expected. In this array, of the 32 genes relating to metabolism and energy homeostasis that were profiled, only *FMO2* showed a significant difference in gene expression ( $p=0.014$ ). However, we had few samples and real differences in gene expression may not have reached the threshold of statistical significance. In Figure 5, the differences in gene expression for genes relating to metabolism between EOMs and OOMs are shown as  $\log_2$  fold change.

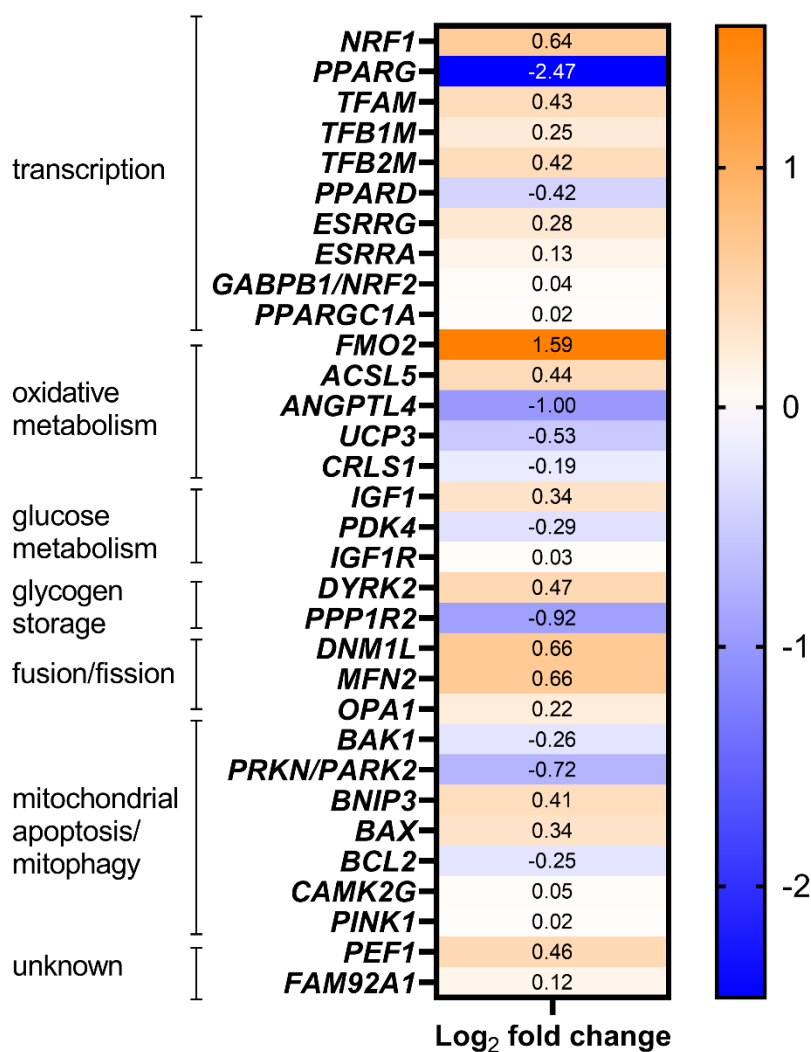


Figure 5. Comparing the expression of genes relating to metabolism in EOMs and OOMs. The  $\log_2$  fold change values are presented. Except for *FMO2* ( $p=0.014$ ),  $p$  values were  $>0.15$ .

Based on previous reports, it was expected that EOM gene expression may differ from the OOMs for genes relating to glucose and glycogen metabolism, oxidative capacity and mitochondrial biogenesis. EOMs preferentially utilize circulating glucose and are reported to have low glycogen stores (Andrade, McMullen et al. 2005, Fischer, Budak et al. 2005, Andrade and McMullen 2006). *PPARG* which encodes the peroxisome proliferator activated receptor- $\gamma$ , a transcription factor relating increased sensitivity to insulin and glucose uptake, showed non-significant lower levels of expression in the EOMs compared to the OOMs ( $p=0.43$ ) although it was previously reported as upregulated in mouse EOMs compared with non-ocular muscles (Andrade, McMullen et al. 2005). The other genes relating to glucose metabolism, including *PDK4* which encodes pyruvate dehydrogenase-4 and reported to have lower expression in EOMs vs limb skeletal muscle, was similarly expressed in the EOMs and OOMs ( $p>0.50$ ), *PPP1R2* which is involved in glycogen storage and therefore expected to have low levels of expression in EOMs, showed non-significantly lower levels of expression in the EOMs compared to the OOMs ( $p=0.46$ ). Apart from *FMO2*, genes relating to oxidative function did not show significant differences between EOMs and OOMs (Fischer, Budak et al. 2005). Although the list of genes relating to metabolism that were profiled in this study is not comprehensive, and OOM metabolism is not expected to be as efficient as the EOMs, this data suggests that OOMs metabolism may bear some similarity to the EOMs.

Comparison of gene expression between the EOMs and OOMs of live donors by qPCR has shown that gene expression in EOMs and OOMs was similar. Differences in myosin heavy chain isoform expression and acetylcholine receptor subunit expression were expected based on previous transcriptomic evidence and the unique contractile properties of the EOMs.

#### 3.4. Novel gene expression data in extraocular and orbicularis oculi muscles

Of 125 genes profiled, 72 genes have not previously been profiled in human EOMs by qPCR. These genes were all expressed ( $Cq<35$ ) in both EOMs and orbicularis oculi muscles including four putative OP-MG genes with poorly characterized biological function (Nel, Jalali Sefid Dashti et al. 2017, Nel, Mulder et al. 2019). These genes are shown in Figure 6.

Category	Genes
<b>OP-MG genes</b>	<i>MKMK2, AKT1S1, SH3BGR, MYL12B, PPP1R12C, PPP1R2, ZFP36L2, HLADPB1, <b>FAM92A1, PEF1</b>, SPTLC3, DDX17, ST8SIA1, <b>FAM136A, FAM69A</b>, CANX, PPP6R2</i>
<b>Muscle regeneration and atrophy signalling</b>	<i>SPTLC1, UGCG, BAK1, TMBIM6, CASP6, XIAP, PIK3CB, PIK3R1, MTOR, MAPK6, HDAC1, SIRT1, WNT3, TWIST1, HGF, WIF1</i>
<b>Mitochondrial biogenesis</b>	<i>PPARD, NRF1, NRF2, TFAM, TFB1M, TFB2M, CRLS1, DNM1L, OPA1, MFN2, ESRRA, ESRRG, PINK1, PRKN/PARK2, BNIP3</i>
<b>MG pathways</b>	<i>CHRNA1, CHRNG, CHRNE, DAF/CD55, ANGPTL4, ACSL5, UCP3, RGS2, NFIX, ENC1, ERFF1, GLIPR2/GAPR-1, DYRK2, GALNT12, ANKRD1, GPNMB, CEBPD, DDIT4, GADD45A, MT1A, FMO2, FKBP5</i>
<b>Reference genes</b>	<i>RPLP0, CSNK2A2</i>

Figure 6. Novel gene expression data in EOMs and orbicularis oculi muscles. Genes with poorly characterized biological function are indicated in bold text.

#### 4. Discussion

Although it was not the main aim of comparing gene expression between EOMs and orbicularis oculi muscles, novel data were found in the samples obtained from live human subjects and not subjected to cautery at the time of resection. Overall, gene expression in the EOMs and orbicularis oculi muscles was similar with the only significant differences in gene expression relating to myosin heavy chain isoform and acetylcholine receptor subunit expression.

Although EOMs have long been considered a unique muscle allotype (Porter, Khanna et al. 2001), differing substantially from non-ocular muscles (including cranial muscles), we hypothesized based on similar physiological characteristics that orbicularis oculi muscles may be a suitable surrogate tissue for EOMs in gene expression studies relating to the pathogenesis of treatment-resistant ophthalmoplegia in MG (see Chapter 3). Despite having few samples, we have shown that patterns of gene expression are similar between EOMs and orbicularis oculi muscles, which corresponds with similarities in embryogenesis and function (Cheng, Liao et al. 2007). The few differences in gene expression reported here are similar to previous reports on EOM microarray data (Fischer, Budak et al. 2005, Porter, Israel et al. 2006). In addition, this work has also shown that putative OP-MG genes identified by genome-wide analyses are expressed in the EOMs and therefore support their biological relevance (Nel, Mulder et al. 2019).

Novel gene expression data in EOMs are described due to the paucity of data available in public databases. A search of the literature to date showed that gene expression data in orbicularis oculi muscles was limited to one previous report which investigated gene expression in human orbicularis oculi surgical biopsy specimens obtained from oculoplastic procedures (Sekulic-Jablanovic, Ullrich et al. 2016). Although it was an additional subanalysis, the comparison of EOM and orbicularis oculi gene expression comprises the most extensive investigation of gene expression in orbicularis oculi muscles in the current literature. The small number of samples in this investigation is a substantial limitation, however the opportunity to sample these orbital muscles from live donors is a rarity. Although half of the samples came from patients with the OP-MG subphenotype, these cases were equally distributed between the EOM and OOM groups and pathological differences in gene expression were therefore not expected to have caused confounding of the results.

In conclusion, gene expression in EOMs and orbicularis oculi muscles is similar, differing mostly in genes involved in contractile function. Orbicularis oculi muscles could therefore serve as a reasonable surrogate tissue for EOMs in gene expression studies.

## References

- Agarwal, A. B., A. J. Christensen, C.-Y. Feng, D. Wen, L. A. Johnson and C. S. von Bartheld (2017). "Expression of schizophrenia biomarkers in extraocular muscles from patients with strabismus: an explanation for the link between exotropia and schizophrenia?" PeerJ **5**: e4214-e4214.
- Agarwal, A. B., C. Y. Feng, A. L. Altick, D. R. Quilici, D. Wen, L. A. Johnson and C. S. von Bartheld (2016). "Altered Protein Composition and Gene Expression in Strabismic Human Extraocular Muscles and Tendons." Invest Ophthalmol Vis Sci **57**(13): 5576-5585.
- Agretti, P., L. Chiovato, G. D. Marco, C. Marcocci, B. Mazzi, S. Sellari-Franceschini, P. Vitti, A. Pinchera and M. Tonacchera (2002). "Real-time PCR provides evidence for thyrotropin receptor mRNA expression in orbital as well as in extraorbital tissues." **147**(6): 733.
- Altick, A. L., C.-Y. Feng, K. Schlauch, L. A. Johnson and C. S. Von Bartheld (2012). "Differences in gene expression between strabismic and normal human extraocular muscles." Investigative ophthalmology & visual science **53**(9): 5168-5177.
- Andrade, F. H. and C. A. McMullen (2006). "Lactate is a metabolic substrate that sustains extraocular muscle function." Pflugers Arch. **452**(1): 102-108.
- Andrade, F. H., C. A. McMullen and R. E. Rumbaut (2005). "Mitochondria are fast Ca<sup>2+</sup> sinks in rat extraocular muscles: a novel regulatory influence on contractile function and metabolism." Investigative ophthalmology & visual science **46**(12): 4541-4547.
- Briggs, M. M. and F. Schachat (2002). "The superfast extraocular myosin (MYH13) is localized to the innervation zone in both the global and orbital layers of rabbit extraocular muscle." Journal of Experimental Biology **205**(20): 3133-3142.
- Chang, W., M. S. Gelman and J. M. Prives (1997). "Calnexin-dependent enhancement of nicotinic acetylcholine receptor assembly and surface expression." Journal of Biological Chemistry **272**(46): 28925-28932.
- Cheng, A. M. S., H. Y. Yin, A. Chen, Y.-W. Liu, M.-C. Chuang, H. He, S. Tighe, H. Sheha and S.-L. Liao (2016). "Celecoxib and Pioglitazone as Potential Therapeutics for Regulating TGF- $\beta$ -Induced Hyaluronan in Dysthyroid Myopathy." Investigative Ophthalmology & Visual Science **57**(4): 1951-1959.
- Cheng, N.-C., S.-L. Liao, I.-J. Wang, I.-C. Lin and Y.-B. Tang (2007). "Fiber type and myosin heavy chain compositions of adult pretarsal orbicularis oculi muscle." Journal of Molecular Histology **38**(3): 177-182.
- Choi, H., A. Charlton, S. Tay, G. Sundar and S. Amrith (2012). "Mitochondrial Changes in Aging Orbicularis Oculi Muscles: Histologic and Genetic Analyses in Elderly Asian Patients." Asia Pac J Ophthalmol (Phila) **1**(3): 180-184.

- Etienne, W., M. H. Meyer, J. Peppers and J. Ralph A. Meyer (2004). "Comparison of mRNA gene expression by RT-PCR and DNA microarray." BioTechniques **36**(4): 618-626.
- Fischer, M. D., M. T. Budak, M. Bakay, J. R. Gorospe, D. Kjellgren, F. Pedrosa-Domellof, E. P. Hoffman and T. S. Khurana (2005). "Definition of the unique human extraocular muscle allotype by expression profiling." Physiol Genomics **22**(3): 283-291.
- Fischer, M. D., J. R. Gorospe, E. Felder, S. Bogdanovich, F. Pedrosa-Domellof, R. S. Ahima, N. A. Rubinstein, E. P. Hoffman and T. S. J. P. g. Khurana (2002). "Expression profiling reveals metabolic and structural components of extraocular muscles." Physiol. Genomics **9**(2): 71-84.
- Hiromatsu, Y., D. Yang, T. Bednarczuk, I. Miyake, K. Nonaka and Y. Inoue (2000). "Cytokine Profiles in Eye Muscle Tissue and Orbital Fat Tissue from Patients with Thyroid-Associated Ophthalmopathy\*." The Journal of Clinical Endocrinology & Metabolism **85**(3): 1194-1199.
- Kaminski, H. J., K. Himuro, J. Alshaikh, B. Gong, G. Cheng and L. L. Kusner (2016). "Differential RNA Expression Profile of Skeletal Muscle Induced by Experimental Autoimmune Myasthenia Gravis in Rats." Front Physiol **7**: 524.
- Kaminski, H. J., L. L. Kusner, K. V. Nash and R. L. J. N. Ruff (1995). "The gamma-subunit of the acetylcholine receptor is not expressed in the levator palpebrae superioris." **45**(3): 516-518.
- Kaminski, H. J., Z. Li, C. Richmonds, F. Lin and M. E. Medof (2004). "Complement regulators in extraocular muscle and experimental autoimmune myasthenia gravis." Exp Neurol **189**(2): 333-342.
- Kitada, M., T. Matsuo, T. Yamane, S. Hasebe and H. Ohtsuki (2003). "Different levels of TIMPs and MMPs in human lateral and medial rectus muscle tissue excised from strabismic patients." Strabismus **11**(3): 145-155.
- Kjellgren, D., L. E. Thornell, J. Andersen and F. Pedrosa-Domellof (2003). "Myosin heavy chain isoforms in human extraocular muscles." Invest Ophthalmol Vis Sci **44**(4): 1419-1425.
- Koltai, H. and C. Weingarten-Baror (2008). "Specificity of DNA microarray hybridization: characterization, effectors and approaches for data correction." Nucleic acids research **36**(7): 2395-2405.
- Koppelkamm, A., B. Vennemann, S. Lutz-Bonengel, T. Fracasso and M. Vennemann (2011). "RNA integrity in post-mortem samples: influencing parameters and implications on RT-qPCR assays." Int J Legal Med **125**(4): 573-580.
- Liu, J.-X. and F. P. Domellöf (2021). "Cytoskeletal Proteins in Myotendinous Junctions of Human Extraocular Muscles." Investigative ophthalmology & visual science **62**(2): 19-19.
- Liu, X.-H., W. A. Bauman and C. Cardozo (2015). "ANKRD1 modulates inflammatory responses in C2C12 myoblasts through feedback inhibition of NF- $\kappa$ B signaling activity." Biochemical and biophysical research communications **464**(1): 208-213.

Lonsdale, J., J. Thomas, M. Salvatore, R. Phillips, E. Lo, S. Shad, R. Hasz, G. Walters, F. Garcia, N. Young, B. Foster, M. Moser, E. Karasik, B. Gillard, K. Ramsey, S. Sullivan, J. Bridge, H. Magazine, J. Syron, J. Fleming, L. Siminoff, H. Traino, M. Mosavel, L. Barker, S. Jewell, D. Rohrer, D. Maxim, D. Filkins, P. Harbach, E. Cortadillo, B. Berghuis, L. Turner, E. Hudson, K. Feenstra, L. Sobin, J. Robb, P. Branton, G. Korzeniewski, C. Shive, D. Tabor, L. Qi, K. Groch, S. Nampally, S. Buia, A. Zimmerman, A. Smith, R. Burges, K. Robinson, K. Valentino, D. Bradbury, M. Cosentino, N. Diaz-Mayoral, M. Kennedy, T. Engel, P. Williams, K. Erickson, K. Ardlie, W. Winckler, G. Getz, D. DeLuca, D. MacArthur, M. Kellis, A. Thomson, T. Young, E. Gelfand, M. Donovan, Y. Meng, G. Grant, D. Mash, Y. Marcus, M. Basile, J. Liu, J. Zhu, Z. Tu, N. J. Cox, D. L. Nicolae, E. R. Gamazon, H. K. Im, A. Konkashbaev, J. Pritchard, M. Stevens, T. Flutre, X. Wen, E. T. Dermitzakis, T. Lappalainen, R. Guigo, J. Monlong, M. Sammeth, D. Koller, A. Battle, S. Mostafavi, M. McCarthy, M. Rivas, J. Maller, I. Rusyn, A. Nobel, F. Wright, A. Shabalina, M. Feolo, N. Sharopova, A. Sturcke, J. Paschal, J. M. Anderson, E. L. Wilder, L. K. Derr, E. D. Green, J. P. Struwing, G. Temple, S. Volpi, J. T. Boyer, E. J. Thomson, M. S. Guyer, C. Ng, A. Abdallah, D. Colantuoni, T. R. Insel, S. E. Koester, A. R. Little, P. K. Bender, T. Lehner, Y. Yao, C. C. Compton, J. B. Vaught, S. Sawyer, N. C. Lockhart, J. Demchok and H. F. Moore (2013). "The Genotype-Tissue Expression (GTEx) project." Nature Genetics **45**: 580.

MacLennan, C., D. Beeson, A. M. Buijs, A. Vincent and J. Newsom-Davis (1997). "Acetylcholine receptor expression in human extraocular muscles and their susceptibility to myasthenia gravis." Annals of Neurology **41**(4): 423-431.

Nel, M., M. Jalali Sefid Dashti, J. Gamielidien and J. M. Heckmann (2017). "Exome sequencing identifies targets in the treatment-resistant ophthalmoplegic subphenotype of myasthenia gravis." Neuromuscul Disord.

Nel, M., N. Mulder, T. A. Europa and J. M. Heckmann (2019). "Using Whole Genome Sequencing in an African Subphenotype of Myasthenia Gravis to Generate a Pathogenetic Hypothesis." Front Genet **10**(136).

Porter, J. D., S. Israel, B. Gong, A. P. Merriam, J. Feuerman, S. Khanna and H. J. Kaminski (2006). "Distinctive morphological and gene/protein expression signatures during myogenesis in novel cell lines from extraocular and hindlimb muscle." Physiol Genomics **24**(3): 264-275.

Porter, J. D., S. Khanna, H. J. Kaminski, J. S. Rao, A. P. Merriam, C. R. Richmonds, P. Leahy, J. Li and F. H. Andrade (2001). "Extraocular muscle is defined by a fundamentally distinct gene expression profile." Proceedings of the National Academy of Sciences **98**(21): 12062-12067.

Rodríguez, M. A., K. Sandgren Hochhard, A. Vicente, J.-X. Liu and F. Pedrosa Domellöf (2019). "Gene expression profile of extraocular muscles following resection strabismus surgery." Experimental Eye Research **182**: 182-193.

- Romero-Kusabara, I. L., J. V. Filho, N. M. Scalissi, K. C. Melo, G. Demartino, C. A. Longui, M. R. Melo and A. N. Cury (2017). "Distinct inflammatory gene expression in extraocular muscle and fat from patients with Graves' orbitopathy." Eur J Endocrinol **176**(4): 481-488.
- Schmittgen, T. D. and K. J. Livak (2008). "Analyzing real-time PCR data by the comparative C(T) method." Nat Protoc **3**(6): 1101-1108.
- Sekulic-Jablanovic, M., A. Palmowski-Wolfe, F. Zorzato and S. J. B. J. Treves (2015). "Characterization of excitation–contraction coupling components in human extraocular muscles." **466**(1): 29-36.
- Sekulic-Jablanovic, M., N. D. Ullrich, D. Goldblum, A. Palmowski-Wolfe, F. Zorzato and S. J. T. J. o. g. p. Treves (2016). "Functional characterization of orbicularis oculi and extraocular muscles." jgp. 201511542.
- Soltys, J., B. Gong, H. J. Kaminski, Y. Zhou and L. L. Kusner (2008). "Extraocular muscle susceptibility to myasthenia gravis: unique immunological environment?" Ann N Y Acad Sci **1132**: 220-224.
- Veeravalli, S., B. A. Omar, L. Houseman, M. Hancock, S. G. Gonzalez Malagon, F. Scott, A. Janmohamed, I. R. Phillips and E. A. Shephard (2014). "The phenotype of a flavin-containing monoxygenase knockout mouse implicates the drug-metabolizing enzyme FMO1 as a novel regulator of energy balance." Biochem Pharmacol **90**(1): 88-95.
- Wu, S.-L., C.-S. J. Yang, H.-J. Wang, C.-L. Liao, T.-J. Chang and T.-C. Chang (1999). "Demonstration of thyrotropin receptor mRNA in orbital fat and eye muscle tissues from patients with Graves' ophthalmopathy by in situ hybridization." Journal of Endocrinological Investigation **22**(4): 289-295.
- Zhu, Y., D. Deng, C. Long, G. Jin, Q. Zhang and H. Shen (2013). "Abnormal expression of seven myogenesis-related genes in extraocular muscles of patients with concomitant strabismus." Mol Med Rep **7**(1): 217-222.

## Appendix figures

Appendix table 1: Reference gene selection

	Average fold change (EOMs/O.Oc)	p value	geNorm (m value)	Bestkeeper (SD; CV)
<i>RPLP0</i>	9.93	0.00002	1.48	1.60; 5.47
<i>ACTB</i>	6.04	0.002	1.57	2.51; 10.06
<i>GAPDH</i>	5.11	0.004	1.89	2.76; 12.25
<i>CSNK2A2</i>	23.99	0.00002	1.38	2.26; 10.32
<i>ACTN2</i>	12.01	0.0006	1.42	1.47; 6.86
<b>Average <i>RPLP0</i>- <i>ACTN2</i></b>	12.00	0.0006	0.43	1.53; 6.05

Appendix table 1. Fold change =  $2^{-\Delta Cq}$  ( $\Delta Cq = \text{EOM } Cq^{\text{ref}} - \text{orbicularis oculi } Cq^{\text{ref}}$ ). “Average fold change” refers to the arithmetic mean of EOM  $2^{-Cq}$  divided by the arithmetic mean of the orbicularis oculi muscles. The p values indicate the results of unpaired t tests comparing EOMs and orbicularis oculi muscles  $2^{-Cq}$  values. The “geNorm m value” refers to the average expression stability value calculated using the geometric mean. SD is the standard deviation and CV is the coefficient of variance.

Appendix table 2: Highly expressed genes

Gene Symbol	Average (EOMs) $2^{-\Delta Cq}$	Average (OOMs) $2^{-\Delta Cq}$	Fold change (EOMs/OOMs )	p value
<i>MYH2</i>	16,55	14,70	1,13	NS
<i>DES</i>	15,96	26,51	0,60	NS
<i>MYL12B</i>	11,18	9,96	1,12	NS
<i>MYH1</i>	7,61	22,36	0,34	NS
<i>MYH3</i>	7,42	0,84	8,84	0,0001
<i>ANKRD1</i>	5,40	1,57	3,44	0,028

<i>CTGF</i>	2,22	0,83	2,67	0,007
<i>DDX17</i>	1,93	1,12	1,73	NS
<i>TMBIM6</i>	1,71	1,67	1,02	NS
<i>SH3BGR</i>	1,32	2,41	0,55	NS
<i>BNIP3</i>	1,12	0,85	1,33	NS
<i>CHRNA1</i>	1,11	0,11	10,00	0,0003
<i>CANX</i>	0,91	0,42	2,16	0,033
<i>NFKBIA</i>	0,83	0,56	1,49	NS
<i>PDK4</i>	0,75	0,92	0,82	NS
<i>ZFP36L2</i>	0,75	0,71	1,05	NS
<i>DAF/CD55</i>	0,70	1,86	0,38	NS
<i>CYR61</i>	0,58	0,93	0,62	NS
<i>DDR2</i>	0,51	0,61	0,84	NS
<i>NFIX</i>	0,48	0,35	1,34	NS
<i>PIK3R1</i>	0,47	0,52	0,91	NS
<i>OPA1</i>	0,47	0,41	1,17	NS
<i>FBXO32</i>	0,47	0,21	2,19	NS
<i>MYH13</i>	0,46	1,63	0,28	NS
<i>PPP1R2</i>	0,44	0,84	0,53	NS
<i>MMP2</i>	0,44	0,72	0,61	NS
<i>FMO2</i>	0,43	0,14	3,01	0,014
<i>NOTCH2</i>	0,42	0,41	1,02	NS
<i>GPNMB</i>	0,41	0,73	0,56	NS
<i>AKT2</i>	0,37	0,53	0,70	NS

Appendix table 2. Highly expressed genes in extraocular muscles (EOMs) and orbicularis oculi muscles (OOMs) listed by highest expression in the EOMs. Comparison of expression in EOMs and O.Oc is presented as fold change and p values represent the statistical significance of these comparisons as determined by unpaired student's t tests or Mann-Whitney U test in the case of *CHRNA1*. P values <0.05 were considered significant.

putative OP-MG genes/ pathways	<i>IL6R<sup>1</sup>, PAX3<sup>1</sup>, AKT2<sup>1</sup>, BAX<sup>1</sup>, BCL2<sup>1</sup>, CASP3<sup>1</sup>, CAPN3<sup>1</sup>, IGF1<sup>1,2</sup>, AKT1<sup>1</sup>, TRIM63<sup>1</sup>, FBXO32<sup>1</sup>, FOXO3<sup>1</sup>, TNF<sup>3</sup>, IL6<sup>3</sup>, MSTN<sup>1</sup>, PPARG<sup>1</sup>, PPARGC1A<sup>1</sup>, CAMK2G<sup>1</sup>, TGFB1<sup>1,4</sup>, PAX6<sup>1</sup>, PAX7<sup>1</sup>, BMP4<sup>1,4</sup>, MYH2<sup>1</sup>, MYOG<sup>1,2</sup></i>
MG pathways	<i>MUSK<sup>1</sup>, PDK4<sup>1</sup>, NFKBIA<sup>5</sup></i>
strabismus	<i>COL1A1<sup>5</sup>, COL8A1<sup>5</sup>, CTGF<sup>1,5</sup>, CYR61<sup>5</sup>, LOX<sup>5</sup>, MMP16<sup>4,5</sup>, MMP3<sup>4,5</sup>, TIMP4<sup>4,5</sup>, TNC<sup>5</sup>, VCAN<sup>5</sup>, DDR2<sup>1,5</sup>, MMP2<sup>1,5</sup>, ANK1<sup>5</sup>, DES<sup>1,5</sup>, NRCAM<sup>1,5</sup>, MYH1<sup>1,5</sup>, MYH3<sup>5</sup>, MYH13<sup>5,6</sup>, GDNF<sup>1,5</sup>, IGF1R<sup>1,5</sup>, CXCR4<sup>1,5</sup>, IL10RA<sup>1,5</sup>, NOTCH2<sup>1,5</sup></i>
reference genes	<i>ACTB<sup>2,7</sup>, GAPDH<sup>3,8</sup>, ACTN2<sup>9</sup></i>

Appendix figure 3. Genes previously reported to be expressed in human EOMs by qPCR array. Ophthalmoplegic myasthenia gravis (OP-MG) genes/pathways refer to the putative genes and pathways from unbiased next generation sequencing studies. Myasthenia gravis (MG) pathways refers to genes relating to the pathogenesis of MG, or those previously dysregulated in the EOMs of rodents with experimental autoimmune MG (Kaminski, Himuro et al. 2016) but later profiled in the EOMs of humans (without MG). References: 1. (Agarwal, Christensen et al. 2017); 2. (Zhu, Deng et al. 2013); 3. (Hiromatsu, Yang et al. 2000); 4. (Kitada, Matsuo et al. 2003); 5. (Agarwal, Feng et al. 2016); 6. (Sekulic-Jablanovic, Ullrich et al. 2016); 7. (Agretti, Chiovato et al. 2002); 8. (Fischer, Budak et al. 2005); 9. (MacLennan, Beeson et al. 1997).

## Chapter 5: Mitochondrial genetic and dynamic studies in ocular fibroblasts of myasthenia gravis patients with ophthalmoplegia: a pilot study

### Abstract

**Introduction:** Histopathological reports and gene expression studies in experimental autoimmune myasthenia gravis models have suggested that muscle mitochondrial metabolism may be impacted in myasthenia gravis (MG). Extraocular muscles (EOMs) are dependent on oxidative metabolism for sufficient energy to support their fast contractility and may be particularly susceptible to mitochondrial dysfunction. We therefore hypothesized that this may contribute to the development of treatment-resistant ophthalmoplegia in MG (OP-MG) in susceptible individuals. **Aim:** To investigate mitochondrial function in opportunistically obtained ocular fibroblasts as a surrogate tissue for EOMs. **Methods:** Patient-derived ocular fibroblasts were cultured from the EOM myotendons of OP-MG cases and non-MG controls after opportunistic sampling. To investigate mitochondrial function in the context of MG, these cells were exposed to homologous MG sera as an *in vitro* application to create an “MG model” for mitochondrial dynamic metabolic stress tests (Agilent Seahorse XF96 assays) and quantitative polymerase chain reaction (qPCR). **Results:** Expression of nuclear-encoded mitochondrial genes and rates of oxidative metabolism were similar between OP-MG (n=2) and control (n=5) ocular fibroblasts at basal levels. Exposure to 5% MG sera for 24 hours induced upregulation of genes regulating mitochondrial metabolism (*PK4* and *ANGPTL4*,  $p \leq 0.041$ ) in all ocular fibroblast cultures regardless of phenotype. However, exposure to MG sera induced a ~2-fold increase in rates of oxidative metabolism in OP-MG ocular fibroblasts but not controls ( $p < 0.015$ ). Control of respiration, calculated as the cell respiratory control ratio, did not differ significantly between OP-MG and control ocular fibroblasts at basal levels ( $p = 0.40$ ) or after exposure to MG sera ( $p = 0.65$ ). **Conclusion:** The altered mitochondrial function triggered by MG sera in ocular fibroblasts derived from OP-MG EOM myotendons suggests that this tissue is responsive to MG sera and reflects upregulated oxidative metabolism. Although we did not find any evidence of mitochondrial insufficiency in ocular fibroblasts of OP-MG cases, the MG-induced upregulation of oxidative metabolism in their EOMs may potentially have direct and/or indirect consequences with other interacting pathways.

Reference: Europa, T. A., et al. (2022). "Mitochondrial bioenergetics in ocular fibroblasts of two myasthenia gravis cases." *IBRO Neuroscience Reports* 12: 297-302.

## 1. Introduction

### 1.1. Mitochondrial function in myasthenia gravis

A review of muscle histopathology in myasthenia gravis (MG) cases (Chapter 2), showed that ultrastructural mitochondrial changes are commonly observed in MG muscle biopsies (Europa, Nel et al. 2019). Mitochondrial enlargement, subsarcolemmal aggregates of mitochondria and abnormal cristae were commonly reported. Although these observations were limited to histopathological findings and not correlated with functional mitochondrial analyses, mitochondrial structure is closely related to function (Vincent, Ng et al. 2016) and structural abnormalities may be associated with aberrant mitochondrial function. Similar ultrastructural mitochondrial changes to those observed in MG skeletal muscle biopsies have been reported in extraocular muscles (EOMs) and non-ocular muscles with poor contractility from non-MG causes. It is therefore uncertain whether these mitochondrial changes relate to MG pathology or whether they are a consequence of reduced contractility in muscles weakened by MG (Chapter 2).

Experimental autoimmune myasthenia gravis (EAMG), induced either by passive antibody transfer or active immunization in rodents, showed upregulation of genes relating to oxidative metabolism in the EOMs, diaphragm and limb muscles suggesting that transcriptional changes relating to mitochondrial function may be induced in the context of MG (Zhou, Kaminski et al. 2014, Kaminski, Himuro et al. 2016). Gene ontology of the differentially expressed genes in EAMG rodent muscles compared with control muscles suggested that EAMG triggered a metabolic shift from glucose to fatty acid oxidation (Kaminski, Himuro et al. 2016). The transcript most highly upregulated in the EOMs of EAMG rodents (compared with controls) was *ANGPTL4*, which was also shown to be upregulated in patient-derived transdifferentiated myocytes of OP-MG cases compared with control-MG cases (Nel, Prince et al. 2019). Although these reports provided transcriptional evidence to suggest altered oxidative metabolism in MG (Zhou, Kaminski et al. 2014, Kaminski, Himuro et al. 2016, Nel, Prince et al. 2019), dynamic tests of mitochondrial metabolism are confined to two cases in which reduced coupling efficiency in MG muscle biopsies were reported (Meijer 1972, Lousa, Gobernado et al. 1983).

Mitochondrial function is important in EOMs, a unique skeletal muscle allotype requiring a constant energy supply to sustain high firing rates (Fischer, Gorospe et al. 2002, Andrade and McMullen 2006, Garcia-Cazarin, Fisher et al. 2010). The EOMs are frequently weak in MG and may manifest treatment-resistant weakness in susceptible individuals (Heckmann and Nel 2017). Although it may not be the primary mechanism, we hypothesized that mitochondrial dysfunction triggered by MG may contribute to the persistent EOM weakness observed in OP-

MG cases despite adequate immune therapies and resolution of weakness in the non-ocular muscles. We therefore investigated dynamic mitochondrial responses in ocular fibroblasts of ophthalmoplegic myasthenia gravis (OP-MG) cases in comparison with controls.

## 1.2. Tissue selection

EOM myotendons were opportunistically harvested from OP-MG cases and non-MG controls undergoing ocular realignment surgeries (see Chapter 3). The EOM myotendons were cultured to produce phenotype-specific ocular fibroblasts. The benefits of using the ocular fibroblast cultures were that:

- (a) they could be expanded to optimise the quantity of cells for testing and
- (b) they could be exposed to different biological stimuli in culture such as active sera from MG patients.

These “perimysial” ocular fibroblasts differ from non-ocular fibroblasts in morphology, gene expression and function and demonstrate specificity for the EOM microenvironment (Kusner, Young et al. 2010). Compared with other fibroblasts, ocular fibroblasts showed trophic support for EOM myoblasts, inducing faster growth and differentiation (Kusner, Young et al. 2010). It is possible that these fibroblasts support EOM regenerative processes.

## 1.3. Investigating basal gene expression in ocular fibroblasts

The investigation of EOM gene expression using a custom qPCR array of 120 genes was previously described in Chapter 3. As ocular fibroblasts were to be used in dynamic metabolic tests as a surrogate for EOMs, OP-MG and control ocular fibroblast cultures were included in this array for comparison. Although ocular fibroblasts are not muscle cells, and substantial differences in gene expression were expected, we were interested to see which pathways would show differences in gene expression to determine whether the ocular fibroblasts are a suitable surrogate tissue for EOMs in dynamic tests of metabolism. Importantly, genes relating to mitochondrial function comprised 32 of the genes profiled and mostly formed part of the PGC-1 $\alpha$  pathway (Figure 1). This pathway regulates mitochondrial biogenesis, insulin-dependent glucose metabolism, hepatic gluconeogenesis and fatty acid oxidation (Arnold, Gill et al. 2014, Duarte, Amorim et al. 2015) and therefore differences in gene expression between the ocular fibroblasts and EOMs related to this pathway would be a relevant consideration in interpreting the results of the metabolic assays. The genes profiled in this pathway are shown in Figure 1.

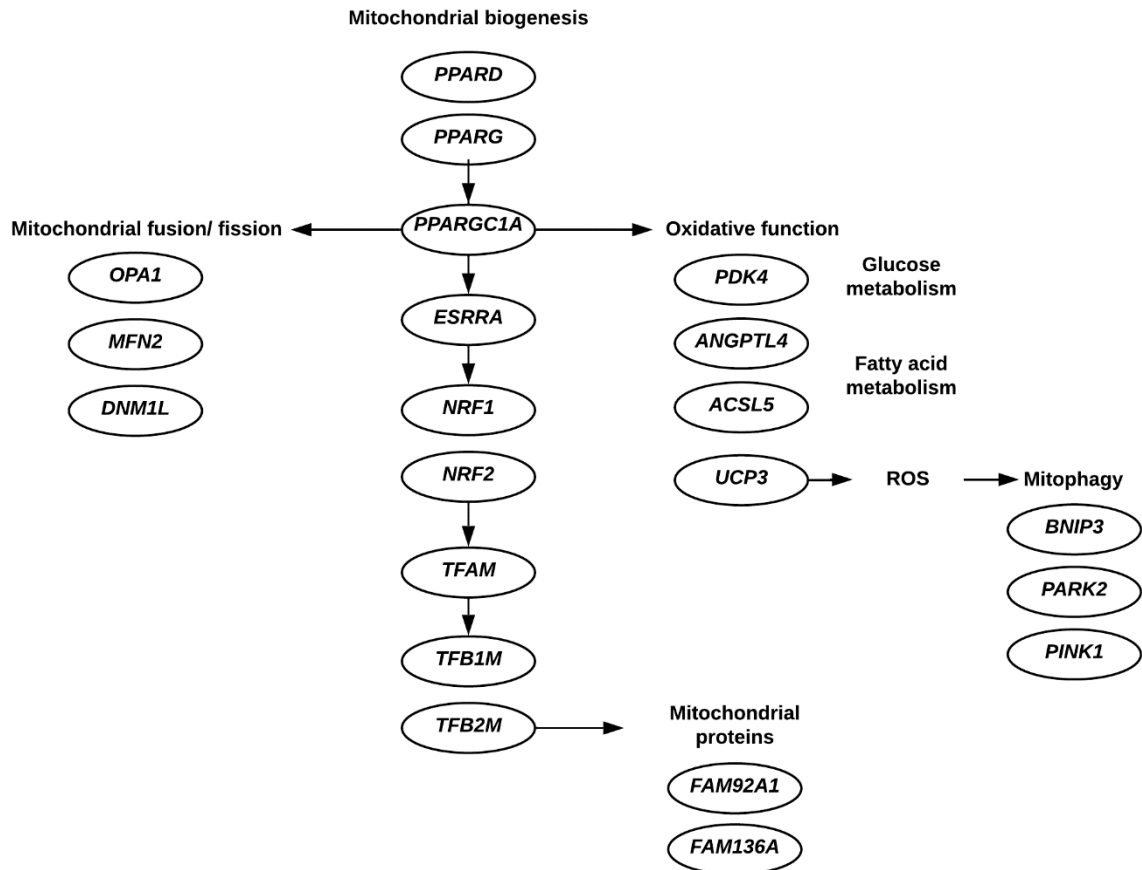


Figure 1. Genes in the PGC-1 $\alpha$  pathway profiled in EOMs and ocular fibroblasts. Reactive oxygen species (ROS).

Next, to ascertain whether there were differences between OP-MG and control phenotypes prior to experimental exposures, the basal expression of the same panel of genes was compared in OP-MG and control ocular fibroblasts.

#### 1.4. Exposure of ocular fibroblasts to myasthenia gravis sera

To investigate whether an MG stimulus may induce transcriptional and/or dynamic effects on oxidative metabolism in ocular fibroblasts *in vitro*, the ocular fibroblasts were exposed to homologous sera of newly diagnosed MG cases with acetylcholine-receptor (AChR) antibody positive MG (See Methods, section 2.1). Previous work showed that myoblasts and transdifferentiated myocytes were responsive to AChR-antibody positive MG sera *in vitro* which induced cytoskeletal changes, apoptosis or transcriptional changes (Luckman, Skeie et al. 2006, Nel, Prince et al. 2019). We therefore reasoned that ocular fibroblasts may also be responsive to MG sera despite not expressing AChRs. It was hypothesized that other factors such as cytokines, circulating microRNAs and other regulating RNA species in MG sera may impact ocular fibroblast function.

### 1.5. Investigating the effects of MG sera on gene expression in ocular fibroblasts

In rodent experimental autoimmune myasthenia gravis (EAMG) models, induced either by passive-transfer (Zhou, Kaminski et al. 2014) or active immunization (Kaminski, Himuro et al. 2016), *PDK4*, *ANGPTL4* and *UCP3*, genes of the PGC-1 $\alpha$  pathway involved in oxidative metabolism, were upregulated in EOMs, diaphragm muscle and limb skeletal muscle which may indicate a significant shift in EOM metabolism. Previously in transdifferentiated myocytes of OP-MG cases, *in vitro* exposure to MG sera caused upregulation of *PDK4* and *ANGPTL4* and downregulation of *UCP3* in comparison with control-MG myocytes (Nel, Prince et al. 2019). Under normal physiological conditions, low levels of expression of *PDK4* and *UCP3* were demonstrated in EOMs compared to non-ocular muscles (Fischer, Gorospe et al. 2002, Fischer, Budak et al. 2005), meaning that the changes in gene expression in the context of MG observed in rodent muscle (EAMG) and in human myocytes exposed to MG sera show a change in metabolism from the normal physiological state. To determine whether similar transcriptional changes would occur in ocular fibroblasts, the expression of *PDK4*, *ANGPTL4* and *UCP3* was investigated in OP-MG and control ocular fibroblasts at basal levels and after exposure to MG sera.

### 1.6. Investigating mitochondrial bioenergetics using live-cell metabolic assays

Live-cell metabolic assays, capable of measuring mitochondrial function in small quantities of live, intact cells, were used to analyse the ocular fibroblasts. Previous methods of measuring mitochondrial function required isolated mitochondria or large amounts of cells that could survive prolonged stirring in suspension (Divakaruni, Paradyse et al. 2014). However, live-cell metabolic assays allow for dynamic assessment of mitochondrial function under more physiological conditions than tests using isolated mitochondria, and may be used to investigate cellular responses to multiple stressors and/or treatments (Divakaruni, Paradyse et al. 2014).

The Agilent Seahorse XF Serial *in vitro* measurements of oxygen and proton concentration were measured to quantify rates of oxidative phosphorylation and glycolysis as the oxygen consumption rate (OCR) and extracellular acidification rate (ECAR) respectively (Brand and Nicholls 2011, Divakaruni, Paradyse et al. 2014). A graphical comparison of OCR and ECAR values was generated to assess the overall metabolic state of the cell viz. quiescent, aerobic, energetic or glycolytic (Figure 2A). To induce dynamic responses to metabolic stress, oligomycin and carbonyl cyanide p-trifluoromethoxyphenylhydrazone (FCCP), were injected simultaneously after establishing baseline measurements. Together, these stressors inhibit ATP synthase and uncouple respiration resulting in maximal OCR and ECAR rates which is referred to as the “stressed phenotype”. A metabolic shift from quiescence to aerobic,

energetic or glycolytic phenotypes indicates increased requirements for ATP for processes such as protein synthesis (Divakaruni, Paradyse et al. 2014). This test provides a general, qualitative assessment of metabolism.

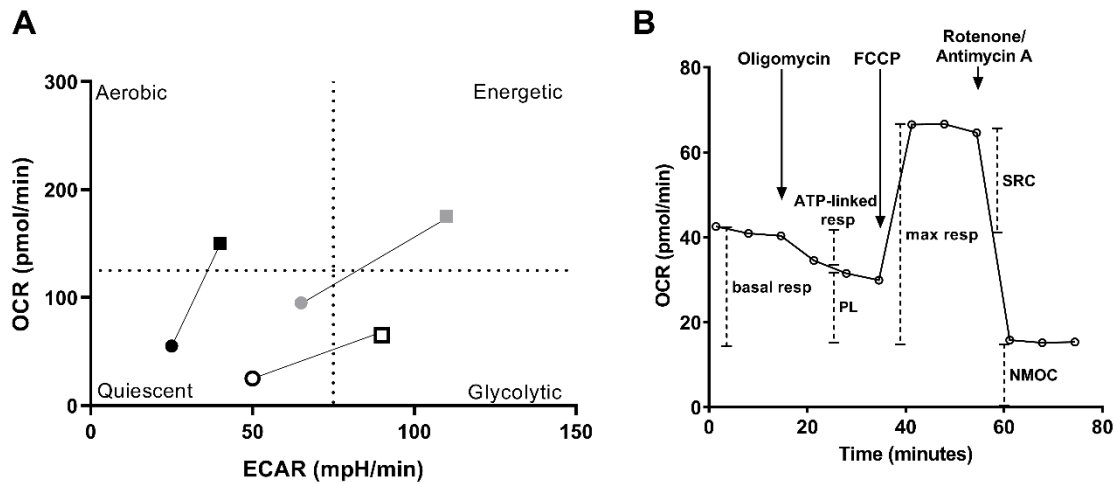


Figure 2. A. Oxygen consumption rate (OCR) is plotted against the extracellular acidification rate (ECAR) to visually assess the general metabolic state of the cell. Baseline measurements in this graph are indicated by circles. Simultaneous injection of the stressors oligomycin and carbonyl cyanide p-trifluoromethoxyphenylhydrazine (FCCP) produces the “stressed” metabolic phenotype which is indicated by squares. B. Illustrative graph showing the parameters of oxidative phosphorylation measured after sequential inhibition of respiratory complexes. described in the Mito stress test. Oxygen consumption rate (OCR); respiration (resp); proton leak (PL); carbonyl cyanide p-trifluoromethoxyphenylhydrazine (FCCP); spare respiratory capacity (SRC); non-mitochondrial oxygen consumption (NMOC). Arrows indicate oligomycin, FCCP and rotenone/antimycin A injections.

A second independent assay, involving the sequential injection of mitochondrial stressors over time (oligomycin, carbonyl cyanide p-trifluoromethoxyphenylhydrazine (FCCP), and Rotenone/Antimycin A) allowed for measurement of dynamic responses in OCR to inhibition of specific respiratory complexes (Figure 2B). Addition of oligomycin, an inhibitor of adenosine ATP-synthase, allows for measurement of ATP-linked oxygen consumption (state 4o) and proton leak (Brand and Nicholls 2011). Maximal respiration is calculated after the addition of FCCP which uncouples respiration from ATP production and is used to calculate the spare respiratory capacity, a marker of respiratory reserve (Brand and Nicholls 2011). A combination of rotenone and Antimycin A inhibits complexes I and III of the electron transport chain respectively, thereby inhibiting mitochondrial respiration and allowing for calculation of the non-mitochondrial oxygen consumption (Divakaruni, Paradyse et al. 2014).

The respiratory control index (RCI) is a well-established measure of mitochondrial sufficiency using isolated mitochondria. An analogous measurement, the cell respiratory control ratio (CRCR) was proposed by Brand et al. for live-cell metabolic assays, as the RCI was calculated in response to controlled exposure to oxidative substrates, which is not possible in intact cells where the cell membrane is impermeable to most commonly-used substrates (Brand and Nicholls 2011). The CRCR is calculated as the ratio of maximal respiration to proton leak (Brand and Nicholls 2011).

As it was postulated that mitochondrial metabolism may be altered in the context of MG, during the functional tests the ocular fibroblasts were exposed MG sera to elicit MG-specific responses. The novelty of these mitochondrial functional tests is that a) dynamic tests of mitochondrial function have not been previously performed in the context of MG orbital tissues and b) tests on live cells of MG cases, which provides a more physiological context and allows for dynamic assessment of mitochondrial function after exposure to different stressors (Brand and Nicholls 2011) have not been previously performed.

The objectives of this chapter relate to performing pilot genetic and dynamic studies in ocular fibroblasts to assess aspects of mitochondrial metabolic pathways in OP-MG cases vs controls. In order to address these aims, cultures of patient-derived perimysial ocular fibroblasts from the EOM myotendons of OP-MG and control cases were established. An additional comparison of gene expression was performed between ocular fibroblasts and EOMs using the custom qPCR array data as described in Chapter 3.

#### Main aims

1. To investigate the impact of MG sera on the expression of selected genes in ocular fibroblast cultures previously altered in EAMG.
2. To investigate bioenergetics in ocular fibroblasts using dynamic tests of metabolism with and without MG sera and the differences between OP-MG and control fibroblasts.

## 2. Materials and methods

### 2.1. Tissue collection and culture of ocular fibroblasts

In highly selected MG cases with an established diagnosis of treatment-resistant ophthalmoplegia and diplopia, ocular re-alignment surgery may be considered to improve visual function (Heckmann and Nel 2017, Rautenbach, Pillay et al. 2017). We acquired resected EOM myotendons from two OP-MG patients, aged 27 (on azathioprine and 10mg prednisone daily) and 42 years (on methotrexate only) at the time of ocular re-alignment surgery, who both had generalised MG with circulating anti-acetylcholine receptor (AChR) antibodies (Heckmann, Owen et al. 2007). For comparison, we acquired EOM tendon specimens from five control patients who were undergoing surgery for strabismus due to non-MG causes (mean age 35 years) (see Table 1). These tissues were obtained with informed consent and approval from the institutional Human Research Ethics Committee (HREC 257/2012 and 602/2020).

Table 1. Patient-derived ocular fibroblast cell cultures

Diagnosis	Age at surgery (years)	Duration of MG (years)
OP-MG	27	16
OP-MG	42	40
secondary esotropia*	56	NA
secondary esotropia*	52	NA
congenital strabismus	14	NA
secondary esotropia*	31	NA
intermittent exotropia	21	NA

Table 1. OP-MG refers to the treatment-resistant ophthalmoplegic subphenotype of MG. EOM refers to extraocular muscle. \*esotropia secondary to blindness as a result of trauma, glaucoma, or congenital cause.

Perimysial ocular fibroblasts were cultured from the myotendinous junctions of medial or lateral rectus EOMs. Each myotendon specimen was finely minced under sterile conditions and then cultured under coverslips in Gibco Dulbecco's Modified Eagle Medium (DMEM) supplemented with foetal bovine serum (10%) and penicillin/streptomycin (1%) at 37°C and 5% carbon dioxide (Figure 3). Fibroblasts appeared after 5 – 7 days (Figure 3B). The ocular fibroblast cultures were expanded and cryopreserved in growth medium and 10% dimethyl

sulfoxide (DMSO) at a freezing rate of 1°C/min (Nalgene cryocontainer) at -80°C before longer term preservation in liquid nitrogen. Cells were used up to passage 9 and were kept in liquid nitrogen storage for 12-18 months for completion of the experiments. Cultures tested negative for mycoplasma.

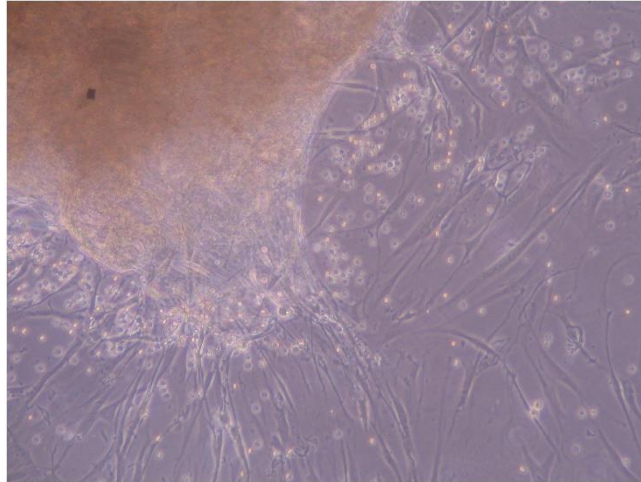


Figure 3. Cultured extraocular myotendon with fibroblast outgrowth after 5 days in culture viewed at 100x magnification.

To mimic the MG stimulus *in vitro*, we exposed OP-MG and control patient-derived ocular fibroblast cultures to growth medium supplemented with homologous MG sera previously stored in 1mL aliquots at -20°C (Nel, Prince et al. 2019) at 5% concentration for 24 hours before qPCR or live-cell metabolic experiments (Figure 4). For comparison, in every experiment where we exposed ocular fibroblasts to MG sera, we performed the same procedures on ocular fibroblasts derived from the same cases in plain growth medium, i.e. we split the cells of each ocular fibroblast culture into “MG-sera treated” and “untreated” groups. The median age of the individuals from whom we received MG sera was 26 years (range 14 - 65 years, n=5). No comorbid disease or infections were present at the time of MG sera collection and all patients had detectable circulating acetylcholine receptor (AChR) antibodies with substantial EOM weakness.

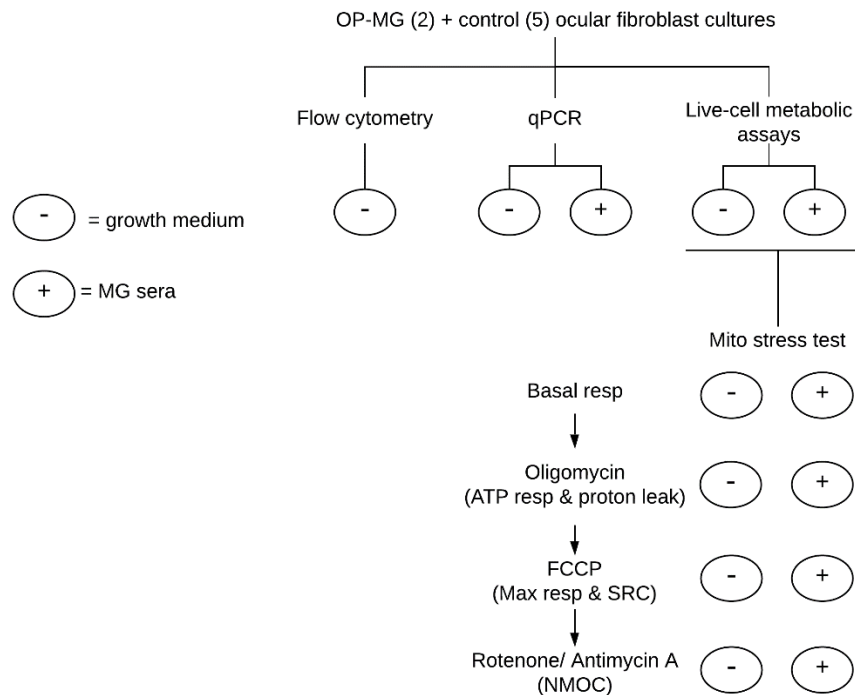


Figure 4. Experiment design and terminology. Ocular fibroblast cultures derived from patients with treatment-resistant ophthalmoplegia (OP-MG) and strabismic controls (without myasthenia gravis (MG) were left untreated in plain growth medium (“-”) or treated with 5% MG sera (“+”) for 24 hours. Quantitative polymerase chain reaction (qPCR); FCCP (carbonyl cyanide p-trifluoromethoxyphenylhydrazone); extracellular acidification rate (ECAR); oxygen consumption rate (OCR); respiration (resp); maximal (max); spare respiratory capacity (SRC); non-mitochondrial oxygen consumption (NMOC).

## 2.2. Flow cytometry

We used flow cytometry (Figure 4) to quantify fibroblast and myofibroblast populations in the cell cultures using immunolabelling with vimentin and  $\alpha$ -smooth muscle actin ( $\alpha$ -SMA) antibodies respectively. The cultured, adherent cells were trypsinized, quantified using a haemocytometer and resuspended in phosphate buffered saline (PBS). Cells were stained, washed in permeabilization solution and marked with the appropriate antibodies. Flow cytometry was conducted using the BD Accuri C6 flow cytometer (Becton Dickinson Biosciences) and the data was analysed using FlowJo (Tree Star Incorporated). The gating strategy excluded dead cells, debris and doublets before quantifying the proportion of vimentin and/or  $\alpha$ -SMA positive cells.

## 2.3. RNA isolation and reverse transcription

RNA was isolated from the ocular fibroblasts using the Roche High Pure RNA kit as per manufacturer protocol, including the in-column DNase treatment to prevent genomic DNA contamination. RNA concentrations were  $>80\text{ng}/\mu\text{L}$  with spectrophometric ratios of  $A_{260}/A_{280} >1.8$  and  $A_{260}/A_{230} >1.7$  as measured by the Nanodrop v.1000. The RNA integrity (RIN) values ranged from 6 - 9 using the Agilent Bioanalyzer. RNA isolation from the EOMs is described in Chapter 3.

For each ocular fibroblast sample used in the qPCR array 40ng of RNA was reverse transcribed (see Chapter 3), whereas in the qPCR experiments investigating the expression of individual genes 300ng of RNA was reverse transcribed using the Promega ImProm-II Reverse Transcription system according to the manufacturer's specifications.

## 2.4. Quantitative polymerase chain reaction (qPCR)

### 2.4.1. Reference gene selection, reverse transcription and qPCR methods

#### *Basal gene expression in ocular fibroblasts and comparisons with extraocular muscles*

Gene expression in four ocular fibroblast cultures (2 OP-MG and 2 control) was investigated. Reference genes for normalization were selected using the geNorm (Vandesompele, De Preter et al. 2002) and Bestkeeper methods (Pfaffl, Tichopad et al. 2004). The details of the reference gene selection are shown in Appendix tables 1 and 2. For the specific methods related to reverse transcription and qPCR array see Chapter 3. Using the same array data for the ocular fibroblasts, basal gene expression was compared between OP-MG (n=2) and control (n=2) ocular fibroblast cultures. An additional analysis was to compare the expression of the genes of interest between the ocular fibroblast cultures (n=4) and EOMs (n=2).

#### *Ocular fibroblast gene expression in the presence of MG sera*

In order to compare the effects of MG sera on gene expression, it was important to identify a stable reference gene in the presence of MG sera. A qPCR array was used to identify stable reference genes for use in subsequent qPCR experiments using ocular fibroblasts with and without MG sera. We evaluated the expression of 10 reference genes in two OP-MG ocular fibroblast lines at baseline and after MG sera exposure using the Qiagen RT<sup>2</sup> Custom Profiler PCR Array plate. *RPLP0* and *CSNK2A2* were determined to be the most stable using the geNORM (Vandesompele, De Preter et al. 2002) and Bestkeeper algorithms (Pfaffl, Tichopad et al. 2004) (Appendix table 3). Based on the reference gene analysis in the exploratory qPCR array, primers for *RPLP0* (*NM\_001002*, *NM\_053275*) and *CSNK2A2* (*NM\_001896*, *XM\_005255799*, *XM\_005255800*, *XM\_005255801*) were obtained from Qiagen.

Quantitative PCR was performed using the KAPA SYBR FAST qPCR Master Mix (Sigma-Aldrich) and the Lightcycler 2.0 (Roche Life Science). QuantiTect primer assays (Qiagen) were obtained for *PDK4* (NM\_002612), *ANGPTL4* (NM\_016109, NM\_139314, XM\_005272484) and *UCP3* (NM\_003356).

## 2.5. Live cell metabolic assays

The Seahorse extracellular flux (XF) 96 analyzer (Seahorse Bioscience, Agilent technologies) was used to perform the live-cell metabolic assays. The assays (Phenotype and Mito stress tests) were each performed with and without 5% MG sera (Figure 4).

### *Preparation of ocular fibroblast cultures*

Ocular fibroblasts were thawed and plated at a concentration of  $\pm 2.5 \times 10^4$  cells/mL. These were expanded in culture until sufficient fibroblasts from each patient cell culture were obtained ( $\pm 1 \times 10^6$  cells in total). These were trypsinized (0.25% trypsin-EDTA) and resuspended to a concentration of  $4 \times 10^4$  cells/100 $\mu$ L for each patient cell culture. These cell suspensions were plated in 96-well plates (80 $\mu$ L per well) in triplicate (passage 6 – 8) and incubated x 24 hours at 37°C and 5% CO<sub>2</sub> to allow cells to adhere. On the day of plating the fibroblasts, the Seahorse XF cartridge was prepared with calibrant and incubated in a non-CO<sub>2</sub> incubator.

### *Preparation of Seahorse XF assay medium*

Agilent Seahorse XF RPMI base medium was supplemented according to the manufacturer's guidelines i.e. 1% glucose (1.0M), 1% pyruvate (100mM) and L-glutamine (200mM). Base pH was maintained at 7.4 using NaOH/HCl if needed. No additional buffers were added.

### *Preparation of compounds*

Compounds oligomycin, FCCP and rotenone/antimycin A were prepared using assay medium at volumes specified in the manufacturer's guidelines. These were then pipetted systematically into the designated injection ports.

On the day of the assay, the fibroblasts were viewed to check that cells were adherent and forming a confluent monolayer. Background correction wells were checked for cells. Prior to the assay, the fibroblasts were washed and incubated in the prepared Seahorse XF assay medium (section 2.5.2) for 1 hour in a non-CO<sub>2</sub> incubator. After machine calibration, the 96-well plate was then loaded into the Seahorse XF 96 machine and the assay was allowed to run.

#### 2.5.1. Phenotype test

After measuring OCR and ECAR at baseline, the 'stressor mix' consisting of oligomycin (1.0 $\mu$ M) and FCCP (1.5 $\mu$ M) was added via the injection ports and the response to the stressor mix was measured.

#### 2.5.2. Mito Stress test

Oligomycin (1.0 $\mu$ M), FCCP (1.5 $\mu$ M) and Rotenone/Antimycin A (0.5 $\mu$ M) were sequentially added (as per Seahorse XF software) to calculate the basal respiration, maximal respiration, spare respiratory capacity (SRC), ATP respiration, proton leak and non-mitochondrial oxygen consumption rate of the ocular fibroblasts.

### 2.6. Data analysis and statistics

#### 2.6.1. Investigations of gene expression

Differential gene expression analysis was performed using the  $\Delta$ Cq method (Schmittgen and Livak 2008) and expressed as fold change or the  $\log_2$  transformed fold change for graphical presentation. Statistical significance of these differences was calculated using unpaired students t tests, or in cases where the sample size was too small, Mann-Whitney-U tests. P values <0.05 were considered significant unless otherwise specified. For the qPCR array data, correction for multiple testing was performed using the Benjamini Hochberg correction. A false detection rate (FDR) of 5% was accepted. Graphs were generated using Prism Graphpad v.8.

#### 2.6.2. Live cell metabolic assays

The Seahorse XF Report Generator was used to calculate and report assay measurements. Between OP-MG and control ocular fibroblast cultures we compared absolute OCR or ECAR values with and without MG sera exposure by unpaired student's t tests as all continuous data was determined to be normally distributed data by Shapiro-Wilk tests. P values  $\leq$ 0.05 (2-tailed) were considered significant. We compared the responses in OCR and ECAR to MG sera exposure between the OP-MG and control ocular fibroblasts, i.e. to see whether the dynamic responses in OCR and ECAR in OP-MG ocular fibroblast cultures were significantly different to controls. These were reported as fold change (MG sera/untreated).

## 3. Results

### 3.1. Flow cytometry verified the presence of ocular fibroblasts in cell cultures grown from EOM myotendons

Flow cytometry was performed on all seven patient-derived cell cultures (Figure 5). Vimentin positive cells comprised 98% (SD $\pm$ 2%) which is consistent with a predominant fibroblast

population. However, a large proportion of the cells in each culture were also immunoreactive to  $\alpha$ -SMA (mean 45%; SD $\pm$ 35%) indicating differentiation into myofibroblasts. Importantly, there was no difference in the proportion of myofibroblasts between OP-MG and control ocular fibroblast cultures ( $p=0.38$ ). These perimysial ocular fibroblast cultures displayed similar morphology and immunophenotyping to those in previous reports (Smith 2004, Kusner, Young et al. 2010).

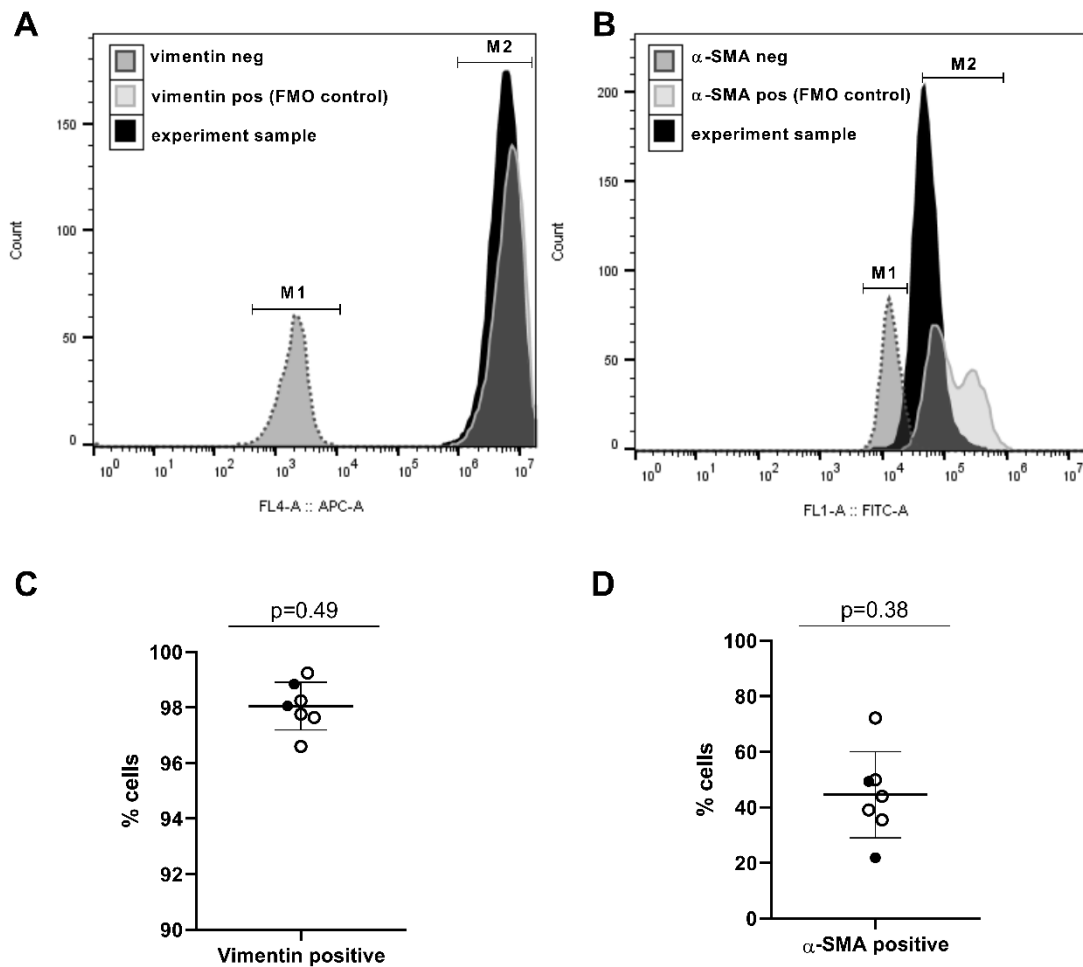


Figure 5. Quantification of fibroblast and myofibroblast populations using flow cytometry. Histograms A and B show, as an example, the results of the gating strategy in one cell culture to determine the proportions of cells immunopositive to vimentin antibodies (A) and  $\alpha$ -SMA antibodies (B). Histograms for the other six cell cultures were similar. M1 indicates the immunonegative population while M2 indicates the immunopositive population. Fluorescence minus one control (FMO). C and D show the percentages of cells in each individual ocular fibroblast culture that were immunopositive for either vimentin or  $\alpha$ -SMA. OP-MG fibroblasts are indicated with black circles while controls are in open circles.

## A. Genetic studies

### 3.2. Ocular fibroblast gene expression involving mitochondrial pathways differs from extraocular muscles

Data was normalized to the reference gene *RPLP0* which was the most stable between the EOMs and ocular fibroblast samples. Comparing the gene expression in ocular fibroblast cultures (n=4) and EOMs (n=2) for an array of 120 genes known to be highly expressed in EOMs and/or skeletal muscle, the genes encoding tumour necrosis factor (*TNF*), the mitochondrial transcription factor *ESRRG*, myogenesis transcription factor (*PAX7*) and interleukin-10 receptor (*ILR10A*) were not expressed in the ocular fibroblasts.

Significant differences in gene expression between the ocular fibroblasts and EOMs are shown in Figure 6 ( $p \geq 0.01$ , FDR 5%). As the ocular fibroblasts are not muscle cells, large differences in gene expression between the EOMs and ocular fibroblasts were shown for 9 genes encoding muscle markers including the myosin heavy chain isoforms (>600-fold,  $p < 0.0009$ ), the intermediate filament desmin (>500-fold,  $p = 0.0014$ ) and genes encoding proteins of the neuromuscular junction including the acetylcholine receptor subunits (*CHRNA1* >5000-fold; *CHRNE* and *CHRNA3* >25-fold,  $p < 0.042$ ) as well as muscle-specific kinase (*MUSK*) which causes clustering of the acetylcholine receptors on the muscle endplate (29-fold,  $p = 0.019$ ). Eight genes involved in pathways relating to muscle regeneration/atrophy including the IGF-1 and IL-6 pathways and the ubiquitin protease system were upregulated in the EOMs ( $p < 0.007$ ).

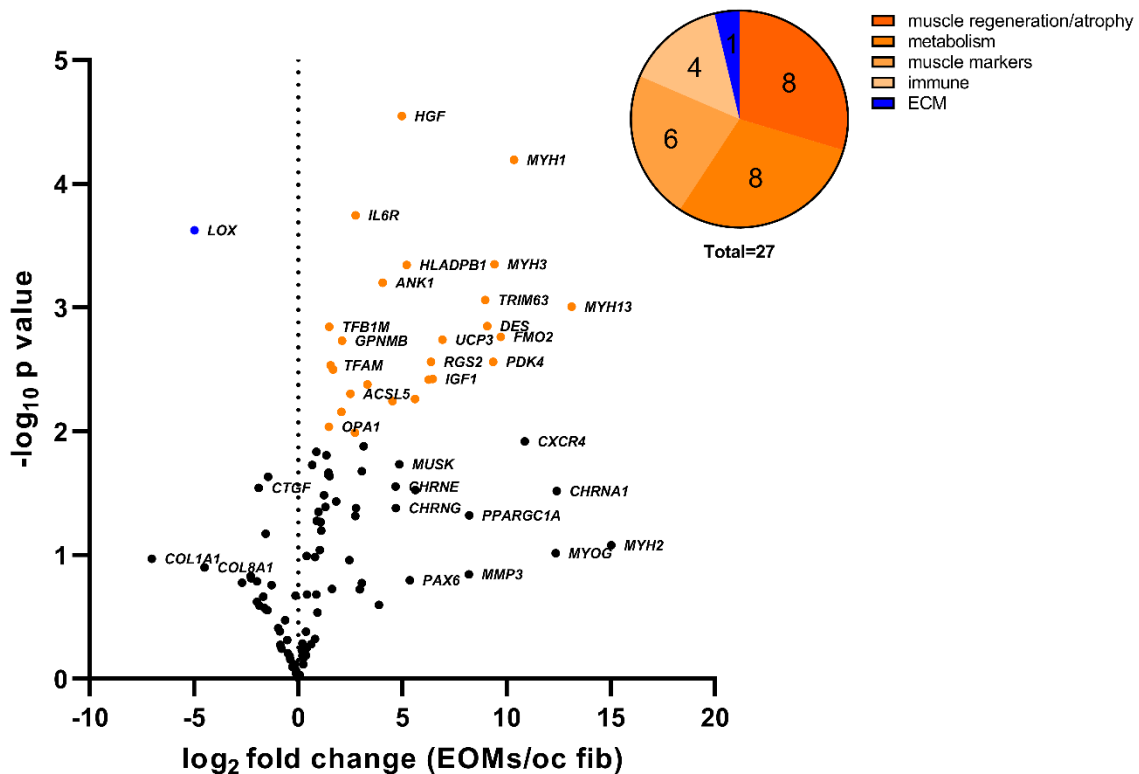


Figure 6. Differences in gene expression between the ocular fibroblasts (oc fib) and EOMs are shown in the volcano plot. Differentially expressed genes reaching statistical significance after Benjamini-Hochberg correction with false discovery rate (FDR) set at 5% are shown in colour. Inset: Pie chart showing the categorization of differentially expressed genes by biological pathway. Extracellular matrix (ECM).

As the EOMs are highly metabolically active compared to the ocular fibroblasts, it was expected that genes relating to glucose and oxidative metabolism would be upregulated in the EOMs. Of 32 genes relating to metabolism that were profiled, half were upregulated in the EOMs ( $p < 0.05$ ) although only 9 reached statistical significance after correction for multiple tests of significance ( $p \leq 0.009$ ). Genes encoding transcription factors involved in mitochondrial biogenesis (*TFAM* and *TFB1M*) and genes regulating glucose metabolism (*PDK4* and *IGF1*) and oxidative metabolism (*FMO2*, *UCP3*, *ACSL5*) comprised the most significantly upregulated genes in the EOMs related to metabolism ( $p \leq 0.007$ ). Genes regulating mitochondrial fission/fusion were also upregulated in the EOMs including *OPA1* ( $p = 0.009$ ), *MFN2* and *DNM1L* ( $p \leq 0.045$ ) while genes relating to glycogen storage, apoptosis and mitophagy did not show significant differences in gene expression.

Four genes involved in the regulation of immune function and inflammatory processes in muscle were upregulated in the EOMs ( $p \leq 0.001$ ). As the ocular fibroblasts were cultured from

EOM myotendons, *LOX*, a gene involved in extracellular matrix (ECM) regulation was upregulated in the ocular fibroblasts compared to the EOMs ( $p=0.0002$ ), together with three other genes relating to ECM regulation but which reached subthreshold levels of significance including the genes encoding connective tissue growth factor (*CTGF*) and collagens (*COL1A1* and *COL8A1*) ( $p\leq 0.13$ ).

Although the ocular fibroblasts are highly specialised and show specificity for the EOM microenvironment, substantial differences in gene expression were shown between the EOMs and ocular fibroblasts particularly in genes relating to muscle-specific pathways and metabolism. This is not surprising as the custom plate was populated with genes known to be expressed in muscle and in EOMs. That genes relating to glucose and oxidative metabolism were more highly expressed in the EOMs highlights the importance of these processes in EOM function. Despite the limitations of performing the dynamic studies in orbital fibroblasts, live cultures of ocular muscles are not possible. Therefore, evidence for dysregulation of these processes in dynamic metabolic assays in the context of MG, albeit shown in ocular fibroblasts rather than EOMs, may shed light on oxidative metabolism in response to MG sera *in vitro*.

### 3.3. Basal gene expression in OP-MG ocular fibroblasts is similar to controls

Basal gene expression was investigated in 2 OP-MG and 2 control ocular fibroblast cultures using the same array data as section 3.2. Here, data was normalized to the reference gene *ACTN2* (Appendix table 2). At basal levels, no significant differences in gene expression were shown between OP-MG and control fibroblasts ( $p\geq 0.07$ ). However, 3 genes with ~3-fold change ( $p\leq 0.15$ ) showed different trends of basal expression in this small sample by phenotype; *FAM69A*, an OP-MG associated gene (Nel, Prince et al. 2019), *FBXO32* and *MT1A*, which were previously upregulated in the EOMs and other muscles of EAMG rodents (Kaminski, Himuro et al. 2016).

As the basal expression in OP-MG and control ocular fibroblasts were similar, we were interested to see if the MG-specific stimulus of *in vitro* MG sera exposure would trigger changes in gene expression and metabolism in the ocular fibroblasts.

### 3.4. MG sera increased gene transcripts relating to oxidative metabolism

Expression of genes *PDK4*, *ANGPTL4* and *UCP3* was investigated in 3 independent qPCR experiments comparing OP-MG ( $n=2$ ) and control ( $n=5$ ) ocular fibroblasts. Normalization of data after MG sera exposure was performed using reference genes *RPLP0* and *CSNK2A2* which showed stability across all fibroblasts ( $p>0.32$ ).

The basal expression of *PDK4*, *ANGPTL4* and *UCP3* was similar in OP-MG ( $n=2$ ) and control ( $n=5$ ) ocular fibroblasts ( $p>0.20$ ) in the 3 independent qPCR experiments as well as in the OP-

MG (n=2) and control (n=2) fibroblasts in the array (section 3.3). However, exposure to 3 of 4 MG sera tested, induced consistent ~2-fold upregulation of *PDK4* (p=0.016) and *ANGPTL4* (p=0.031) in all ocular fibroblast cultures, regardless of phenotype. *UCP3* expression levels remained unchanged (Figure 7). Although the effects of MG sera did not show differences between OP-MG and control phenotypes (p>0.61), the transcript levels of *PDK4* and *ANGPTL4* in seven ocular fibroblast cultures and with reproducibility, showed that MG sera upregulated the expression of these two genes.

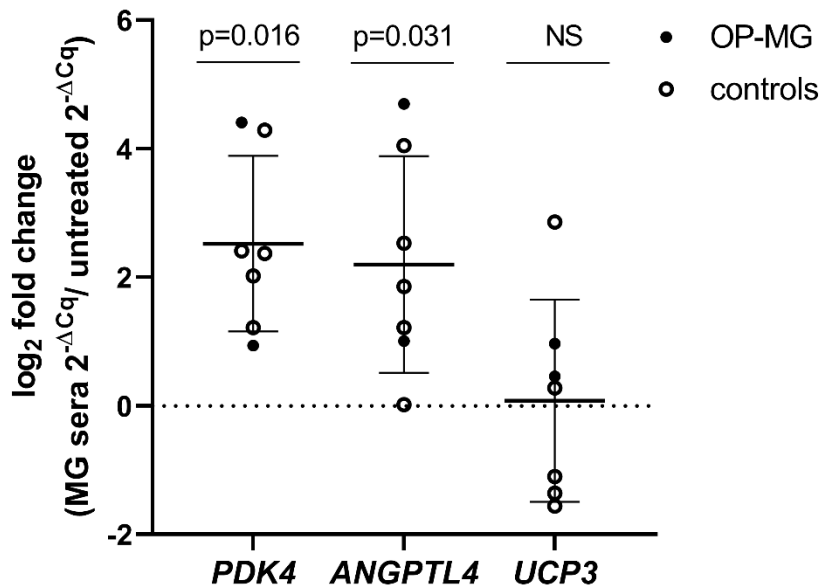


Figure 7. MG sera induced upregulation of *PDK4* and *ANGPTL4* but not *UCP3* in ocular fibroblasts (OP-MG and controls). Each data point represents the log<sub>2</sub> fold change in response to 1 of 3 MG sera (5% x 24 hours) for seven ocular fibroblast cultures in 3 independent experiments performed in duplicate (averaged). The p values were calculated by Mann-Whitney U tests. Not significant (NS).

Taken together, gene expression of candidate targets of mitochondrial pathway genes in ocular fibroblasts have shown that although it may differ from EOMs, in both OP-MG and control ocular fibroblast cultures, MG sera induced significant upregulation of 2 genes in the PGC-1 $\alpha$  pathway that increase oxidative metabolism suggesting that MG sera may impact mitochondrial function.

## B. Dynamic studies of mitochondrial function in ocular fibroblasts

### 3.5. MG sera induces a more energetic phenotype in OP-MG ocular fibroblasts

Phenotype tests (n=3) were performed on all ocular fibroblast cultures. Without MG sera exposure, all the ocular fibroblast cultures showed similar states of quiescence at baseline (Figure 8A). With exposure to 5% MG sera for 24 hours, the OP-MG ocular fibroblasts became more “energetic” than the controls with increased rates of oxidative phosphorylation (OCR) and glycolysis (ECAR) (Figure 8B).

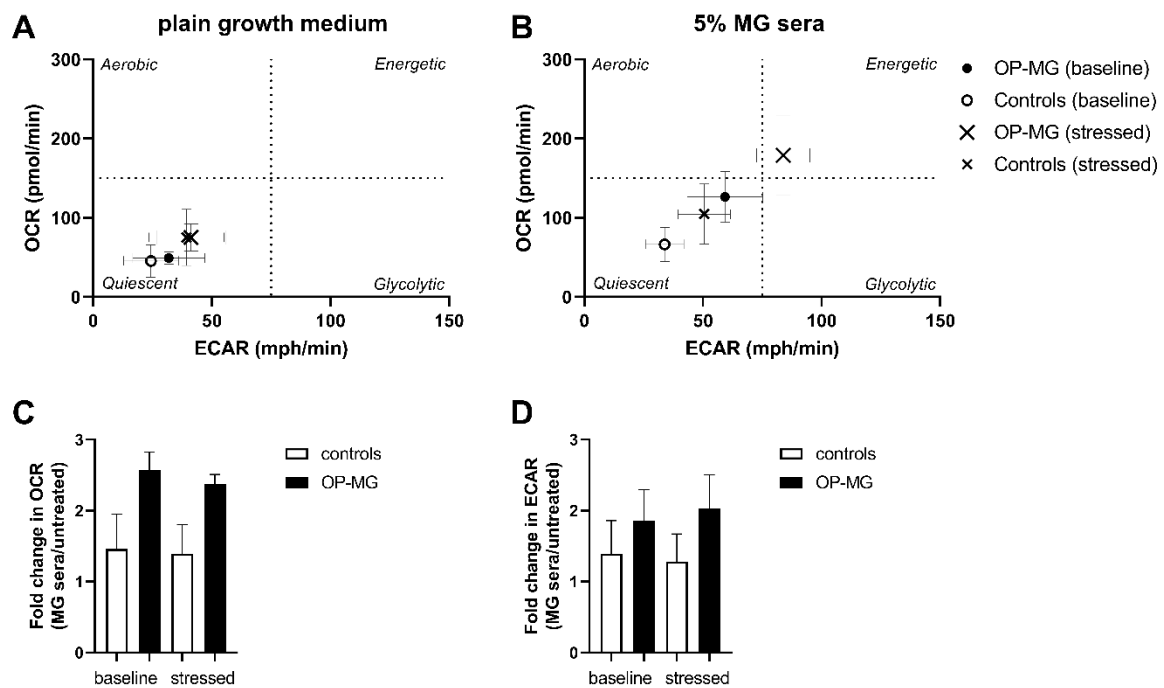


Figure 8. A. OP-MG and control ocular fibroblasts have similar metabolic phenotypes in plain growth medium. B. OP-MG ocular fibroblasts become more “energetic” after exposure to MG sera. “Stressed” values are indicated by X symbols. For both A and B, average values for OP-MG and controls are presented (n=3; each plated in triplicate). C. The fold change values in OCR in response to MG sera. D. The fold change values in ECAR in response to MG sera.

Although the experiments were performed using five different MG sera, two did not induce significant changes in metabolic parameters compared to untreated conditions in any of the ocular fibroblast cultures (data not shown), whereas three sera showed similar results across replicate experiments. The OCR of the OP-MG ocular fibroblasts increased to 1.9-fold higher than the controls (p=0.031) and the ECAR to 1.75-fold higher (p=0.030). Figures 8C and 8D show the fold change in OCR and ECAR values in response to MG sera exposure which is higher in the OP-MG ocular fibroblasts than the controls. After the addition of stressors

(oligomycin and FCCP), a similar increase in OCR and ECAR was seen in both OP-MG and control ocular fibroblasts (1.5-fold) with and without MG sera.

The results of the phenotype tests showed that although the basal metabolism of the OP-MG and control ocular fibroblasts is similar, exposure to MG sera induced increased metabolic activity in both glycolytic and oxidative pathways.

3.6. MG sera increased all parameters of oxidative phosphorylation in OP-MG ocular fibroblasts but not controls

Two independent Mito stress test assays were performed on all ocular fibroblast cultures and the results were consistent. As seen in the phenotype tests, without MG sera stimulation, the average OCR values for the OP-MG ocular fibroblasts were similar to controls ( $p=0.34$ ). However, the basal OCR levels of the two OP-MG cases differed more widely than controls in both independent experiments (OP-MG OCR SD=33.5 vs 2.6 for controls).

With 24-hour exposure to 5% MG sera, the OCR of the OP-MG ocular fibroblasts from both cases increased 1.6-fold overall ( $p<0.001$ ) while the average control ocular fibroblast OCR remained the same. The increase in OCR of OP-MG ocular fibroblasts in response to MG sera exposure (Figure 9) was observed across all parameters of OCR measured ( $p<0.05$ ) i.e., basal respiration, maximal respiration, ATP-linked respiration and non-mitochondrial oxygen consumption except the proton leak which showed a trend towards significance ( $p=0.09$ ). No change was observed in the controls.

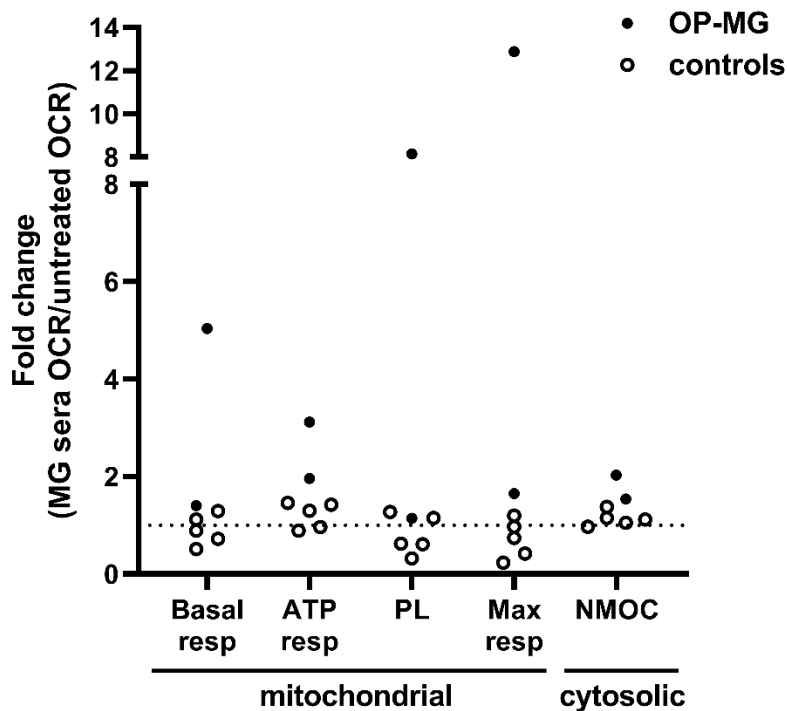


Figure 9. Mito stress tests. MG sera-induced changes in measures of oxygen consumption rate. Each data point represents the fold change in oxygen consumption rate (OCR) for each ocular fibroblast culture (OP-MG=2; controls=5) in response to myasthenia gravis (MG) sera (5% for 24 hours) from untreated OCR levels in two independent experiments (performed in triplicate). Differences in fold change between OP-MG and ocular fibroblasts were significant for all parameters ( $p \leq 0.049$ ) except the proton leak ( $p = 0.09$ ). Respiration (resp); non-mitochondrial oxygen consumption (NMOC); proton leak (PL). Unpaired student's t tests were used to compare  $\log_2$  fold change values between OP-MG and controls (log-normal distribution).

The cell respiratory control ratio (CRCR), i.e. the ratio of maximal respiration to proton leak, was similar in OP-MG and control ocular fibroblasts at basal levels ( $p = 0.40$ ) and after exposure to MG sera ( $p = 0.63$ ) and does not show evidence of mitochondrial insufficiency in OP-MG ocular fibroblasts (Brand and Nicholls 2011).

In summary, the basal metabolism of the OP-MG and control ocular fibroblast cultures was similar however, exposure to MG sera from three different homologous donors increased glycolysis and oxidative phosphorylation parameters in OP-MG ocular fibroblasts and not controls. Dynamic responses to mitochondrial stressors did not show evidence of mitochondrial insufficiency in OP-MG ocular fibroblasts. Although preliminary, these results

suggest that the regulation of mitochondrial pathways in certain individuals may be altered in response to MG sera.

#### 4. Discussion

The pilot studies described here related to the effect of MG sera on mitochondrial bioenergetics in patient-derived ocular fibroblasts and support previous gene expression studies in animals in which it was reported that oxidative metabolism may be induced in the context of MG (Kaminski, Himuro et al. 2016). We found that this may be more vigorous in ocular fibroblasts from two OP-MG cases. We demonstrated, in all seven ocular fibroblast cultures exposed to MG sera for 24 hours, similar transcriptional changes in two mitochondrial pathway genes to what was observed in EAMG rodent muscles. Although we were interested in the MG-sera induced differences between OP-MG and control ocular fibroblasts at gene transcript level, we did not find differences between the two phenotypes. In addition, we did not demonstrate evidence of mitochondrial insufficiency in the OP-MG ocular fibroblasts based on the cellular respiratory control rate, a calculated indicator of mitochondrial coupling efficiency (Brand and Nicholls 2011), which contrasts with the findings in two cases of loosely coupled respiration in mitochondria isolated from MG muscle rather than fibroblasts (Meijer 1972, Lousa, Gobernado et al. 1983).

Although it was not a principal aim, we compared the gene expression between the EOMs and ocular fibroblasts between a number of genes representing muscle mitochondrial pathways to inform our interpretation of bioenergetic studies in ocular fibroblasts as a surrogate for EOM tissue. Therefore, inferences from the mitochondrial functional studies performed in ocular fibroblasts may not accurately represent the mitochondrial efficiency in EOMs of OP-MG cases. However, the induced mitochondrial energetic profile shown in the OP-MG ocular fibroblasts after MG sera exposure suggests that regulation of mitochondrial function is altered by an MG-specific stimulus and possibly differently in OP-MG cells. Recent work has shown that regulation of mitochondrial function is complex, involving a network of pathways regulated by both nuclear and mitochondrial genomes (Duarte, Amorim et al. 2015). Therefore, even small changes in mitochondrial metabolism, as may be triggered by MG, may have major downstream consequences. Besides ATP production, other mitochondrial functions including calcium homeostasis and apoptosis (Duarte, Amorim et al. 2015) may be impaired. In muscle, this may impact contractility or induce atrophy.

MG sera exposure induced upregulation of *PDK4* and *ANGPTL4* in the ocular fibroblasts. These genes were previously reported to be upregulated in EAMG models (Kaminski, Himuro et al. 2016) and in transdifferentiated myoblasts exposed to MG sera (Nel, Prince et al. 2019). These genes are downstream targets of peroxisome proliferator-activated receptor gamma coactivator 1-  $\alpha$  (PGC-1 $\alpha$ ) a central transcriptional activator of mitochondrial biogenesis and oxidative metabolism, that modulates metabolic adaptation of cells/ tissues to internal or

environmental metabolic stress (Austin and St-Pierre 2012). Increased expression of these genes in the ocular fibroblasts suggests an adaptive response to metabolic stress induced by MG sera.

Although we have not included control sera in these experiments, previous reports found that in contrast to 1-10% MG sera (AChR-antibody positive and negative), control sera, including healthy controls and cases with non-MG antibody-mediated conditions, did not induce any morphological changes in cultured myoblasts or lymphocytes after at least 24 hours (Luckman, Skeie et al. 2006, Auret, Abrahams et al. 2014). Although the absence of healthy control human sera may be a limitation, the use of plain growth medium as a control eliminated potential confounding factors of undiagnosed diseases in the control cases.

In conclusion, despite the major limitation of only two OP-MG samples, this pilot study suggested differential responses in dynamic tests of mitochondrial metabolism between perimysial ocular fibroblasts of patients with treatment-resistant myasthenic ophthalmoplegia vs controls after exposure to MG sera. This data would support the hypothesis of altered susceptibility to MG-associated changes in oxidative metabolism in MG.

## References

- Andrade, F. H. and C. A. McMullen (2006). "Lactate is a metabolic substrate that sustains extraocular muscle function." *Pflugers Arch.* **452**(1): 102-108.
- Arnold, A.-S., J. Gill, M. Christie, R. Ruiz, S. McGuirk, J. St-Pierre, L. Tabares and C. Handschin (2014). "Morphological and functional remodelling of the neuromuscular junction by skeletal muscle PGC-1 $\alpha$ ." *Nature Communications* **5**: 3569.
- Auret, J., A. Abrahams, S. Prince and J. M. Heckmann (2014). "The effects of prednisone and steroid-sparing agents on decay accelerating factor (CD55) expression: implications in myasthenia gravis." *Neuromuscul Disord* **24**(6): 499-508.
- Brand, M. D. and D. G. J. B. J. Nicholls (2011). "Assessing mitochondrial dysfunction in cells." *Biochem. J.* **435**(2): 297-312.
- Divakaruni, A. S., A. Paradyse, D. A. Ferrick, A. N. Murphy and M. Jastroch (2014). Analysis and Interpretation of Microplate-Based Oxygen Consumption and pH Data. *Methods in Enzymology*. A. N. Murphy and D. C. Chan. New York, Academic Press. **547**: 309-354.
- Duarte, F. V., J. A. Amorim, C. M. Palmeira and A. P. Rolo (2015). "Regulation of Mitochondrial Function and its Impact in Metabolic Stress." *Curr Med Chem* **22**(20): 2468-2479.
- Europa, T. A., M. Nel and J. M. Heckmann (2019). "A review of the histopathological findings in myasthenia gravis: clues to the pathogenesis of treatment-resistance in extraocular muscles." *Neuromuscul. Disord.*
- Fischer, M. D., M. T. Budak, M. Bakay, J. R. Gorospe, D. Kjellgren, F. Pedrosa-Domellof, E. P. Hoffman and T. S. Khurana (2005). "Definition of the unique human extraocular muscle allotype by expression profiling." *Physiol Genomics* **22**(3): 283-291.
- Fischer, M. D., J. R. Gorospe, E. Felder, S. Bogdanovich, F. Pedrosa-Domellof, R. S. Ahima, N. A. Rubinstein, E. P. Hoffman and T. S. J. P. g. Khurana (2002). "Expression profiling reveals metabolic and structural components of extraocular muscles." *Physiol. Genomics* **9**(2): 71-84.
- Garcia-Cazarin, M. L., T. M. Fisher and F. H. Andrade (2010). "Glucose Uptake in Rat Extraocular Muscles: Effect of Insulin and Contractile Activity." *Invest. Ophthalmol. Vis. Sci.* **51**(12): 6364-6368.
- Heckmann, J. M. and M. Nel (2017). "A unique subphenotype of myasthenia gravis." *Ann. N. Y. Acad. Sci.*
- Heckmann, J. M., E. P. Owen and F. Little (2007). "Myasthenia gravis in South Africans: racial differences in clinical manifestations." *Neuromuscul. Disord.* **17**(11-12): 929-934.
- Kaminski, H. J., K. Himuro, J. Alshaiikh, B. Gong, G. Cheng and L. L. Kusner (2016). "Differential RNA Expression Profile of Skeletal Muscle Induced by Experimental Autoimmune Myasthenia Gravis in Rats." *Front Physiol* **7**: 524.

- Kusner, L. L., A. Young, S. Tjoe, P. Leahy and H. J. Kaminski (2010). "Perimysial fibroblasts of extraocular muscle, as unique as the muscle fibers." Invest. Ophthalmol. Vis. Sci. **51**(1): 192-200.
- Lousa, M., J. Gobernado, A. Gimeno and M. Gosalvez (1983). "Mitochondrial function in myasthenia gravis." Eur. Neurol. **22**(1): 53-57.
- Luckman, S. P., G. O. Skeie, G. Helgeland and N. E. Gilhus (2006). "Effects of myasthenia gravis patient sera on human myoblast cultures." Acta Neurol Scand Suppl **183**: 28-32.
- Luckman, S. P., G. O. Skeie, G. Helgeland and N. E. Gilhus (2006). "Morphological effects of myasthenia gravis patient sera on human muscle cells." Muscle Nerve **33**(1): 93-103.
- Meijer, A. E. F. H. (1972). "Morphologie, histochemie und biochemie mitochondrialer skelettmuskelkrankheiten." Acta Histochem. Suppl. **12**: 333-334.
- Nel, M., S. Prince and J. M. Heckmann (2019). "Profiling of patient-specific myocytes identifies altered gene expression in the ophthalmoplegic subphenotype of myasthenia gravis." Orphanet J Rare Dis **14**(1): 24.
- Pfaffl, M. W., A. Tichopad, C. Prgomet and T. P. Neuvians (2004). "Determination of stable housekeeping genes, differentially regulated target genes and sample integrity: BestKeeper–Excel-based tool using pair-wise correlations." Biotechnol. Lett. **26**(6): 509-515.
- Rautenbach, R. M., K. Pillay, A. D. N. Murray and J. M. Heckmann (2017). "Extraocular Muscle Findings in Myasthenia Gravis Associated Treatment-Resistant Ophthalmoplegia: A Case Report." J Neuroophthalmol.
- Schmittgen, T. D. and K. J. Livak (2008). "Analyzing real-time PCR data by the comparative C(T) method." Nat Protoc **3**(6): 1101-1108.
- Smith, T. J. (2004). "Novel aspects of orbital fibroblast pathology." J. Endocrinol. Invest. **27**(3): 246-253.
- Vandesompele, J., K. De Preter, F. Pattyn, B. Poppe, N. Van Roy, A. De Paepe and F. Speleman (2002). "Accurate normalization of real-time quantitative RT-PCR data by geometric averaging of multiple internal control genes." Genome Biol. **3**(7): research0034.0031.
- Vincent, A. E., Y. S. Ng, K. White, T. Davey, C. Mannella, G. Falkous, C. Feeney, A. M. Schaefer, R. McFarland, G. S. Gorman, R. W. Taylor, D. M. Turnbull and M. Picard (2016). "The Spectrum of Mitochondrial Ultrastructural Defects in Mitochondrial Myopathy." Scientific reports **6**: 30610-30610.
- Zhou, Y., H. J. Kaminski, B. Gong, G. Cheng, J. M. Feuerman and L. Kusner (2014). "RNA expression analysis of passive transfer myasthenia supports extraocular muscle as a unique immunological environment." Invest. Ophthalmol. Vis. Sci. **55**(7): 4348-4359.

## 5. Appendix

Appendix table 1: Reference gene selection for qPCR comparing EOMs and ocular fibroblasts

	Average fold change (EOMs/ocular fibroblasts)	p value	geNorm (m value)	Bestkeeper (SD; CV)
<b><i>RPLP0</i></b>	<b>0.11</b>	<b>0.063</b>	<b>1.46</b>	<b>1.87; 7.67</b>
<i>GAPDH</i>	0.11	0.66	2.57	2.89; 15.8
<i>CSNK2A2</i>	0.07	0.057	1.84	2.76; 17.3
<i>ACTN2</i>	0.09	0.003	1.99	1.61; 10.13
Average <i>RPLP0</i> - <i>ACTN2</i>	0.08	0.023	1.57	1.74; 8.64

Appendix table 1. Extraocular muscles (EOMs); Fold change =  $2^{-\Delta Cq}$  ( $\Delta Cq = \text{EOMs } Cq^{\text{ref}} - \text{ocular fibroblasts } Cq^{\text{ref}}$ ). “Average fold change” refers to the arithmetic mean of OP-MG  $2^{-Cq}$  divided by the arithmetic mean of the controls. The “geNorm m value” refers to the average expression stability value calculated using the geometric mean. SD is the standard deviation and CV is the coefficient of variance.

Appendix table 2: Reference gene selection for qPCR comparing OP-MG and control ocular fibroblasts

	Average fold change (OP-MG/controls)	p value	geNorm (m value)	Bestkeeper (SD; CV)
<i>RPLP0</i>	1.07	0.95	2.13	1.54; 6.52
<i>GAPDH</i>	1.30	0.82	2.84	3.85; 21.46
<i>CSNK2A2</i>	1.78	0.60	2.13	3.04; 20.02
<b><i>ACTN2</i></b>	<b>1.34</b>	<b>0.61</b>	<b>2.95</b>	<b>0.63; 4.28</b>
Average <i>GAPDH</i> - <i>CSNK2A2</i>	1.52	0.70	1.10	3.45; 20.80

Appendix table 2. Ophthalmoplegic myasthenia gravis (OP-MG); Fold change =  $2^{-\Delta Cq}$  ( $\Delta Cq = \text{EOMs } Cq^{\text{ref}} - \text{ocular fibroblasts } Cq^{\text{ref}}$ ). “Average fold change” refers to the arithmetic mean of OP-MG  $2^{-Cq}$  divided by the arithmetic mean of the controls. The “geNorm m value” refers to the average expression stability value calculated using the geometric mean. SD is the standard deviation and CV is the coefficient of variance.

Appendix table 3: Assessing the impact of MG sera treatment on reference gene stability in OP-MG ocular fibroblasts

Reference Gene	Average fold change (Fold change <sup>A</sup> ; fold change <sup>B</sup> )	Paired t test (p value)	geNorm m value	Bestkeeper SD; CV
<i>TFRC</i>	1.03 (1.71; 0.35)	0.833	0.867	0.58; 2.42
<i>HPRT1</i>	1.87 (2.68; 1.06)	0.466	0.730	0.38; 1.50
<i>B2M</i>	0.50 (0.08; 0.92)	0.300	0.797	0.61; 3.09
<i>PPIA</i>	2.13 (3.51; 0.75)	0.715	0.787	0.62; 2.54
<i>ACTB</i>	0.87 (1.06; 0.68)	0.633	0.752	0.25; 1.54
<i>GUSB</i>	0.88 (0.91; 0.85)	0.311	0.751	0.51; 1.97
<i>RPLPO</i>	0.79 (0.81; 0.77)	0.175	0.670	0.27; 1.56
<i>TBP</i>	1.64 (2.28; 1.00)	0.499	0.637	0.44; 1.62
<i>CSNK2A2</i>	0.84 (0.72; 0.97)	0.423	0.700	0.21; 0.86
<i>AP3D1</i>	1.74 (0.79; 2.70)	0.753	1.186	0.57; 2.53

Appendix table 3. Fold change =  $2^{-\Delta Cq}$  ( $\Delta Cq = \text{MGS } Cq^{\text{ref}} - \text{untreated } Cq^{\text{ref}}$ ). Average fold change was calculated between the two cell lines used in this experiment (identified as A and B in this table). The “geNORM m value” refers to the geometric mean. SD is the standard deviation and CV is the coefficient of variance.

## Chapter 6: Concluding remarks

In this investigation of the molecular genetic pathogenesis of the treatment-resistant ophthalmoplegic subphenotype of myasthenia gravis (OP-MG), triangulation of data from clinical observations of MG cases with ophthalmoparesis, systematic review of MG muscle biopsy histopathology, gene expression analyses and dynamic metabolic assays in patient-derived orbital tissues, was used to identify the underlying pathogenetic mechanisms of OP-MG and to verify previous hypotheses generated by next generation sequencing studies.

It was previously recognised that a subphenotype of myasthenia gravis cases with ocular manifestations developed persistent ophthalmoplegia and/or ptosis despite the use of standard immune therapies although their non-ocular muscles responded well to therapy (Heckmann and Nel 2017). The ophthalmoplegic subphenotype was previously defined by persistent EOM weakness despite adequate treatment and resolution of weakness in non-ocular muscles after a period of two years (Heckmann and Nel 2017). We aimed to determine, through clinical observations, at which critical point this treatment resistance may develop. Analysis of observational data in new cases in their first year of immune therapies (Chapter 1), suggested that this critical period may be as early as 7 months (median time to resolution) and 40% of cases demonstrated persistent EOM weakness after one year of therapy of  $\geq 1$  EOM ( $\approx 20\%$  multiple EOMs). However, in clinical practice we observed that some patients improved after one year of treatment. Delay to diagnosis and initiation of immune therapies (from symptom onset) was shown to be an unfavourable prognostic factor. This demonstrated the importance of early identification of “at-risk” cases who may warrant alternative strategies relating to immune therapies. These results also suggested that with prolonged reduced contractility and/or untreated MG, pathological changes such as neurogenic atrophy, fibrofatty replacement and mitochondrial abnormalities may develop at the level of the muscle, contributing to the development of treatment resistance in susceptible individuals after a critical period. Taken together, a prognostic biomarker is required to identify which individuals are at greatest risk of developing ophthalmoplegic MG.

Although the evidence was limited to a few case reports, a review of histopathological changes in MG muscle biopsies showed that fibrofatty replacement and ultrastructural features of mitochondrial stress were observed in significantly weak EOMs (Chapter 2). There was some evidence, from EOM biopsies of MG cases as well as paralysed EOMs from other causes, to suggest that the EOMs may be more susceptible to the effects of reduced contractility than non-ocular muscles. Gene expression studies in EAMG models showed that transcriptomic changes in denervated muscles could be observed as early as 7 days (Iqbal, Ostojic et al. 2013, Graham, Harlow et al. 2018). We hypothesized that reduced contractility induced by MG

may trigger a cascade of atrophy signalling pathways, thereby contributing to the development of treatment resistance.

In the comparison of gene expression in OP-MG and non-MG control orbital muscles, atrophy signalling pathways featured prominently in the dysregulated pathways supporting previous histopathological findings. Although altered gene expression might be expected in these important muscle pathways in muscles affected by a synaptic transmission defect, the dysregulated pathways including atrophy signalling, muscle contractility and mitochondrial homeostasis were observed in muscles which were not overtly weak and provided some insight into the molecular-genetic changes which may occur in the EOMs of susceptible individuals in the context of MG.

Inferred co-expression networks from gene expression data in orbicularis oculi muscles of OP-MG and control cases suggested that the putative OP-MG genes/pathways function in a dysregulated network and supported the hypotheses of the previous genomic studies (Nel, Mulder et al. 2019). Repression of several genes in the OP-MG pathways suggested miRNAs, biological regulators of gene expression, as a potential mechanism of action resulting in downregulation of genes of interest. MiRNAs associated with the repressed genes and previously shown to be highly expressed in EOMs were identified in public miRNA databases (Zeiger and Khurana 2010, Chou, Shrestha et al. 2018). Interestingly, several of the repressed genes were previously identified as having OP-MG associated variants in the 3'UTR regions which would support miRNAs as the underlying pathogenetic mechanism (Nel, Jalali Sefid Dashti et al. 2017). These miRNAs require further investigation as they may be useful as diagnostic or prognostic biomarkers or serve as therapeutic targets in the future.

Ultrastructural evidence of mitochondrial stress was frequently observed in histopathological reports on MG muscle biopsies, including both non-ocular muscles and EOMs, regardless of the MG serotype (Chapter 2). In this project, gene expression data from comparison of OP-MG and control orbital muscles and dynamic bioenergetic studies in perimysial ocular fibroblasts suggested that mitochondrial metabolism may be dysregulated in the EOMs of OP-MG cases in the context of MG. However, this is preliminary data was the result of a pilot study performed opportunistically using a small number of ocular fibroblast samples. This could not be reproduced due to the rare opportunity of sampling these ocular tissues from MG cases. Taken together, the previous evidence from EAMG models and histopathological reports (Chapter 2), gene expression studies (Chapter 3) and bioenergetic assays using ocular fibroblasts (Chapter 5) suggest that mitochondrial function may be altered by MG and that the EOMs of individuals with OP-MG associated gene variants may be most susceptible. It is well established that the EOMs have an abundance of mitochondria compared with non-ocular

muscles and that the mitochondrial metabolism of the EOMs is uniquely regulated to support their high energy requirements (Andrade, McMullen et al. 2005, Andrade and McMullen 2006, Garcia-Cazarin, Fisher et al. 2010). Although the primary function of the mitochondria in muscle is to produce energy for contractile activity, mitochondrial pathways intersect with other important muscle pathways including muscle regeneration and atrophy signalling (Tryon, Vainshtein et al. 2014). Therefore, altered mitochondrial metabolism in OP-MG EOMs may not only impact contractility but also perpetuate the dysregulation of these other pathogenetic pathways.

Figure 1 shows the intersection of the pathogenetic pathways hypothesized to contribute to the development of the treatment-resistant OP-MG subphenotype. We showed that patients who started treatment earlier and had higher doses of steroids and/or rescue therapies in the form of intravenous immunoglobulin (IVIG) or plasma exchange (PLEX) in the first year of treatment experienced resolution of ophthalmoparesis earlier (Chapter 1). This suggests that in these cases, arresting the ongoing autoimmune mechanisms earlier and allowing regeneration of AChR receptors on the muscle endplate potentially attenuated the secondary effects of functional denervation leading to EOM atrophy. Therefore, earlier identification and treatment of MG cases, and particularly those who are most susceptible to the development of treatment-resistant ophthalmoplegia will be important in the initial treatment phases.

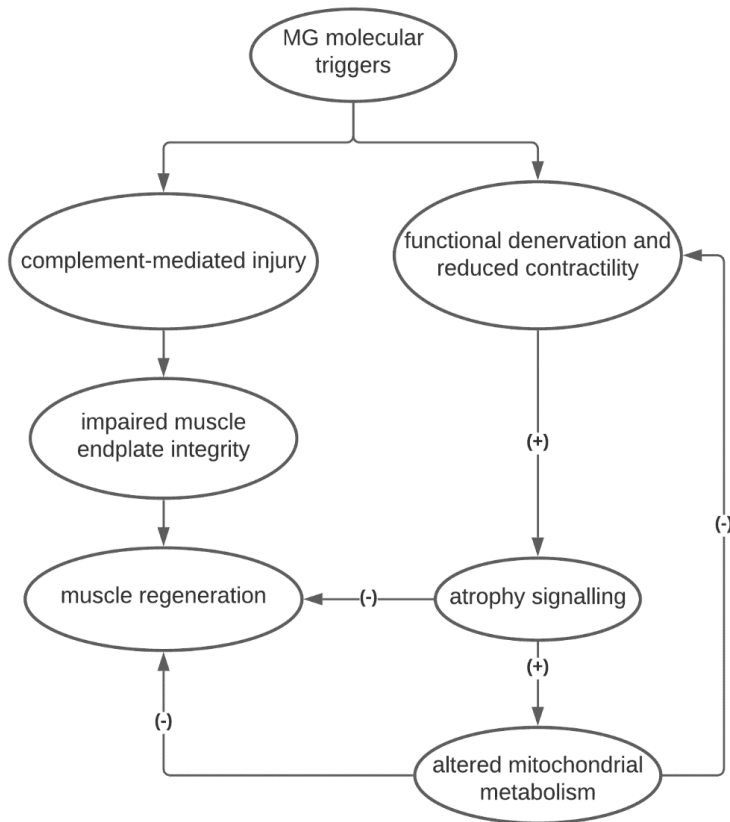


Figure 1. A schematic figure demonstrating the intersection of the pathogenetic mechanisms hypothesized to contribute to the development of the treatment-resistant ophthalmoplegic subphenotype in myasthenia gravis (MG).

It is possible that higher steroid doses or more rapid escalation in initial dosing may be useful in achieving earlier resolution of ophthalmoparesis, however this decision in the clinical setting would have to be made with consideration of comorbid conditions like diabetes, potential adverse effects of steroid use and the possibility of initial clinical deterioration, particularly in those with severe generalized disease. In a small blinded randomized controlled trial, low doses of prednisone were effective in improving ophthalmoparesis however these patients had mostly mild weakness (Benatar, McDermott et al. 2016). Further randomized controlled trials will be necessary to evaluate the efficacy and safety of higher doses of prednisone in the resolution of ophthalmoparesis. We noted in a small number of cases, that those who had severe generalized MG and required rescue therapies in the form of IVIG or PLEX had earlier resolution of ophthalmoparesis, although these patients also received higher doses of steroids. However, these immune therapies which are more invasive and more costly are reserved for cases of severe generalized MG and not for cases with ocular manifestations only and therefore not appropriate in cases of OP-MG. As in the case of IVIG/PLEX, other biological immune therapies used in MG are directed towards severe generalized symptoms

rather than ocular symptoms. For example, rituximab has been shown to be effective in patients with generalized symptoms of MuSK-MG (Narayanaswami, Sanders et al. 2021). As most cases of MG have circulating AChR antibodies which initiate a complement mediated attack at the muscle endplate, complement inhibitors have been investigated in clinical trials and eculizimab has been approved for use in refractory generalized AChR-MG (Howard Jr, Utsugisawa et al. 2017, Narayanaswami, Sanders et al. 2021). However, this agent carries a risk of meningococcal meningitis and vaccinations are therefore required. Complement inhibitors are also very costly and not yet feasible for use in our current clinical setting. As the EOMs have lower expression of complement regulators (Soltys, Gong et al. 2008) and may be more susceptible to complement-mediated damage, in the future these agents may be of use in carefully selected OP-MG cases.

Studies documenting the findings of orbital MRI in MG patients, have shown evidence of atrophy and fatty replacement of EOMs (Farrugia, Robson et al. 2006, Velonakis, Papadopoulos et al. 2021). It was suggested that MRI may be useful in identifying EOM atrophy early on and without EOM biopsy which may help with prognostication and counselling of patients regarding the expected clinical outcome (Velonakis, Papadopoulos et al. 2021). Atrophy of the craniofacial muscles mainly in MuSK-MG is well-established in the literature (Huda, Woodhall et al. 2016) however this may be reversible as was shown in a single case of a patient with atrophy of the tongue which resolved with immune therapies over a period of three years (Takahashi, Kawaguchi et al. 2010). We suspect however, that the EOMs may be more susceptible to the mechanisms inducing atrophy in MG, which may trigger a vicious cycle (see Figure 1), impacting on other muscle pathways in susceptible individuals.

The limitations encountered in this project related to the investigation of a rare disorder for which biological samples are rarely available. Due to the small sample sizes, statistical analyses may have been underpowered and limited the interpretation of results. However, the results from these studies in gene expression and dynamic metabolic assays supported previous hypotheses generated from comprehensive next generation sequencing analyses and suggested that the association signals identified are real.

This work has provided a basis for future research for the development of a biomarker for the early identification of susceptible individuals which may influence decisions regarding immune therapies early in the course of the disease.

## References

- Andrade, F. H. and C. A. McMullen (2006). "Lactate is a metabolic substrate that sustains extraocular muscle function." *Pflugers Arch.* **452**(1): 102-108.
- Andrade, F. H., C. A. McMullen and R. E. Rumbaut (2005). "Mitochondria are fast Ca<sup>2+</sup> sinks in rat extraocular muscles: a novel regulatory influence on contractile function and metabolism." *Investigative ophthalmology & visual science* **46**(12): 4541-4547.
- Benatar, M., M. P. McDermott, D. B. Sanders, G. I. Wolfe, R. J. Barohn, R. J. Nowak, M. Hehir, V. Juel, H. Katzberg, R. Tawil and G. Muscle Study (2016). "Efficacy of prednisone for the treatment of ocular myasthenia (EPITOME): A randomized, controlled trial." *Muscle Nerve* **53**(3): 363-369.
- Chou, C.-H., S. Shrestha, C.-D. Yang, N.-W. Chang, Y.-L. Lin, K.-W. Liao, W.-C. Huang, T.-H. Sun, S.-J. Tu, W.-H. Lee, M.-Y. Chiew, C.-S. Tai, T.-Y. Wei, T.-R. Tsai, H.-T. Huang, C.-Y. Wang, H.-Y. Wu, S.-Y. Ho, P.-R. Chen, C.-H. Chuang, P.-J. Hsieh, Y.-S. Wu, W.-L. Chen, M.-J. Li, Y.-C. Wu, X.-Y. Huang, F. L. Ng, W. Buddhakosai, P.-C. Huang, K.-C. Lan, C.-Y. Huang, S.-L. Weng, Y.-N. Cheng, C. Liang, W.-L. Hsu and H.-D. Huang (2018). "miRTarBase update 2018: a resource for experimentally validated microRNA-target interactions." *Nucleic acids research* **46**(D1): D296-D302.
- Farrugia, M. E., M. D. Robson, L. Clover, P. Anslow, J. Newsom-Davis, R. Kennett, D. Hilton-Jones, P. M. Matthews and A. Vincent (2006). "MRI and clinical studies of facial and bulbar muscle involvement in MuSK antibody-associated myasthenia gravis." *Brain* **129**(Pt 6): 1481-1492.
- Garcia-Cazarin, M. L., T. M. Fisher and F. H. Andrade (2010). "Glucose Uptake in Rat Extraocular Muscles: Effect of Insulin and Contractile Activity." *Invest. Ophthalmol. Vis. Sci.* **51**(12): 6364-6368.
- Graham, Z. A., L. Harlow, W. A. Bauman and C. P. Cardozo (2018). "Alterations in mitochondrial fission, fusion, and mitophagic protein expression in the gastrocnemius of mice after a sciatic nerve transection." *Muscle & nerve* **58**(4): 592-599.
- Heckmann, J. M. and M. Nel (2017). "A unique subphenotype of myasthenia gravis." *Ann. N. Y. Acad. Sci.*
- Howard Jr, J. F., K. Utsugisawa, M. Benatar, H. Murai, R. J. Barohn, I. Illa, S. Jacob, J. Vissing, T. M. Burns and J. T. Kissel (2017). "Safety and efficacy of eculizumab in anti-acetylcholine receptor antibody-positive refractory generalised myasthenia gravis (REGAIN): a phase 3, randomised, double-blind, placebo-controlled, multicentre study." *The Lancet Neurology* **16**(12): 976-986.
- Huda, S., M. R. Woodhall, A. Vincent and J. M. Heckmann (2016). "Characteristics Of acetylcholine-receptor-antibody-negative myasthenia gravis in a South African cohort." *Muscle Nerve* **54**(6): 1023-1029.

- Iqbal, S., O. Ostojic, K. Singh, A. M. Joseph and D. A. Hood (2013). "Expression of mitochondrial fission and fusion regulatory proteins in skeletal muscle during chronic use and disuse." Muscle & nerve **48**(6): 963-970.
- Narayanaswami, P., D. B. Sanders, G. Wolfe, M. Benatar, G. Cea, A. Evoli, N. E. Gilhus, I. Illa, N. L. Kuntz, J. Massey, A. Melms, H. Murai, M. Nicolle, J. Palace, D. Richman and J. Verschuuren (2021). "International Consensus Guidance for Management of Myasthenia Gravis." 2020 Update **96**(3): 114-122.
- Nel, M., M. Jalali Sefid Dashti, J. Gamielidien and J. M. Heckmann (2017). "Exome sequencing identifies targets in the treatment-resistant ophthalmoplegic subphenotype of myasthenia gravis." Neuromuscul Disord.
- Nel, M., N. Mulder, T. A. Europa and J. M. Heckmann (2019). "Using Whole Genome Sequencing in an African Subphenotype of Myasthenia Gravis to Generate a Pathogenetic Hypothesis." Front Genet **10**(136).
- Soltys, J., B. Gong, H. J. Kaminski, Y. Zhou and L. L. Kusner (2008). "Extraocular muscle susceptibility to myasthenia gravis: unique immunological environment?" Ann N Y Acad Sci **1132**: 220-224.
- Takahashi, H., N. Kawaguchi, S. Ito, Y. Nemoto, T. Hattori and S. Kuwabara (2010). "Is tongue atrophy reversible in anti-MuSK myasthenia gravis? Six-year observation." Journal of Neurology, Neurosurgery & Psychiatry **81**(6): 701-702.
- Tryon, L. D., A. Vainshtein, J. M. Memme, M. J. Crilly and D. A. Hood (2014). "Recent advances in mitochondrial turnover during chronic muscle disuse." Integr Med Res **3**(4): 161-171.
- Velonakis, G., V. E. Papadopoulos, E. Karavasilis, D. K. Filippiadis and V. Zouvelou (2021). "MRI evidence of extraocular muscle atrophy and fatty replacement in myasthenia gravis." Neuroradiology **63**(9): 1531-1538.
- Zeiger, U. and T. S. Khurana (2010). "Distinctive patterns of microRNA expression in extraocular muscles." Physiological Genomics **41**(3): 289-296.

## List of abbreviations

<b>Abbreviation</b>	<b>Term</b>
AChEIs	Acetylcholinesterase inhibitors
AChR	acetylcholine receptor
ACTH	adrenocorticotrophic hormone
AF	atrophic fibres
AMP	adenosine monophosphate
ANOVA	analysis of variance
ATP	adenosine triphosphate
AZA	azathioprine
CI	confidence interval
COX	cytochrome C oxidase
CRCR	cell respiratory control ratio
CT	computed tomography
DMEM	Dulbecco's Modified Eagle Medium
DMSO	dimethyl sulfoxide
EAMG	experimental autoimmune myasthenia gravis
ECAR	extracellular acidification rate
ECM	extracellular matrix
EOM	Extraocular muscle
FCCP	carbonyl cyanide p-trifluoromethoxyphenylhydrazone
FCMR	fibrocellular and fatty muscle replacement
FDR	false discovery rate
GMG	generalised myasthenia gravis
HIV	human immunodeficiency virus
HR	hazard ratio
Ig	immunoglobulin
IGF-1	insulin-like growth factor 1
IMCL	intramyocellular lipid
IO	inferior oblique
IQR	interquartile range
IR	inferior rectus
IVIG	intravenous immunoglobulin
LR	lateral rectus
LRP4	lipoprotein receptor-related protein 4
MFD	myofibrillary disarray
MG	myasthenia gravis
mg	milligrams
MGFA	Myasthenia Gravis Foundation of America
MIF	multiply-innervated fibres
miRNA	microRNA
MR	medial rectus
MTX	methotrexate
MuSK	muscle-specific kinase
NGS	next generation sequencing
NMJ	neuromuscular junction

NMOC	non-mitochondrial oxygen consumption
NSIT	non-steroid immunosuppressive therapy
OCR	oxygen consumption rate
OM	ocular manifestations
OOM	orbicularis oculi muscle
OP-MG	Ophthalmoplegic myasthenia gravis
OR	odds ratio
PBS	phosphate buffered saline
PGC-1 $\alpha$	peroxisome proliferator-activated receptor- $\gamma$ coactivator
PI3K	phosphoinositide-3 kinase
PL	proton leak
PLEX	plasma exchange
PM	post mortem
PPC	positive plate controls
Pred	prednisone
QMG	quantified myasthenia gravis score
qPCR	quantitative polymerase chain reaction
RA	rheumatoid arthritis
RIN	RNA integrity number
RNA-seq	RNA sequencing
RNS	repetitive nerve stimulation
ROS	reactive oxygen species
RsR	resolution ratio
RT	reverse transcription
SD	standard deviation
SFEMG	single-fibre electromyography
SIF	singly-innervated fibres
SNP	single nucleotide polymorphism
SO	superior oblique
SR	superior rectus
SRC	spare respiratory capacity
SSA	subsarcolemmal aggregates
TAO	thyroid-associated ophthalmopathy
TCA	tricarboxylic acid
UCP3	uncoupling protein 3
WES	whole exome sequencing
WGS	whole genome sequencing
ZBS	Z-band streaming
$\alpha$ -SMA	$\alpha$ -smooth muscle actin